APPLICATION OF IEC 61850-90-5 STANDARD-BASED PREDICTIVE DYNAMIC STABILITY SYSTEM

by

Nande Fose

Thesis submitted in fulfilment of the requirements for the degree

Master of Engineering: Electrical Engineering

in the Faculty of Engineering and the Built Environment

at the Cape Peninsula University of Technology

Supervisor: Dr. S. Krishnamurthy

Bellville Campus

Date submitted: 23rd February 2023

DECLARATION

I, Nande Fose, declare that the contents of this thesis/dissertation represent my own unaided work, and that the thesis/dissertation has not previously been submitted for academic examination towards any qualification. Furthermore, it represents my own opinions and not necessarily those of the Cape Peninsula University of Technology.

23rd February 2023

Signed **Date**

ABSTRACT

With the rapid growth of intermittent renewable energy sources across all power grid networks and the fact that loads cannot be considered passive; there is a growing need to develop new methods and technologies for real-time monitoring and control of the power grid. Part of this is because power grids are becoming more complex. In many countries around the world, recent widespread blackouts have demonstrated the need for more reliable and precise tools for tracking, regulating, and protecting the power system. There are important biases in the prediction of the state of the power system, which is the key method used today to provide the real-time model of the system, arising mainly from the complexity and geographical delivery and separation of the electricity network. The decreased stability margin at which power systems work these days has forced the power industry to come up with new ideas to ensure the integrated power system operates continuously and efficiently. In this regard, it has become important to implement Wide Area Monitoring, Protection and Control (WAMPAC) systems in order to better manage the grid, to improve the efficiency of system usage, to ensure the security of supplies, and to make synchrophasor measurements more prominent, offering consistent real-time data. The development and deployment of the synchronized Phasor Measurement technology in many network locations has introduced a promising way to secure power networks from unwanted conditions.

From time to time, a series of unpredictable and conflicting contingencies can lead to angular instability of the power system and even blackouts if not adequately handled by an out-of-step (OOS) protection system. The key contribution of this research work, to the theory of Out-of-Step protection, is the identification and isolating after a given disruption of many unstable swings. The method of out-of-step condition detection is based on system-wide generation sources supplying an Eskom transmission network in the Western Cape Province with the Western Grid with 765kV and 400kV voltage levels. The proposed defense scheme involves an optimally placed PMU for fast detection of system analogue quantities.

Therefore, the research work aims to investigate the IEC 61850-90-5 standard for Predictive dynamic stability maintaining system using Phasor Management Units (PMU) for an out of step condition of synchronous generator at a Palmiet pump storage generating station of the Eskom West Grid test system. A framework to investigate the power system rotor angle stability during steady state and transient stability occurrence in DIgSILENT PowerFactory® software is first developed for non-real time simulation studies.

A Lab-scale implementation to test an out-of-step algorithm when a severe fault occurs in a busbar fed by Pump storage generators in Real-Time Digital Simulator (RTDS) will be carried out, software-based Phasor Measurement Unit (PMU) is incorporated to test and validate the IEC-61850-90-5 standard. The power system modelling and simulation are performed in the RSCAD-FX for the proposed multi-area power system network.

Key words: Out-of-step protection, dynamic stability, predictive system, IEC61850-90-5, multi-area power systems, PMU, PDC, WAMP

ACKNOWLEDGEMENTS

I wish to thank:

- First and foremost, my husband for the time granted to focus on project and undying support during this journey .
- Exceptionally my academic supervisor Dr. Senthil Krishnamurthy for his insight counsel and guidance throughout this project, the words of encouragement and patience were vital in making this thesis possible.
- My appreciation also goes to the entire Center for Substation Automation and Energy Management systems (CSAEMS)

The financial assistance of **CSIR DSI-Interbursary Support (IBS) Programme** towards this research is acknowledged. Opinions expressed in this thesis and the conclusions arrived at, are those of the author, and are not necessarily to be attributed to the National Research Foundation.

DEDICATION

This thesis is dedicated to my late mother Nozuko Mamfenguza, her teachings and love towards her children will forever be cherished.

GLOSSARY

Power Swing: A difference in three phase power flow that occurs when the angles of the generator rotor shift forward or slow down relative to each other in response to changes in load magnitude and direction, line switching, generation failure, faults, and other device disturbances.

Power System Stability: The capacity of the power system to recover and maintain stability after being subjected to disruption.

Rotor Angle Stability: It refers to the ability of synchronous generators in a linked power system to continue running at the same time after a disruption.

Out-of-Step Condition: A power swing that can lead to pole slippage of a generator or group of generators for which some corrective action must be taken.

Pole Slip: A situation in which the generator or group of generators, terminal voltage angles (or phases) go past 180 degrees relative to the rest of the connected power grid.

Algorithm: A step-by - step process to solve a problem or perform a task, particularly on a computer.

DIgSILENT: Power systems modelling, analysis and simulation software for applications in generation, transmission, distribution and industrial systems.

DFT: Discrete Fourier Transform converts samples from a sampled signal into a set of complex co-efficient of sinusoidal frequencies. This transform essentially converts samples from the time domain to the frequency domain.

IEC 61850-90-5: Technical report to ensure conformance of synchrophasor communication with the IEC 61850 standard

R-GOOSE: Routable Generic Object-Oriented Substation Event to ensure cyber secured transmitted data sets of the IEC 61850-90-5 standard.

GPS: It is the global positioning system that is comprised of 24 satellites in geostationary orbit around the earth.

IEEE-C37.118.1: The international standard for synchrophasor measurements in power systems. Specifies conformance communication criteria for phasor measurement units.

Power system security: The power grid can withstand changes in the power system without disrupting system operation. It connects system strength and contingencies.

Synchrophasor: Phasors measured simultaneously at different locations within the power network and synchronised in real-time.

RTDS: Real-Time Digital Simulator for power systems. It can simulate any modern power grid system in real-time.

FACTS: The static equipment used for the AC transmission of electrical energy is known as the Flexible Alternating Current Transmission System. It is designed to improve controllability and increase the ability to shift power. It is usually a computer based on power electronics.

NOMENCLATURES

WANs	:	Wide Area Network
PDCs	:	Phasor Data Concentrators
PMUs	:	Phasor Measurement Units
FACTS	:	Flexible Alternating Current Transmission System
GPS	:	Global positioning system
DSM	:	Dynamic System Monitoring solutions
DSE	:	Dynamic state estimator
PSB	:	Power Swing Blocking (PSB)
OOS	:	Out-Of-Step condition
OST	:	Out-Of-Step tripping
SCADA	:	Supervisory Control and Data Acquisition systems
RTU	:	Remote terminal units
EMS	:	Energy Management System
OMS	:	Outage Management System
WAMPAC	:	Wide-Area Monitoring, Protection, Automation and Control
RTDS	:	Real-Time Digital Simulator
IED	:	Intelligent Electronic Device
R-GOOSE	:	Routable Generic Object-Oriented Substation Event
IPP's	:	Independent Power Producers
DG	:	Distributed generator
FDR's	:	Electrical feeder
DDSE-T	:	Distributed Dynamic System Estimation at relay level
EHV	:	Extra High Voltage
VT	:	Voltage Transformer
CT	:	Current Transformer
RTDM	:	Real-Time Dynamics Monitoring
AC	:	Alternating current
DC	:	Direct current
AVR	:	Automatic voltage regulator
PSS	:	Power System Stabilizer
SPSG	:	Salient pole synchronous generator
GSU	:	Generator step up transformer
ICE	:	Internal Combustion Engine

TABLE OF CONTENTS

LIST OF FIGURES

LIST OF TABLES

1 CHAPTER ONE

INTRODUCTION

1.1 INTRODUCTION

The power system is often subject to numerous disruptions during steady state activity that leads to voltage instability. System engineers and developers are trying to develop the most robust power system structure capable of dealing with all potential contingencies. There is, however, a slight risk of contingencies where an unexpected scenario of complex events can contribute to power system instability. As an out-of-step regime, angular instability is one of the most dangerous states of instability in the power structure. Due to the limited capacity of the transmission lines, the short circuits and the lack of generation, the generated power cannot be successfully transmitted to the load. Then, some parts of the power system generator which continues to operate asynchronously with the remaining part of the system in response to the generation / load imbalance.

The out-of-step condition cannot be sustained for long time duration as it may pose negative impact on the power system equipment and its integrity. The last resort to prevent a potential power grid from failing is the regulated black outs of the network into many electrically separated islands. The goal of this division is to try to maintain the balance within each island (Begovic, 2005). At its inception, power systems were designed to transmit power to places geographically close to generation stations. This feature made power systems very stable, which means that power systems were worked well beyond their stability limits. A small or significant disruption would not disrupt the system, nor would the ability to produce power be affected. As the use of electrical power became more widespread in the early twentieth century, the need to transmit power over long distances became inevitable. This, along with the rise in network size, has changed the way power systems are run. Power grids are now being forced to run closer to their reliability limits. The higher the energy demand, the higher the increase in production, and the lack of new transmission lines have caused the system to hit stressed conditions more frequently and the system to collapse (Dobson, 2002).

Government agencies have imposed restrictions on power utilities and on system operators to comply with regulations that seek to guarantee the reliable operation of the bulk power system. This is one of the reasons why, in recent years, control and security of the network has become an important area of research. New and more precise protection philosophies and operational guidance are being applied around the grid with the development and implementation of Phasor Measurement Units (PMUs). The concept of a phasor synchronized with the power system was introduced in the 1980s and standardized for the first time in 1995 with the IEEE 1344 standard (Martin, 2011). In 2011, as a result of joint work between IEEE and IEC, IEEE Standard C37.117-2005 was split into two parts. IEEE C37.118.1: the structured way of calculating synchrophasor, and IEEE C37.118.2: the data transfer criteria stated. The establishment of this task force marked the formal beginning of the IEC TR 61850-90-5 production, which was first published in 2012.

In this research, a new IEC 61850-90-5 standard based out-of-step protection scheme for predictive dynamic stability system is presented. This scheme uses phasor measurement data collected in different parts of the system to predict the loss of synchronism between generators. This protection scheme will be tested on different dynamic models in order to evaluate its performance during stable and unstable swings.

1.2 AWARENESS OF THE PROBLEM

With load demand rising every day, however, stability issues cannot occur frequently when they do, their impact may be huge. In fact, it can be confidently claimed for many utilities that dynamic stability becomes the most significant risk facing the network operator in the course of cascading events and extreme contingencies. State owned Power utilities are forced to explore new ways of producing power by adapting interconnection of energy renewables to its existing grid. However, in as much as expanding their Grid they still have an obligation to maintain a secured and stable to customer service points, with this said even if an Independent Power Producer (which is the large scale and leading renewable energy utilities) is to be connected to Eskom / Municipal grid the integrity of their energy production shouldn't be compromised. Such system is a multi-variable complex electrical network with a number of generators, load points, buses, and interconnecting transmission lines. Long, heavily loaded transmission lines that interconnect power systems are susceptible to power swings; subsequently to an event such as a failure or variances in the power system configuration, such oscillations can be generated. Power swing oscillations occur because the system shifts after an incident from one stable point of equilibrium to another stable point of equilibrium.

The system will lose synchronism when the system has unstable oscillations, and when this occurs, we can consider the system to be in an out-of-step state. These phenomena can be plotted with respect to a distance relay characteristic as shown in Figure 1 and as described in more detail in (Tziouvaras & Hou , 2004)

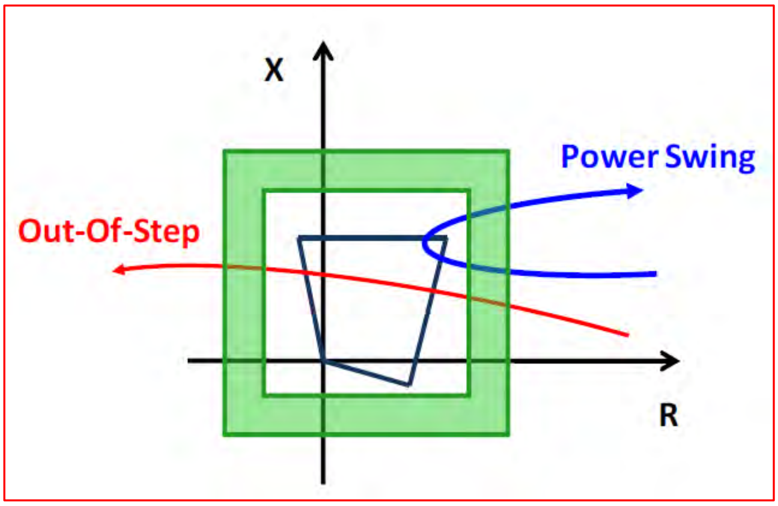

Figure 1.1: Impedance trajectory presented to distance relays during power swings (Tziouvaras,2004).

If measures are not taken to avoid undesirable protection operations during stable power swings, this can result in excessive outages or blackouts.

1.2.1 Power system Stability

Power system stability refers to a power system's ability to recover an appropriate operating state after it has been exposed to usual or abnormal disturbances (Kundur, etal, 1994) this operating state is accomplished if the system voltage and frequency levels remain similar to their minimal values. Analysis of the power system stability is alienated into three categories: voltage stability, angular stability and frequency stability.

- **Voltage stability**: Is the power system's ability to sustain appropriate voltage levels across the grid while the network experiences change in its operating condition; these changes typically occur in the form of load increments. Voltage instability is a complicated phenomenon that usually occurs with inadequate reactive assistance when the system is heavily loaded (Novosel, 2010). Under these conditions voltage begins to drop drastically in parts of the network, giving rise to what is known as voltage collapse.
- **Angular stability**: Refers to the power system property to remain in synchronous operation after a system disturbance has been impacted. These disruptions can be of different nature and magnitude, such as changes in load, three phase faults, tripping of the transmission line, loss of generating units, etc. After a disturbance, angular stability is achieved if all generating units remain synchronized.
- **Frequency stability**: refers to the capability of a power system to sustain steady state frequency after an occurrence of significant disruption between system generation and load.

Grid Code CC6.1 allows the national grid to ensure that the transmission system operates under certain technological, design and operational requirements that specify acceptable variations in frequency & voltage, quality of the waveform and fluctuations in tension. To fulfil this responsibility National Grid must be in a position to track and record these measurements at appropriate locations (National Grid code standard). This standard is governed by the use of DSM solutions (Dynamic System Monitoring), is compulsory for use at certain 400kV, 275kV, 132kV and other lower voltage substations to offer data on a substation and system-wide basis of “System Dynamic behaviour. This enables the post-event review of system events to help determine the cause of particular system incidents and provide a better understanding of the overall actions of the power systems. This knowledge is often used as part of system stability evaluations, allowing network vulnerabilities to be found that feed into transmission strengthening. All electricity utilities are mandated to abide by this standard and failure for utilities to meet the targets comes with a fine which in essence state owned utility running costs will be increased.

1.2.2 Existing Monitoring Systems

Grid conditions are detected by Supervisory Control and Data Acquisition Systems (SCADA) approximately every 5 seconds, which is considered too slow to track complex grid events. They do not normally track main indicators, such as phase angles. SCADA information is not regularly time-synchronized and time-aligned, and this information is not widely transmitted across the grid. In addition, the systems commonly used at substations and grid link points are outdated, running on old technologies that are not sufficient for the changing network. In essence, they all perform similar tasks, but not all feed into the central network, which makes it very difficult to interpret and compare data (Phadke, 1993).

This large number of systems contributes to an unacceptable degree of complexity as well as commissioning and maintenance issues. In essence, the operation of existing monitoring systems operates through the provision of analogue voltage and current data from the secondary side of the instrument transformers. This is then sampled / digitized for processing, all at different resolutions. Various applications are carried out from this point in order to provide information on the current state of the electricity network, but direct comparisons at the measurement point without high-precision time synchronization are not possible.

A complex and wasteful amount of data processing arises from the present configuration of the substation networks, with some of the legacy monitoring data to be obtained manually from dial-up systems such as the public switch telephone network.

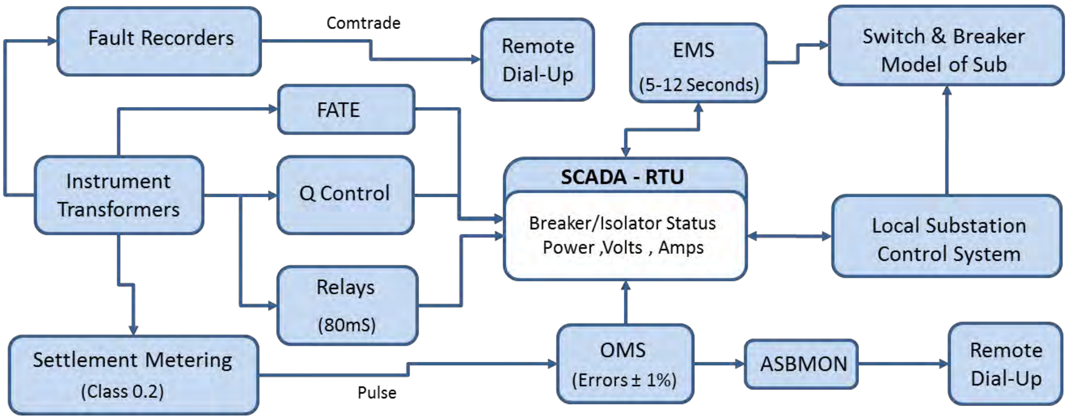

Figure 1.2: substation SCADA systems

1.2.3 Exploitation of Wide Area Monitoring, Protection and Control

The requirements for flexibility and adaptability of future electricity grids to integrate IPPs call for development of Wide-area monitoring, protection and control (WAMPAC) applications. Transmission system management generally requires "Wide-Area" communication architectures and WANs. From the point of view of the power system, the word "Wide-Area Monitoring, Protection, and Control (WAMPAC)" or any number of other words starting with "wide-area" are all used to denote large-scale, global power system management, including the transmission system (John Wiley & Sons, 2014).In addition to conventional SCADA, wide-area measurement systems (WAMS) are being built on many transmission networks. They include measurements of bus voltages and current due to the transmission circuits with the magnitudes and phase angle. This information is transmitted to the Control Centre, calculated over a large area, and is used for the following applications (John Wiley & Sons, 2012):

- Prediction of the state of the power system
- Surveillance and cautioning of the power system
- Event investigation of the power system

Apart from the global explosion of System Integrity Protection Schemes (SIPS) programs, developments such as synchronized measurements provided from the Phasor Measurement Units (PMU), have sufficiently advanced to enable commercial implementation of WAMPAC.

Such technical advancements and changes in the design of power grids mean that introducing specific WAMPAC exertion is equally feasible and warranted, and as such a sensible acquisition is needed (Novosel, et al , 2008).

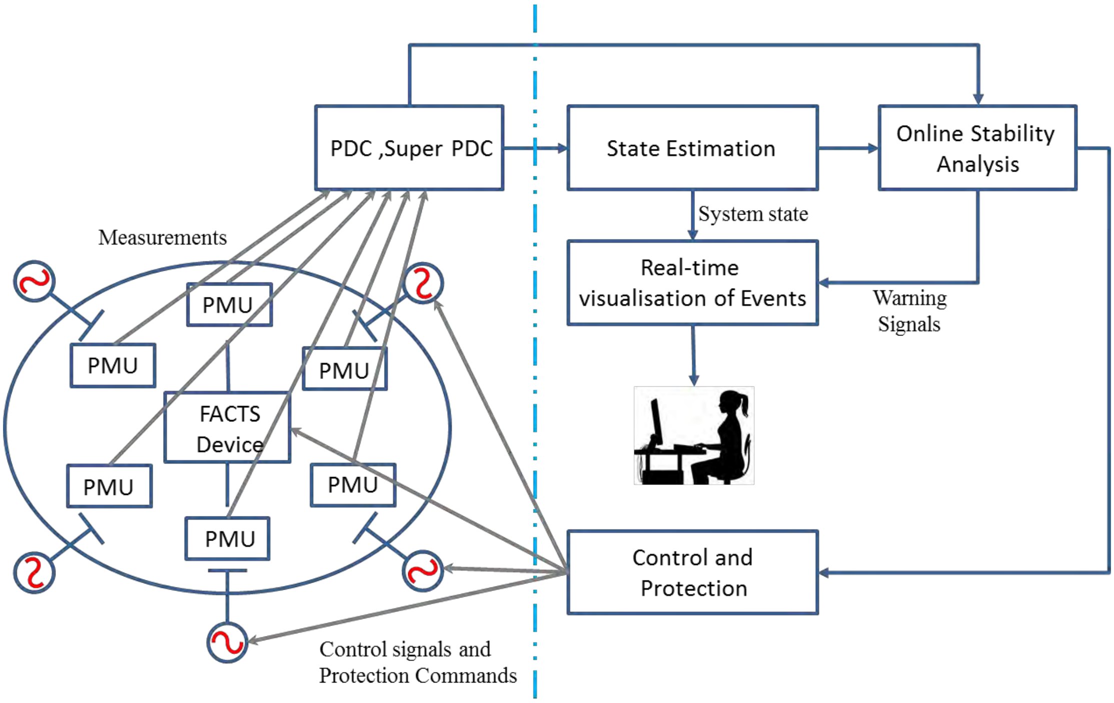

Figure 1.3: Simplified representation of WAMPAC (John Wiley & sons, 2014).

Synchronization of time is an important part of WAMPAC; it is not, however, a modern phenomenon in power systems or a new application. As power systems and telecommunication technologies have progressed, the timeframe over which synchronized information is measured and transmitted has been gradually reduced from seconds to milliseconds and now microseconds. The Phasor Measurement Units are currently in use and are considered to be the most detailed time-synchronized measurement technology for WAMPAC applications available to power engineers and system operators. Advances in computer and microprocessor technologies, and the availability of GPS signals, have enabled this technology.

The security and importance of the synchronized measurement technology, like PMUs, PDCs, is currently being fully realized through the implementation of large-scale projects around the world.

This research will present an application of predictive IEC-61850-90-5 standard based out-of-step protection scheme which is based on real time dynamic stability surveillance, for Utility's Generation system and Transmission system as these two Divisions are the big role players for Eskom's/Municipalities Electricity service delivery. Substation Automation is the new age for protection system thus implementation of synchronized measurement technology will be realized to its full extent through the deployment of a new algorithm for Flexible Alternating Current Transmission system simulated in RTDs to epitomise real world condition. The cost of introducing synchronized measurement technology continues to decline and its efficiency continues to improve as a growing number of integrated substation devices (devices that provide the functionality of relays, meter, fault recorders and other Intelligent Electronic Devices (IEDs) in a single device) begin to offer standard PMU functionality. Subsequent to the development of this new algorithm and once a satisfactory WAMPAC system with scalable structural design has been built; compared to the benefits gained, the incremental cost of adding these acquisitions is low., as the algorithm will be supported by IEC 61850 communication protocol to improve power system state prediction and event analysis.

1.3 Problem Statement

The key cause of the most cascaded blackouts in most countries was found to be lack of system's situational awareness. This conclusion proved the need for more efficient, precise, and dependable equipment to control the power system in real time. The main tool that is used to achieve this functionality in modern energy management systems (EMS) presently is fairly operated to its limits and quite slow to retrieve direct interpretation of the plant status at a particular time as it uses telephone network to dial-up remote sites.

In Eskom particularly system estimations are conducted in a compacted manner based on serial measurements that are composed in the control center where the SE is executed every couple of minutes. Steady-state system models are utilized, while different measurements of Electrical quantities inclusive of voltage and current quantities, active and reactive power flows and injections are made available through supervisory control and data acquisition System (SCADA). Nevertheless, the convolution, the scope and the geographical dimension of the project in degree of modern power systems imposes substantial prejudices in the configuration and system estimation execution.

The implementation and continuous development of phasor measurement installations Units (PMUs) have been opened to provide highly precise coordinated measurements upturn the possibility to monitor the power system more effectively and accurately. System Estimation is one of the main control functions of the power system that can be modernized on the basis of Synchronized measurement equipment and substation automation advances. Prejudices in current state evaluators can be removed using combination PMU measurements with highly precise, three-phase and asymmetric models of power systems, so suggests (Farantatos & Huang, 2011).

By making use of the new technology a new algorithm can be developed by employment of IEC 61850-90-5 standard based for predictive dynamic stability maintaining system as a new solution to these problems. Conventional out-of-step detection techniques are discussed and compared with proposed algorithm. The proposed method is advantageous as it exhibits sensing capabilities for unstable swings faster than conventional methods thus it monitors a wide range of system components.

Problem statement: To investigate the application of IEC61850-90-5 standard for a predictive out-of-step protection scheme response which is based on a real-time dynamic monitoring of the system achieved through implementation of virtual phasor measurement unit in HIL lab bench setup with RTDS for real time simulation and analysis in order to improve the network management, protection and event analysis in power system protection studies.

1.4 RESEARCH AIMS AND OBJECTIVES

The research serves to improve the existing system reliability of Western Grid based on synchrophasor measurements of the predictive out-of-step protection which is realized through real-time dynamic system monitoring. Furthermore, the application will be enhanced by the incorporation of an IEC-61850-90-5 standard for messaging and exploitation of R-GOOSE application to improve the functionality of Wide Area Network Monitoring, Protection and Control and expand this novel application to the Smart Grid protection field.

1.4.1 Objectives

- To conduct a literature review on predictive dynamic stability maintaining system for out-of-step condition and applications of phasor measurement unit (PMU), phasor data concentrator (PDC) units and R-GOOSE applications in WAMPCS.
- To study and understand the predictive dynamic stability maintaining system within in wide area monitoring, protection and control system (WAMPCS).
- To study, understand the engineering configuration of a phasor measurement unit (PMU), phasor data concentrator (PDC -can use SEL RTAC) units for WAMPCS.
- Modelling and simulation of the proposed two-area or multi-area power system network in DigSilent and RSCAD-FX software suite of RTDS.
- Develop a new algorithm for an out-of-step condition with SEL700G generator protection and SEL-421-line protection IED's (both relays have out-of-step protection, the other one uses the functionality as main protection function whilst the other one employs it as the sub protection function to provide back-up protection to system generators)
- To perform the relay engineering configuration setting to predict out-of-step condition.
- To perform the IEC61850-90-5 configuration for out-of-step condition.
- To implement Hardware-in-the-loop simulation using RTDS and test the out-of-step condition occur between the two power systems.

1.5 HYPOTHESIS

The case study to be considered in the thesis is the mesh loop, multi-area areas power system network for Eskom Western Grid geographical area with reference to IEC-61850-part 90-5 standard. A possibility exists for developments of a system protection & control Planning with enhanced State-estimation that comprise of discrete-time control schemes with continuous feedback control systems using PMU measurements. This implementation will permit for innovative automated and integrated intelligent algorithms and enhanced system reliability, such as dynamic setting variations at the mercy of strained system conditions. Developing an algorithm with protection philosophy based on systems requirements, and by conducting protection co-ordination studies. Accurate fault location for transmission lines is of essential significance power systems restorations, decreasing outage time, improving power system dependability and cutting the utility operational costs. The assumption for intelligent islanding & resynchronization is formulated the system control may isolate the transmission system in a governed manner to ensure that, in every island molded, adequate loads can remain linked and are judiciously balanced by the remaining parts of generation in the same portion through the alienated transmission network. The application of the IEC 61850-90-5 standard employs permission digital out-of-step protection to be done in an intelligent, reliable and cost-effective way.

1.6 DELIMITATION OF RESEARCH

The proposed research focuses only on the application of IEC61850-90-5 in predictive dynamic stability system. The research will analyze in detail the network management and state estimation that is used for out-of-step protection at the moment throughout the power system (inclusive of generating and transmission sites) and thereafter develop a new algorithm of a continuous predictive dynamic stability maintaining system. The proposed special protection scheme will be modeled with the use of area subsystem techniques; set up as well a simulated network using DigSilent and RSCAD software suite of RTDS in Centre of Substation Automation and Energy Management Systems lab environment.

1.6.1 Within the scope

- **Wide-Area severity indices**: Various types of measures, features, or indices will be investigated in the research to assess dynamic protection. Many methods proposed use direct measurements taken from the power system, whereas others use measured indices.
- Develop a scheme that uses synchrophasor technology that will take measurements at separate geographic locations and determine from comparing the measurements that an unstable power swing is underway and trip the affected CB of generators off the grid to house-load for re-synchronizing once the grid is stable.

- Analyze real-time synchronized measurements for system’s pre-fault and post-fault states.
- The real-time implementation of the protection scheme will then be done in the Real-Time Automation Controller (RTAC) for exporting those parameters into the database to be used in the RSCAD-FX environment.
- Perform case study for distance algorithm based out-of-step protection
- Employ PMU measurements by implementation of IEC-61850-90-5 standard to improve the system integrity protection

1.6.2 Out of scope

Since the IEDs (SEL-700G and SEL-421) to be used in the research work are built in a scalable, lightweight, and cost-effective package to provide comprehensive protection, integration and control features. For small to large machines the SEL-700 series relays provide basic to complete generator security. The relay offers complete intertie and generator protection. The SEL-700G Relay offers dual feeder protection for a network application of a multi-machine integrated wind generator including overcurrent protection for feeders, transformers, etc. On the other hand, SEL-421 Relay offers single-pole and three-pole tripping and reclosing with synchronism check, circuit breaker monitoring, circuit breaker failure protection, and series-compensated, line protection logic, relay is a high-speed transmission line protective relay. The relay includes high-resolution data collecting and reporting along with thorough metering and data recording.

Only out-of-step protection function will be dealt with in the protection aspect, all metering, monitoring, control and communications functions will be realized in full extent for this research work.

The OOS function is not available on the SEL700G IED due to limited licensing resources, for the lab for practical work, only SEL-421 will be bench tested in the practical aspect of the study.

1.7 Motivation of the Research Project

Study of protection and reliability of the power system requires proper assessment of system conditions and stability during small and severe disturbances. A power network has constant voltage, frequency, and the power angle characteristics for all synchronous generators at a steady state. But the load on a power network is never a constant and so there are always disturbances. In addition, power plants are being run closer to their full loadability due to deregulation of the electrical energy markets. Expansion of transmission networks to meet future demand growth is hindered by environmental constraints. As such, power systems are more susceptible to serious turbulences such as faults and lightning strikes on critical parts of the equipment (Phadke, 2008).

Small disturbances of sustained instability and temporary instability are major threats to the security of the power system, which may result to out-of-step conditions. Most out-of-step protection systems installed in our national grid use local measurements, i.e. voltage and current measurements at one end of the transmission line. The disadvantage of this scheme is its inability to have knowledge of the other parts of the complex power grid. Although the out-of-step tripping system is well designed and properly set, it still has a number of disadvantages in minimizing the effects of the disturbance. Special Protection Schemes are required in this context, which obtain the data from more than one location and process decisions in wide area orientation. More recent technological advances in microprocessor-based relays, combined with GPS receivers for synchronization and accurate time stamping, provide synchronized measurements called synchrophasors (Palizban, 2007).

The necessity for wide-area situational surveillance receives significant attention following the (year) load shedding/ blackouts in South Africa. Reinforced by technological progression as well as funding mechanisms, this motivates for interconnection of Independent Power Producers in the existing grid which is a great aspect to retain system integrity in case the current generating capacity and transmission load is under stressed. However, the deprivation of wide-area conspicuousness would still prevent early identification of the system status, as current SCADA systems perceive grid situations every 4 to 6 seconds, with which is relatively too slow to trace dynamic events on the lattice. Thus, having wide-area situational awareness can prevent the Western Interconnection outages i.e. planned or unplanned outages. As the phasor data Phasor data and applications will give network workforces and designers first-time insight into what is happening on the grid at high resolution, over a wide area in time synchronized mode, and where needed, in real-time.

Despite such swift progress in PMU technology, the use of synchro phasors is largely restricted to offline analysis and real-time monitoring of the system. Restricted access in infrastructure, data quality problems, and data analysis restrictions, unavailability of production grade software tools and slow acceptance of technology are one of a few of the challenges. These demanding complications motivated the decision to investigate application of IEC-61850-90-5 predictive dynamic stability system.

With Load demand increasing every day, power utilities such as Eskom is forced to explore new ways of producing power by adapting interconnection of energy renewables to its existing grid. However, in as much as expanding their Grid they still have an obligation to maintain a secured and stable to customer service points, with this said even if an Independent Power

Producer (which are the large scale and leading renewable energy utilities) is to be connected to Eskom grid the integrity of Eskom's energy production shouldn’t be compromised. Enhancement of the grid stability through IEC 61850 communication standard-based protection would be of great benefit. Synchronizing Generators of the two parties i.e. Eskom and IPPS can be quite complex and needs not to be taken lightly as this would result in major power outages so implementation of such IEC 61850-90-5 standard based predictive dynamic stability system would maintain a smart constant generating grid owing to its fast detection and fault isolation when an out-of-step condition is detected thereby improving key performance system indexes are that put in place to govern Eskom's energy supply and failure for utilities to meet the targets comes with a fine so in essence Eskom's revenue could also be increased.

1.8 ASSUMPTIONS

The Eskom West grid power system network will be used as a generic test system network in this project. Modifications will be done to meet the purpose of achieving the study objectives. The DIgSILENT PowerFactory® software will be utilized for all the necessary simulation functions. To validate the proposed methods, the Real-Time Digital Simulator (RTDS) will be employed for real-time simulation. The laboratory testbed successfully mimics the power system grid network. Most significantly, because the test incorporates the physical protective device interface, it accurately reflects the protection scheme's real-world implementation. The proposed algorithm facilitates relay cooperation in different operating ways and allows rapid fault seclusion compared to traditional protection systems, taking into account various grid situations and fault conditions.

1.9 RESEARCH DESIGN AND METHODOLOGY

In this research thesis project is to assess the rotor angle stability of the Western Cape grid generating units in the presence of a power swing, as well as the effect of this power swing phenomena on the plant in the context of a known event (planned and unplanned contingencies). The research further considers the network expansion subsequent to the fault occurrence in the system. The control scheme based on the IEC 61850-90-5 standard will improve both hardwiring and communication between the pump storage (peak station) and the control center. The new algorithm is tested on the 7-bus system which is a portion of Western grid transmission network with two IPP’s, Electra (Wind) and integrated at distribution level. Case studies considering the renewable units connected to the Eskom grid will be evaluated for various power swing locations. Real-time phasor measurements from the Phasor Measurement Unit (PMU) software models and PMU hardware synchronized to the Common Time Reference (GPS) will be streamed for dynamic state estimation. In order to test the performance of the proposed scheme, the Eskom Western grid network is modified to a 7-bus as seen in Figure 1.4:

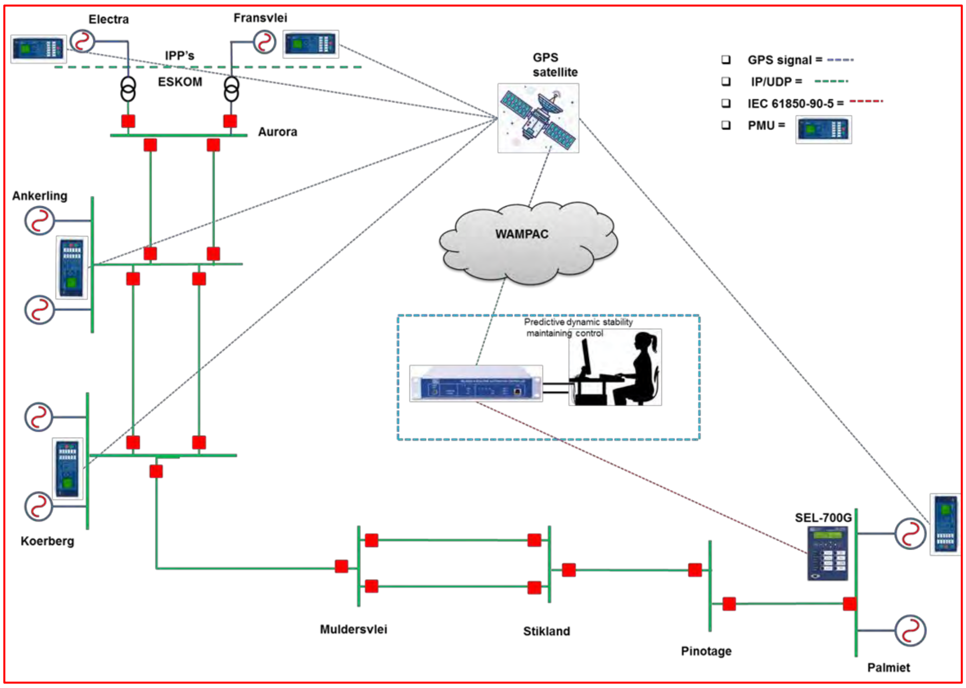

Figure 1.4: Network diagram for the modified Predictive system

The Western Cape transmission network is shown is a network reference, with all the generation sources in the province up to Mpumalanga generation pool. However, the original version of this network system imposed some constraints for the proposed algorithm for the following reasons:

- The scope of the research is only limited to Western grid geographical area so taking full context of it will require network parameters of Source ties between the two provinces.
- There are too many IPP's connected to the Western grid therefore the network visibility will be limited when the research work model is simulated on software.
- The power flow will be non-directional and the phasor quantities from Mpumalanga generation won't be easily accessible for the study.

The communication criteria for the system under test may be summarized as in the following table.

Table 1.1: Acting devices in the algorithm execution.

Name	Description of Role
PMU	Calculates synchrophasors
IED	Receives PMU info, predicts dynamic stability & control of power systems and send protection commands to relevant bays.

The available technology allows us to achieve the aforementioned goals. The study's goal is accomplished using research methods such as a literature review, theoretical framework, modelling and simulations, and documentation.

1.9.1 Literature review

There are numerous rotor angle detection systems already in use, and this thesis focuses on establishing a viable predictive scheme to be used in dynamic system. This is because the traditional schemes employed in generation system can no longer provide adequate state estimation. The knowledge gained through reading related books, journals, conference papers and the internet create a path to the desired objectives.

1.9.2 Methods of protection and monitoring

Because of the complexity of the system integrated with IPP’s, monitoring and protection functions must be considered. To carry out these functions, various protection methods and their aspects must be thoroughly examined and comprehended. These protection solutions employ one or more protective devices. The protection plan used is determined by the voltage level of the system as well as the type of equipment to be safeguarded. Distance protection is more suitable for the transmission system than all other protection schemes for OSS tripping function, and it is performed by using a distance (impedance) protection relay. The literature now available states that distance protection relays are frequently employed as the primary or backup for line protection for the following reasons: they increase the protection scheme's overall reliability index, and they can manage high fault resistance (Joós & Pradhan , 2007).

This dissertation looks at the point of pump storage power plant which is often called upon a grid during peak hours, therefore loss of synchronism protection is crucial at this node. This will be monitored using a generator protection device which encompasses a mho impedance based out-of-step protection. Another distance relay will be optimally placed in the outgoing transmission line of the power station to provide back-up protection to the generator OOS relaying when called upon to do so, it also incorporates a mho distance element for this functionality.

With the IEC-61850-90-5 standard the system situational awareness is made easy as part of a protective scheme that addresses all SAS-compliant protection features. The IEC 61850-90-5 standard employs PMU's which are optimally placed in various generating units and the available communication channels are supported by the intelligence of these devices. The communication standard contributes to improving system monitoring capabilities. The subsequent chapters contain further in-depth information about the approaches taken in developing the protection schemes.

1.9.3 Simulations

An algorithm of protection function technique for generator rotor angle instability is developed using simulation software and put into practice on a modified Eskom West grid network. The DIgSILENT PowerFactory® simulation platform is used to model the modified network. The real-time digital simulation (RTDS) platform is used to validate the proposed protection scheme's working principles. Utilizing this platform is intended to allow for real-time evaluation of the designed scheme's performance. The phasor measurement unit available in RSCAD-FX software is used to release the IEC-61850-90-5 communication standard for the logic of the protection scheme configured using ArcSELarator quickset settings confirmation settings. The simulation results of the OOS protection scheme are examined for out of step blocking and out of tripping of the SEL-421 relay, using the COMTRADE fault events files within the RSCAD-FX runtime environment and the signals from the actual IED.

1.9.4 Data collection

The Eskom utility grid is used as a case study in this dissertation. Data for test system is given from Table 5.1 to Table 5.5 in chapter 5 of this thesis. For further protection scheme development using a different simulation environment, the parameters and results of the DIgSILENT-developed protection scheme are gathered. These various simulation platforms' functionalities of the OOS protection schemes are being contrasted. Comparing the established control across many platforms will require an accurate evaluation of the behavior of the proposed scheme for successful and efficient real-time implementation.

1.10 THESIS CHAPTERS

The research thesis is divided into 9 chapters and appendices as described in the following subheading topics:

1.10.1 Chapter 1

This chapter discusses the background of the research, the purpose, the objectives, the awareness of the problem, the motivation for the research, the problem statement, the hypothesis, the delineation of the research, the project assumptions, the research design and methodology, the thesis chapter breakdown, and the overall conclusion drawn from the research work.

1.10.2 Chapter 2

This section outlines the existing methods available in literature for power system state estimation, the current state-of-the-art protection technology used, its estimation and its biases and limitations are covered in this chapter. Furthermore, a study of literature on real-time transient stability assessment methodologies to monitor rotor angle stability of a generator are extensively discussed. The benefits of IEC-61850-90-5 application to advance the OOS schemes are also well studied. Several articles on advanced predictive dynamic stability maintaining system were evaluated.

1.10.3 Chapter 3

In this chapter, a detailed theory for synchronous generators and transmission lines effect on power system stability. The approaches used to assure rotor angle stability in conventional power system grids during stable and unstable power swings are also specified.

1.10.4 Chapter 4

This chapter discusses the protection relaying principles of synchronous generators with which detailed settings calculation for proposed OOS logics for the 2 optimally placed IED's (SEL700G and SEL-421) are configured , each presenting a distinct algorithm from the other. Other available protection functions for a generator are also discussed briefly for the sake of completeness of generator protection theory so that several interesting aspects may be explored further for future work.

1.10.5 Chapter 5

This chapter describes system modelling of the modified Eskom test system network I DigSilent PowerFactory®. To validate the settings calculated in chapter 4, time-domain simulation is performed taking into account the rotor angle stability of the 2 parallel synchronous generators at palmiet pump storage taking into consideration the whole detailed model of Eskom west Grid. Quasi-Dynamic simulation studies are also taken into contrast for better system situational awareness and system planning studies. Critical clearing time for protection aspect is also obtained through simulation scan studies within the DigSilent software.

1.10.6 Chapter 6

This chapter discusses the modelling of the test system in RSACAD-FX interface to perform studies for stable load flow convergence on offline mode of RDTS non-real time simulation and design of synchronous generator control variables.

1.10.7 Chapter 7

This chapter outlines the Hardware-in-the loop hardwired approach for the system under study to assess the accuracy of settings and the real physical protection relay's (SEL-421) detection and isolation of unstable power fluctuations. The OMICRON CMC356 is utilized in a secondary current injection technique to supply the proper low power voltage and current signals to the physical relay, which is set and monitored by the AcSELerator Quickset software.

1.10.8 Chapter 8

The chapter outlines the implementation of IEC-61850-90-5 for a predictive dynamic stability system by realization of software PMU placed on RTDS HIL testing. The CMC356 receives data from a phasor measurement unit (PMU) installed in the Eskom west grid system on RSCAD draft. Data sampling & phasor estimation will be performed from PMU by sampling voltage and currents then estimate synchrophasor values that are sent and received by the IED, with which the IED then IED decides that a portion of system is to be separated if a pole slip is detected on one of the Palmiet pump storage generating units in order to avoid an out-of-step occurring in the system.

1.10.9 Chapter 9

In this chapter based on the results a conclusion is drawn and recommendations are offered. Further work to improve on these new developments is also suggested along with the novelty of this thesis work towards electrical power utilities.

Appendices

Figures absent from the body of the thesis documents, modeling parameters, and some results are significant attachments offered under appendices section.

1.11 CONCLUSION

This chapter presented a generic overview of the importance of IEC-61850-90-5 out-of-step phenomena in the power system electrical protection aspect. It also concentrated on the thesis objectives and layout, which would be employed to accomplish the study objectives. The thesis research questions, problem statement and research methodology are outlined here.

2 CHAPTER TWO

LITERATURE REVIEW

2.1 INTRODUCTION

When power systems are running under pseudo-steady-state conditions, all electrical variables are within operational bounds and power systems normally operate near to their nominal frequency (Acosta, etal, 2021). The safe and efficient operation of the electrical power system, however, may be compromised by some operating conditions that push the electromechanical variables beyond of permitted bounds (Chamorro, et al, 2021). The power system is unable to attain a new operating equilibrium point when it is subject to a significant disturbance. This is seen as an unstable circumstance (Kundur, et al, 2014). Electrical power is subject to rapid variations due to power system breakdowns, line switching, generator disconnection, and the loss or application of huge blocks of load, whereas mechanical power input to generators is generally continuous .The oscillations in synchronous machine rotor angles caused by these system disturbances can lead to significant swings in power flow (Sanchez, et al, 2018). The system may remain stable and revert to a new equilibrium state, experiencing what is known as a stable power swing, depending on the degree of the disturbance and the actions of the power system controls.

The electrical output power of a generator is greatly decreased by a close-in transmission failure. The generator rotor accelerates in relation to the system due to the resulting differential between the electrical power and mechanical turbine power, increasing the generator rotor angle. If the generator rotor angle has increased by the time the fault is fixed, the electrical power is then restored to a level that corresponds to that value. By essentially removing one or more transmission components from service, clearing the fault weakens the transmission system, if not permanently. When the defect is fixed, the generator's output of electrical power surpasses that of the turbine. As a result, the unit slows down, which lessens the momentum the rotor had built up due to the malfunction (Basler & Schaefer, 2008). The generator will be momentarily steady on the initial swing and will move back toward its operational position if there is enough retarding torque after the fault clearing to compensate for the acceleration during the fault. The power angle will increase if the retarding torque is insufficient until synchronism with the power system is lost. The amount of time it takes for a transmission system fault to clear affects the stability of the power supply (Alhejaj & Gonzalez-Longatt, 2016). A faster fault-clearing time ensures that the rotor stops accelerating much more quickly and that there is enough synchronizing torque to recover with a significant safety margin. Thus, protection engineers must make sure that transmission systems are equipped with fast acting protection.

This section provides the background information of currently existing technologies related to the research along with a literature review of the research efforts on these topics. In particular, the first part summarizes the current state-of-the-art protection technology used, its estimation and its biases and limitations will be dealt with. Different kinds of traditional out-of-step schemes are presented then a brief comparison will provide summary on the present state-of-the-art protection schemes of an out-step protection on generation segments and that of transmission system application, this information is given as background information content since the current existing schemes are contrasted with new developed proposed scheme which protects the interconnected power system.

Furthermore, a study of literature on real-time transient stability assessment methodologies which were proposed and developed previously will be done. The conditions for a robust and effective online transient stability monitoring tool are discussed along with the advantages of integrating IEC 61850-90-5 standard. Lastly there is a short overview to PMUs to illustrate the characteristics of its technology, and how it can be utilized to create advanced predictive dynamic stability maintaining system, such as the one proposed.

2.2 AN OVERVIEW OF POWER SYSTEM STABILITY

Synchronous generators are the main source of electrical energy production and are essential to the stability of the traditional linked power system. The synchronous generators are designed to enable electromechanical coupling of their rotors, causing them to rotate simultaneously under typical working conditions. The generator's shaft rotates at a frequency of 50Hz when everything is coordinated and stable (Johnson et al., 2017). The classification of power system stability brought about a critical understanding of the system's instability and the impact of its perturbations. Classification can also be used to analyze and identify important elements influencing stability as well as strategies to be applied to increase stability (Kundur et al., 2004).

The rotor angle, frequency, and voltage are three variables that affect the behavior of the power system. These three components of the power system grid are primarily caused by either a fault event or a shift in load demand. While frequency and voltage can have either a short-term or long-term basis, the duration of the disturbance caused by rotor angle can have a short-term base (3 to 5 seconds after the disturbance, and it can be 10 to 20 seconds for enormous systems). The classification of the stability of the power system is shown in Figure 2.1 below. The factors that can cause power system instability and the magnitude of the disturbance are also displayed with which the effects of rotor angle stability group are further explained as it is the main focus of this study. This classification will be extremely helpful for computation strategies and stability predicting (Kundur et al., 2004).

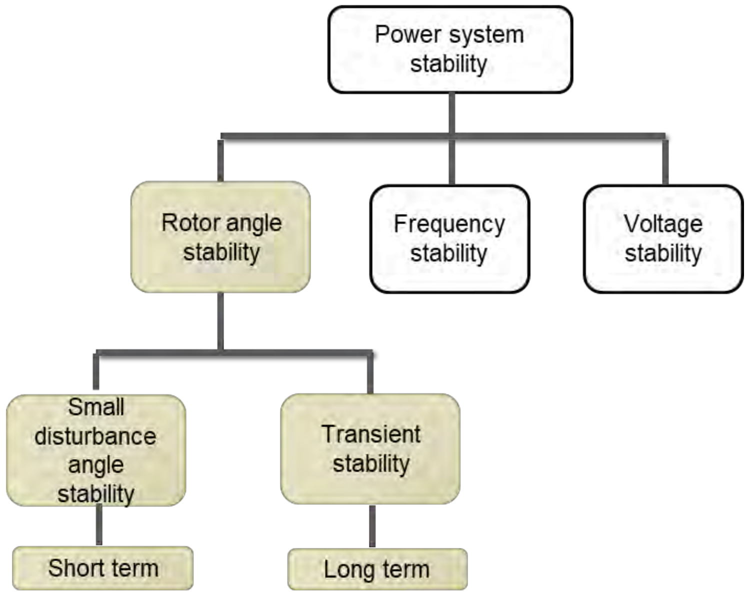

Figure 2.1: Classification of Power system stability (Kundur, etal, 2004)

2.2.1 Rotor Angle stability

A number of studies have examined the rotor angle stability to be the ability to maintain the synchronism of interconnected generators both the mechanical torque and the electromagnetic torque of these generators are kept constant. To support this claims authors (Sallam & Malik, 2015) suggests that the synchronous generator's prime mover (turbine) turns the rotor using mechanical force. The electrical torque opposes the direction of rotation, whereas the mechanical torque will be in that direction. Due to the excitation system response in the fault, the electrical output power varies more quickly than its mechanical counterpart. The rotor speed will fluctuate due to an imbalance in the applied torques (mechanical and electrical), which will affect the relationship between the rotor's magnetomotive force and the resultant rotor and stator magnetic fields. It is anticipated that the electricity system would be able to endure such disruptive occurrences and resume normal functioning.

One of the three key factors influencing the stability of a power system is rotor angle stability. Small-signal stability and transient stability are additional categories for rotor angle stability, and these disturbances occur for brief periods of time, this idea is also evident in the famous works of (Kundur, etal., 2004).

2.2.1.1 Transient stability

The capacity of the power system to resume normal operation after experiencing a major disturbance for a brief period is known as transient stability. Transmission line faults may be to blame for this. By dividing this form of electrical torque disturbance into two parts—the synchronizing torque and the damping torque—it can be resolved. Any alterations to the system can be regulated by the exciter system. The exciter must supply greater magnetic flux if the torque is insufficient to counteract variations in rotor angle. The exciter system should quickly deliver a stronger positive voltage to the generator field if the mechanical torque exceeds the electrical torque. On the other hand, the exciter should supply a stronger negative voltage to the field generator and inhibit any changes that would cause instability when the electrical torque is greater than the mechanical torque (Sallam & Malik, 2015).

Figure 2.2 shows how the grid-connected generator is anticipated to perform at point O, where P_m (mechanical power) typically equals P_e (electrical power). In the event of a grid disturbance, the generator's electrical output power will drop to zero, shifting the rotor angle or power angle from δ_0 to δ_1 in the area where the disturbance is resolved. According to the power angle curve post-fault, the electrical output power is restored to its usual level at point one. The protective system may have isolated the malfunctioning portion of the system because the new curve is lower than the one before the breakdown. The exciter system will suppress the difference in both powers at point 3, where the electrical power is greater than the mechanical power and causes a decline in rotor motion. The generator will subsequently return to the area where it normally operates. This will only be accurate if the exciter system can react promptly to changes in the system (Sallam & Malik, 2015).

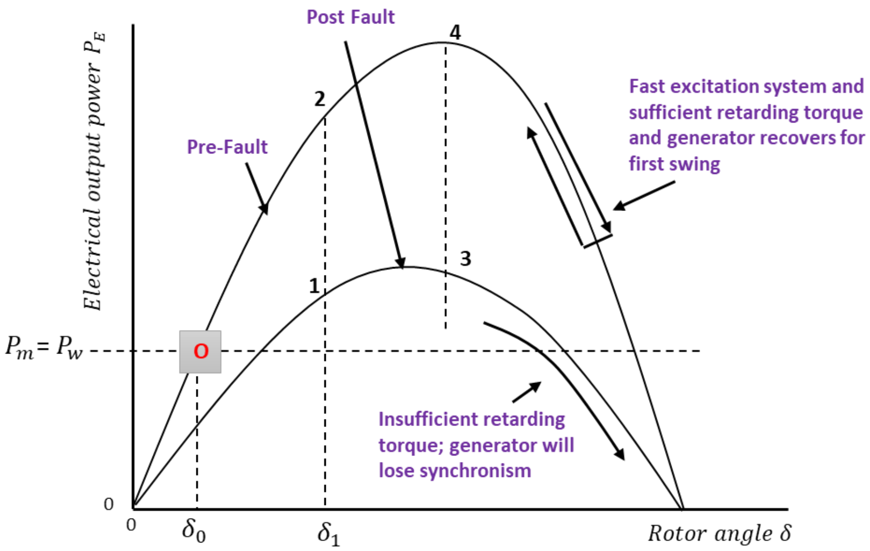

Figure 2.2: Rotor angle transient stability analysis (Sallam & Malik, 2015)

2.2.1.2 Small signal transient stability

The ability of the electricity grid to continue operating in a stable state after being impacted by a minor disturbance is known as small-signal stability, also known as small-disturbance stability. This form of disturbance is so minor that its impact on the power system can be examined using a classical generator linear system (Gu et al., 2019).

Consider Figure 2.3 below, where the power angle is 0 and the mechanical power is equal to the electrical output power at O. The electrical output power Pe1 at point 1 will decrease in the case of a little disruption, which will cause the rotor to accelerate further in an effort to shift point O back. The mechanical power Pm will in this case be greater than the electrical output power. Electrical power is more than electrical output power at point 2. As a result, the rotor will slow down and return to operating point O. Due to damping oscillation, the power system becomes steady once more (Sallam & Malik, 2015).

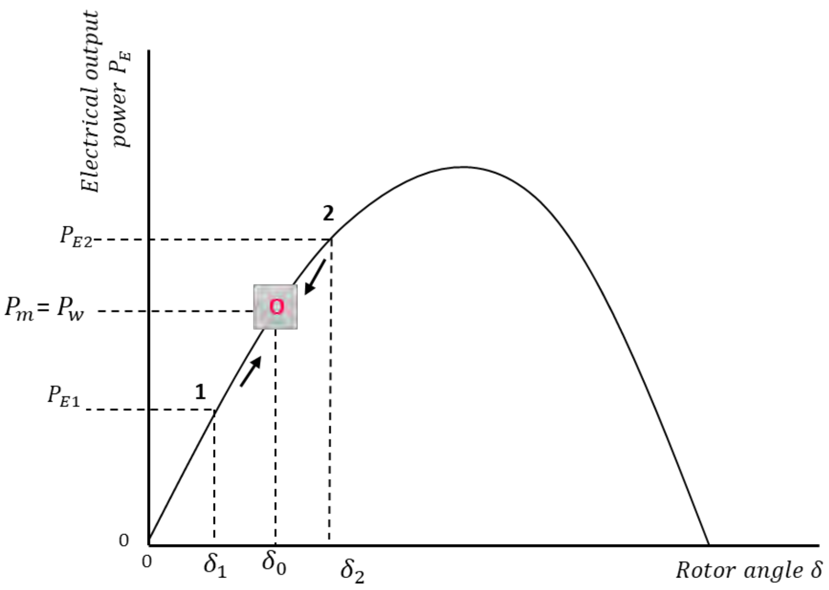

Figure 2.3: Oscillation curve of rotor angle during small signal stability (Sallam & Malik, 2015)

2.2.2 Voltage stability

The ability of the power system to keep the voltage levels at all buses within acceptable ranges after the power system was perturbed is known as voltage stability. This will aid in avoiding power outages or the collapse of the power system grid (Johnson, et al., 2017).

Much of the early work of (Kundur, 1994) centres around the study of voltage instability which is caused by system fault disruption, increase in load and operational contingencies. There will be a voltage drop when the electricity passes via inductive reactive in a transmission system. Voltage instability may happen if reactive power is not appropriately maintained. While one of the buses' voltage magnitudes reduces when reactive power increases, a system is deemed unstable. When the sensitivity of the voltage and reactive power is negative, the system is unstable; when it is positive, the system is stable. This implies that the voltage of the buses must likewise rise (positive sensitivity). When the rotor angle moves beyond 180 degrees and the generators lose synchronism with one another, voltage instability may result

The receiving end power increases and decreases before it reaches saturation when the load demand is increased by decreasing Z_{LD}, as shown in Figure 2.4 below. As a result, the greatest amount of power is transferred at this time, and the power factor is at unity (cosØ=1). Additionally, as the voltage drops, the current rises. This occurs during normal operation, that is, before the line impedance and load impedance are equal. It should be observed that the current is growing rapidly relative to the rate of voltage drop before the line impedance equals the load impedance. As a result, power transfer increases at the receiving end. The voltage reduction is greater than the current increase, which causes the load power to decrease as the load impedance decreases more and approaches the line impedance (Kundur, 1994).

The author further points out that the system will decide to regulate voltage and utilize all available apparatuses, such as an automatic underload tap changer in the event a transformer is used to raise the load impedance to be greater than the line impedance in order to preserve the voltage, once the voltage and current reach the critical operation point where the line impedance is equal to the load impedance. The system will be unstable owing to voltage if the voltage at the buses is lower than the acceptable level (Kundur, 1994).

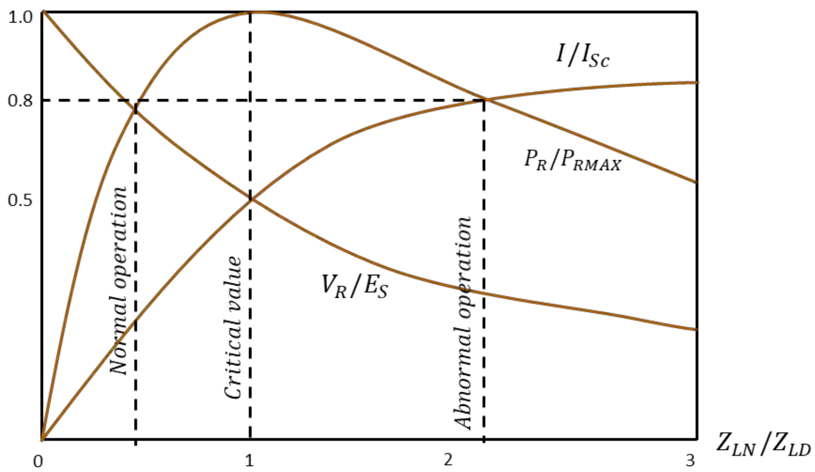

Figure 2.4: Relationship between power, voltage and current at the receiving end (Kundur, 1994)

Voltage stability can be caused by minor or major disturbances. They must be addressed independently in order to gain a better understanding of the analysis. This implies that the impact of minor disturbances must be investigated independently from the impact of significant system disturbances. Voltage stability in the conventional system can be increased by utilizing tap changing transformers, which alter the transformer, booster transformer, series and shunt capacitors, and synchronous phase modifiers. Due to the direct relationship between voltage and frequency, modifications to system bus voltages also had an impact on the system's frequency stability point.

2.2.3 Frequency stability

In his recent work (Kundur, et al, 2004) discovered that the ability of a power system to maintain constant frequency in the case of a system upset that causes a power imbalance between load and generation is known as frequency stability. Without interrupting the power supply, the power system should maintain or restore an equal power balance between the generation and the load. A sustained frequency fluctuation that trips loads or generating units is the cause of the instability. Increased load demand, a lack of synchronism between the generation units, and transmission line problems can all cause these frequency changes. When there are insufficient control and protection measures, equipment failure to adapt to system changes might have an influence on frequency stability.

Due to the dynamic behavior of the power system during disturbances, frequency stability can further be divided into three types: short-term or transient, mid-term, and long-term frequency stability. The recovery of the system from a disruption within a short window of time (10 seconds at most) is referred to as short-term frequency stability. The system's restoration time of a few seconds to a few minutes indicates mid-term stability (typically, about 10 seconds to less than 10 minutes). After being subjected to a major disturbance, the long-term stability takes up to 10 minutes for the system to return to its usual operational condition. Mid-term and long-term stability analyses, however, are typically viewed as one element because they involve the same factors as studies on power system stability (Kundur, 1994).

2.3 OVERVIEW OF POWER SYSTEM PROTECTION

A power system protection system is an auxiliary system which identifies the power system faults and isolates the failed equipment as early as possible so that the remaining power system stays intact. A typical protection system consists of current and voltage transformers, protective relays, circuit breakers, wiring or control schematics, a communication system and a coordination methodology with other relays, fuses and active controls. Protective relay is a piece of equipment whose function is to detect abnormal system conditions or defective devices and to initiate a proper control response. Popular control reactions are trip commands to the circuit breaker, warning signals to the power system operator and, in some situations, the closing of the circuit breaker.

Study of the protection and reliability of power systems needs careful evaluation of system conditions and stability in case of minor and severe disruptions. At steady state, a power system has features of constant voltage, frequency and the power angle for all the synchronous generators. However, the load on the power system is never constant hence the perturbations are always present. Moreover, owing to deregulation of electrical energy markets, power networks are being run closer to their full loadability. Expansion of transmission networks to cater for future load demand suffers limitations due to the environmental constraints. As a result, power systems are more exposed to severe turbulences like faults and lightning strokes on critical pieces of apparatus. This can be counter acted by performing studies of power system operating conditions (Shaik, 2017).

The operating conditions of the system can be divided into five different states, mainly for the purpose of evaluating power system security and designing suitable control and protection schemes. To be precise they are categorized in the following:

- Normal state
- Emergency state
- Warning state
- In extremis state
- Restorative state

These five functional states along with potential state transitions are represented in Figure 7

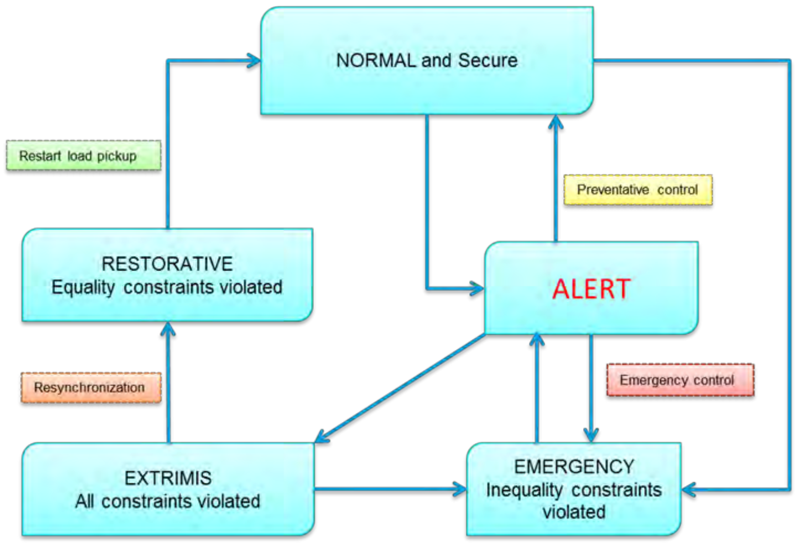

Figure 2.5: Power system state change over diagram

- **Normal and secure state**: In this state, all device variables are within the usual range, without complete equipment. With differences in equality and inequality being met, the system is in a stable state. Equal constraints apply to the equilibrium between produced power and load demand, whereas the limitations of inequalities, such as currents, voltage and frequency, set the limits of certain system variables. In safe situations, without violating any equality and inequality restrictions, the device is able to withstand a single contingency.
- **Alert state**: If the system's safety level falls below some predefined threshold, the system then enters a warning state called 'insecure.' The variables within the system are still within limits. System operators must be alert and maintain continuous monitoring of the limits of equality and inequalities. Nevertheless, in the event of any

crisis, the lack of reserve margins could lead to a breach of certain inequality constraints, leading to a transition from the alert to an emergency state. In that instance, some machinery can operate above their rated capabilities. If the severity of the disruption is very high, the system will directly change its state to in extremis state from alert state.

- **Emergency state**: The system enters the emergency state if protective controls malfunction or if there is a major disturbance. The transition may occur either from a normal state or from an alert state to that state. In emergency situations, the voltage levels of the different buses fall below the stability limits, and the system components are overloaded, thus breaching the limitations of inequality. By initiating successful control strategies such as fault clearing, fast valving, re-routing of power excitation control, generation tripping, and load shedding, the system can be restored to warning status.
- **Extremist state**: If the emergency management mechanisms fail while the system is in a state of emergency, the system will enter an in-extreme state. The scheme is beginning to break down into parts or islands. Some of these islands may still have adequate generation to satisfy the load, but the system equipment is overloaded, and the balance of active power is also disrupted. Overloaded generators are beginning to cause cascade outages and potential 'blackout. To save as much system as possible from a wide range of blackouts, regulated actions such as shedding load and well-ordered system operation are required.
- **Restorative state**: This state means that control measures that aim to restore the dignity of the power system are being enforced. The system can transit back alert state or directly to normal state, subject to the present operating conditions. The control activities can be performed either by the operators or automatically from the central energy control centre.

According to (Huang, 2015), the major source of the cascaded blackouts in olden times was known to be absence of system's situational awareness which motivated a necessity for Linear State Estimation as the fundamental function of Energy Management System (EMS) on which all other optimization, regulation, and security functions are based. To track the power systems accurately, a lot of the network's electrical quantities should be measured. This requires a considerable amount of expenditure which is not economically effective and control systems would be vulnerable to errors or failures while measuring. Consequently, various state estimation approaches have been suggested in the past to assess the optimum estimate of the system states, including unmeasured parameters based on system models and other network measurements.

2.3.1 The Energy Management System evolution

In the high voltage transmission network, an energy management system (EMS) tracks and controls the network flows. Hardwired analogue systems with meters and switches were used at early control centers. Thumbwheels have been used to modify field operating setpoints. With the advent of digital computers, modern-day EMS functions were initially developed in the 1970's. Computer rapid processing capabilities were utilized to solve broad and complex mathematical problems efficiently. Such EMS roles have continuously developed in the last several decades (Giri et al, 2012). Most traditional state estimators considered the steady state system model whose measurements were available via SCADA system. The measurements are sent to the centralized control centre via local remote terminal units (RTUs), which monitor and control the system as a whole.

Power system state estimation requires a variety of quantities to assess the state of the system. The measurement data used by state estimator is a subset of "real-time" data collected from SCADA system that includes voltage magnitudes, current magnitudes, power flow values and power injections. State estimator also includes a "static" database containing information about circuit breaker connection and the bus segment that is often stored in the control centre (Vallapu, 2015). EMS technologies have evolved according to the following market and organizational goals:

- Real-time monitoring of network conditions.
- Optimizing grid operating conditions.
- Maintaining system frequency.
- Performing what-if studies.
- Assessing grid stability.

The SCADA measurements are usually sent to the EMS every two to 10 seconds (Giri, et al, 2012). This was deemed appropriate because EMS was designed primarily to monitor normal and alert states. The need of electrical utilities to enhance their service and the need to accommodate new technologies in a smart grid with smart sensor penetration and distributed generation (DG) result in the system estimation's need for much higher time resolution and precise time synchronization to address emerging monitoring , control and security needs that cannot be met by the traditional SCADA. While the current approach to EMS applications have evolved in a piecemeal manner over the past few decades, where the various implementations operate independently using their own models and formats. Although these tools have been enhanced, the implementations are still based on decades-old core technology and software architectures, built separately for their own particular purposes, mostly with legacy code implementing old algorithms, and optimized for sequential hardware computing.

Most current applications have closely coupled and non-separable modules of their various components. The internal code is very old and sometimes not standardized. Furthermore, external data interfaces are unfavourable, the user interface is poor, and generally there is no centralized engine to house the numerical methods used in the application. It's very tedious to upgrade or expand such applications. It's often easier to completely create new software. It is highly difficult if not impossible to achieve interoperability for such applications.

According to (Vallapu, 2015) it can be summarized that in its current state the power system estimation is not proficient of picking up the dynamic behavior of the system. As it can only provide information about control in the context of a series of stable states. This also restricts the wide area governor actions on the system to be very slow since it is usually performed manually by network operators. These applications can comprise, for example, generation dispatch amid units, redirection of power flow, profile controls of reactive power and voltage, static security calculation and control, load conjecturing. In general, fast automatic control during faults and transients is provided only locally on a component basis and therefore does not take into account the wide area system behavior.

2.3.2 Need for Dynamic state prediction

While tracing is a stress-free / smooth way to track variations of the power network, it does not encompass unequivocal physical moulding of the system's time behavior (Rampelli, et al, 2017). 'Dynamic State Estimation' has been developed to avoid this. The physical moulding of the dynamic essence of the system will be applied. This implies that with the aid of the instantaneous state vector and the physical characteristic of the system, the Dynamic System Estimation envisages the instantaneous state of the power network. Thus, anticipating has a lot of advantages when carrying out security studies and the operator will have sufficient time to conduct control action. Dynamic state estimation typically expands the principle of static state estimation by means of the power network’s vigorous states, such as speed and/or acceleration of the generator. Dynamic System Estimation forecasts the state vector for the following time instant with the aid of the current state along with acquaintance of the network’s physical model. The benefits of this extra prediction step are listed below:

- Security scrutiny may be carried out in advance, giving the system operator extra time to execute control action in the event of an emergency.
- It assists in classifying and discarding bad data.
- To avoid hostile conditioning by substituting quasi measurements with high quality values.
- Irregularities like Topological errors, variations in the system can be identified.

The Dynamic State Estimator is normally carried out in a distributed state manner (Farantatos et al, 2011), at the stage of substations. Local (substation) variables are used to predict the conditions of the substation, but also the conditions of the busses at the other edges of the lines / circuits linking the substation of interest to the neighbouring substations. Dynamic state estimation dependent on substations utilizes information from relays, PMUs, meters, FDRs, etc. only in substations, thereby eliminating all disputes related to data propagation and associated time latencies. It operates at rates comparable to those indicated by the C37.118 synchrophasor standard.

However, dynamic system estimation was not widely spread, let alone applied, since without the phasor measuring units with GPS synchronization, implementation of these principles could not be feasible. Most related publications are based on simplified dynamic models of power systems; they use Kalman filter algorithms for the estimation procedure (Zhenyu, et al, 2007), and are virtually unsuitable for large-scale and real-time implementation. Research study attempts have also been made on dynamic system estimation using computational intelligence methods such as artificial neural networks (Sinha and Mondal, 1999).

2.3.3 PMU-Based Dynamic State Estimation

The Phasor Measurement Unit (PMU) (Meliopoulos, et al, 2005) is a promising technology that can revolutionize state estimation. PMUs provide synchronized measurements where synchronization is achieved by means of a GPS (Global Positioning System) clock providing a synchronizing signal with a potential accuracy of 1 µsec. This time accuracy is translated into 0.02 degrees U.S. power frequency (60 Hz) accuracy. The technology therefore provides a means of measuring phase angles with a precision of 0.02 degrees. This means that quantities taken, or phasors computed by time reference, at one location are globally valid. This form of synchronized calculation removes problems stemming from the broad geographic separation of power system components. The technology's initial use is defined in (Meliopoulos, Zhang, et al, 1994). When added in addition to the fundamental estimator, the harmonic state estimator is only a linear state estimator as defined in (Meliopoulos, Zhang, et al, 1994). The system was put into service between 1993 and 1998.

Several publications (Chakrabarti et al, 2009) have discussed the advantages of incorporating synchronized measurements into an established nonlinear estimator. In addition, state estimators, which use only PMU measurements and thus turn out to be linear estimators, have also been proposed (Yang et al 2011). Another benefit is that the implementation of PMUs has allowed both the magnitude and phase of electrical quantities to be determined locally and the state estimation procedure to be distributed. The PMU technology therefore opens up the possibility of developing distributed state estimation approaches which have been an important research subject in recent years (Van Cutsem and Ribbens-Pavella, 1983). This is the basic idea for the definition of Super calibrator (Ebrahimian and Baldick, 200). The technology is established on a robust hybrid state estimation formulation. This is a bit of a combination of the conventional formulation of state estimation and the GPS-synchronized formulation of measurement using an expanded collection of accessible data. The basic idea is to provide pattern-based error correction from all known sources of error.

In order to expand and strengthen renewable integration studies, variable renewable generation patterns (wind , solar and others) and their correlations with conventional generation systems can be analyzed, subject to the availability of resource data synchronized with other PMU data and a large set of historically measured data (Palizban, 2007). For example, renewable resource variability can be quantified using measured historical data that can be used in renewable IPP impact studies for the selection of worst-case, spatial / temporal circumstances. Furthermore, utilizing data based on PMUs, different distributed resources based on renewables can be better tracked, handled and regulated conceptually. Although PMU-based online applications can benefit from organizational aspects, the design process should take advantage of the availability of PMU data during the planning phase. This is integration process is shown in Figure 2.6 below.

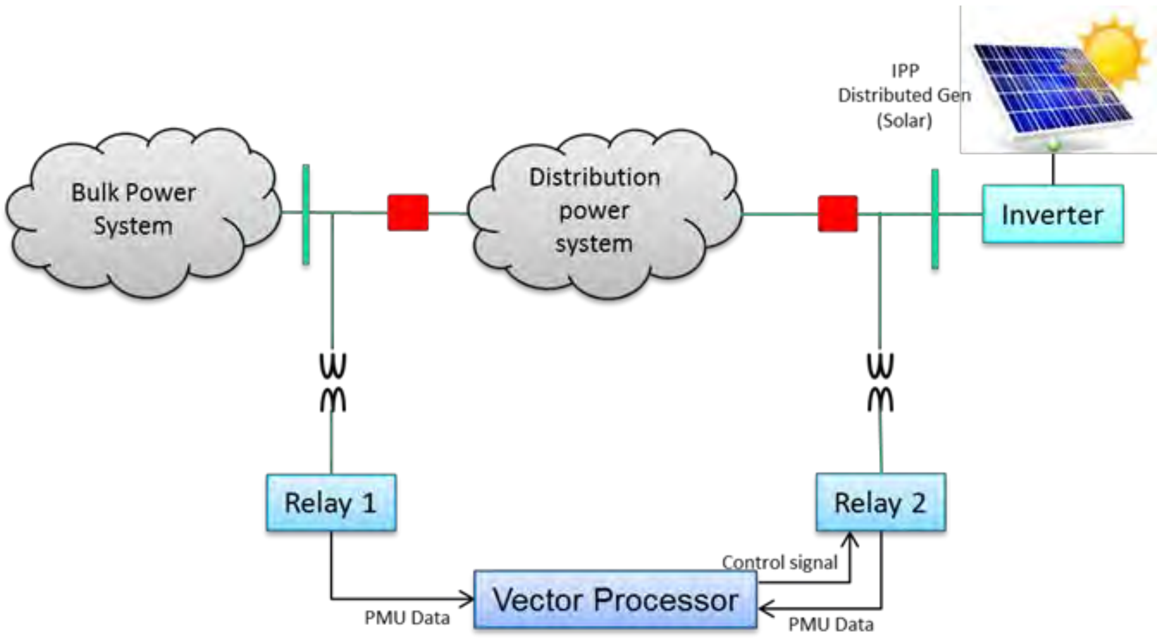

Figure 2.6: IPP integration using PMU data

PMU-based dynamic system estimation plays a big role in power system protection as it offers distributed dynamic system estimation at relay level (DDSE-T). The DDSE-T takes into account both the mechanical and electrical dynamics of the power system and is implemented with accurate time-domain component models; that is, real time-domain waveforms are used not only to capture fast dynamics but also the exact frequency of each waveform. The DDSE-

T is carried out in a distributed manner at the relay level for each power system component, and the DDSE-T inputs are the component's measurements (voltages, currents, and any other observable quantities) in time-domain waveforms.

The basic concept is to enforce the DDSE-T continuously using a comprehensive state and control model of one single component (protection zone) under normal operating conditions. By checking the confidence level of the DDSE-T, which reflects how well the measurements fit with the component model under normal operating conditions, it is possible to determine whether the component under monitoring suffers from internal fault. If the confidence level is high, the component is under normal operation, while if the confidence level is low, the component is under abnormal operation (fault curers inside the component) (Huang, 2015).

The benefit of this protection scheme based on dynamic state estimation is that there is no need to know the details for the rest of the network and no relay coordination settings is needed. The protection based on dynamic state estimation can be further developed to address many more problems with power systems. The ability of the dynamic state estimation to validate the protection zone model as well as the ability to expand it into parameter state estimation opens the possibility of using the relays as the gatekeeper of different system equipment.

2.4 OUT-OF-STEP PROTECTION PHILOSOPHY

Power systems run very similar to the nominal frequency under steady state conditions and retain all bus voltages between 0.95 and 1.05 per unit. A balance between active and reactive power generated and consumed is established, and the system frequency normally varies below + /- 0.02Hz. Any change in generation, load demand, or network transmission causes the change in power flow through the system until new equilibrium is reached. These changes take place continuously and are expiated by the control systems. Therefore, they customarily have no damaging influence on the power grid or its protection systems.

Extreme failures, switching of heavily loaded transmission lines or loss of excitation in large synchronous machines result in abrupt changes in electrical power, while the mechanical power input to the generator stays constant. Such turbulences cause fluctuations in the rotor angle of the system and can result in extreme power flow swings. This state is called 'out-of-step' (OOS) situation (Shaik, 2017).

Out-of-Step state, or unstable power swing, refers to the operating situation where a group of generators is not synchronized with the rest of the machines in the network. This state of the power system is highly undesirable because of the stress it brings to the system; some effects of this phenomenon are large cyclic power flows, high currents in the network and cyclic torque oscillations in the generators (Horowitz and Phadke, 2014). Upon finding this circumstance corrective steps should be taken to isolate asynchronously running parts of the network.

At least a number of OOS detection methods and algorithms are well-known and used more or less successfully (Sauhats et al, 2017), they are as follows:

- Distance algorithm-based methods
- The Ucosϕ algorithm
- Energy function-based method
- Angle control-based methods

(McDonald and Tziouvaras, 2005) realized that not all methods find their realistic application, however methods based on distance algorithms and methods based on angle control are commonly employed. Typically, distance algorithm-based OOS protection is incorporated into TL impedance protection terminals and monitors how the impedance trajectory crosses the protection zone. The main drawback of the method is that in the case of an OOS regime, impedance path does not necessarily cross the protected zone of the particular protection terminal. Thus, it is difficult to coordinate the chosen network splitting place and the response of the specific security terminal for all possible OOS regime scenarios, which can lead to unregulated network islanding.

(Antonovs et al, 2014) also coincide with the above authors that angle control-based methods are frequently used on compensation schemes or compound schemes where they detect angle difference between generated system's voltages measured at critical network locations. By so doing, the violation of angle stability is determined from the rise of the controlled angle value exceeding maximum limit which signifies the initiation of loss of stability then OOS protection will operate.

(McDonald and Tziouvaras, 2005) further notes that alternatively, in relation to the rate of change in angular velocity or frequency shifts and second angle derivatives, the loss of stability can be measured by both of these estimated values having the same sign.

However, some theorists such as (Haddadi et al, 2019) have argued that though some methods and algorithms have no actual implementation they might slightly be realized through integration of large-scale renewable energy where characteristics of these resources may result into mal operation of the legacy power swing protection schemes. These logicians are at pains to point out that the use of energy function-based method could be applicable when OOS protection tripping, or blocking is dependent on the amount of kinetic energy that needs to be converted to potential energy. For energy function-based methods the variation in kinetic and potential energy is premeditated in real time from the local power flow and angle measurements across the line. The system must be able to completely absorb the kinetic energy for transient stability. If the kinetic energy is not fully converted into potential energy, then the system will become unstable. So kinetic energy is zero for a stable swing when potential energy reaches a limit, and kinetic energy is not zero (positive) for an unstable swing when potential energy reaches a maximum. This can be supposed of as a multi machine version of the more simplistic area criterion to assess system stability.

2.4.1 Interconnected grid and Conventional OOS protection

(Berdy, 1979) reflects that two decades ago the impedance characteristics for power system network (generator, transformer, and feeders) were such that an event of loss of synchronism would generally occur in the transmission systems. Transmission line relaying or out-of-step relaying schemes could rapidly perceive the loss of synchronism and in most cases the system(s) could be isolated without the need for generators to trip. In his paper he alluded that with the arrival of Extra High Voltage (EHV) system which comprises of large generators, huge transformers and with the need to expand transmission system, the impedance in the system have changed substantially. Impedance on a generator and step-up transformer has enormously increased while that of the system has drastically decreased. Under these circumstances then out-of-step relaying on both generators and transmission line has to be catered for.

(Berdy, 1979) further concedes that it is not a simple procedure to apply out-of-step relaying schemes to a generator owing to the complexity of the system. The accurate application of such schemes normally requires extensive stability studies to determine the following:

- Loss of synchronism characteristics (impedance loci).
- Maximum generator slip.
- Stable swings characteristic.
- Expected fault current levels in the relays.

In his previous studies (Berdy, 1975) he found that generally, you can’t make use of the normally applied generator zone protection to protect against loss of synchronism suchlike, differential relaying, and time delayed overcurrent system back up etc. However, he noted that the loss of excitation relay may to some extent provide protection, but it cannot be relied upon to detect synchronization failure of the generator under all system conditions. Thus, in the event of a loss of synchronism the electrical centre is situated in the region from the high voltage terminals of the generator step-up transformer down into the generator, a discrete out-of-step relay must be accorded to protect the unit. Such protection may also be needed even if the location of the electrical centre originates out in the system and the system protection is slow or can't even detect a loss of synchronism. Pilot wire relaying or phase comparison relaying used in transmission lines won't detect a loss of synchronism.

(Haddadi et al, 2019) observed that in the modern power system with a great scale of integrated wind generation, the power swing features of the power system changes and may lead to mal-operation of the legacy Power Swing Blocking (PSB) and Out-of-step (OOS) protection schemes. In their view they suggest that the electrical center of a power network may perhaps frequently move owing to increased levels of wind generation, as a result it would be crucial to revise the optimum region of the OOS protection taking into account the impact of several factors, suchlike the type of wind generator, control scheme and fault-ride-through function, not forgetting level and capacity of the wind generation. Authors of (IEEE/NERC Task Force, 2018) proffer that, generation resources that are inverter based such as but not limited to wind generation, comprise of fault response characteristics that differ from conventional synchronous rotating generation and primarily depend on their converter control scheme. Owing to this, the impact of these resources on bulk system protection has of late gained the attention of the power systems community and the performance of several legacy protection schemes i.e., distance protection and negative sequence-based protection schemes have been latterly studied.

The IEE/NERC task force further stresses that, when performing load/fault studies of systems with inverter-based resources it should be recognized that positive sequence dynamic model tools might not record the conditions in which these resources may trip, since they often use phase-based quantities instead of a positive sequence value. Therefore, engineering judgment should be applied to understand the degree to which tripping would also take place for these studies taking into consideration that the inverters are to be connected to transmission level that will weigh heavily on decision making of which type of OOS protection to be used.

(Tziouvaras & Hou, 2004) say, if a small generator is to be connected in a transmission line suchlike IPP shown in figure 9, a decision on whether clearing times on line 2 and 3 needs to be revised for cater for adequate stability of the generation. In most cases, relaying of an existing stepped distance scheme may have to be substituted by schemes that are communication assisted in order to enhance clearing speed and guarantee stability. Protection configuration on line 1 has no effect in the stability of the connected generation, since if line 1 is tripped it will be lost anyway.

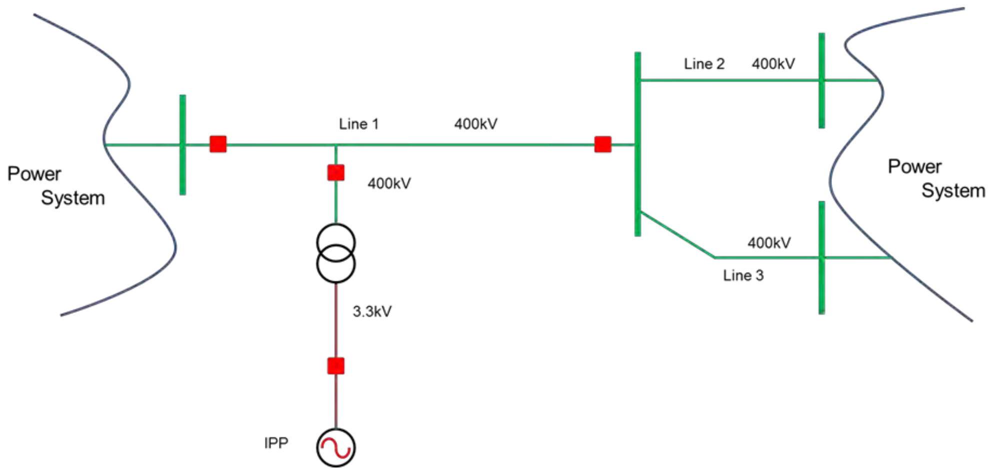

Figure 2.7: IPP connected to transmission line

Nowadays, heavily loaded transmission lines are run around the world whereby the transmitted power and line impedance increase by enormous scale, this might have an influence in power system stability and OOS is the fundamental phenomena of stability protection function (Krata et al, 2014). The authors put emphasis on the fact that during the process of losing system stability, variations in the voltage and current frequency may occur in each affected points of the system therefore an application of frequency difference method may be deployed in long transmission lines besides the already known methods which is impedance based, equal area criterion etc. Frequency algorithm uses currents on local bus and frequency differences within voltage and current on local and remote locations, whereby the frequencies are computed based on synchrophasor measurements with which its output functions send a trip signal to isolate circuit breakers of the affected region.

Out-of-Step tripping should not be implemented in all lines. Separation points should be carefully selected to save the system after an OOS tripping, as (Jacome et al, 2011) utter.

2.4.1.1 State of the art: Generation conventional OOS relaying

(Manunza, 2009) conveys that OOS condition in Synchronous generators is often due to torsional stress from internal mechanism and electro-magnetic flux of generator CB, thus a suitable protection setting of OOS (ANSI type 78 device) must diminish these stresses, however the preference of which co-ordination to use is never a simple task, even in those instances where transient stability study was done. Furthermore, various relays may apply different algorithms owing to the loss of synchronism characteristic as viewed from the terminals of each generator. (Berdy, 1979) also agrees that it would be necessary to briefly study the characteristics of a loss of synchronism situation before considering the out-of-step relaying equipment and its implementation. Berdy stipulates that when two power system areas or two interconnected systems lose synchronism, significant differences in voltages and currents can occur in the systems. When the quantities are in phase the voltages are at maximum and currents are at minimum, however when they are 180° out of phase the voltages tend to be at minimum then the currents will be at maximum. Such fluctuation of the quantities may be used to detect the loss of synchronism phenomena although it may take up to several slip cycle to point out if they were actually due to loss of synchronism. The current level due to loss of synchronism can be denoted from generator as the following equation;

$$I = \frac{E'_q + E_s}{X'_d + X_T + X_s} \tag{2.1}$$

Where I = per unit generator current

E'_q= per unit generator voltage behind transient reactance

E_s= per unit equivalent system voltage

X_T= per unit transformer reactance

X_s= per unit system impedance

However, the determining factor which has the biggest influence on the relay current in this equation is impedance seen by the system. With which the value of this impedance most scheme calls for is equal to the of generator and transformer reactances;

$$X_s = X'_d + X_T \tag{2.2}$$

(Farantos, 2012) points out that there's a fast and effective way to detect and visualize loss of synchronism which is by taking ratio of voltage to current or impedance. During this process, as seen at the line terminal the impedance can differ depending on the angular separation between the systems. This impedance variance can be readily identified, and the systems separated before the completion of a single slip cycle. According to this author OOS condition in generators is mainly carried out by distance relays that observe the impedance trajectory. (Berdy, 1979) recommends the CEX-CEB blinder scheme to protect the generator from loss of synchronism. To measure the progressive shift in impedance as will occur during a loss of synchronism and to trigger tripping when the angle between generator and system voltages is 90 degrees or less, this scheme utilizes three impedance measuring units and logic circuitry. Switching at this angle (90 degrees or less) is usually recommended in order to reduce the burden on the circuit breaker(s). When properly implemented, this scheme is capable of initiating tripping during a loss of synchronism condition on the first half slip cycle. Since synchronism loss is generally a balanced three-phase phenomenon, the relay units used in this scheme are single-phase devices, and only need to be.

This author further concedes that although the CEX-CEB scheme is usually applied to the generator terminals, there are certain instances where it can be best applied to the step-up transformer's high voltage terminals and the settings approach is not a complicated technique since it uses preliminary graphical R-X diagram approach to track the trajectory of the impedance (blinders or circles).

(Rebizant & Feser, 2001) argue that an application of artificial intelligence techniques to OOS protection may be applied paying exceptional attention to fuzzy logic conjecture algorithms which is much faster and more reliable detection when it comes to generator loss of synchronism. The decision is made within a period of approx. 500ms after the fault inception, thus providing ample time for effective tripping signal to protect the generator from stress and maintain the reliability of the power system. The scheme is realised through performing recognition pattern that entails suitably chosen signal sampling vector criterion, whereby the deciding values have to be hitherto estimated with the aid of dedicated digital processing algorithms from existing power system signals. Phase voltage and current orthogonal components are calculated first using full-cycle Fourier filters, on the basis of which further criterion signals are determined.

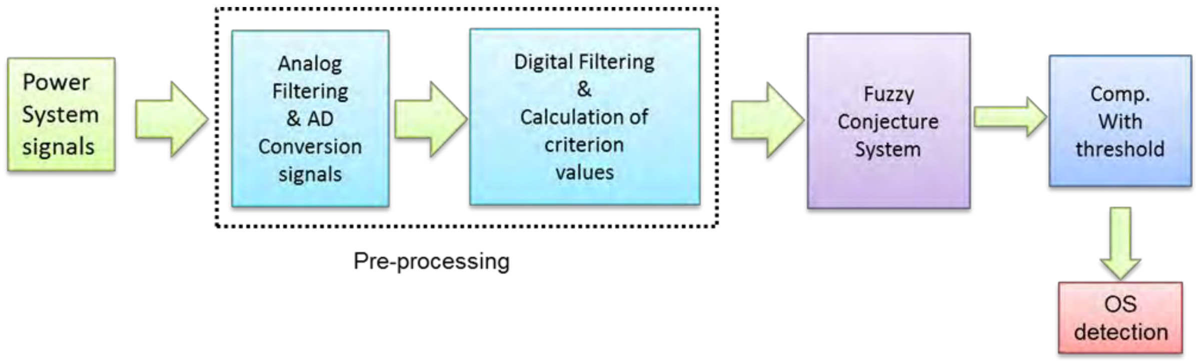

Figure 2.8: The Fuzzy logic-based OOS protection structure (Rebizant & Feser, 2001).

On the above logic it is presumed by the author that the fuzzy inference systems 1 is detected for OS conditions and for stable patterns output equal to 0 is assumed. A threshold of 0.5 is predetermined to classify if the relay should or should not operate and this is distinguished by if the value is lower than the threshold then the relay should be stable and if it exceeds the threshold then the OOS is detected by the relay.

(Yaghobi, 2016) highlights that with the increasing smart protection technology the conventional OOS detection/ protection is not limited to the previously mentioned methods, there’s another advanced technique to swiftly detect this abnormality in the local bus of protected generator. This algorithm utilizes angular velocity and the acceleration seen from the generator’s magnetic flux that is obtainable at the relay location, whereby this relay is commissioned such that it discriminates between stable and unstable circumstances independent of the existing conventional generator protection without any coordination studies/settings. Furthermore, the machine size, the configuration of the power system and its parameters does not affect the performance of this algorithm. The magnetic flux is the main criterion on this OOS protection since in a salient-pole synchronous generator the magnetic flux varies cosinusoidally with the angle between the magnetic axes of the rotor and the stator coil, as the rotor turns.

The author argues that although powers system's switching transients may affect the machine terminal voltage causing it to change very quickly, this occurrence doesn't affect the machine's magnetic flux owing to its highly inductive characteristic thus giving out precise measurement for this phenomenon. He further concludes that it should be noted that, it should be remembered that the magnetic flux is a local variable in the system and this criterion can change locally due to the occurrence of the fault, whereas the current and voltage of the stator are overall external variables that are influenced by various factors. Air-gap flux per pole analysis is therefore an adequate criterion for OOS detection in electrical machines.

In his opinion (Berdy, 1975) suggests that generally during an out-of-step condition, it is not recommended practice to trip generation. It is felt that, wherever possible, it is more beneficial to split the transmission system and preserve all generations connected to the system or portions of it. With this strategy, generation will be ready and available to re-synchronize the system and pick up the load. There will of course, be exceptions to this rule, but the outcomes of such tripping should be carefully assessed.

2.4.1.2 State of the art: Transmission conventional OOS relaying

According to (Hou &Tziouvaras, 2004), the philosophy of OOS relaying in transmission systems is simple and straightforward i.e., during stable swings, avoid the tripping of any power system component and protect the power system in unstable or OOS conditions. However, a controlled tripping approach needs to considered reducing the loss of load and retaining maximum continuity of service. The author denotes that since transmission lines are generally long, the impedance seen by the lines during the fault is often modelled as the shunt reactance between the faulted point and ground. For this reason, impedance protection is usually employed to protect against OOS conditions in such lines, since its tripping is already controlled by zones of tripping. The (IEEE Power System Relaying Committee, 2005) reports that in many applications, the necessary settings for the power swing blocking (PSB) and out-of-step tripping (OST) elements could be difficult to calculate. In order to calculate the fastest rate of potential power swings, detailed stability studies with various operating conditions must be conducted for these applications. Actually, for stable power swings for which the system should recover and remain stable, some transmission line relays may operate. The committee complicates matters further when it writes that during OOS conditions, instantaneous phase-overcurrent relays can operate if the line current during the swing exceeds the relay's threshold setting. Likewise, the ones with directional element will operate if the swings surpass pickup and polarizing voltage setting, however the time-delayed ones are less likely to operate although this is dependent on the time delay setting of the relay and current magnitudes of the swings.

The working group emphasizes that impedance relays respond only to positive-sequence quantities. During an OOS condition the positive-sequence impedance seen at a line terminal change as a function of the phase angle d, amongst the two equivalent system sources. The distance relay elements most vulnerable to trip during a power swing would be Zone 1 distance relay elements, with no deliberate time delay, therefore the use of concentric characteristic schemes may help prevent such mal operations as these schemes are capable of detecting and checking power swing condition before any of the impedance tripping zones is entered which permitting the tripping elements to block if desired. However, on heavy loaded transmission lines this concept may have a drawback due to load encroachment as this will limit the reach of higher impedance zones. Some of the concentric characteristic used for PSB and OST are shown in figure 2.9 below.

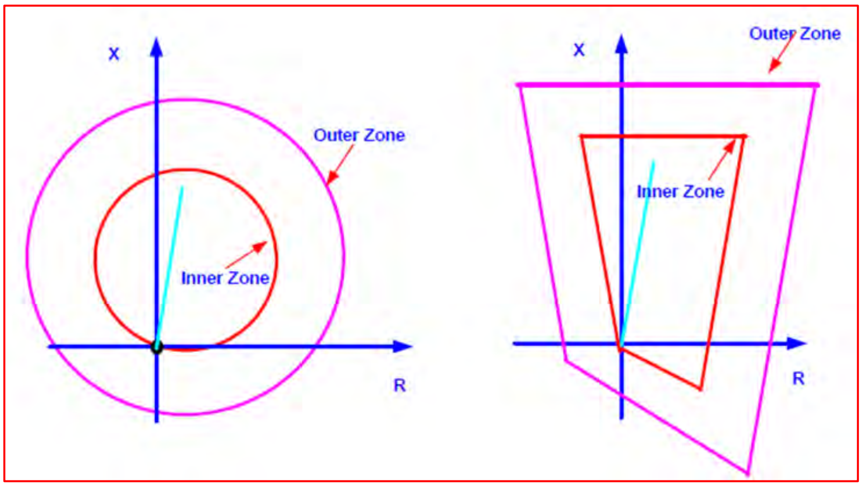

Figure 2.9: concentric mho and quadrilaterals respectively (IEEE PSRC, 2005)

On the other hand (Farantatos, 2012) argues that the safest and commonly used OOS protection detection is the traditional mho relay with 2 blinders, as shown in figure 12 below. The scheme uses impedance trajectory to identify power OOS condition, where it should restrict tripping for loads outside of the blinders and the principle is based on measuring the time it takes for an impedance vector to travel definite delta impedance. The time calculation begins when the outer blinder (RRO) is crossed by the impedance vector and ends when the inner blinder (RRI) is crossed, if the measured time exceeds the predetermined setting of delta time, then OOS situation is present on the system. The essence of this author’s argument is that for power swing detection applications, one advantage of the blinder method is that it can be used independently of the characteristics of the impedance zones. He further concludes that single blinder scheme has also been previously proposed and realized in earlier years, but they exhibit a weakness since tripping is normally delayed to avoid overstresses of the opened breaker when an unstable swing is detected, this then concurrently leads to requirement of repetitive several stability simulations prior to setting the relay. Figure 2.10 below provides illustration of a double mho blinder scheme:

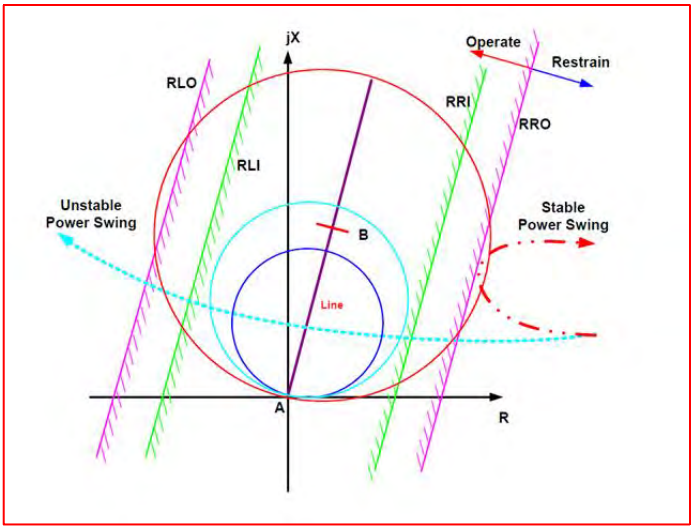

Figure 2.10: mho relay 2-blinder scheme (Farantatos, 2012)

In his earlier study, (Abdelaziz, 1998) explored new adaptive OOS detection through neural networks techniques using stochastic backpropagation training algorithm. The principle basically used prediction from various line outages whereby sample values are computed to obtain ideal discrimination results simulated at 5 different stages to enhance the response of the relay under varying network conditions. The author further acknowledges that there are many benefits of using neural networks for OOS prediction known to literature, as the schemes provides a capability to trigger early isolation for non-recoverable swings while avoiding tripping for recoverable ones. The researchers insist that for certain cases, the algorithm adjusts the optimal output in the training set which then leads to a different decision boundary for the neural network trained from this data, which thereby reduce a large percentage of trips to no-trips causing the scheme to have less false trips. This is realized by classifying a region with “trip” to 1 and the region with “no-trip” to 0 then the algorithm will compute and check the neighbours of every trip to weigh the probability of present OOS condition, if at least 2 of the number of “no-trips” surround a “trip”, the target trip output will be modified to no-trip.

Though (Heo et al, 2007) concede with the above authors that exploring various ways of conventional impedance algorithms might enhance the OOS detection on transmission lines. However, Heo and his co-researchers insist that such relays only track apparent impedance, which is an indirect function of the angle of the generator, and the relay cannot cope with the out-of-step situation of very rapid power swings, which can also cause harm to transmission lines if not detected quickly enough. They proposed an OOS protection algorithm where the angular velocity and angular acceleration are computed as a function of system voltage.

Only voltage measurements seen via the VT are used for the relay, thereafter the voltage signal is passed through the anti-aliasing filter as shown in figure 13. The resulting signal is then digitized via the emulation of the A / D converter until it is eventually used in the out-of-step detection algorithm as seen in Figure 2.11 below.

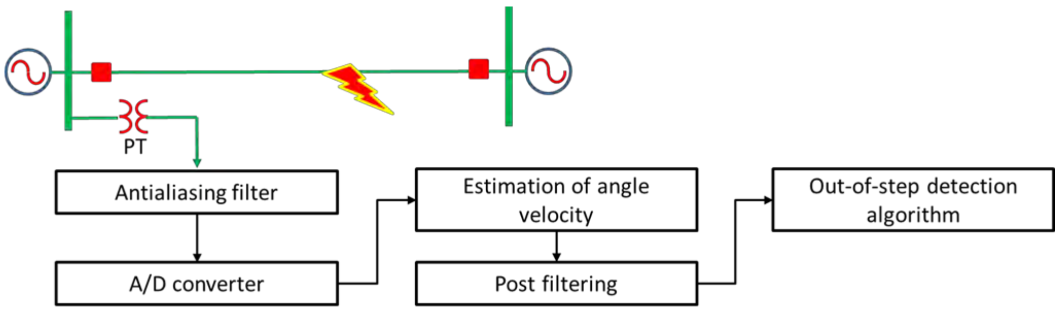

Figure 2.11: Block diagram of frequency deviation of voltage OOS algorithm (Heo et al, 2007).

In this scheme OOS detection can be carried out without the need for current measurements, the only critical variable is the local voltage measurements. It also presents a novel process since the out-of-step condition can be detected earlier than the traditional out-of-step relay with single blinder characteristics, thus it presents much higher reliability and speed to save the disturbed generator and power system from further damage. Yet a sober analysis from (Krata et al, 2014) reveals that it's not really necessary to monitor frequency deviation of voltage on the local bus to enhance higher probability of OOS detection, the authors suggest an implementation of a new frequency difference-based scheme for multi-terminal transmission system.

The algorithm uses three criterion for an OOS detection to be meat, the first works such that threshold value for frequency difference concerning current and voltage at the local bus has to be known, secondly frequency of remote and local terminal should deviate inversely with which regression coefficient is utilized as an indicator for that situation. The third one check if the frequency differences between local and remote end exceeds the threshold to avoid false signal it also validates if the signs of the frequencies are opposite. This approach is said to be very universal, as it can handle almost all of the complex situations that could be presented by OOS.

Philosophers such as (Hashemi & Sanaye-Pasand, 2019), cite that one can implement current-based OOS protection to enhance pre-existing line differential protection on transmission system. The reasons for doing so are arguably significant in efforts to maintain a stable and reliable system protection at no extra cost. This algorithm makes use of current phasors measured at both ends of the line. In this approach controlling the rate of change of line current $\left(\frac{d(I)}{d_t}\right)$, the fault and OOS can be discriminated. The line current typically jumps to a high level whenever a fault occurs, resulting in a high $\left(\frac{d(I)}{d_t}\right)$. Afterwards, the line current becomes almost fixed when the fault is not removed, which causes the rate of change to be approximately 0. On the other hand, the magnitude of the line current changes steadily and constantly during unstable power swings or OOS. Therefore, $\left(\frac{d(I)}{d_t}\right)$ should be greater than zero and smaller than a threshold setting for the OOS condition.

It is worth mentioning that CT saturation is not a concerning factor in the algorithm since the saturation arises due to the presence of DC components in the fault current which is less likely to happen when there's power swings. Additionally, this approach exhibits a novel technique that prevents bogus OOS detection from adjacent lines. The aforementioned algorithm is depicted in Figure 2.12.

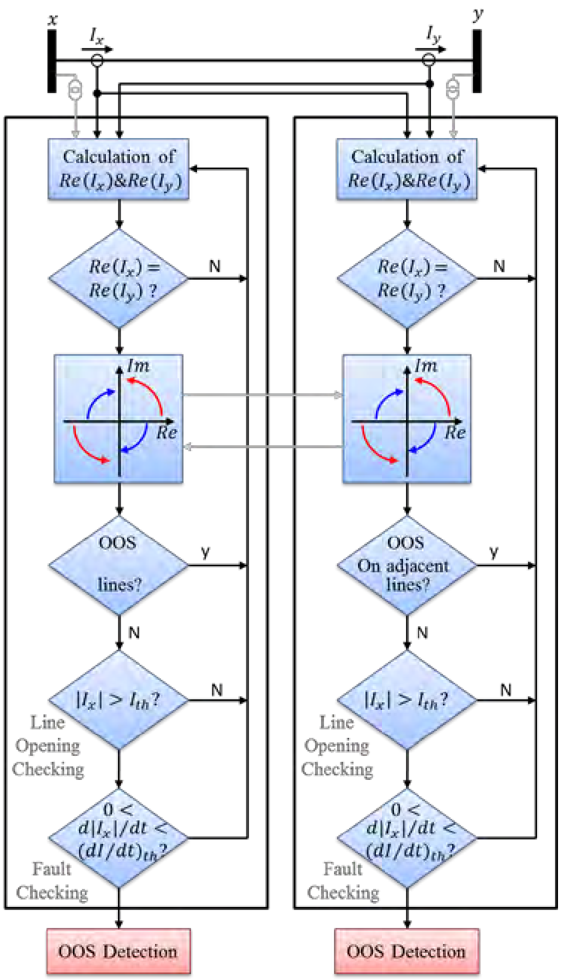

Figure 2.12: Current-based OOS algorithm for line differential schemes (Hashemi & Sanaye-Pasand, 2019).

2.4.2 PMU-based Out-of-step relaying

According to (Phadke & Thorp, 2009), synchrophasor measurement began in 1986 with attempts to investigate whether the power system stability monitoring and protection can't be enhanced. The authors highlight that indeed application of phasor measurement units has enhanced the bulk power system protection whereby the available system quantities such like; bus voltage magnitudes, real and reactive power flows and injections, and status of the breaker are measured to estimate the state of the system often referred to as "State estimation algorithms". However, (Laverty et al, 2013) argues that the application of PMU's dates back to the early 1980's when measurements were carried out between Montreal and SEPT-ILES for voltage phase angles, and Bonanomi 's parallel efforts in 1981. Nonetheless, the PMU technology available today was then emerged by Phadke et al in 1986 to shed new light on synchronised clocks which the previous studies did not completely address.

In Laverty et al view, the application of PMUs has been historically limited to transmission systems due to their cost, but recent developments of PMU in electronic sectors reduced the cost of assembling which consequently dropped prices drastically making them attractive tool throughout the utility, including embedded generation and distribution systems. The author further concedes that ever since the market various types of PMUs have since been realized such like; GridTRAK PMU, DTU PMU and the openPDC each expressing a wide range of pros and cons than one another. (IEEE Std C37.118-2005) for synchrophasor measurements, highlights that although different vendors are given commercial platforms to compete against each other they are guarded under the same standard to promote use of a technology through consistency and create confidence among users while adhering to assurance conformance.

(Singh et al, 2011) says that it is important to note that PMUs promote ground-breaking solutions to conventional utility problems and give power system engineers a wide variety of potential benefits, including but not limited to; improved precise snap shots of post-disturbance analyses which are obtained through GPS synchronization and advanced protection may be applied based on synchronized phasor measurements, with options to enhance the overall system response to disastrous events. This author further concedes that PMUs exhibits optimal benefits when incorporated with FACTS controllers to mitigate sub synchronous oscillations by employing global positioning satellite systems to transmit satellite positional coordinates from which GPS may be used to determine the location of a receiver station on Earth. A typical phasor measurement unit is shown in Figure 2.13 below.

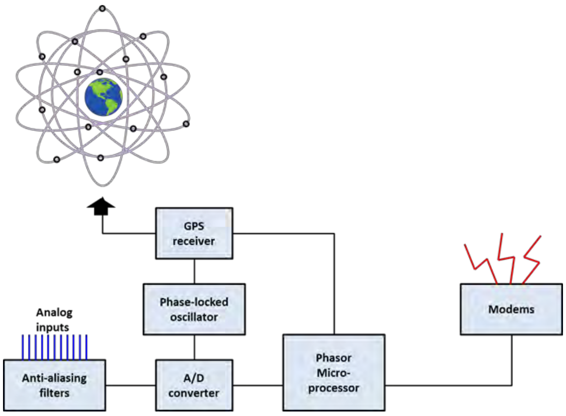

Figure 2.13: Block diagram of PMU (Singh, et al, 2011)

In his study (Shaik, 2017) introduced the out-of-step protection based on synchrophasors for two area system. The author's literature explores that the electrical centre in this system is a point that corresponds to the half of the total impedance between the two sources. The proposed algorithm requires that the electrical centre be between the two relays that receive the measurements of the synchrophasor. The angle difference between these voltages is determined using the voltage synchrophasors of the buses at both ends of the line. To define the unstable power swing conditions, the slip frequency and acceleration are used. The algorithm's flow chart is depicted in the Figure 2.14 below.

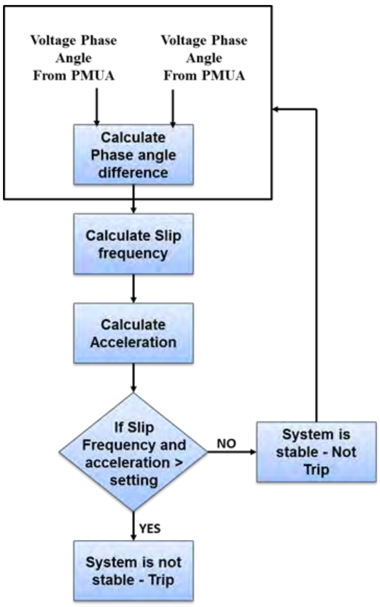

Figure 2.14: PMU-based OOS flow chart (Shaik, 2017).

Most literature studies revealed that PMUs are can efficiently perform when used on predictive schemes based on energy approach commonly referred to as dynamic state estimator (DSE), in his research (Farantos, 2012) suggest that the algorithm is performed at the substation level using only the local measurements available from PMUs, meters, FDRs, etc. in the substation, thereby eliminating all issues related to data transmission and associated time latencies. This strategy allows for a very high DSE update rate that can go up to more than 60 executions per second. Using the results of the DSE, the generator total energy can be tracked and monitored, if it is greater than the peak value of its potential energy. When the total energy is greater than the barrier value, instability is observed. The real-time dynamic state of the substation, as obtained from the dynamic state estimation results, encompasses the real-time operating condition of the substation generators, that is; the angle of the generator torque, the speed of the generator, the acceleration of the generator, etc. All this information helps to characterize and predict the dynamic stability of the system and distinguish if the system is out of step.

(Regulski et al, 2018) also cite that recent studies of PMU application and positioning in the power system provides a number of advantages over traditional OOS schemes, they imply that the PMU is practically configuration-free since it doesn’t require all system parameters to operate properly. With multiple PMUs smarter activities are achieved like areas that lost synchronism are precisely detected to reduce number circuit breakers opening.

2.5 WIDE-AREA MONITORING, PROTECTION, AUTOMATION AND CONTROL

(Cigre- WG B5.14, 2016) workgroup seminal contributions have recognized that in response to the recent global increase in disruptions and grid congestion, the trend towards increasing Wide-Area, Monitoring, Protection, Automation and Control (WAMPAC) adoption is clearly seen through the deployment of advanced WAMPAC applications. A series of recent studies has indicated that a typical architecture of these advanced applications utilizes synchrophasor measurements seen from PMUs throughout the network with which time synchronization is an integral aspect. Time synchronization is however a known concept to previous studies but have advanced from standard to standard. It was reported in literature that synchronized measurements have specific implementation challenges that occur due to the engagement of multiple users with different specifications in the development of WAMPAC systems based on wide area. A fully integrated architecture is required if this diversity is to be properly addressed when designing WAMPAC solutions. In addition, the correct selection of WAMPAC technologies is necessary for cost effective tools that support congested and complex grids management.

In the light of reported WAMPAC technologies it is conceivable that the structure is hierarchical and can be divided into two main levels: regionally and globally. At local level sensed information is processed, synchronized, and archived automatically by a monitoring and control centre known as the Phasor Data Concentrator (PDC), (Bertsch et al, 2005). This information is then sent for inference, calculation, control and protection purposes to a global data concentrator for real-time dynamics monitoring (RTDM) framework. The authors highlight that the input data may be inadequate, correlated, inconsistent dynamically, and in different styles or modalities. Monitoring provides vital data to be analysed and used to avoid deterioration of the power system for control and protection functions; this is of course achieved through real-time monitoring systems.

The most known to literature and utilized protocol for real-time exchange of synchronized phasor measurement data is IEEE C37.118 standard. The standard addresses the synchronized phasor concept, time synchronization, time tag implementation, standard measurement compliance verification process, and message formats for phasor measurement unit (PMU) communication. However new research studies recognised that in order to harmonize with the IEC 61850 power utility automation standard and to address some of the gaps not addressed in IEEE C37, the IEC 61850-90-5 technical report has been established.

2.5.1 IEC TR 61850-90-5

It was reported in literature that the latest accessible synchrophasor measurement technology deployed in power grids around the world is the result of more than two decades of deployment. These infrastructures, from PMUs and PDCs to Super PDCs (SPDCs) and application systems in control centres, have been implemented and developed using the IEEE C37.118 standard at various hierarchical levels. A recent study by (Firouzi et al, 2017) concluded that attempts have been made to migrate from IEEE C37.118 to IEC 61850-90-5 with the introduction of IEC 61850-90-5 in 2012. Although new systems could easily follow the new standard, updating the system components already built to support the new IEC protocol is a challenge. This is a barrier to moving to the new standard and, more importantly, interoperability.

(Firouzi, 2015) is at pains to point out that regardless of the protocol challenges the standard addresses cyber security requirements which were not addressed by the IEEE standard. A more comprehensive description of the use cases of the protocol which are commonly used in substation can be found in the standard itself as the working committee putted so much effort to realize and compile the report in the favour of Electrical engineers. However, it is important to note that the protocol is for transferring digital state and time synchronized power measurement over wide area, thus no hardwiring is needed as it uses routable profiles of IEC 61850-8-1 GOOSE and IEC 61850-9-2 SV packets as shown in Figure 2. below.

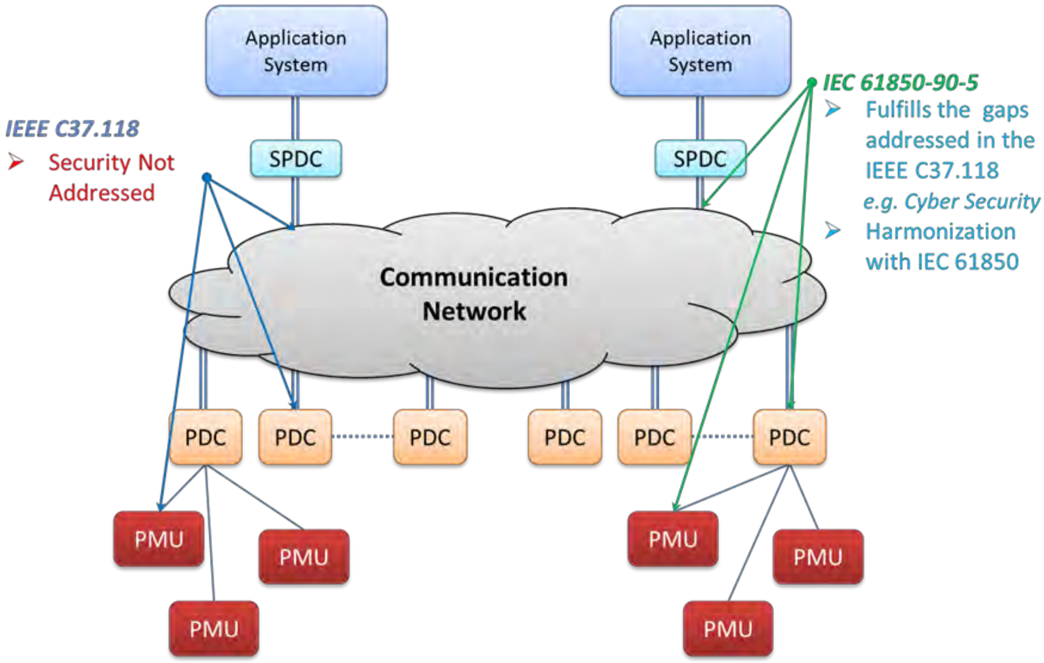

Figure 2.15: Probable scenario for future WAMPAC Systems' architecture (Firouzi, 2015).

2.5.1.1 R-GOOSE

In the previous studies Generic Object-Oriented Substation Event (GOOSE) message were constrained to peer-to-peer communications between multifunctional IEDs used within the substation over local area network (Apostolov, 2017). He concedes that the success of using GOOSE messages for applications of substation protection makes it desirable for use in communication over wide area networks between IEDs. These are systems that impose various conditions on peer-to - peer interactions. The literature reflects that while GOOSE messages have already been utilized in protection and automation applications outside of the substation, the fact that they are distributed over wide-area networks renders them vulnerable to cyber-attacks. Thus, the concept of Routable GOOSE has been introduced and addressed by the IEC TC 57 working group 10.

For IEC 61850-90-5 session protocol; the sending of event driven information e.g., GOOSE, control block needs to be defined and remain unchanged from the original IEC 61850-8-1 so as to acquire backward compatibility. However, a new functional constraint will need to be added to LN0, (IEC TC 57 working group 10):

- RG – Specifies a routable GOOSE functional constraint for packets based upon the profile defined in the technical report. The control blocks with this constraint will be defined as ROUTABLE-GOOSE-CONTROL-BLOCK (R-GoCB).

In the application standard the client/server A-profile for profile mapping enables the transference of GOOSE as specified in IEC 61850-8-1 to be sent in a secure and routable manner. These APDUs are meant to be used with a minimum of modifications as seen from the Figure 2.16 below.

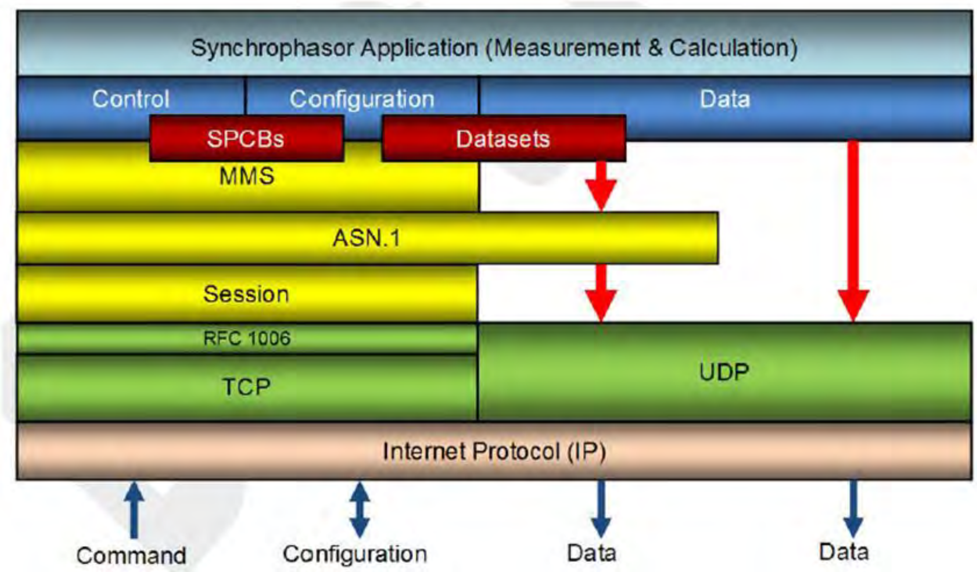

Figure 2.16: general service mappings (IEC TR 61850-90-5).

The A-Profiles are generally comprised of the existing GOOSE Application Protocol Data Units (APDUs) encapsulated or tunnelled using the session protocol specified in this standard.

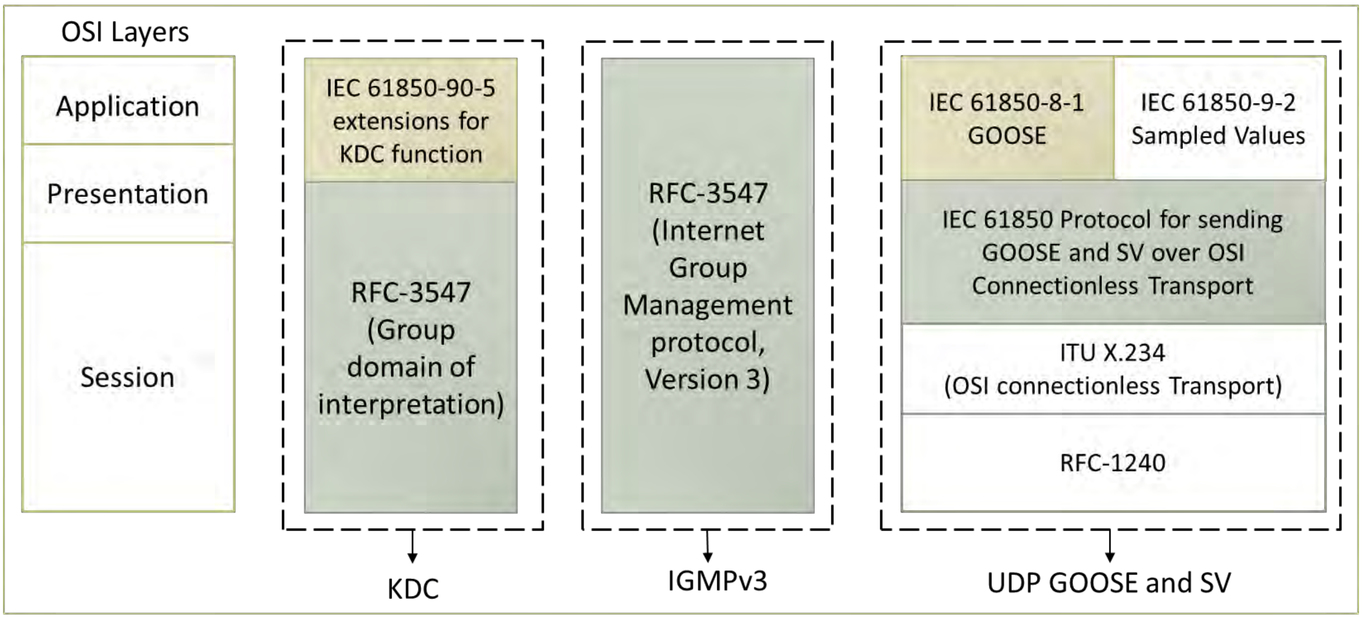

Figure 2.17: A-profiles (IEC TR 61850-90-5).

In his study (Firouzi, 2015) suggested that you can actually implement a IEE-IEC gateway that is capable of working in an embedded device with minimal hardware requirements (no operating system, minimal memory, etc.), allowing synchrophasor streams to be easily transmitted across wide-area networks, reducing latencies in real-time applications. The research presents “Khorjin” library algorithm to serve for this gateway. Khorjin library is designed to receive and parse Routed-SV and Routed-GOOSE messages and to provide the sub-scribed applications with the raw synchrophasor data extracted, as shown in Figure 2.18. The author further highlights that another part of the Khorjin is designed to receive PMU / PDC synchrophasor data using the IEEE C37.118.2 protocol, map PMU data to the IEC 61850 data model and publish either Routed-Sampled Value or Routed-GOOSE format IEC 61850-90-5 messages.

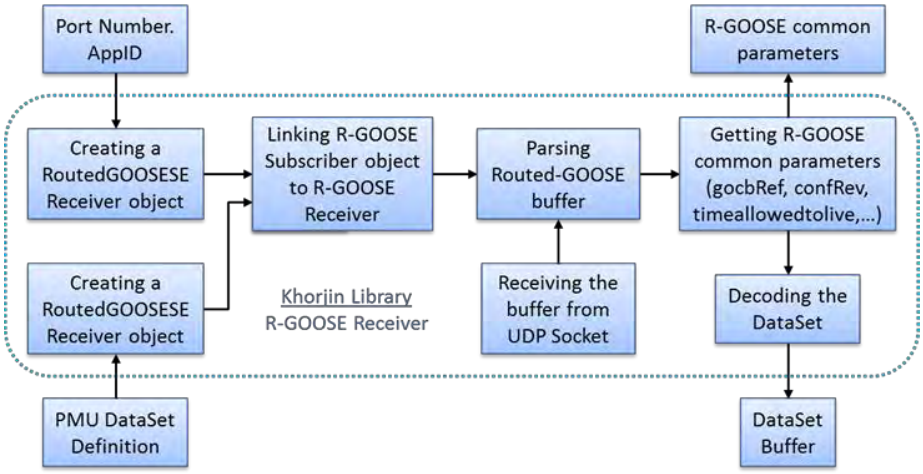

Figure 2.18: Khorjin library R-GOOSE parser algorithm

2.5.1.2 Predictive dynamic stability maintaining system

A more systematic and theoretical analysis of the IEC TR 61850-90-5 standard have been explored by the working group. Where they closely looked for an appropriate indicator that would denote the occurrence of a disruption with a gradual onset of 5 s to 10 if an out-of-step condition arises in a loop or a mesh network connecting two or major power systems. For the case use when an OOS detected the algorithm can avoid the OST condition from occurring by subsequently splitting system at a particular point. An out-of-step condition can be established, and it is possible to avoid the out-of-step from happening by eventually splitting the system at a particular stage. The system consists of PMUs used to collect data which are located at each major point of the power system; the IED allows the power system to be separated. Within a communication network, the IED and PMU are linked.

The method employed applied in this case works such that each PMU transmits the voltage angle to the IED for its own portion of the power system. The IED compares the angles between the PMUs, and the future angle is anticipated. If the anticipated angles between system A PMUs and system B PMUs surpass pre-determined values, the IED decides that there will be an out-of-step condition and the CB will be triggered. Alternately, under normal conditions, the IED calculates the angular difference between PMUs. Whereby, this change in angular difference is determined from the generator rotor angle (speed) or frequency deviation when a disturbance occurs.

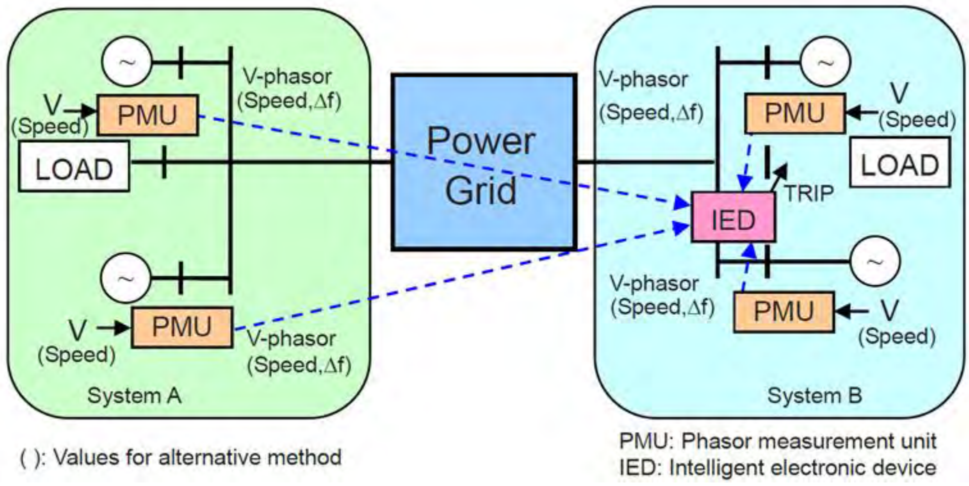

Figure 2.19: predictive dynamic stability use case diagram (IEC TR 61850-90-5).

However, it is important to note that the algorithm poses time constraints with which may be critical to note in design application stages; the drawbacks of this use case are such that control steps have to take place within a short period of time. For future predictions, this program predicts a voltage angle difference of 15ms to 200ms, thus control is executed to break part of the systems when the expected angles surpass the predetermined values.

2.6 IMPLEMENTATION OF REAL-TIME DIGITAL SIMULATOR

RTDS Technologies Inc. introduced the first Real-Time Digital Simulator for commercial use in 1991 using a Digital Signal Processor (DSP) (RTDS, 2014). In order to evaluate the performance of a high voltage direct current converter, the RTDS was interfaced with the controller. In that simulator, analogue and digital components were combined. Since then, RTDS has expanded and evolved into one of the most widely used commercial real-time simulators. The first small-scale digital simulator for testing the components of the power system in real-time was presented by authors (Kuffel, et al, 2010) and was based on the parallel computing system's multifunctional standard. It was called the Digital Transient Network Analyzer (DTNA). The DTNA could model electromechanical transients, ac/dc interactions, and electromagnetic transient events up to 3 kHz.

Real-time detection systems, also known as RTDS, can be made up of intricate arrangements of sensors, tools, software, and procedures. They hold enormous promise to enhance exposure decision analytics when applied to occupational and environmental health and safety. But as RTDS implementation becomes more complicated, there is a greater chance of running into serious problems.

Advanced connectivity, whether to a base station like a tablet or laptop or directly to a telemetry system connected via cellular data connection, Wi-Fi, or other means, is a developing feature in DRIs. By removing manual local storage transfers, improving data retrieval rates (by the hour, minute, or second rather than by the day or event), and seamlessly integrating with database software, advanced connectivity improves the flow of data from instrument to laptop to database, allowing users to more easily transport or analyse their data (RTDS, 2014).

A freshly created and developed phase domain synchronous machine model is now part of the RTDS. This paradigm is put into practice in the RTDS environment using the embedded phase domain technique (Dehkordi, et al, 2005). Phase domain describes how machine inductance values vary depending on the rotor position and saturation level. The phrase "embedded" denotes the network solution's incorporation into the machine's differential equations solution. When compared to the traditional interfaced approach, this method performs numerically better (Dehkordi, et al, 2010). The inductance matrix of the machine can be calculated by the phase domain synchronous machine model using either the MWFA approach or the dq-based method:

- **DQ-Based Approach**: In this method, it is expected that not only will the healthy windings produce a distributed magnetomotive force (MMF) that is perfectly sinusoidal, but also that the MMF resulting from the defective windings will also be sinusoidal. The benefit of this technology is that users do not need to be aware of the geometry of the rotor and the distribution of the windings. The non-sinusoidal distribution of the windings, however, prevents this approach from displaying the phase-belt harmonics (third, fifth, and seventh harmonics) (RTDs user’s manual 2020).
- **MWFA-Based Method**: This approach, which is based on the modified winding function approach, takes into account the actual distributions of the windings when calculating their inductances. The rotor pole design, the number of stator slots, the actual distribution of the windings, and the number of poles are the only minimal data needed to apply this model. The phase-belt harmonics are accurately represented by this method, as opposed to the dq-based approach (Dehkordi, et al, 2005)

The open loop method, according to authors (Marttila et al., 1996), can be used to test some equipment for protection and control; in this kind of test case, feedback from the equipment reaction to the modelled system is not required. When it is believed that the equipment's action timing in response to power system events will not affect the equipment's response to subsequent changes in the power system, this test is appropriate.

Whilst authors (McLaren et al., 1992) are in pains to point out that closed loop method posses a better benefit as it enables thorough testing and research into the effectiveness of protective relays under extremely realistic settings (McLaren et al., 1992).

The implementation of the closed loop test can be done after the open loop test has been completed and the protective relay's replies have been verified as being accurate. The protective relay response signals (actuator: trip signals) are supplied back to the RTDS for closed-loop testing, enabling the user to monitor the trip signals and circuit breaker status through the Run Time window in the RSCAD software environment.

The author (De Oliveira, 2008) claims that real-time digital simulator (RTDS) testing of numerical distance relays gives users greater reliability and achieves the highest levels of performance and functionality, which are subsequently applied to power transmission systems. The performance of the numerical distance relay for the CEMIG 500 kV transmission lines was examined by the author (Energy Company of Minas Gerais-Brazilian Energy Utility).

In distribution networks, problems with protection arise from the high penetration of distributed generation (DG). By using Controller Hardware-in-the-Loop (CHIL) to evaluate the protective relays and Power Hardware-in-the-Loop (PHIL) of the PV inverter and wind energy system, the authors (Papaspiliotopoulos et al., 2014) investigated this difficulty. These simulation tests aided in the verification of the DG's effect on protection plans.

Through GTAO and amplifiers, the secondary current and voltage are supplied to the protective relay, and the relay reaction is connected to the actual power systems.

2.7 DISCUSSION OF LITERATURE REVIEW

In the early years of OOS detection methods, traditional impedance algorithm has been used across the world. Despite the fact that the basic idea behind OOS protection has not changed, an incredible number of scholarly articles have addressed the problem of detecting and coordinating the OOS protection scheme. The most widely used method is the impedance-based, classical method, which is followed by more recent methods like R-Rdot swing-centre voltage (SCV)-based technique, wide area synchrophasor-based technique, equal-area criterion-based technique, heuristic algorithms, and decision trees. Additionally, some previous work proposes a neural network-based detection technique and suggests employing an adaptive network-based fuzzy interface to apply fuzzy logic (ANFIS). However, the arrival of PMUs in the early 1980s changed the concept of Out-of-step protection such that reliability and speed have been enhanced and system splitting could be achieved with a total isolation of the affected area. Most studies have relied on local bus phasor computation for the PMU’s to be able to detect a disruptive situation.

With the aid of IEEE Std C37.118, communication gateway for PMUs to send and receive information from other devices in the system in 2005 a predictive and situational awareness of the networks was realised. However, this algorithm was susceptible to cyber hacks thus a need for IEC 61850-90-5 standard which provides cyber security was developed. Many conventional OOS detection techniques were proposed, and lab tested but they never really found their practical real-world implementation. A graph showing number of OOS publications over the years and the table presenting algorithms of OOS detection reviewed in this research work are shown below:

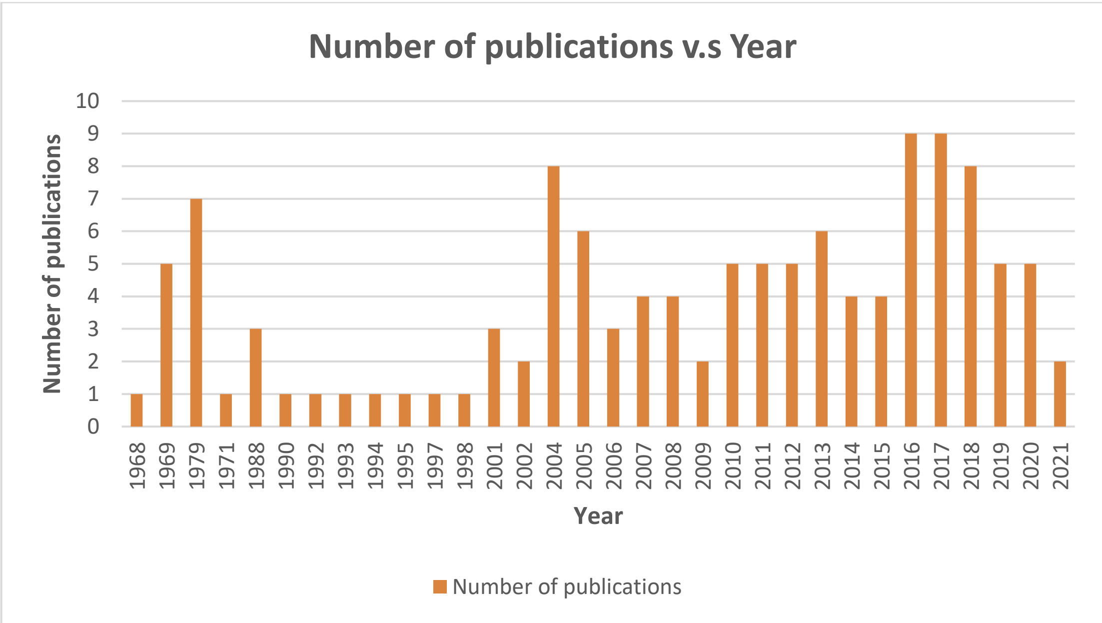

Figure 2.20: Literature review bar graph

Reference	Application	Algorithm	Standard/protocol	Network considered	Real life implementation
(Berdy, 1975)	Generator OOS	Single-blinder mho scheme	N/A	N/A	yes
(Hou & Tziouvaras, 2004)	OOS protection Enhancements	Double-blinder mho scheme	N/A	N/A	yes
(Rebizant, & Feser, 2001)	Generator OOS	Fuzzy logic	ATP-generated power system signals	N/A	No
(Abdelaziz, 1998)	Adaptive OOS detection	Neural networks	stochastic backpropagation	N/A	No
(Hayes at al, 2002)	OOS relaying	Neural networks	confusional filtering criterion	176-bus model of the western United States	Yes
(Heo et al, 2007)	OOS detection	frequency deviation of voltage	Digital filters based on discrete Fourier transforms	N/A	No
(Yaghobi, 2016).	Generator OOS	Magnetic flux as the main criterion	N/A	SMIB and a TMIB power network	yes
(Brahma, 2007)	OSB function for OOS relays	Wavelet Transform	PSCAD/EMTDC	N/A	No
(Hashemi & Sanaye, 2019).	Line Differential enhancement	Current-based method	PSCAD/EMTDC	IEEE 39-Bus System	No

(Jacome, 2011)	Setting OST & OSB	Impedance based	Dynamic PMU simulations	Peru Substation	No
(Shaik, 2017)	Modern OSS protection	Synchrophasor-based	Real-time tests (RTDS)	Kundur two area system	Yes
(Qiao et al, 2013)	Theoretic Approach to PMU placing	greedy algorithm	N/A	IEEE 14-bus system	No
(Wen et al, 2012)	Special protection schemes	C-RAS logic	IEC 61850-8-1 GOOSE message	SCE transmission grid	Yes
(Yuri et al, 2012)	Wide-area security assessment	PMU-based	Hyperplanes	N/A	No
(Ivankovic et al, 2017)	WAMPAC OOS system	PMU-based	Hardware-in-the-loop	N/A	yes
(Firouzi, 2017)	IEC 61850-90-5 application	Khorjin library R-GOOSE parser algorithm	Real-time platform (RTDS)	N/A	No
(Apostolov, 2017)	R-GOOSE Application	R-GOOSE	IEC 61850-90-5	N/A	Yes
(Ali et al, 2016)	Performance comparison of PMUs	N/A	IEEE C37.118.2 and IEC 61850-90-5	N/A	No

(Sauhats et al, 2017)	Transmission OOS protection	Angle-control based	IEC 61850	Latvian power system network 330 kV	Yes
(Jacobsen et al, 2020)	Multi-machine synchronous islanding	PMU-based	Physical lab test bed	N/A	No
(Gonzalez-Longatt et al, 2021)	Transmission OOS protection	Impedance based	Hybrid co-simulation and cyber-physical approach	Mongolian Transmission system	Yes

2.8 CONCLUSION

This chapter gave a general review of the stability of the power system and the factors that affect it. An overview of previous research on generator rotor angle stability pertaining out-of-step detection and out of step blocking by different researchers has also been discussed. The previous researchers concentrated on creating innovative methods for detecting loss of synchronism in large, interconnected power system. The existing schemes are still effective, but they need to be improved in order to handle the power system's evolution and allow for the integration of renewable energy sources. The benefits introduced by incorporating an IEC-61850-90-5 standard to the OOS phenomena has also been given by various studies each owing to the need for interoperability of IEDs and PMUs. To suit the current monitoring system used in the power system, the protection algorithm needs to be adaptable.

This thesis focuses on developing a novel approach based on exported synchrophasor measurements for designing a predictive dynamic stability maintaining system based on IEC 61850-90-5 gateway for a multi-area power system oscillations is presented. For the optimum location of the PMUs, a new approach will be used based on combined modal participation factor and binary integer programming. To obtain maximum efficiency on the scheme Out-Of-Step tripping must not be configured in all the lines. Islanding points should be carefully selected in order to save the system after out-of-step tripping and avoid reoccurrence of the OOS condition again.

The proposed scheme takes the advantage of direct transient stability analysis methods by computing the angular difference from synchrophasors of the system. As a result, the out-of-step situations are predictable faster than the conventional methods; this will contribute to this increasing demand of smart grid as it pertains to the IEC61850 standard and substation automation.

Chapter 3 entails the theoretical aspect of power system stability, the synchronous generator design in relation to the power system stability is also covered along with the generator excitation and governor controls.

3 CHAPTER THREE

Theoretical synopsis of power system stability and Generator Design

3.1 INTRODUCTION

Power system stability has been broadly discussed in literature as a property of a power system that enables it to remain in a state of equilibrium under normal operating conditions and to regain back an acceptable state of equilibrium after being subjected to a disturbance. The study of the dynamics of the power system under disturbances is necessary for power system stability. The ability of a power system to resume normal or steady performance following exposure to disturbances is referred to as stability. Power system instability can be conceptualized from a classical perspective as a loss of synchronism (i.e., some synchronous machines moving out of step) when the system is subjected to a specific disturbance. Steady state, transient, and dynamic stability are the three types of stability that are problematic.

It is important to note that the system used for research study is a dynamic model, hence one of its essential and crucial characteristic is its flexibility to operate in different conditions owing to variability of load demand, so it is imperative to analyse the flexibility of this concept. The three-phase power system is taken to be balanced to make the analysis simpler. A balanced three-phase system is the foundation for the analysis of the steady-state and dynamic power system models (Kundur, et al, 2004).

The analysis of the system model characteristic along with that of synchronous machines will be derived and discussed according to the following flow chart.

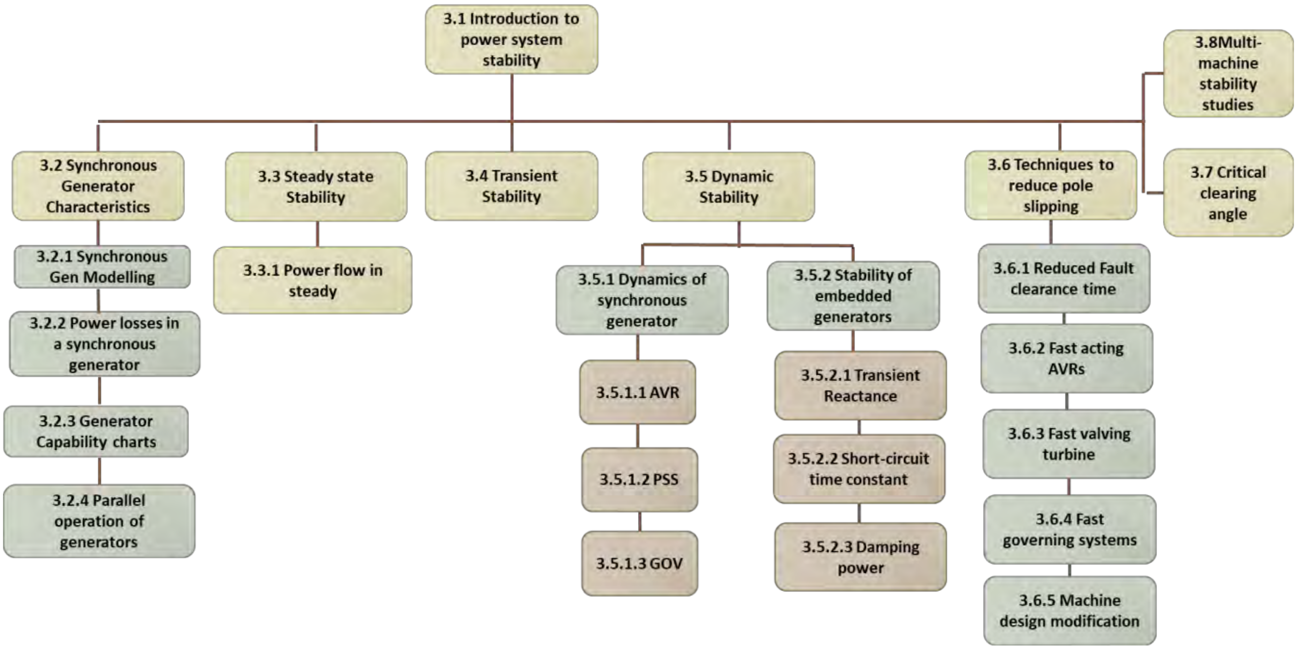

Figure 3.1: Overview of power system stability synopsis

3.2 SYNCHRONOUS GENERATOR CHARACTERISTICS

Synchronous or alternating current generator is a specific type of generator that is capable of converting mechanical energy into alternating current electrical energy. The principle of operation of the synchronous generator is as follows: A direct current is applied to the rotor winding, which then generates a rotor magnetic field. The rotor is then turned by a prime mover (e.g., steam, water, etc.) creating a rotating magnetic field (Klempner & Kerszenbaum, 2018). This rotating magnetic field induces a 3-phase voltage set in the generator's stator windings. This DC power supply generate the magnetic field on the rotor blades which can provided by slip rings and brushes or by a unique DC power supply design mounted on the shaft of the rotor as shown in Figure 3.3 (a) below. A rotor is the large rotating electromagnet inside the synchronous generator stator, as shown in Figure 3.3 (b).

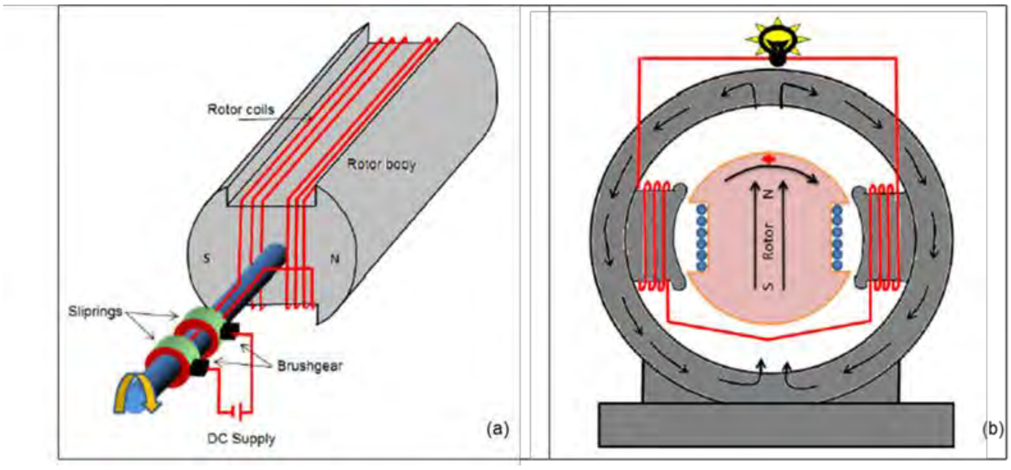

Figure 3.2: Generator rotor with electromagnetic coil (Beukman, et al, 2011)

A synchronous generator's rotor is a sizable electromagnet with magnetic poles that may or may not be conspicuous in design (Salient and non-salient pole). Salient pole rotors are typically used for rotors with 4 or more poles with teeth opening on Kaplan turbines and has low speed, whilst non-salient pole rotors are typically used for rotors with 2 to 4 poles with a smooth surface on a pelton wheel and has high speed.

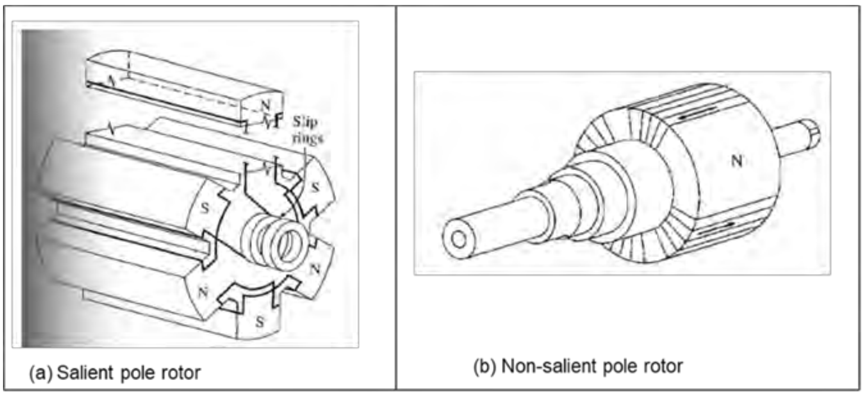

Figure 3.3: Diagram of rotor configurations (Klempner & Kerszenbaum, 2018).

DC power of synchronous generators is said to be supplied by slip rings or brushes, while this is true for small machines; large machines require brushless exciters to deliver this DC current. A brushless exciter is a tiny ac generator with the field and armature circuits located on the stator and rotor shaft, respectively. A 3-phase rectifier circuit, which is installed on the generator shaft as well, converts the exciter generator's three-phase output to direct current before feeding it to the main dc field circuit (Beukman, et al, 2011). We can modify the field current on the main machine without slip rings and brushes by adjusting the small dc field current of the exciter generator, which is housed on the stator. A brushless exciter requires minimal maintenance because there are no mechanical contacts between the rotor and stator. In a brushless exciter circuit, a diminutive three phase current is rectified and utilized to provide the field current of the exciter, which is situated on the stator. For this research application are parallel generators at Palmiet pump storage are of focus, the machines act as synchronous generators when call upon to during peak hours of national generation otherwise act as motors most of the time pumping water to and from steenbras dam.

3.2.1 Synchronous generator modelling

A three-phase generator has three windings that are displaced 120 degrees apart, as shown in the simplified diagram below Figure 3.5 The voltages induced are also displaced 120° apart to create a balanced system currents with which at any point in time their sum is always zero, hence why a neutral is not required as there is no return path for current flow. Which is an advantage for large industries that employ 3-phase motors as their prime drivers as what they receive from supply system is what they're directly consuming in turn. This results in enormous saving in material and cost when building transmission and distribution systems.

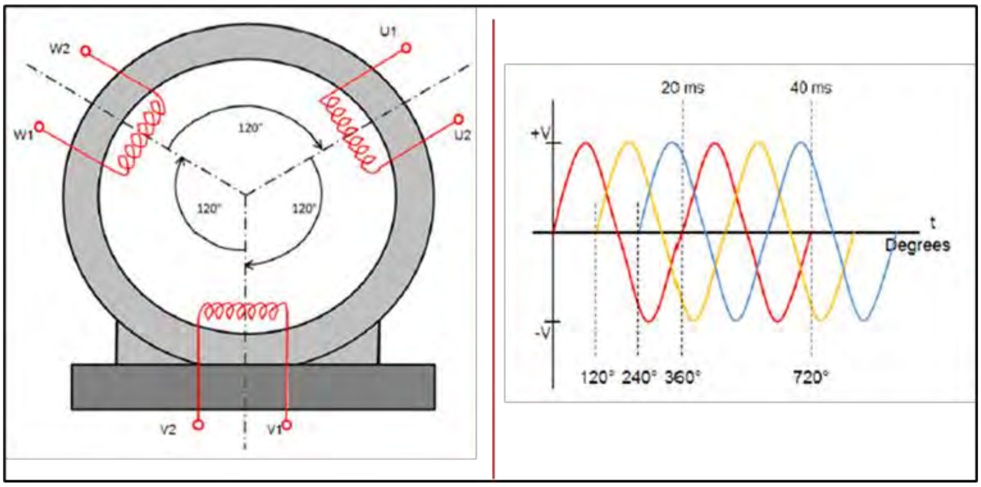

Figure 3.4: Voltage winding distribution in a 3-phase generator (Beukman C. etal, 2011)

Synchronous generators are, by definition, synchronous, which means that the electrical frequency produced is locked in or synchronized with the generator's mechanical rate of rotation. The rotor of a synchronous generator is an electromagnet to which direct current is applied. The magnetic field of the rotor points in the direction that the rotor is turned. This is an important variable for when the generator accelerates to maintain synchronism with the system. Thus, the rate of rotation of the magnetic field in the in such a machine is relative to the stator electrical frequency by:

$$f_e = \frac{n_m p}{120} \tag{3.3}$$

Generators can be operated in two modes: lock mode and free mode. The generators produce power based on the rotational speed of the prime mover when in lock mode. The generator's operation in free mode is determined by the mechanical torque applied to it. The angular velocity of the generator, which one of the principal parameters in a prime mover that varies with time when the generators are loaded, can be used to monitor the frequency in the generators. The expression can be used to calculate the frequency on the mechanical side of the generator. Whereby ω is the rotational speed of the generator in units of radian per second.

$$f = \frac{\omega}{2\pi} \tag{3.4}$$

The mechanical torque provided by the prime mover (turbine) is balanced by an electromagnetic torque in the opposite direction caused by the interaction of the magnetic flux and the current flowing in the stator windings. This is illustrated in the following formula where it is seen that the power produced by the generator is directly proportional to the torque on the drive shaft.

$$P = \tau\omega \tag{3.5}$$

Where: τ = torque, NM

ω = rotational speed, rad/s

The rotor shaft must be designed to transmit the rated torque, and the stator must be able to withstand a similar torque reaction. In practice, the design must also be able to withstand the much higher torques produced during fault conditions (Klempner & Kerszenbaum, 2018).

There are basically 3 types of relationships that need to be found for a synchronous generator:

- Field current and flux relationship
- Armature resistance
- Synchronous reactance

The magnitude of the induced internal generated voltage in a given stator is:

$$E_A = \sqrt{2}\pi N_c \phi f = K\phi\omega \tag{3.6}$$

Where; K is a constant depicting the edifice of the machine, ϕ is flux in it and ω is its rotation speed. Since flux in the machine is determined by the field current passing through it, the internal generated voltage is proportional to the rotor field current as shown in the Figure 3.6 below.

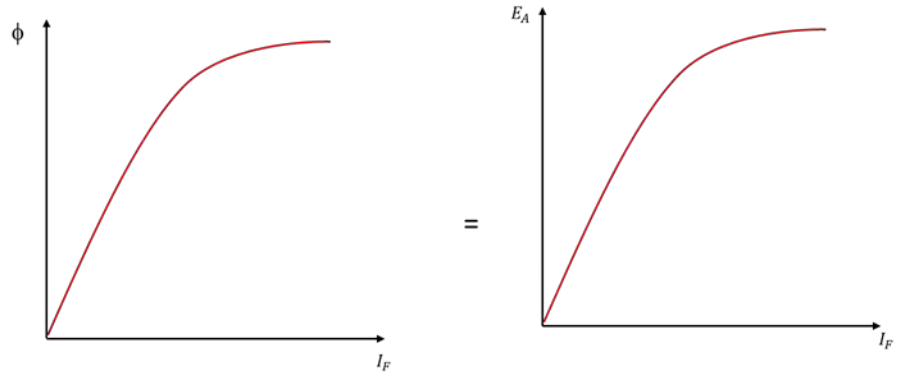

Figure 3.5: Magnetization curve of a synchronous machine (Klempner & Kerszenbaum, 2018).

The voltage generated internally in a single phase of a synchronous machine E_A is not always the voltage seen at its terminals. Only when there is no armature current in the machine does it equal the output voltage V (Beukman, et al, 2011). The following are the reasons why the armature voltage E_A is not equal to the output voltage V:

- Air-gap magnetic field distortion caused by current flowing in the stator (armature reaction)
- The armature coils' self-inductance
- Resistance of the armature coils

When a synchronous generator's rotor spins, a voltage E_A is induced in its stator. When a load is connected, a current begins to flow, producing a magnetic field to form in the machine's stator. Then the induced stator magnetic field B_s adds to the main magnetic field from the rotor B_R affecting the entire magnetic field and consequently also the phase voltage is affected in the process.

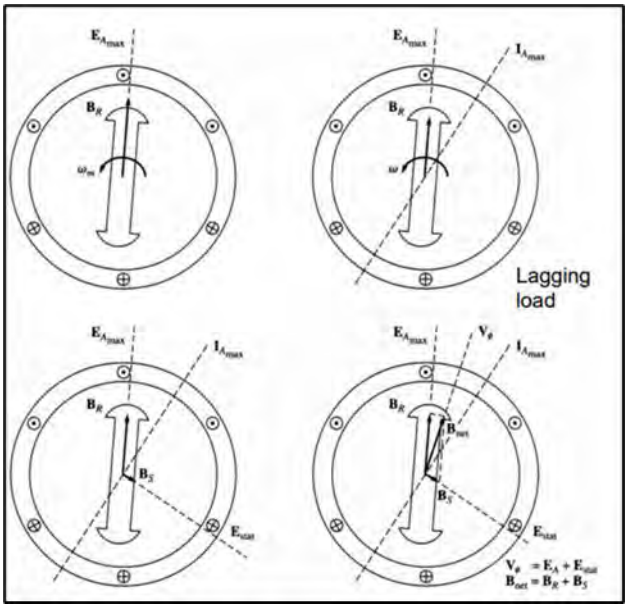

Figure 3.6: Armature reaction of synchronous machine (Klempner & Kerszenbaum., 2018)

Then the effects of the armature reaction on the phase voltages are modelled such that the voltage E_{Stat} sits at an angle of 90° behind the plane of I_A, assuming that the voltage E_{Stat} is directly proportional to the current I_A. When X is a constant of proportionality, the armature reaction can be expressed as:

$$E_{Stat} = -jXI_A \tag{3.7}$$

Therefore, the armature reaction voltage can be modelled as an inductance in series with the internally generated voltage:

$$V_{\phi} = E_A - jXI_A \tag{3.8}$$

However, adding to the armature reactance effect, the stator coil has a self-inductance L_A (X_A is the corresponding reactance) and the stator has resistance R_A. The phase voltage can then be expressed as:

$$V_{\phi} = E_A - jX_SI_A - R_AI_A \tag{3.9}$$

Where X_S is the combined reactance of armature and self-inductance reactance ($X+X_A$) which makes up the synchronous reactance of the machine. An equivalent circuit of a synchronous generator is shown if figure below. A DC source powers the rotor field circuit, which is modelled by the inductance and resistance of the coils in series. In series with R_F is an adjustable resistor R_{adj} that controls the flow of field current. The rest of the equivalent circuit consists of the models for each phase. Each phase has an internally generated voltage with a series inductance X_S and a series resistance R_A.

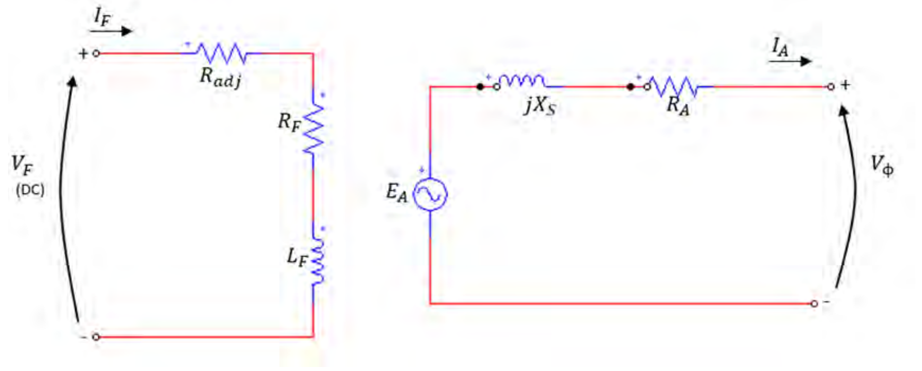

Figure 3.7: The per-phase equivalent circuit of a synchronous generator (Klempner & Kerszenbaum, 2018).

A 3-phase generator may be connected in star or delta configuration, Ideally, the terminal voltage should be the same for all 3 phases since we assume a symmetrically connected load. If it's not balanced, a deeper technique is required. From this assumption it is then apparent that the phasor diagrams of synchronous generator are similar to that of power transformers for all 3 power factor conditions (unity, lagging and leading power factor).

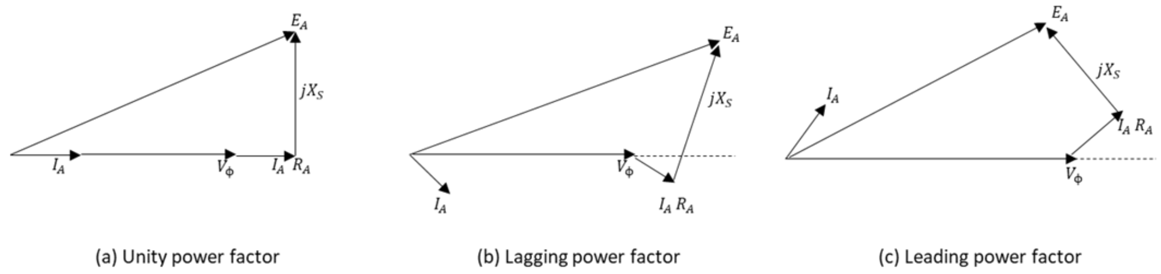

Figure 3.8: Synchronous generator phasor diagrams

For a specified phase voltage and armature current, a larger internal voltage E_A is required for lagging loads than for leading loads. Therefore, a larger field current is required to get the same terminal voltage since $E_A = k\phi\omega$ because it has to be kept constant to keep a continuous frequency. Alternatively, for a given field current and magnitude of load current, the terminal voltage is lower for lagging loads and higher for leading loads.

3.2.1.1 **Power characteristics for an ideal synchronous generator**

The interaction between the stator flux and the field winding flux dominates the typical response of synchronous machines. As a result, the power/load angle characteristic is sinusoidal. The steady state real and reactive power load angle characteristics for a machine coupled to an infinite bus and supplying a balanced set of voltages are provided by:

$$P_{ss} = \frac{1}{R^2 + XdXq}\left[V^2\left(\left(\frac{Xd - Xq}{2}\right)\sin 2\delta - R\right) + EVZ\sin(\delta + \theta)\right] \tag{3.10}$$

$$Q_{ss} = \frac{1}{R^2 + XdXq}\left[EVZ\cos(\delta + \theta) + V^2\left(\left(\frac{Xd - Xq}{2}\right)\cos 2\delta - \left(\frac{Xd + Xq}{2}\right)\right)\right] \tag{3.11}$$

Where $Z = \sqrt{R^2 + Xq^2}\ and\ \theta = \sin^{-1}\frac{R}{Z}$. E is the voltage rating of the machine for various loadings.

The field flux linkage will typically remain constant after a change in operating condition because of the lowest field resistance. The current transient that results from a quick change in stator current, such as one brought on by a short circuit, can be divided into two parts. The first element is known as the sub-transient element and the second as the transient element. Other circuits than the field winding on the machine rotor are responsible for the sub-transient component (Gupta & Lynn, 1980). In salient pole machines, these circuits are given by damper windings, but in round rotor machines, the circuits for induced eddy currents to flow are provided by the solid steel rotor. For this dissertation these parameters are paramount when dealing with RMS/EMT simulation in DigSilent chapter 5 and RSCAD-Runtime simulation in chapter 7 as they define short circuit limit values for synchronous generator.

Two connected circuits are formed by the field and damper winding circuits. Both are at rest in relation to each other, yet both rotate in relation to the stator. There are two-time constants in these two circuits: a small sub-transient time constant and a larger transient time constant. The impedance of the stator influences both of these time constants. If the stator is short circuited, the time constants are given by their short circuit values T_d' and T_d'', whereas if the stator is open circuited, they take on their open circuit values T_{do}' and T_{do}'' (Anderson & Fouad, 1977).

The direct axis sub transient reactance, X_d'', determines the magnitude of the stator current during the sub transient period, whereas the transient magnitude is determined by the direct axis transient reactance, X_d'. Tdo" and Td" are typically 0.125 and 0.035 seconds. The sub transient period is less interesting than the transient period since pole sliding has a much longer time period than these values. When configuring protective relays or computing plant ratings, the sub transient duration is critical for the machine's short circuit characteristics. Because the typical values for Tdo' and Td' are 6 and 1.5 seconds, the transient duration is of great importance when evaluating the pole slipping characteristic (Anderson & Fouad, 1977).

In general, there are two types of synchronous machines to consider. The salient pole type and the round rotor. Round rotors are commonly employed in high-speed, two-pole generators powered by steam turbines. For lower speed multiple pole pair generators, such as hydro generators, salient pole designs are used. For both types on no load conditions a pole slip is unlikely to occur since there essentially little mechanical input power to propel the rotor into a pole slip.

3.2.2 Synchronous generator power losses

Understanding the source of losses in synchronous machines as well as their structure and uses is crucial in order to model the effects of non-ideal operating conditions on a synchronous generator's losses. As a result, an overview power losses is provided in this subsection as these will be evident in load-flow studies of DigSilent simulation chapter with which the generated power does not match the output power on loads since the test system is not a classical one but rather a dynamic system which has a variety of loads.

This subsection presents the losses in electrical generating machines, with a focus on ohmic losses and core losses. A common way to define the loss components in synchronous generators is to categorize them according to their origin and mechanisms. Most of the losses generated in the machine are resistive losses, pole surface core losses and stator core c losses. Resistive losses in the stator and rotor account for about 50-60% of the total losses in a generator. Losses in the stator core and the rotor pole surface account for around 20% of the total losses (J. Tervaskanto 2018). Mechanical losses, such as bearing friction and rotor windage, account for a sizable component of the losses. However, mechanical losses are often assumed to be constant across the different operating points of the machine. Therefore, mechanical losses are not examined in this study.

- **Resistive Loses**-Losses in the stator winding, rotor bars, rotor winding, and extra resistive losses are the different types of resistive losses. The resistive losses in the rotor winding are caused by the DC current required to magnetize the poles. Additional losses produced by an alternating current have two basic components. First, the conductor's skin effect and eddy currents, which result in uneven current distribution and further losses. Second, because of the stray fields in the machine, more losses are brought about in the stator coils. Due to the air-gap flux pulsation, the rotor bars experience resistive losses. Due to conductivity of the material, currents flowing in a conductor may result into DC losses:

$$P_{cu} = RI^2 = \frac{l}{\sigma A} I^2 \tag{3.12}$$

Where A refers to the cross-sectional area, l the length and σ is the conductivity of the material. This then concludes that all the losses found in the material are dependent on the operating temperature of that material. Electrical machinery winding temperatures can reach

140°C. The conductivity can be adjusted to any given temperature θ using a professional approximation for more precise loss estimation:

$$\sigma = \sigma_{20}\,[\frac{1}{1+\alpha(\theta-20°C)}] \tag{3.13}$$

Where α in the expression refers to the conductor temperature co-efficient. Assuming a perfectly balanced system for 3-phase electrical machines the losses can be projected as:

$$P_{cu} = 3R_p I_n^2 \tag{3.14}$$

where R_p is the phase resistance and I_n is the nominal current. The reference operating temperatures for electrical machines are typically defined as 95°C for temperature class B machines and 115°C for temperature class F machines in accordance with IEC 60034-2-1 standard. However, according to Equations 3.11 and 3.10, the maximum winding temperatures can be 135°C or 155°C, which would result in higher losses.

In addition to the DC losses, the electrical machine's magnetic field and current variations over time cause eddy currents to form in its windings and other conductive components. In essence, eddy currents in the conductors of electrical equipment are related to two phenomena. The first is the skin- and proximity effect, which is brought on by the conductors' internal alternating stator current and nearby conductors (Islam 2010). Additionally, the conductor's fluctuating stray fields that pass through the conductor in the winding ends and stator slots. In other words, a conducting material will experience a current when exposed to a time-varying magnetic field. The current also generates a magnetic field that is in opposition. A from this phenomenon one can argue that an alternating current in the conductor creates an alternating magnetic field, which in turn creates an electric field that opposes the change in current density. The centre of the conductor experiences the strongest opposing electric field, pushing electrons to the conductor's edge. Uneven current distribution in the conductor causes radial resistance changes in the conductor (Sadarangani 2006). Because the losses in the conductors are greater than just the DC resistance, it is necessary to estimate a separate **AC resistance** coefficient for greater accuracy. Equation 3.10 can be used to calculate the AC resistance by adding a particular eddy current coefficient, k_r:

$$R_{ac} = k_r \frac{l}{\sigma A} \tag{3.15}$$

The fraction of the AC and DC resistances in the slot-embedded portion of the winding is known as the eddy current factor k_r:

$$k_r = \frac{R_{AC}}{R_{DC}} \tag{3.16}$$

The equations above are frequently used to calculate resistive losses in the stator core region and rotor magnetization losses. The end winding effects and the losses on the rotor pole surface, and damper bars amongst other losses are often referred to as additional synchronous machine losses. (Karmaker 1992) presents that these losses are a consolidation of the losses in the following areas of the machine:

- Loss in stator teeth, yoke iron due to stray flux
- Loss in the rotor pole surface
- Loss from constructional sources i.e., rotor eccentricity
- Loss in the end plates and winding ends

Stray fluxes penetrating the end area in axial direction, generating eddy current losses, cause losses in the winding ends and end plates. The geometry of the winding end has a significant impact on end winding losses. The end winding leakage inductance can be used to estimate the losses at the winding ends.

The harmonics in the air-gap flux cause the rotor pole surface and rotor bar losses. Time harmonics, which vary with time, and space harmonics are two types of harmonics. Time harmonics can be generated by, for example, the machine's power supply. The space harmonics are produced by the machine slotting and the non-sinusoidal distribution of the coils. The permeance variations of the stator slot-tooth cause ripples in the air-gap flux density as the slot opening size changes (Pyrhonen et al. 2013). Additionally, the coils are spatially displaced, resulting in variations in permeance as a function of space angle. The time and space harmonics cause the air-gap flux to pulsate, resulting in eddy current losses on the rotor poles, particularly the damper bars. Moreover, harmonics can be caused by unbalanced phase currents or rotor constructional eccentricity.

- **Iron losses (core losses)-**Losses in electrical steel are referred to as iron losses or core losses. The majority of the iron losses occur in the stator core and on the rotor pole surface, where the ferromagnetic iron core is subjected to a time-varying magnetic field. Total iron losses are classified as hysteresis loss, eddy current loss, and excess loss.

$$P_{fe} = P_{hy} + P_{ed} + P_{ex} \tag{3.17}$$

The power used by the magnetic domains during a change in magnetic orientation is known as hysteresis loss, whereas the traditional eddy current losses are increased when iron currents caused by changing magnetic fields are induced. Localized, microscopic eddy currents are thought to be the source of excess losses near the moving magnetic domain walls

(Boon & Robey 1968). The domain walls that separate the magnetic domains and the iron losses are connected. The ferromagnetic steel sheets are made up of several magnetic domains with various magnetic moment axes. The magnetization gradually shifts to match the direction next to it between the domains, inside the wall area. The movement of the domain walls, on the other hand, is not continuous and is determined by impurities or defects in the material surrounding the walls. The magnetization direction jumps between local energy minimums, resulting in a nonlinear relationship between B and H and material losses. The hysteresis loss is the energy consumed in the domain during the change of magnetization direction. A hysteresis loop, which depicts the relationship between magnetic flux density and magnetic field strength, is frequently used to describe the B h relation. The hysteresis loop also displays magnetic flux density saturation and the amount of remanence magnetism in the material when the magnetic field strength is reduced to zero. A graphical description of the procedure is presented in Figure 3.10 below.

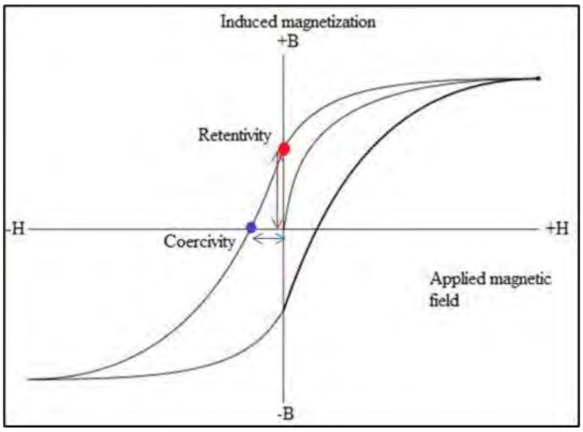

Figure 3.9: Schematic diagram of hysteresis loop (Pyrhonen et al. 2013)

The machine's time-varying magnetic field induces eddy currents in the stator's steel sheets, known as classical eddy currents which are similarly generated as resistive losses. When the flux density changes rapidly, a voltage is induced along its path. According to I^2 R, power loss is caused by material resistivity. The classical eddy current model assumes that the magnetic flux density in the material is uniform. However, the material's microscopic structure causes additional eddy current losses, also known as the excess loss. Excess losses are defined as any losses that cannot be explained by eddy current or hysteresis losses. According to (Roshen 2007), the excess losses are microscopic eddy current losses induced around the moving domain walls of the material during magnetization. Because the domain walls account for only a small portion of the total area of the material, the magnetization within the wall area must be much greater than the average magnetization of the material. As a result, the eddy currents around the walls must be greater than the classical eddy current model with uniform magnetization predicts.

- **Losses due to unbalanced voltage** -Voltage imbalances in power systems can occur as a result of unbalanced loads, large single-phase loads, or blown fuses. Unbalance can also be produced by electrical machines if the number of winding turns is not equal or if the rotor is misaligned. Unbalanced voltages cause a variety of issues in electrical motors and generators. Even minor voltage imbalances can cause significantly higher current imbalances, resulting in additional losses and heating. Furthermore, unbalanced conditions create a counter rotating field in the airgap, causing pulsations in the air-gap flux and additional losses on the rotor pole surfaces and damper bars.

A three-phase system can be represented by symmetrical components, with three phasors representing the system's phases. The magnitudes of the voltages are sinusoidal, equal in, and 120 degrees apart in a perfectly balanced system. Unbalanced systems can have unequal voltage magnitudes, shifted phase angles, or phase distortion. To analyse system unbalance, divide the components into zero sequence U_0, positive sequence U_1, and negative sequence U_2 voltages.

$$\begin{bmatrix} U_0 \\ U_1 \\ U_2 \end{bmatrix} = \frac{1}{3}\begin{bmatrix} 1 & 1 & 1 \\ 1 & a & a^2 \\ 1 & a^2 & a \end{bmatrix}\begin{bmatrix} U_a \\ U_b \\ U_c \end{bmatrix} \tag{3.18}$$

Where the stator voltages are denoted by U_a, U_b and U_c then:

$$a = e^{j\frac{2\pi}{3}} \tag{3.19}$$

Any three-phase system can be divided into positive, negative, and zero sequence components using the above equations. Because there is no neutral path for zero sequence current in electrical machines, the zero-sequence component can be ignored. As a result, an unbalanced system has both positive and negative sequence components (Von Jouanne & Banerjee 2001). The positive sequence component represents three equal phasors that are 120 degrees displaced and have the same phase sequence as the original phasors. Only a positive sequence component generates positive torque in a perfectly balanced system. In an unbalanced system, a negative sequence current will flow. The negative sequence component's phase order is opposite that of the positive sequence component, resulting in counter-rotating flux in the airgap. The generated flux rotates in the opposite direction as the positive flux, lowering the output speed and torque. Furthermore, because the negative sequence impedance is low, the negative sequence voltage can generate a large negative sequence current.

The positive and negative fluxes rotate in opposite directions at the synchronous frequency. The constructive and destructive sequence fluxes combine twice per revolution, resulting in twice-line-frequency air-gap flux pulsations and currents on the rotor pole surfaces. These currents cause additional losses, which are most noticeable on the rotor bars, which have a high conductivity compared to the surrounding rotor core material. Furthermore, the negative sequence component results in additional losses on the stator winding. Because of the phase imbalance, total stator winding losses increase. When only one phase carries the nominal current, the losses are three times higher than in the perfectly balanced case.

(Daniel Donolo et al. 2016) investigated the effects of negative sequence voltage on the core losses of an induction machine and discovered that the losses caused by the negative sequence component are negligible when compared to the losses caused by the positive sequence component. IEC has defined a maximum negative sequence current to limit unwanted effects in rotating electrical machines. The maximum continuous negative sequence current for an indirect cooled SPSG must be less than 8% of the nominal, and 5% for direct cooled SPSGs, according to IEC 60034-1. In fault conditions, the same standard defines a maximum negative sequence current as:

$$\left(\frac{I_2}{I_n}\right)^2 t \tag{3.20}$$

Where t is the duration of the fault. The maximum value for directly cooled SPSGs is 15 seconds, and the maximum value for indirectly cooled SPSGs is 20 seconds. A more general definition for voltage unbalance levels can be found in IEC Electromagnetic compatibility standard 61000-2-2, which defines maximum unbalance as a ratio of 2% between the positive and negative sequence $\frac{U_2}{U_1}$ voltages. However, because the terminal voltage of synchronous generators is generally adjusted by the AVR, the applicability of voltage unbalance may not be as reasonable as current unbalance for SPSGs. (Brekken and Mohan 2007) investigated methods for reducing airgap flux pulsation in a doubly fed wind generator by injecting a negative sequence component into the rotor current. It was discovered that compensating negative 27 sequence current can not only reduce unwanted torque and power pulsations, but also compensate for current imbalances and mechanical wear.

Energy is frequently produced using salient pole synchronous generators. Generators can be used in islanded networks or as an emergency backup power source in remote locations when combined with internal combustion engine as a prime mover. It is important to note that for a generator to perform at heightened efficiency the converted input power needs to be relative to the output power of the machine:

$$P_{conv} = 3E_A I_A cos\gamma \tag{3.21}$$

Where γ is the angle between E_A and I_A

Then the output real and reactive power will be:

$$P_{out} = 3V_\phi I_A cos\theta \quad (3.22)$$

$$Q_{out} = 3V_\phi I_A sin\theta \quad (3.23)$$

To simplify the phasor diagram, an assumption can be made that the armature resistance R_A is negligible and that the load connected to it is lagging in nature. This results in the phasor diagram shown below:

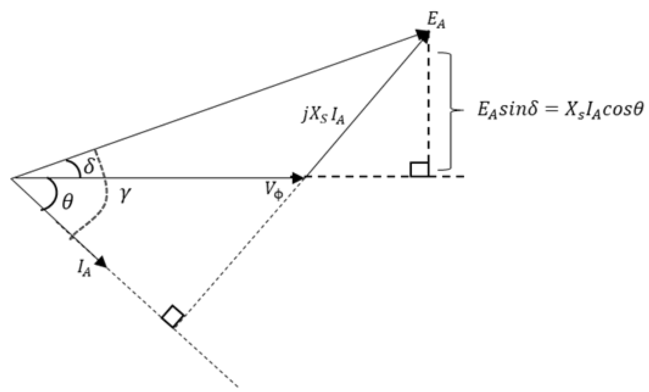

Figure 3.10: Simplified phasor diagram of synchronous generator (Brekken and Mohan 2007).

Based upon the above phasor diagram a new expression for output power can be attained:

$$P = \frac{3E_A sin\delta}{X_s} \quad (3.24)$$

Looking at this new expression it is quite discernible that power is reliant on:

- The angle between V_ϕ and E_A which is δ.
- The machine's torque angle is identified as δ.

3.2.3 Generator capability chart

Generator operators utilize the generator capability, or operating chart, to display the operational limits of the generator. Its two axes are actual and reactive power. It is a function of control room operators to ensure that generators when connected to the grid are operated within their design limits which are clearly defined on the capability charts provided by for each turbogenerator (Nilsson & Mercurio, 1994). Referring to the charts shown in Fig 3.17 the limits are as follows:

- Rotor excitation limit
- Stator current limit

- Turbine power limit
- Practical stability limit
- Theoretical stability limit

At any time, the working point of a generator can be checked by plotting the loading of megawatts and megavars (or the power factor), and this point must lie within the limits above. Operation at lagging power factors outside the limits of rotor and stator current will result in overheating of the generator windings. This can be checked by plotting the loading of real power and reactive power and this point must lie inside the limits above. On the other hand, operation of leading power factor outside the limits of the practical stability line could result in the generator falling out of synchronism with the system, and violent disturbances could occur. Such a condition would have to be corrected by reduction of megawatt loading and increasing the rotor excitation of the synchronous generator concerned (Nilsson & Mercurio, 1994).

Under normal conditions, the rotor current must not be exceeded, as it will cause overheating of the rotor windings and damage to the insulation. The main exciter will be overloaded which might cause sparking at the brushes. This also explains why the loading of the prime mover and hence the generator output should not exceed the full-load rated value. It is also paramount that the rotor is kept within its operating stability limits which means that at all times there must be sufficient excitation to prevent pole slipping or hunting.

A snapshot of a schematic of a typical stability diagram is shown in Figure 3.12 below. The diagram represents the load capability characteristic for a turbine generator. The chart indicates that so long as the operating point of the machine is within the envelope plane, then the generator is not overloaded and neither unstable.

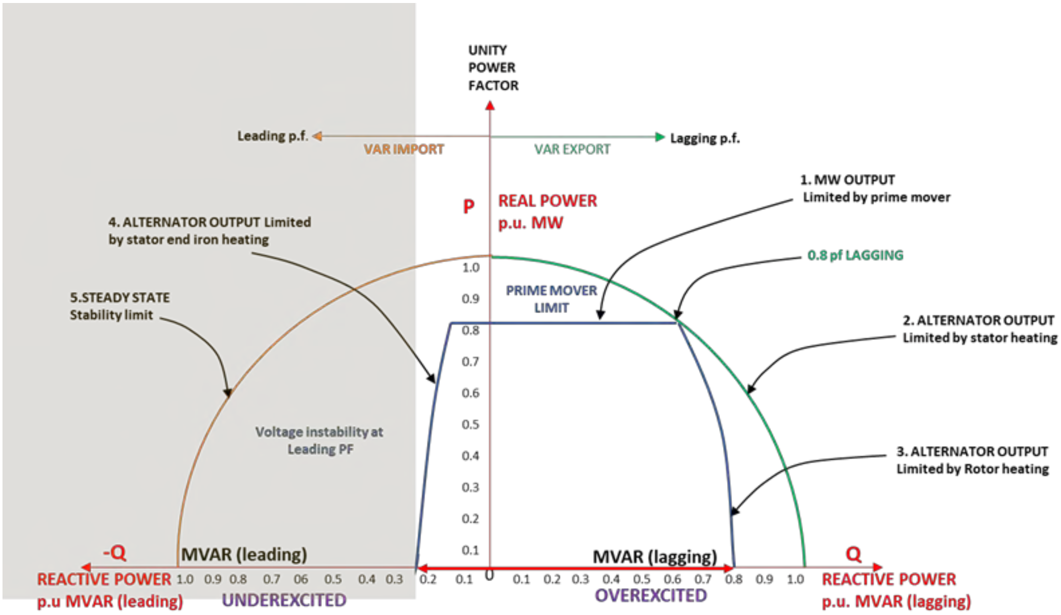

Figure 3.11: Synchronous generator stability diagram (Nilsson & Mercurio, 1994).

X_q of a generator determines the theoretical stability limit. X_d parameter is most usually used when discussing round rotor machines. X_d and X_q are approximately equivalent in a round rotor machine. the practical stability limit line given by Alternator output due to stator end iron heating indicates that the generator is always operated to the right of the theoretical stability limit. This allows for load fluctuations and increases the transient stability margin in the event of a power supply short circuit fault (Nilsson & Mercurio, 1994).

The generator could run longer than its theoretical stability limit. The generator can be operated at load angles up to 130 degrees depending on the impedance of the interface linking it to the system. This raises the generator's capacity to absorb reactive power above the - $\frac{-V^2}{Xd}$ level of theoretical stability limit. The theoretical no-load level becomes $\frac{-V^2}{Xq}$ if the AVR is able to supply negative field current. The generator is likely to become unstable during power system short circuit problems, therefore operating beyond the stability limit does not happen in practice (Eberly & Schaefer, 1995).

It is standard practice to install minimum excitation limiter circuitry to embedded generator AVRs in order to avoid the absorption of large amounts of reactive power during high system voltages, even if some generators are not required to have any reactive power absorbing capabilities. This stops the generator from overheating due to excessive grid voltages and pulling out of step. In most cases the control of the amount of reactive power supplied is also done by National Control, who monitor the voltage at various points on the grid through SCADA protocol communications. They then issue instructions to different units type of to increase or decrease their excitation accordingly.

3.2.4 Parallel operation of generators

Since electricity cannot be stored, it must be used as it is generated. As a result, it is critical that the amount of electricity required at any given time correspond to the amount of electricity generated. More generating units must be brought online as demand grows. This is planned in advance because starting-up and shutting-down operations for many types of power plants are slow and complicated. Economics are also important because some power plants generate electricity at a lower cost than others. To account for variations in demand and unforeseen generating constraints, the system requires some generating capacity reserves. Spinning and standby reserve are examples of these (Beukman, et al, 2011). Spinning reserve is available when generators are not fully loaded, whereas standby reserve is available when generators are off load but can be quickly started up and loaded (gas, hydro, and pumped storage). When all reserves are depleted, Eskom will be forced to reduce demand through voluntary, and eventually involuntary, load shedding.

Because electricity demand fluctuates, different types of power plants are required to meet the fluctuating demand in the most efficient and effective manner. Power stations are classified into two types: base load stations and peak load stations. shedding. So, considering this demand, various generators need to be connected in parallel to inject different sources in the grid (Eskom power system course manual, 2011).

An isolated synchronous generator that supplies its own load independently of other generators is extremely rare in today's world. In this study the generators in subject operate in parallel, so to say in all Eskom generating units, generators are ran parallelly. In all typical generator applications, multiple generators operate in parallel to supply the power required by the loads. There were clear benefits to be seen in such operations as:

- A group of generators can supply a greater load than a single machine.
- Having multiple generators increases the reliability of the power system because the failure of one of them does not result in a total loss of power to the load.
- Having multiple generators running in parallel allows for the removal of one or more of them for shutdown and preventive maintenance.

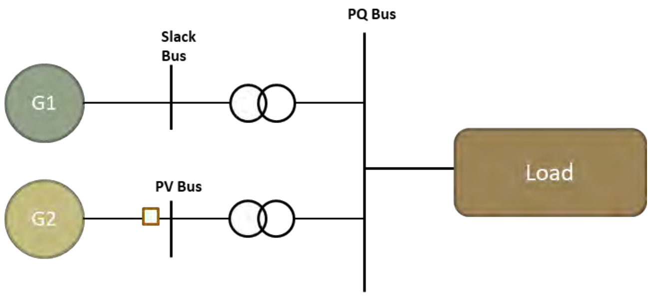

Figure 3.12: A generator being paralleled with the running grid (Beukman, et al, 2011).

Figure 3.13 depicts a synchronous generator G1 powering a load, with another generator G2 about to be paralleled with G1 by closing the switch. If the switch is closed randomly, the generators may be severely damaged, and the load may lose power. If the voltages in each conductor are not exactly the same, there will be a very large current flow when the switch is closed. To avoid this issue, all three phases must have the matching voltage magnitude and phase angle as the conductor to which they are connected.

To the following paralleling conditions must be met in order to achieve this match (Eskom power system course manual, 2011):

- The two generators' rms line voltages must be equal.
- The phase sequence of the two generators must be the same.
- The two a phase, phase angles must be equal.
- The frequency of the new generator, known as the approaching generator, must be slightly higher than the running system's frequency.

These conditions are applied when synchronising the generators to the system. However, for this operation to be fully realised, conditions between the busbars and the machines needs to be fulfilled also (Eskom power system course manual, 2011).

- The voltage of the incoming machine needs to be the same as the system busbar voltage.
- The frequency of the incoming machine must be the same as the busbar frequency.
- The phase of the generator voltage must be identical with the phase of the busbar voltage relative to the feeders.

Large power transients will occur until the generators stabilize at a common frequency if the frequencies of the generators are not very nearly equal when they are connected together. The frequencies of the two machines must be very close, but not exactly equal (Beukman C. etal, 2011). They must differ by a small amount so that the phase angles of the approaching machine change slowly with respect to the phase angles of the running system. The angles between the voltages can thus be observed.

When paralleling generators, regardless of the original source of power, all prime movers tend to behave similarly - As the power drawn from them increases, so does the speed at which they turn. In general, the decrease in speed is nonlinear, but a governor mechanism is usually included to make the decrease in speed linear with an increase in power demand. Whatever governor mechanism is used on a prime mover, it is always set to provide a slight drooping characteristic as load increases. For this research this variable is evident in the parameters of governor control to the generators in the simulation chapters (Chapter 5 and Chapter 6). The equation defines the speed droop (SD) of a prime mover.

$$SD = \frac{n_{nl} - n_{fl}}{n_{fl}} \times 100\% \tag{3.25}$$

Where n_{nl} is the prime-mover speed at no load and n_{fl} is the prime-mover speed at full load. Most generator prime movers have a speed droop of 2 to 4%. Furthermore, most governors have some kind of set point.

After synchronising, an alternator is loaded by adjusting the governor setting to admit more steam. This tends to advance the rotor, and a synchronising or load current flows from the machine to the busbars. However, this needs to correspond to an exact balance of driving and resisting torques in order to keep the machine in step. The greater the rate of admission of steam to the prime mover, the greater the load is assumed by the generator. The governor setting can be altered by remote control from switchboard, to provide desirable rate of steam admission. Figure 3.14 shows some examples of governor set points for speed-versus -power and frequency-versus-power curves respectively.

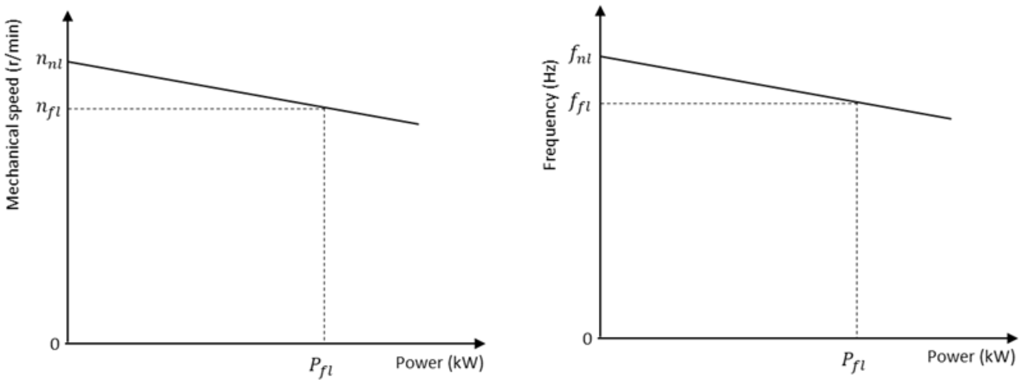

Figure 3.13: Governor setpoint curves (Beukman C. et al, 2011).

It is important to note that changing the excitation does not alter the power output, but rather changes in the amount of reactive load are seen. In a generating station, the loads are shifted from one machine to another by manipulating the governor settings and the reactive power is controlled by the excitation. An increased excitation to the machine causes it to take an increased share of the lagging reactive power. At the same time there is a tendency to raise the busbar voltage since the machines are relieved of some of their lagging current components. Figure 3.14 depicts the result of connecting a generator in parallel with another of the same size. The fundamental constraint in this system is that the sum of the real and reactive powers supplied by the two generators must equal the P and Q demanded by the load. The frequency of the system is not constrained to be constant, and neither is the power of a given generator. Figure 3.15 illustrates the power-frequency diagram for such a system immediately after G2 has been paralleled to the line.

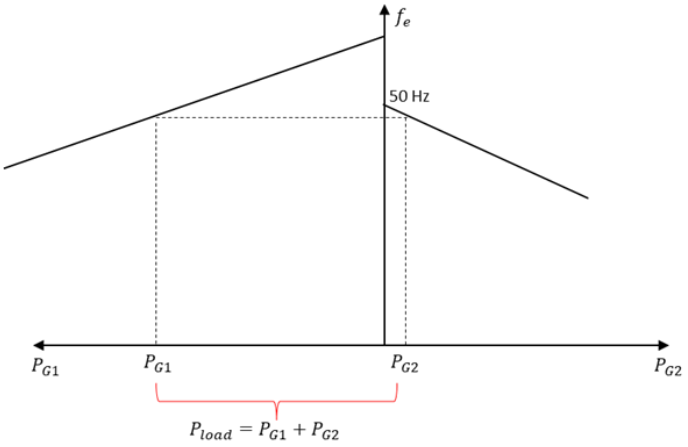

Figure 3.14: House diagram at the moment G2 is paralleled to the system (Beukman C. et al, 2011).

If the slopes and no-load frequencies of the speed droop (frequency-power) curves of the generators are known, the powers supplied by each generator and the resulting system frequency can be calculated quantitatively. Thus, when two generators of comparable size operate in parallel, a change in one of their governor set points affects both the system frequency and the power sharing between them. Ideally, only one of these quantities should be changed at a time.

When a synchronous generator is connected to a power utility grid, the power system is frequently so large that nothing the generator operator does has much of an impact on it. The concept of an infinite bus idealizes this idea. An infinite bus is a power system with such a large capacity that its voltage and frequency remain constant regardless of how much real and reactive power is drawn from or supplied to it, such a system is shown in Figure 3.16, while Figure 3.17 depicts the reactive power-voltage characteristic.

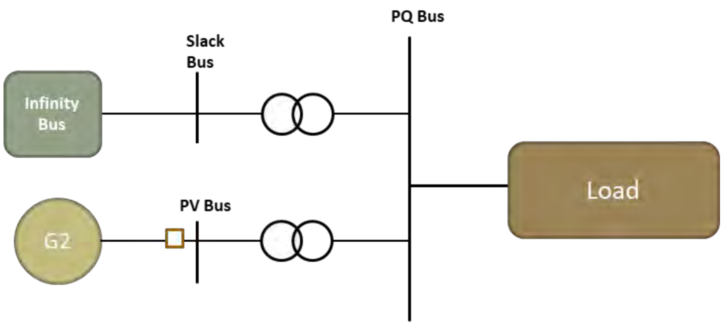

Figure 3.15: Synchronous generator in parallel with infinite bus (Beukman C. et al, 2011).

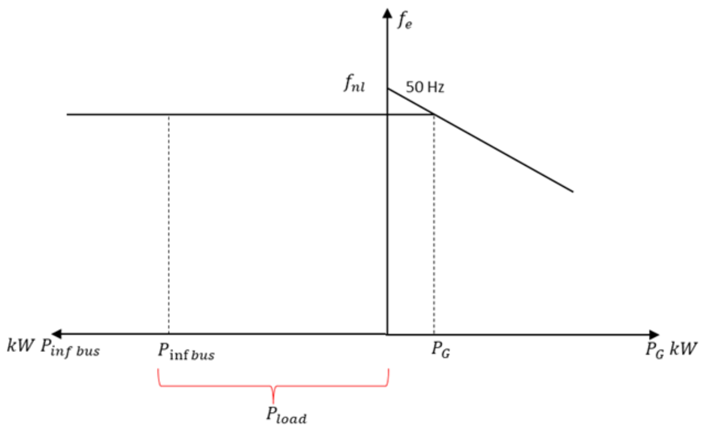

Figure 3.16: House diagram for generator paralleled with infinite bus

When the excitation is changed the amount of electromagnetic flux in the machine is altered accordingly. This would normally change the voltage at the generator terminals. But when the machine is synchronised to a large grid the voltage is fixed by the average voltage of all the generators. So, changing the excitation of one machine does not really affect the system voltage. To summarize when a generator is connected to an infinite bus (Eskom power system course manual, 2011):

- The system to which the generator is connected controls the frequency and terminal voltage of the generator.
- The generator's governor set points control the real power supplied by the generator to the system.
- The field current in the generator regulates the reactive power supplied to the system by the generator.

The situation is similar to how real generators work when connected to a large power system

3.3 STEADY STATE SYSTEM ANALYSIS

The response of a synchronous machine to a progressively rising load is referred to as steady-state stability. It is primarily concerned with determining the upper limit of machine loading without losing synchronism, given that the loading is steadily increased. As the three stages of the power system are conceptualised as generation, transmission, and distribution. The system is complete with a number of components at each level. Synchronous generators, which are the primary sources of power generating, are found on the generation side. Power transformers, transmission lines, cables, capacitors, and reactors make up the transmission network. Power transformers, distribution lines, and a range of loads, including residential, commercial, and industrial loads, are also components of distribution networks. Industrial and commercial loads can include machinery loads like induction motors, whereas residential loads can include lighting and heating loads. These various component kinds have an impact on the way the power system functions (Tomsovic & Venkatasubramanian, 2005).

The system is believed to be stable in a steady state, which can occur before or after the disruption. In a steady state, the power generated equals the total of power losses and load power demand, and the power system frequency is stable which is often regarded as 50Hz in the South African grid. The steady-state analysis focuses on the economic and reliability aspects of the power system. Power flow analysis is used to determine voltages, real and reactive powers, and other system parameters in order to study the system's steady-state operation. This is the method employed for network analysis planning and operation (Tomsovic & Venkatasubramanian, 2005).

3.3.1 Power flow in a steady state

The goal of a power flow study (also known as a load-flow study) is to ascertain the voltages, currents, and real and reactive power flows in a system under specific load conditions. for this dissertation this concept will be very useful when simulating and validating load flow studies in Chapter 4 and 5 (DigSilent PowerFactory® and RSCAD-FX respectively). Planning ahead and taking many hypothetical scenarios into account are the goals of power flow analyses. Can the remaining transmission lines in the system handle the necessary loads without going beyond their rated values, for instance, if a transmission line needs to be pulled off the air for maintenance? (Johnson, et al., 2017). Power system planning engineers often need to bother themselves with a number of nodes in the system under study as the basic load-flow analysis is derived from nodal equations for instance in a 3-bus system the equation will be:

$$\begin{bmatrix} Y_{11} & Y_{12} & Y_{13} \\ Y_{21} & Y_{22} & Y_{23} \\ Y_{31} & Y_{32} & Y_{33} \end{bmatrix} \begin{bmatrix} V_1 \\ V_2 \\ V_3 \end{bmatrix} = \begin{bmatrix} I_1 \\ I_2 \\ I_3 \end{bmatrix} \tag{3.1}$$

where I_i is the current injected at each node, V_i are the bus voltages, and Y_{ij} are the components of the bus admittance matrix.

Relationship between the per-unit current injected into the system at bus I and the per-unit real and reactive power supplied to the system at that bus is given by:

$$S_i = V_i I_i^* = P_i + jQ_i \tag{3.2}$$

where P_i and Q_i are the per-unit real and reactive powers, and V_i is the per-unit voltage at the bus. I_i^* is the complex conjugate of the per-unit current injected at the bus.

Each bus is related with the 4 variables P, Q, V, δ. Meanwhile, each bus is related to two power flow equations. The two of the four variables in a power flow analysis are defined, while the other two are uncertain. In this manner, we have exactly as many equations as there are unknowns. The known and unknowable variables are influenced by the bus type. A power system's buses can be categorized into one of three categories:

- **Load bus (P-Q bus)** - a bus that specifies the real and reactive power and for which the bus voltage is determined. Load buses are those without generators. V and δ are unknown in this context.
- **A generator bus (P-V bus)-** is a bus where the magnitude of the voltage is defined and maintained constant by altering the field current of a synchronous generator. In addition, we assign real power generation to each generator based on economic dispatch. Q and are unknown in this δ context.
- **The slack bus (swing bus)-** is a particular generator bus that serves as the reference bus. Its voltage is supposed to be constant in both amplitude and phase (for example, $1\angle 0°$ pu). P and Q are unknown in this context.

It is important to note that the power flow equations are non-linear and so cannot be solved analytically. Solving such equations necessitates the use of a numerical iterative procedure. A conventional method is then followed:

- Make a Y-bus bus admittance matrix for the power system.
- Estimate the voltages (both magnitude and phase angle) at each bus in the system.
- Input the power flow equations and calculate the deviations from the solution.
- Update the estimated voltages using various well-known numerical techniques (for example, Newton-Raphson or Gauss-Seidel).
- Repeat step 5 until the deviations from the solution are as small as possible.

3.4 TRANSIENT STABILITY

The response to large disturbances, which can produce considerable changes in rotor speeds, power angles, and power transfers, is referred to as transient stability. Transient stability is a quick phenomenon that usually manifests itself within a few seconds. It is normally caused by sudden outage of a line or sudden application or removal of loads.

Determine whether or not synchronism is maintained after the machine has been subjected to significant disruptions is the goal of transient stability investigations. For a rapid forecast of stability, the equal area criterion can be applied (Saadat, 2005). Think about a synchronous machine that is linked to an infinite bus bar. The swing equation derived from second order differential in terms of constant inertia without considering damping is given by:

$$\frac{H}{\pi f_0}\frac{d^2\delta}{dt^2} = P_m - P_e = P_a \tag{3.26}$$

Where P_m is the mechanical power and P_e is the electrical power of the machine, P_a is the accelerating power. Scenarios for the equal criterion are depicted in Figure 3.2 below.

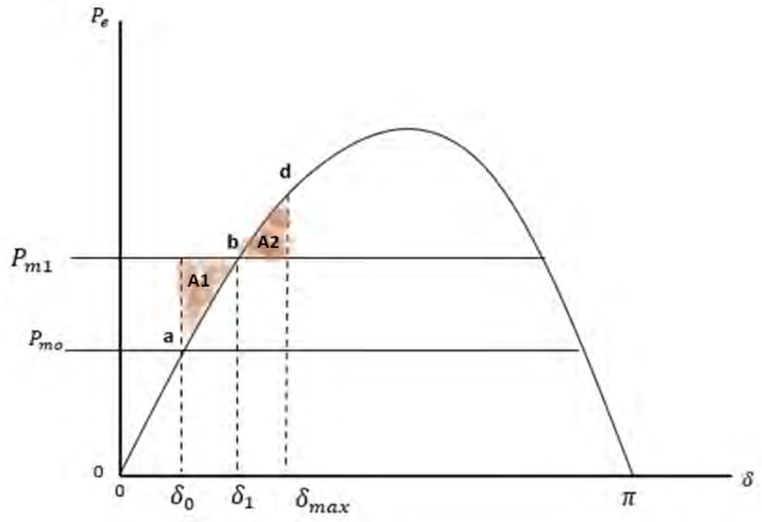

Figure 3.17: Sudden change of load in equal criterion (Saadat, 2005).

The horizontal line P_{m1}represents a sudden step rise in input power. Because $P_{m1} > P_{e0}$, the rotor's accelerating power is positive, and the power angle increases. The rotor's excess energy during the initial acceleration can then be deduced (Saadat, 2005).

The electrical power increases as δ increases, and when $\delta = 1$, the electrical power matches the increased input power P_{m1}. In the case of $P_m < P_e$, the rotor decelerates toward synchronous speed until $\delta = \delta_{max}$. The greatest additional power P_m that can be applied to ensure stability can be determined using the equal area criterion.

3.5 DYNAMIC STABILITY

Dynamic stability is the ability of a system to respond to tiny perturbations that cause oscillations. If these oscillations don't become larger than a specific amplitude and disappear promptly, the system is said to be dynamically stable. If the amplitude of these oscillations keeps increasing, the system is dynamically unstable. This kind of instability typically results from connections between control systems (Johnson, et al., 2017).

Due to increased complexity, increasing uncertainties, and market demands induced by changing types of loads and generation, future power systems may operate closer to their stability limit. Corrective control and stabilization are becoming potentially practical methods for enabling safer system operation. This research effort is to focus on the impact of dynamic maintaining system on the synchronous generators when there's power swing, hence it is crucial to explore the characteristics of synchronous machines in relation to rotor angle stability. Also being explored are control techniques to stabilize the test system.

3.5.1 Dynamics of a synchronous generator

The Kinetic Energy of the Rotor at Dynamics of a Synchronous Machine is where define the inertia constant H such that where it follows that M is also defined. Using G (generator MVA base) as the starting point. For the time period of interest say 1s, the rotor's speed changes by an inconsequential amount as it travels through Dynamics of Synchronous Machine then after it surpasses this period it changes rapidly (Saadat, 2005). H constant can be defined such that:

$$GH = KE = \frac{1}{2} M w_{se} MJ \tag{3.27}$$

Where G = three-phase MVA rating (base) of machine

H = inertia constant in MJ/MVA or MW.sec/MVA

Dynamic models must be incorporated in the power system simulation tool in order to measure the contribution of the dynamic features of the components of a power system. To simulate synchronous and asynchronous machines, for example, the control systems of the voltage regulator and the speed governor must be included. The power system stabilizer must be incorporated in the synchronous generator model for further research, such as small signal stability (Farmer, 2001). For the this study these dynamic models will be very useful in simulation chapters to monitor the rotor speed against rotor angle for out-of-step detection.

3.5.1.1 Automatic voltage regulator and excitation system

The excitation system's primary role is to supply direct current to the synchronous generator's field winding. Figure 1 depicts how this fits into the synchronous machine's overall system paradigm. The excitation system should automatically modify the excitation field in order to maintain the terminal voltage under normal and abnormal network disturbance situations (Farmer, 2001).

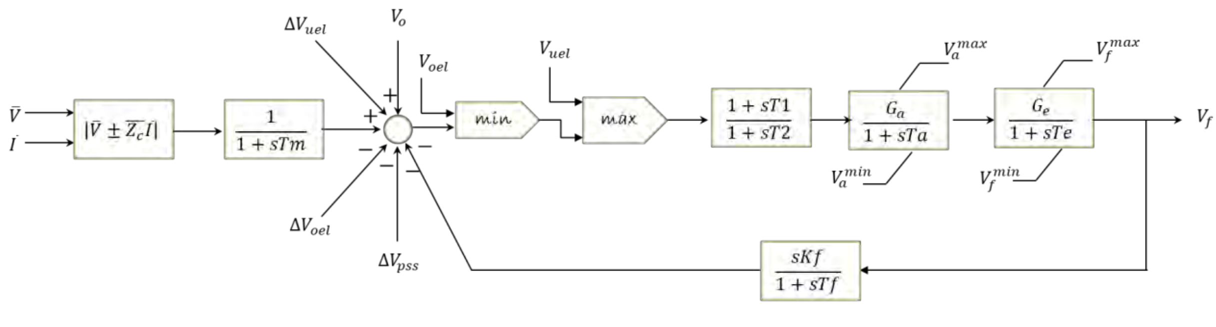

Figure 3.18: AVR and excitation model simple generic model (Van Cutsem, 2017).

The excitation system model is based on Std 421.5, 5th edition, published in 2005 by the Institute of Electrical and Electronics Engineers. This will serve as the foundation for the explanation of the parameters to take into account while setting up the simulation model that follows later in the dissertation.

3.5.1.2 Power system stabilizer

For static accuracy, a large loop gain is necessary, however this "cause[s] an undesired dynamic response and possibly instability The power system stabilizer (PSS) is placed in series with AVR to address this issue see Figure 3.19. The addition of time (T_a, T_e, and T_2) results in a phase advance and is the primary source of the small signal stability problem. The complex eigenvalues connected to the unstable mode will be moved to the required area of the complex plane by the introduction of the PSS (Van Cutsem, 2017).

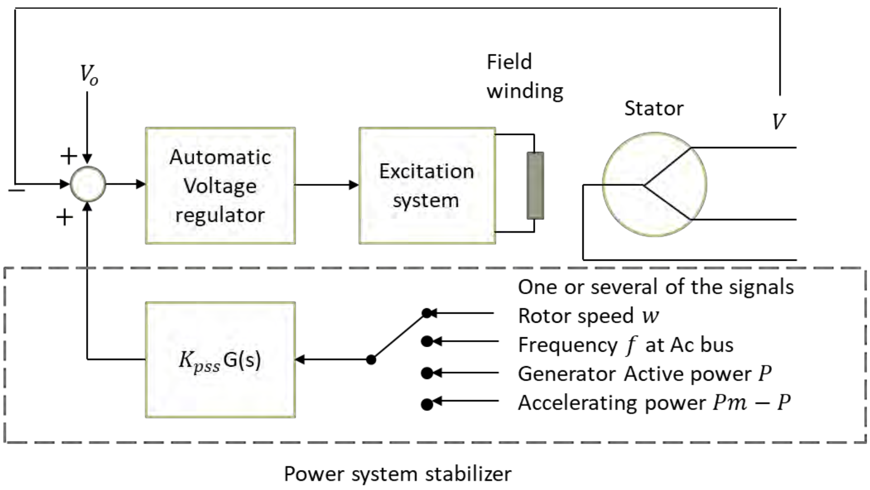

Figure 3.19: PSS added to lessen phase progress brought on the series time restrictions (Van Cutsem, 2017).

3.5.1.3 Speed/turbine governors

Governors are not examined during first swing transient stability investigations, mostly because the governor's responses during these events are ignored. In essence governors are neglected if the duration of the dynamic study is less than 10 seconds. Their main purpose is to control turbine speed and/or load. The full thermal cycle for a speed governor is depicted in Figure 3.19. The illustration identifies the speed governor as SG, the control valves as CV (notice that the SG adjusts these during normal operation), the intercepted valve as IV (which is closed when over speeding), the main stop valve as MSV, and the reheating stop valve as RSV (which is activated during an emergency) (Bickel, 2018).

Figure 3.19 also shows how the shaft's speed is tracked and the valves are appropriately opened to regulate the steam flow. The feedback of the speed error to control the gate position is the main mode of operation for the speed/load control function.

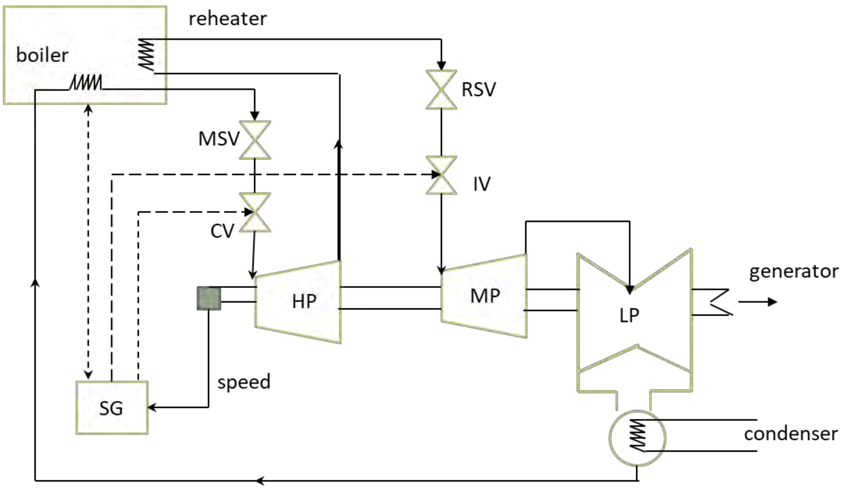

Figure 3.20: Position of speed governor in thermal cycle (Bickel, 2018).

3.5.2 Stability of embedded generator: Pole slipping probability

In comparison to bigger grid-type generating sets that are connected to transmission circuits, embedded generators that run in parallel with utility distribution systems are more likely to experience transient instability. Utility distribution systems' low inertias, small time constants, and lengthy fault clearance durations are to blame for this. The ability of a generator to generate forces that act to return it to equilibrium after a transient disturbance is known as transient stability. Switching activities, electrical problems, and load variations can all result in transient disturbances (Saadat, 2005). This subsection explores the parameters which have most effect on stability of fixed generators in electrical grid.

The distribution system of the regional electricity companies can be regarded of as an endless bus for the majority of embedded generators, whose frequency and voltage are unaffected by the functioning of the embedded generator. Because the one machine-infinite bus model is the most fundamental system for stability analysis, this simplifies the discussion of stability. The system can be represented as a two-machine system, which can also be easily analysed, if the regional electricity companies' bus is not infinite (Farmer, 2001).

The variables that impact the stability of synchronous generators can be divided into two groups: those that are influenced by the generator and its control equipment and those that depend on the setup and operation of the system to which the generator is linked. The inertia of the generator and the direct axis transient reactance are the two key generator parameters that have the largest influence on stability. The inertia constant, H in kWs/kVA, is the most usable measure of generator inertia. The fundamental advantage of utilizing H over alternative rotational inertia metrics is that its value is reasonably constant across a large variety of generator sizes and kinds, making machine comparisons easier (Farmer, 2001).

3.5.2.1 Transient Reactance Xd' & Inertia Constant

In terms of stability, the higher the generator's H value, the more stable it will be. The machine load angle at which the fault is removed decreases with increasing inertia for a given fault clearing time. Because the machine requires more acceleration energy to move its rotor, it appears less responsive and better capable of withstanding a mismatch between generator input and output powers. As it influences the amplitude of the generator's transient power load angle characteristic, the direct axis transient reactance, Xd', is also an important metric of transient stability. This provides a stronger decelerating force on the generator rotor after a transient disturbance, which aids stability.

3.5.2.2 Short Circuit Time Constant, Td'

When it comes to short circuit problems, the parameter Td' comes in handy. Td' is the time it takes for the machine's reactance to move from the transient value Xd' to the synchronous value Xd after a transient. With this adjustment comes a commensurate drop in the generator's output power capabilities, and hence its ability to produce decelerating forces in reaction to a disturbance. The continuous flux theorem does not hold if the generator is subjected to a severe fault that is cleared in a few hundred milliseconds due to the decrease in flux generated by the fault (John Wiley & Sons, 2012). Because embedded generators have higher per unit resistances than larger grid type generators, they have smaller time constants.

3.5.2.3 Damping Power Provided by Generator and AVR

The damping power that the generator produces is another element that might affect stability. This primarily depends on the machine's damper winding type, the level of armature/tie-line resistance, and the AVR parameters. By exerting a decelerating force on the rotor during rotor acceleration, a positive damping coefficient will promote stability. The AVR employed determines the impact that the sum of the armature and tie line resistance has on the damping coefficient (Van Cutsem, 2017). A drop in the damping coefficient due to an increase in resistance will cause the machine to become negatively damped if the AVR is not in use. This damping is the machine's natural dampening. If the AVR is in use, a rise in resistance causes the AVR's damping to increase. A large resistance can enhance overall damping since the AVR's damping predominates over the generator's natural damping.

However, a mistuned AVR may exacerbate the damping. The damping may turn negative if the AVR's loop gain is set too high. The high gain required to achieve a modest steady state voltage error will stay high during transient disturbances if the AVR lacks an adequate value of stabilizing derivative feedback signal. This may cause rotor oscillations to grow in size until the generator loses stability and pole slippage takes place. Dynamic instability is what this is known as, and the AVR frequently needs to be enhanced with additional stabilizing feedback signals to avoid it (Van Cutsem, 2017).

3.5.2.4 Governors of Generator

The governor may significantly improve the critical clearing time, depending on the governor/prime mover set employed. The critical clearing time can be enhanced by governor action if the system's total time lag between the governor and prime mover is minimal. Since the governor won't intervene during the transient under consideration's one-second timeframe, the effect of governor activity is frequently ignored in books on transient stability. This might be accurate for a three-stage combination of high, medium, and low-pressure steam turbines, however fast valved steam turbines, gas turbines, and diesel generators don't fit the assumption during an over-speed condition prior to a power reduction. The governor and prime mover system will have little impact on the critical clearing time if it has a large time lag since its time constants will effectively make it inactive during the first swing of a transient disturbance (Van Cutsem, 2017).

3.5.2.5 Protection Characteristics of the Generator-Connected System

The effective transfer impedance between the generator and the infinite bus, as well as the protection clearance times for faults, are the two main external factors that affect a generator's transient stability margins. The most important factor in maintaining stability is protection clearance time, because the longer the fault exists on the system, the longer the generator's power transfer capabilities are disrupted. Protection clearance periods for high power transfer transmission circuits are typically in the range of several power system cycles. As a result of the flaw, just a little quantity of accelerating energy is produced. As a result, the generator rotor should not accelerate significantly (John Wiley & Sons, 2012).

Engineering recommendation G59 specifies that the generator should be withdrawn from the system "when a system fault occurs that results in an unacceptable deviation of the voltage or frequency at the point of supply". Because power system defects might cause unacceptable deviations at the point of supply, G59 specifies that all short circuit faults cause the generator to be disconnected. If this is accomplished, pole slipping should not occur as a result of short circuit failures. In practice, however, the generator is not disconnected for all external short circuit failures. As a result, pole slipping is possible. Furthermore, the aforementioned description requires that a pole slipping generator be unplugged in the event of voltage or frequency disturbances.

3.5.2.6 Resistance Effect on Stability

High stator and inter-tie resistances may diminish the generator's natural damping capabilities, hence reducing the stability margin. The influence of high resistance values on dynamic stability is the most-biggest worry in an embedded generation context. A high resistance value found in a lengthy length of cable, along with a poorly damped machine, low performance AVR, and poorly damped governor, could result in a negative damping value. This could lead the machine to oscillate with increasing amplitudes until the generator loses stability (Farmer, 2001).

Because the power lost in the resistance acts as a burden on the generator and lowers the accelerating power entering the rotor, increased resistance can also help stability for close-up short circuit problems.

3.5.2.7 Fault Type effect on Stability

Lower stability limits for a given fault duration result from less power transmission from the generator due to decreased fault impedance. The 3-phase problem is the most serious defect in terms of severity. Two phase, two phase, and single phase to earth faults are thus present. According to (Kimbark,1994) the difference in fault severity decreases as the fault duration increases, although there is a considerable difference for faults lasting 200ms or more.

3.5.2.8 Earthing effect on Stability

The level of power mismatch generated by a failure depends on the system's zero sequence impedance, or Zo, which in turn depends on the impedance of unbalanced faults. An unbalanced fault's severity lessens as Zo rises in relation to the location of the fault. It can be seen that a two phase to earth fault would change into a two-phase fault if the extreme of an infinite value of Zo is taken into account. Therefore, grounding through impedances is preferable from the perspective of stability to using solid grounding approaches. In contrast to reactors, grounding resistors near generators are more advantageous since they add additional brakes to the generator during imbalanced faults (Kimbark,1994).

3.5.2.9 Generation System Configuration effects on Stability

In some embedded setups, several embedded generators are centralized at a single location. The generators can be clustered together and behave as one larger generator if they are all linked to the same bus. A site's ratio of infinite bus to machine ratios will decrease from the perspective of stability by adding additional generation. The generators will be more susceptible to instability if the ratio falls too low, which will reduce their ability to restore synchronization after disruptions (Farmer, 2001).

Stability is also impacted by step up transformers since they might increase the generator's stator circuit impedance. The exchange of synchronizing power between the generator and grid will be reduced if the transformer has a high impedance, resulting in a reduction in the stability margin. Because the transformer will partially load the generator, it may increase stability for close-proximity terminal problems.

3.6 TECHNIQUES TO REDUCE PROBABILITY OF POLE SLIPPING

There are many additional techniques to increase power system transient stability that will lessen the chance of pole slipping, though it is feasible to install relays to terminate generators when they pole slip. The many changes that can be made to the power system to enhance transient stability are covered in detail in the subsections that follow, as are the changes that can be made to the machine's design to mitigate the effects of pole slippage.

3.6.1 Reduced fault clearance times

Reducing the duration of a fault minimizes the accelerating energy that goes into increasing the machine rotor angle, which reduces the load angle swing for the fault and increases the possibility of stability. This is one of the most successful means of boosting transient stability, although reducing fault clearance time necessitates costly adjustments to the existing utility's protection, as well as protection changes at neighbouring facilities (Clark & Feltes, 1989). Circuit breakers can also be upgraded to improve fault clearance times. An oil circuit breaker's total running time may be 100ms or more, but an SF6 or vacuum circuit breaker's total operating period may be 50ms.

3.6.2 Fast acting voltage regulators

When a defect is present, voltage regulators can apply field forcing to the generator, boosting the machine's power output when the fault is fixed. This increases the amount of decelerating energy that is available and improves stability for a specific fault duration. Flux linkage will be reduced by the influence of armature response during a failure, particularly if the generator's reactive power output is high. Reduced machine flux linkage results in lower output power and, thus, worse machine stability. A few hundred millisecond defect will result in a large reduction in flux linkage (Dineley, 1991).

Fast AVRs might help to increase the transient stability of the first swing, but they also diminish the dynamic stability margins for subsequent swings. The generator may maintain stability for the initial swing but lose synchronism in later swings if the damping reduction is too significant. Additional stabilizing feedback signals must be incorporated into the AVR to address this dynamic instability.

A quick AVR will help to sustain flux levels that would have otherwise decreased by forcing the levels of excitation during the fault. Despite the fact that AVRs can dramatically increase flux levels during faults, their impact on the size of the initial swing in load angle typically only results in a few degrees of decrease. They are most useful when there are lengthy fault clearance timeframes (Dineley, 1991).

3.6.3 Fast valving turbine

This technique greatly lowers the mechanical input power to the generator during a malfunction, speeding up the response time of steam turbine prime mover systems. As a result, it reduces the rotor's accelerating power while increasing its decelerating power. The steam valves entirely close during a quick valving action in about 80 to 200 milliseconds, reducing the output power of the steam turbines. This strategy needs a way to measure rotor acceleration. The technology does significantly improve transient stability for steam turbine generators if an acceleration-related control signal can be produced (Wiley & Sons, 1987).

3.6.4 Fast governing systems

The essential clearing time can be extended with the aid of a quick reaction controlling system, however pole slipping, and transitory instability cannot be completely avoided. According to one stability study, adding the governor to the model reduced the gas turbine generator's crucial clearing time by 40ms. Depending on the kind and level of sophistication of the system under consideration, the temporal constants of prime mover and governor systems might vary greatly. Even while governors can't totally stop pole slipping, they are by far the most crucial element to take into account when re-synchronizing a unit after pole slipping has taken place. If a rapid regulating system is not first disengaged, a pole slipping generator will re-synchronize after one pole slip cycle (Wiley & Sons, 1987).

3.6.5 Machine design modifications

The machine's characteristics can be altered during the design phase, which will increase the machine's transient stability. Numerous innovative machine designs have been proposed in previous studies that generate output characteristics similar to those of synchronous machines while resolving the transient stability issue.

The machine's inertia constant and transient reactance are the two key variables that can be altered. Since more energy is stored in the rotating mass, a machine with a higher inertia constant is said to be "stiffer." As a result, more acceleration energy will be needed to achieve a given load angle variation. A heavier and hence more expensive machine rotor is necessary for a greater inertia constant (Dineley, 1991).

More deceleration energy will be available during and after transient disturbances like failures thanks to a machine with a lower transient reactance. The machine output power is increased further as a result of the transient saliency brought on by the difference in transient reactances between the direct and quadrature axes, and the load angle at which the peak occurs is shifted to a value greater than 90°. Low transient reactance values will result in a longer rotor, which will increase the generator's size and cost (Dineley, 1991).

One advancement makes it possible to maintain the machine load angle regardless of the load power factor, enabling the machine to absorb reactive power up to the stator's thermal limit without sacrificing transient stability. It accomplishes this by employing a divided winding rotor, of which one half is in charge of supplying the torque required to maintain the rotor in synchronism. The other half is in charge of controlling the machine's reactive power, applying positive or negative excitation based on the load's power factor. It is possible to maintain a constant machine load angle of 40°. The disadvantage of the design is the extra cost of the excitation system because thermal differential expansion and contraction issues arise as a result of the multiple rotor windings carrying various excitation current levels (Seshanna, 1982).

By releasing the rotor magnetic field from being fixed to the rotor, another machine invention eliminates the issues with synchronous stability and, consequently, pole slipping. The rotor features a polyphase excitation winding that is activated by polyphase slip frequency voltages that are in the right order and phase. The desired characteristics of synchronous and asynchronous devices can be realized in this way. The machine can operate with slip while maintaining output power characteristics that are comparable to those of a traditional generator. The effectiveness of the excitation system affects machine stability, and the advantages of the new scheme are offset by the increased cost of the excitation system needed (Seshanna, 1982).

3.7 CRITICAL CLEARING ANGLE AND CRITICAL CLEARING TIME

When a system defect develops, δ starts to increase under the impact of positive accelerating power, and if δ gets very big, the system will start to become unstable. If the system is to stay stable and the equal area criteria is to be met, there is a crucial angle within which the fault must be eliminated. The critical clearing angle is the name given to this angle.

Critical clearing time is the amount of time that the synchronous generator must have in order to maintain its ability to maintain synchronization. When the rotor angle increases, the electric power system becomes unstable. The change in power is significantly impacted by this increase in, making it possible to identify the key clearing time by measuring the rotor angle. When a disturbance happens and the system is unable to handle it, it is said to be unstable. The entire system is impacted by this instability. To prevent any disruptions, it is vital to establish the critical clearance time (Farmer, 2001).

Numerous investigations into transient stability have been done. Previously, numerical integration of nonlinear differential equations was still employed for transient stability analysis. This method can give a general overview of the stability of the power system due to transitory symptoms and is highly accurate at determining crucial clearance time in a multi-machine power system. The iteration phase of this method takes a long time due to the lengthy numerical integration required to determine the critical clearing time. When used in transient stability analysis, this is quite ineffective. Because of the systemic disturbances' tendency to change in a predictable pattern. As a result, a method that can compute CCT with a faster and more precise iteration is needed. The method used in this research is a simulation scan of RMS/EMT injections found in DigSilent chapter 5.

3.8 MULTI-MACHINE STABILITY STUDIES

Since the complexity of the numerical computations rises with the number of machines taken into account in a transient stability study, the equal-area criterion cannot be applied directly in systems where three or more machines are represented. In transient stability investigations, the following presumptions are frequently used to reduce the computational burden of system modelling and its associated system complexity (Dineley, 1991):

- Each machine receives a continuous mechanical power input.
- There is very little damping power.
- A constant transient reactance in series with a constant transient internal voltage can be used to represent each machine.
- Each machine's mechanical rotor angle coincides with δ.
- All loads can be thought of as shunt impedances to the ground, with values based on the conditions that existed just before the transient conditions.

Studies that use this model are known as classical stability studies, and the system stability model based on these assumptions is known as the classical stability model. Consequently, two first stages are needed in the multi-machine situation.

- A production-style power flow program is used to determine the steady-state pre-fault conditions for the system.
- After establishing the pre-fault network representation, it is changed to take into account both the fault and the postfault circumstances.

This phenomenon is to be noted since the system used in this research incorporates multi-machine configuration system, hence such approach will be used for stability studies.

3.9 CONCLUSION

Energy is frequently produced with salient pole synchronous generators. Generators can be utilized in islanded networks or as an emergency backup power supply in remote places when paired with ICE as a prime mover. In this chapter the overall design and performance of a synchronous generator has been discussed taking into account the effects of connecting / paralleling it with the infinite grid system. The machine electromagnetic losses were also presented with which the information aided with the calculation of these non-idealities on power losses. The chapter also addressed the techniques of reducing the probability of pole slipping of synchronous while on design stages. However, when synchronous generators are connected with the grid, they are still more likely to pole slip as they have low inertias. The next chapter presents protection relaying principles of synchronous generators.

4 CHAPTER FOUR

Protection Relaying Principles for Synchronous Generators

4.1 INTRODUCTION

Protective relays play a critical role in the power system at all levels, including power generation, transmission, and distribution. Because these devices control the actuation of circuit breakers, relays must operate with high reliability and selectively isolate faulted sections. Furthermore, existing power systems are growing in complexity and are operating with more uncertainty due to increasing renewable generation. The ability of protective relays to accurately identify and quickly isolate short-circuit faults is integral to maintaining a reliable and stable power system. However, it can be challenging to maintain coordination of remote backup protection, such as Zone 3 distance elements, in the presence of stressed system conditions. Moreover, conventional power system protection approaches consider completely dispatchable generation, central management of static relay settings, and relays without capabilities for real-time awareness of system topology changes or largescale generation swings. The analysis of the effect of out-of-step conditions on distance protection is discussed in literature. During system disturbances, generators in a large, interconnected power system form coherent groups of machines swinging with respect to each other.

Chapter 3 addressed the challenges associated with synchronous generators when system stability and quality of supply are concerned therefore to prevent these generators from corrupting the supply to utility customers. The regulating authorities have produced guidelines that define the general protection requirements for protection against all types of faults and abnormal operating conditions, and they require the utilities to ensure that the embedded generators will not degrade the quality of supply to other customers.

The power system under study is dynamically as it comprises of various loads such as commercial, residential, and industrial loads, it is important to note the transient load change caused by loadshedding which is a recurring factor in the South African grid currently, produce a progressive drop in bus voltages which is often associated with most rotor angle instability between the multi-machines in the system. This characteristic becomes important insight to help with a well-planned OOS protection design for such system where various loads are incorporated.

It is then crucial to explore the framework of relaying for synchronous generators when interfaced with the power system network. Furthermore, this chapter solely provides analysis of SEL-700G (main protection) and SEL-421(distance backup) settings configuration and application for these generators in relation to the system.

4.2 SYNCHRONOUS GENERATOR PROTECTION

The primary function of protective relaying is to cause the rapid removal of any element of a power system from service when it suffers a short circuit or begins to operate in any abnormal manner that may cause damage or otherwise interfere with the effective operation of the rest of the system. The second function of any protective relaying system is to provide location and type of failure indication (Horowitz & Phadke, 2008). The figure below illustrates the distinct one-line diagram of the power system.

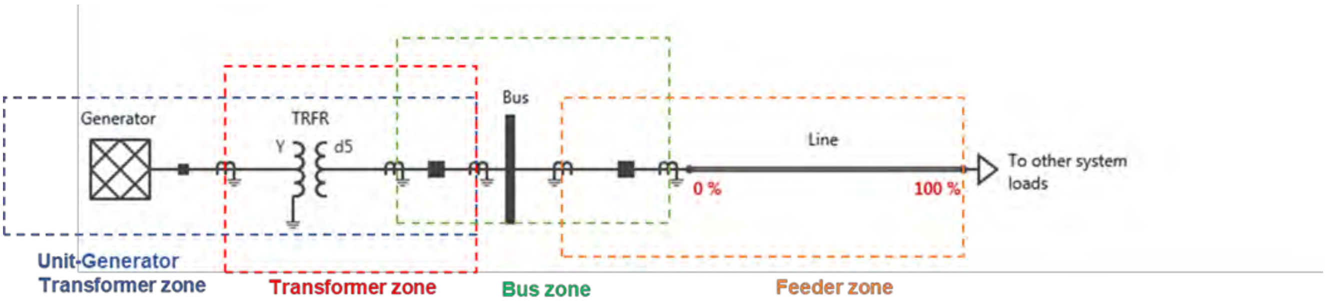

Figure 4.1: Electrical power system one-line diagram

To ensure the overall stability and security of the power system, protection engineers develop broad protection and control mechanisms in addition to the traditional local and zonal protection strategies shown in Figure 4.1.

Any protective relaying system has the following functional characteristics (Blackburn & Domin, 2006):

- Reliability is comprised of two components: - dependability, which refers to the degree of certainty that a relay will function correctly, and security, which refers to the level of confidence that the relay system will not malfunction. The relay's ability to prevent unnecessary operation for faults or abnormal conditions outside of its designated operating zone.
- Selectivity: the protective relay's ability to distinguish between a faulted and non-faulted section. Selectivity or relay coordination is critical to ensuring maximum service continuity with the least amount of system disconnection.
- Sensitivity refers to a protective relay's ability to operate as quickly as possible within its primary protection zone while delaying operation in its backup protection zone.

Generator protection is made up of several protection elements that safeguard the system against abnormal conditions and faults. The severity of the protection system determines the degree of monitoring functions for such systems; however, any protection system should be able to provide adequate protection and initiate a complete shutdown if a fault is detected (Fitzgerald & Kingsley,1971).

Principles of generator protective relaying will be defined according to the following flow chart with the 78 element being of interest to the study objective for lab scale implementation.

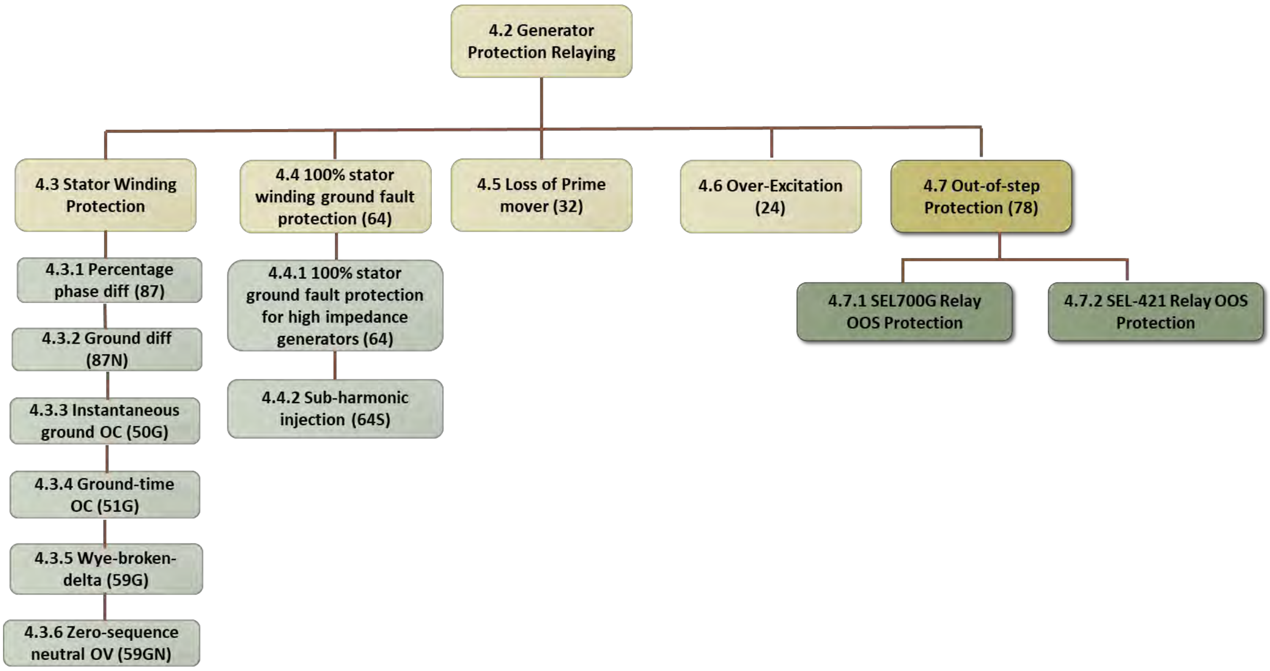

Figure 4.2: Principles of Generator Protection Relaying overview

4.3 STATOR WINDING PROTECTION

Ground faults are the most common generator faults reported. Internal faults in stators are caused by insulation breakdown caused by winding contamination from factors such as dust and oil. Contaminants collect on the coil surfaces outside the stator slots. Overvoltage, overheating of the windings, or mechanical damage caused by faults can all cause insulation deterioration. In the event of an overvoltage. These situations are usually caused by lighting or switching surges, as well as unbalanced loading or a loss of cooling, resulting in overheating. The following are some stator fault protection methods:

4.3.1 Percentage Phase Different Protection (87)

Although phase faults are uncommon in generators, they must be protected in the event that they occur. These faults form in the winding end turns, where all three phases are in close proximity. The danger with these faults is that they frequently transform into ground faults, making their detection a high priority. This relay is most commonly used in such situations (Blackburn & Domin, 2006). This protection relay operates for internal faults where the relay detects sufficient fault current. This relay is insufficient for faults near the neutral and should be replaced with a more effective scheme. Differential protection functions work by comparing the phase currents on both sides of the object to be protected. The relay generates an operate signal if the differential current of the phase currents in one of the phases exceeds the set start value of the stabilized operation characteristic or the instantaneous protection stage. In

Figure 4.3, the current in the restraint coil causes the contact to open, while the current in the operating coil causes the contact to close. When the operating current exceeds the restraining value by a certain percentage, the relay contacts close. The percentage is known as the relay's slope. This configuration automatically increases the operating coil current required for tripping as the fault current and CT error increase (Gwala & Saha, 2015).

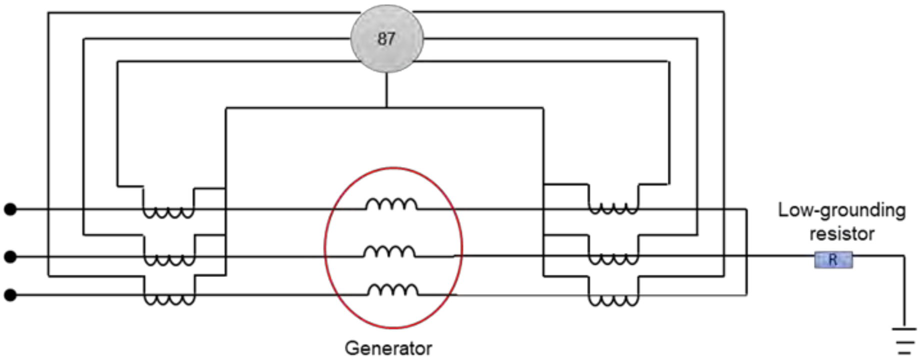

Figure 4.3: Percentage phase differential protection (Gwala & Saha, 2015).

The drawback of this relay is that if the generator is grounded using a high impedance technique, it will not operate in the event of stator winding faults. The fault current is decreased on grounded generators with high impedance to the point where the relay loses sensitivity to the fault. This relay's inability to detect turn-to-turn faults that occur on the same phase due to current difference is another flaw.

4.3.2 Ground differential protection (87GN)

This component is used to protect the generator from internal ground faults. It can only detect faults up to 10% of the generator's neutral. This scheme must be properly configured to avoid unnecessary tripping for external faults, Figure 4.4 depicts this 87GN phenomena (Gwala & Saha, 2015).

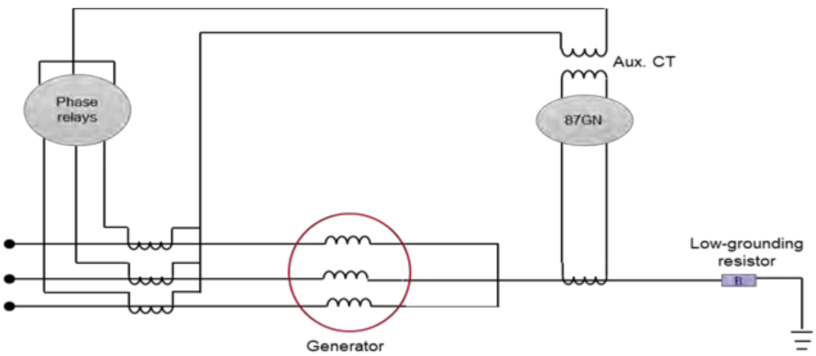

Figure 4.4: Ground differential protection (Gwala & Saha, 2015).

As previously stated, low resistance grounded systems experience high fault currents, necessitating sensitive and high-speed differential protection for generators, making this scheme more suitable than phase differential relays.

4.3.3 Instantaneous ground overcurrent protection (50G)

This protection scheme, also known as the self-balancing differential ground relay scheme, detects faults close to the generator neutral. This relay protects against internal ground faults of low magnitude. Its operation is based on the toroidal current transformer, which is connected to the phase and neutral terminals of the generator, as shown in Figure 4.5. The transformer allows for the measurement of ground current generated by the generator. If the output of the current transformer exceeds the set threshold, the generator will shut down instantly. When there is an external ground fault, the current transformer output remains zero. As a result, this configuration allows you to safely set the relay to a low value for maximum generator protection.

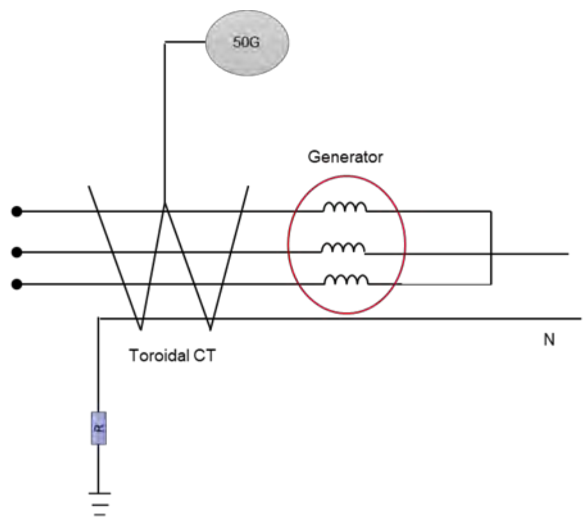

Figure 4.5: Instantaneous ground overcurrent protection (Gwala & Saha, 2015).

4.3.4 Ground time-overcurrent protection (51G)

This scheme protects against un-cleared feeder faults that the instantaneous ground overcurrent relay may miss. These relays provide dependable sensitive ground fault protection. Faults near the generator terminals can cause significant damage due to high fault currents. This condition can be avoided by combining a time-overcurrent relay with an instantaneous ground overcurrent protection relay (Gwala & Saha, 2015).

4.3.5 Wye-broken-delta voltage transformer ground overvoltage protection (59G)

This scheme is mostly used on grounded high impedance generators. It detects both ground faults and zero sequence neutral overvoltage components. This is accomplished by monitoring the voltage across the voltage transformer's broken delta secondary winding (Gwala & Saha, 2015).

4.3.6 Zero-sequence neutral overvoltage protection (59GN)

On high resistance grounded machines, this element is often used. The overvoltage relay is tuned to the fundamental frequency of the system and does not operate for third harmonic voltages obtained at the generator neutral. The assembly of the zero-sequence voltage protection for unit connected generator is shown in Figure 4.6 (Gwala & Saha, 2015).

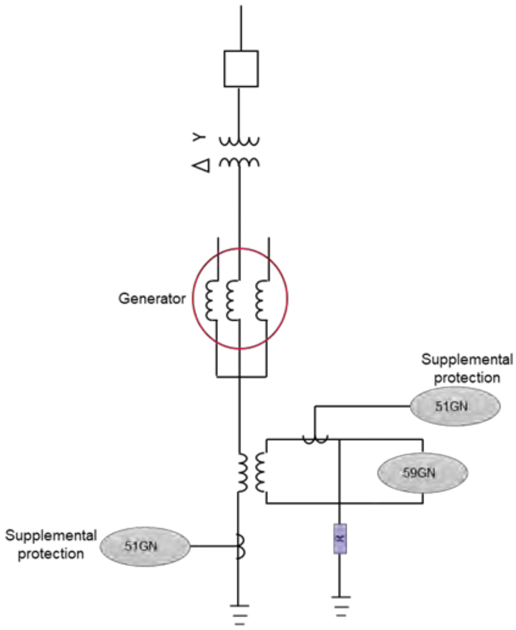

Figure 4.6: Zero-sequence voltage protection in high impedance grounded machine (Gwala & Saha, 2015).

4.4 100 % Stator Winding Ground Fault Protection (64)

The above-mentioned protection schemes cannot provide 100 percent stator winding protection for high impedance grounded generators. The stator winding is completely protected by 100 percent ground protection and a generator neutral breaker. The above schemes can only protect 5 to 95 percent of the stator winding. The remaining 5% is unprotected, and while a fault occurring at this point may not cause significant damage, reoccurrence of the fault on the same winding may result in turn-to-turn faults. The fault current at the neutral points of the generator may not be sufficient to operate the relay.

4.4.1 100% Stator Ground Fault Protection for High Impedance Generators (64G)

The 100% stator ground element is appropriate for providing the ground fault function on high impedance grounded generators with a high resistance or reactance to the system ground. Generators produce harmonic voltages, with the third order being the most powerful. These harmonics are in phase and can be obtained as zero sequence quantities at the generator neutral. When there is a fault at the neutral, the third harmonic voltage at the neutral is reduced to zero, while the third harmonic voltage at the generator terminal is increased to the total third harmonic voltage produced by the machine, as shown in Figure 4.7. These characteristics are then used to detect ground internal faults in the stator winding (Fitzgerald A. and Kingsley C. 1971).

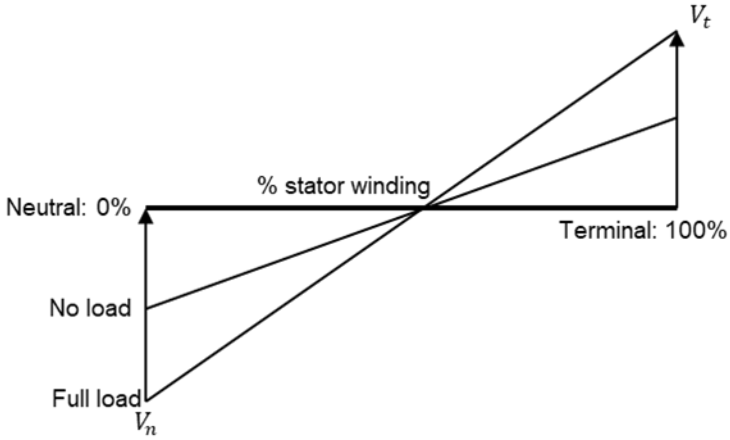

Figure 4.7: 3rd Harmonic voltages under normal conditions (Fitzgerald A. and Kingsley C. 1971).

4.4.2 Sub-harmonic Injection (64S)

The injected voltage is used in this method to detect ground faults along the stator. A transformer is used to inject voltage between the grounding element and ground. A distribution transformer, reactor, or resistor can be used as a grounding element (Mozina, 2009). The injected voltage has a low subharmonic frequency, typically a quarter of the system frequency. The currents generated by the injected voltage are constantly measured. Normally, this current flows through the stator winding shunt capacitances to ground; however, when a ground fault occurs, the shunt capacitances short-circuit and the magnitude of the current increases. Based on this principle, the relay can detect the occurrence of a ground fault by measuring the magnitude of the current (Daquiang, et al, 2002).

The advantage of this function is that the low injection frequency boosts the impedance of the stator capacitance reactance, increasing the element's sensitivity and dependability This method also uses a coupling filter to block the fundamental frequency component of the signal, and the current is measured for the entire quarter of the system frequency (12.5 or 20 Hz cycles) that is used. Due to the additional equipment needed for the injection of voltage, this method has the disadvantage of being costly. The principle of this protection method is shown in Figure 4.8.

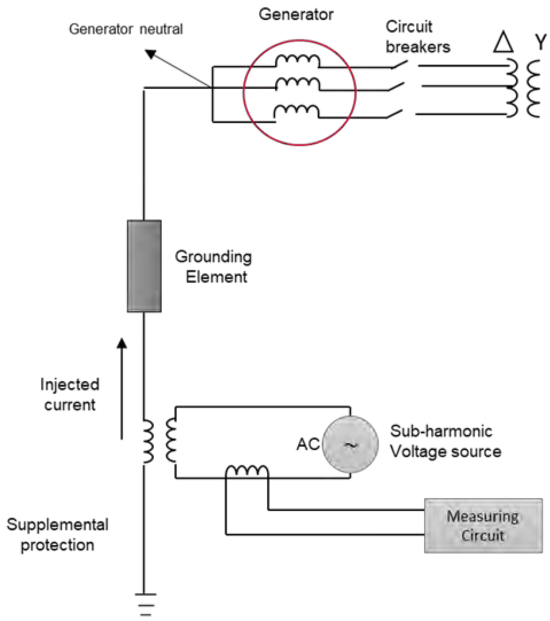

Figure 4.8: Method for sub-harmonic injection (Gwala & Saha, 2015).

4.5 Loss of prime mower (32)

When the synchronous generator loses its mechanical input while it is still running, it is said to have lost its prime mover. The generator enters reverse power mode and begins to function like a synchronous motor if the generator field is still excited. In steam turbines, the loss of steam can cause lead distortion and softening of the blades, which can be very harmful to the generator if left unattended. This condition's damage also lessens the turbine's effectiveness and capacity to balance heating, resulting in hot spots that stress the turbine. This failure is protected using the reverse power relay protection (32). The real-power flow from the generator terminals can be measured by generator protection relays (Gwala & Saha, 2015).

This protection element operates such that when the measured real-power falls below the element setting, the protection relay detects a loss of prime mover condition, a definite timer is started, and eventually a trip signal is issued. This is schematically shown in Figure 4.9 below.

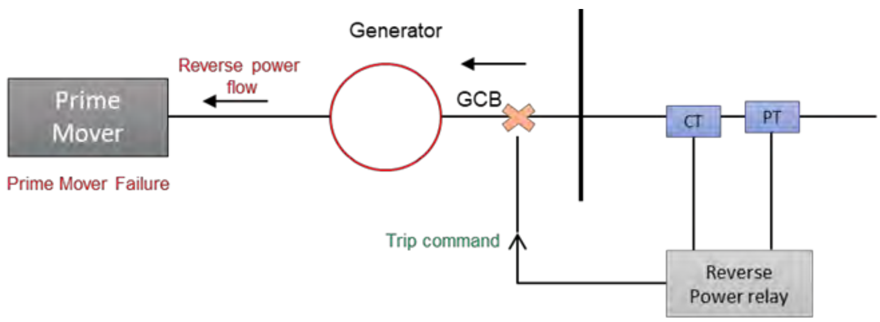

Figure 4.9: Loss of prime mover protection (Gwala & Saha, 2015).

4.6 Over-excitation (24)

A generator stator core is built with a maximum magnetic flux density in mind. If the generator is operated above this density, eddy currents and other conductive components will cause significant damage to the stator core in a short period of time. The magnetic flux in the core is proportional to the winding voltage divided by the winding impedance. With increasing voltage or decreasing frequency, the flux in the core increases. The generator voltage is determined by the number of turns in the output winding and the rate of flux in the magnetic core (Reimert. D, 2005). Over excitation of a synchronous generator or transformer occurs when the voltage to frequency ratio exceeds 105% for a generator operating at full load or 110 % for no load, according to the [IEEE PES gen protection standard guide]. Over-excitation of generators or transformers causes saturation of the stator magnetic core, resulting in stray flux induction in non-laminated components.

The protection relay detects overexcitation by estimating the flux in the magnetic path using the voltage/frequency ratio. If the voltage to frequency ratio exceeds the threshold settings, the protection relay will detect this and trip the main breaker. The time delay curves can be definite-time or inverse-time.

4.7 Out of Step Protection (78)

Generators connected in parallel with one another or in parallel with the grid operate at the same frequency and voltage as the network to which they are linked. The generators are given a buffer and are tuned to be able to handle system disturbances. If one of the bonding forces between the generators becomes insufficient to keep the generators linked, it loses synchronism and is said to be out of step with the other generators. The out-of-step condition causes high peak currents, winding stresses, pulsating torques, and mechanical resonances within the generator, necessitating its removal from the system. Out-of-step tripping (OOST) relays are commonly used to achieve this separation. Out of step protection should be applied as soon as it is detected to prevent operational issues with the rest of the network, and the affected generator should be isolated from the system. Previously, electrical centres were located on the transmission system, and as a result, transmission line out of step protection was provided without the need to trip generators (Gwala & Saha, 2015).

As previously discussed in literature the following schemes are used for out of step protection:

- Single MHO Scheme
- Single Blinder Scheme
- Double Blinder Scheme
- Double Lens and Concentric Circle Scheme

The single blinder is the most common of these schemes. The tripping characteristic of various types of out-of-step protection schemes is defined as a two-dimensional area defined on an R-X impedance plane. An example of 78 relay is shown in Figure 4.10 below:

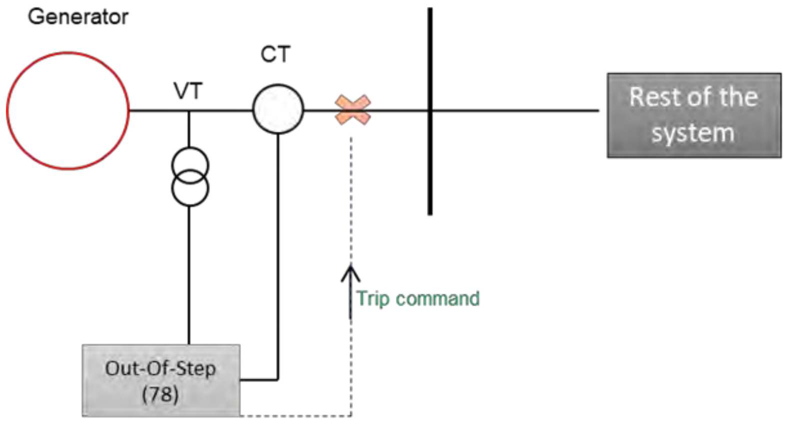

Figure 4.10: Out-of-step protection relay (Gwala & Saha, 2015).

If the disturbance is not severe, the system remains stable, and the generator's load angle oscillates (i.e., the angle increases and decreases in synchronism with the power system oscillations). A system that is "stable" may or may not be well damped. It is never desirable to trip when there's stable power swings. When generators experience out of step conditions, OOST relays isolate them from the power grid. It is common for nearby generators and transmission system terminals to be affected by the system, oscillations comparable to those experienced by the OOS generator. It is frequently desirable that none of these other facilities trip during the generator OOS event. These facilities could require Power Swing Blocking(PSB) relays are required to avoid unwanted tripping. Some OOST relay characteristics only provide OOST capability, whereas others can provide OOST and PSB capabilities.

The traditional method for detecting the OOS condition is to examine the location of the apparent impedance seen from the generator terminals. Transient stability studies (as simulated in DigSilent chapter of the thesis) can determine whether or not the generator will remain in synchronism in the face of various power system contingencies. The impedance seen by the generator during the OOS condition between one generator and another or between one generator and the system varies depending on the voltage and the angular difference between the generator and the other generators or the system. When the two systems are in phase with each other, that is, when the angular difference between the two systems is zero, the voltage at the generator's terminal is at its maximum and the current is at its minimum. When the two systems are perfectly out of phase (180° apart), the voltage at the generator terminals is at a minimum and the current is at a maximum. Appropriate protective devices and associated logic measure voltage and current variations to determine whether or not an OOS condition exists.

The critical clearing angle δ_c, is often used to describe the boundary between a stable system response and an unstable "runaway" response to a disturbance. This is the angular difference that cannot be exceeded. The linked system will not be able to recover. This value is crucial in the configuration of several OOST relay schemes. δ_c = 120° is a common rule of thumb. Stability studies, on the other hand, are required to determine the actual δ_c value. These studies typically model cases with increasing fault clearing times at critical system locations until the system model becomes unstable. The critical clearing angle δ_c, is identified by the maximum angle in the last stable case. Furthermore, these studies identify the swing rates that are critical for the proper operation of several out-of-step relay characteristics. Because the critical clearing angle and system swing rates can change depending on system configuration, the studies required to obtain conservative results can be quite extensive (Blackburn & Domin, 2006).

The relays calculate (measure) an apparent impedance that varies with time during power system oscillations. This variation in measured or calculated apparent impedance can cause the generator impedance protection elements to malfunction if they are not properly set. The best way to demonstrate how the impedance fluctuates while a power system oscillates is to use a straightforward equivalent system, such as the two generators with EMF E_S and E_R shown in Figure 4.11. As depicted in Figure04.12, E_R lags the sending voltage E_S by an angle δ_S.

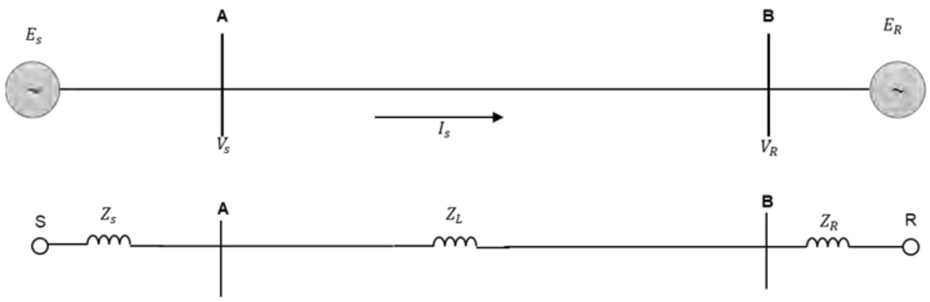

Figure 4.11: System Equivalent for power system oscillations (Blackburn & Domin, 2006).

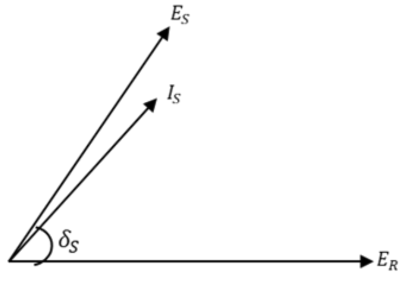

Figure 4.12: Relationship between ES and ER (Blackburn & Domin, 2006).

It is assumed that the protective relay, an impedance-sensing component, is situated at the generator terminals where V_S is the voltage and I_S is the current flowing from S to R.

This then yields the voltage VS observed by a relay at the generator terminals:

$$V_S = E_S \angle \delta_S - I_S Z_S = I_S Z_L + I_S Z_R + E_R \tag{4.1}$$

The current seen by the relay is then given by:

$$I_S = \frac{E_S \angle \delta_S - E_R}{Z_S + Z_L + Z_R} \tag{4.2}$$

According to the phasor diagram in Figure 4.13, the current I_S induces a voltage drop in the system components. As more load is transferred, the value of δ_S, which represents the phase difference between E_S and E_R, rises.

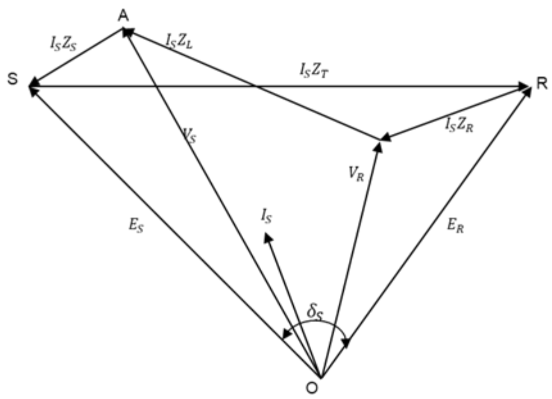

Figure 4.13: Voltage phasor diagram for the equivalent 2 source system (Blackburn & Domin, 2006).

I_S and δ_S are variables that are affected by power transfer. The increase in load transferred causes an increase in I_S and δ_S. As a result, the size of the vector V_S/I_S is reduced. If the load increment is large enough, the impedance perceived by the relay (V_S/I_S) can migrate into the relay operational zones. The electrical centre of the system is defined as the point at where the impedance locus intersects the total impedance line between S and R. The two generators are now 180° out of phase with each other. As the locus moves to the left, the angular divergence goes beyond 180°, and the two-systems re-enter phase. Once the two generators are back in phase with each other, we may say that one slip cycle has been accomplished (n=1).

The locations of the impedances are circles with the circle's centre on an extension of the total impedance line Z_T for values of $n \neq 1$. It can be demonstrated that for values of n>1, the impedance during an OOS state is located above the system's electrical core (above 1/2 Z_T).

In contrast, for n1 values, the impedance is located below the electrical centre. In Fig. 3.30, this is depicted. When creating initial settings for relay applications, it is acceptable to take the simpler scenario where n=1 into account. Although in order to show, at least roughly, the range of the system swing locus in situations of stressed system conditions like low system (receiving) voltage and system equipment outages as well as the response of the generator voltage regulator to such conditions, instances for n>1 and n<1 are also relevant (Blackburn & Domin, 2006).

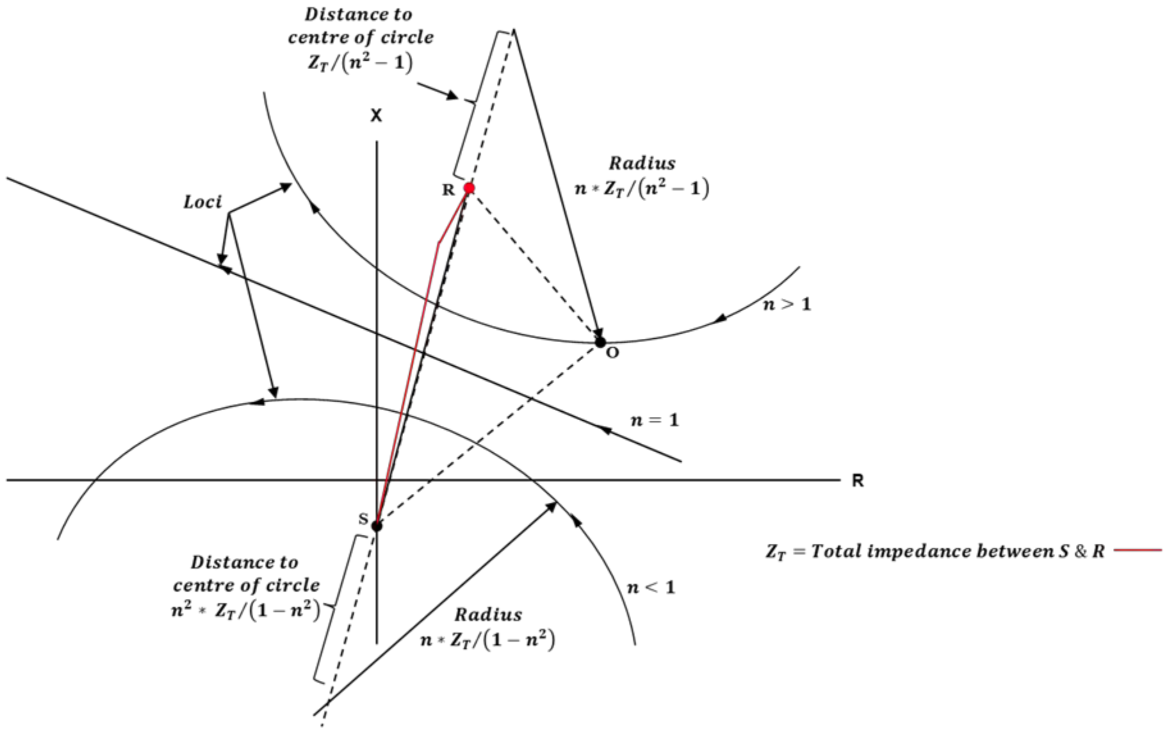

Figure 4.14: OOS characteristic for the case n=1, n>1 and n<1 (Blackburn & Domin, 2006).

Measuring fluctuations in system impedance aids in detecting an Out-of-Step problem and creating OOS protection strategies. These schemes' settings are crucial to system reliability and stability. The schemes must be configured to immediately isolate a machine, not just to minimize harm but also to keep instability from spreading to other parts of the system.

4.7.1 SEL700G RELAY OOS PROTECTION

The transmission system has expanded and continues to strengthen as demand for electrical power has increased; generator impedances have increased due to improved generator cooling methods, allowing for greater MVA capacity. As a result of these advancements, electrical centres have been moved into generator step transformer units and the generator itself, which has increased stresses on both components. As a result, the need for out of step protection at the generator was identified due to electrical centres of swings that affect the generator but cannot be detected by network protection. The overcurrent relays used for generator protection are unable to detect this condition reliably (Reimert, 2005). Amongst the variety of other protection functions of not interest to this thesis study, SEL 700G offers a complete protection against out-of-step of generators. The relay provides, metering, monitoring, control, and communication functions. There are also RTD-based protection and flexible analogue and digital input/output options.

This IED contains out-of-step element to detect out-of-step conditions between two or more electrical sources. It is critical to detect and isolate an out-of-step condition as soon as possible because the resulting high peak currents, winding stresses, and shaft torques can be extremely damaging to the generator and the associated generator step-up transformer. The device implements two tripping schemes: Single and double blinder schemes. However, for the purpose of this thesis a double blinder scheme will be applied for a compact protection against system dynamics.

4.7.1.1 Double-Blinder Scheme

The design of a double blinder system is more complicated than that of a single blinder scheme. If the inner blinder is configured to result in a measured angle smaller than the essential clearance angle, or the blinders and timer are set to indicate a higher swing rate than projected from stability tests, the double blinder settings may result in tripping for an otherwise recoverable swing. To ensure secure scheme operation, more detailed stability modelling to establish key clearing angle and swing rates is required. However, for OOST applications, a greater critical clearing angle say 150°, can simplify the analysis. The scheme interprets the event as a fault if the actual time between the outer and inner blinders is less than the delay timer setting. In this situation, out-of-step protection is ineffective. However, the event is regarded as a swing condition if the actual transit time exceeds the setting. The system perceives blinder crossings time delays pickups.

For a double-blinder scheme to be effective, mho element 78Z1 and two blinder pairs: outer resistance blinder 78R1 and inner resistance blinder 78R2 are incorporated. To detect out-of-step conditions, this scheme employs timer 78D as part of its logic. If the positive-sequence impedance remains between the two blinders for more than 78D seconds and advances further inside the inner blinder, the scheme declares an out-of-step condition. Once an out-of-step condition is established and the positive sequence impedance exits the mho circle, the logic will issue an out-of-step trip. A diagram of Mho double-blinder is illustrated in Figure 4.15 below.

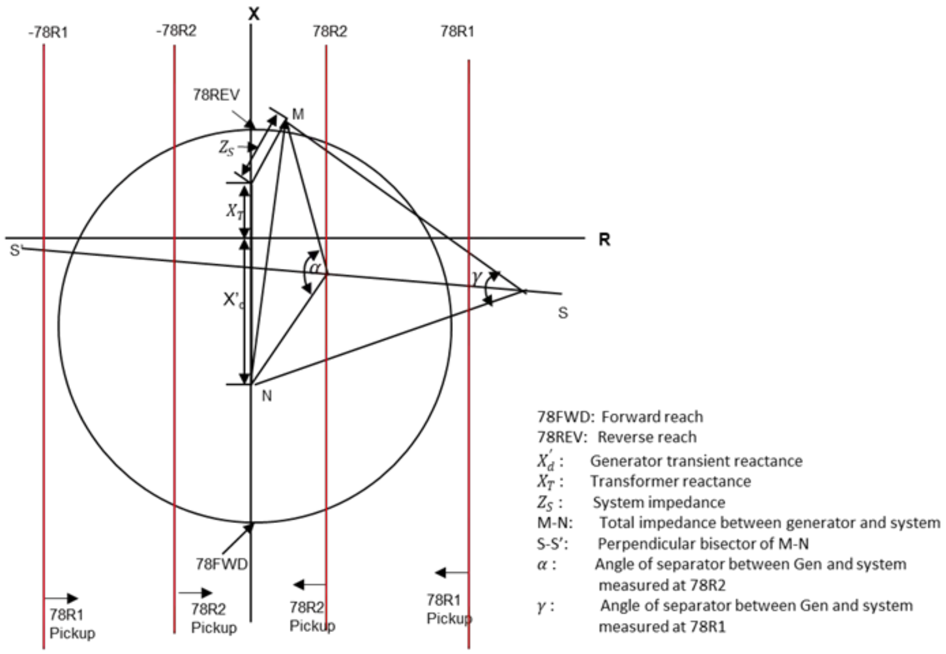

Figure 4.15: Double-Blinder Scheme operating Characteristic (SEL700G instruction manual)

When the relay detects an out-of-step condition, it asserts the Relay Word bits (SEL700G IM):

- When the positive-sequence impedance remains between the outer and inner blinders for longer than 87D seconds, Relay Word bit SWING is activated (78R1 asserts, mho element 78Z1 may or may not be asserted).
- When the impedance trajectory progresses deeper inside the inner blinder, the Relay Word bit OOS detects it (78R1, 78R2, and mho element 87Z1 asserts).
- When the impedance trajectory leaves the mho circle, the rising-edge triggered timer with pickup delay 78TD and 78TDURD dropout delay begins timing. Relay Word bit OOST remains picked up for 78TDURD seconds after pickup delay time 78TD expires.

Table 4.1: Relay Word Bit Definitions for the SEL-700G OOS element

Word Bit	Definition
78R1	Out-of-step right blinder or outer resistance blinder
78R2	Out-of-step left blinder or inner resistance blinder
78Z1	Out-of-step mho element
SWING	Double blinder: 78R1 and 78R2 assert or only 78R1 asserts
OOST	Out-of-step trip
78D	Out-of-step delay
78TD	Out-of-step trip delay
78TDURD	Out-of-step trip duration
OOSTC	Out-of-step torque control

The device uses this scheme to distinguishes between short-circuit faults and out-of-step conditions by measuring how long the impedance trajectory remains between the two blinders. The trajectory is kept between the two blinders. During short-circuit faults, the impedance moves either inside the inner blinder or between the two. Blinders are applied almost instantly, ensuring that the 78D does not time out. Either case, keeps the out-of-step element from picking up.

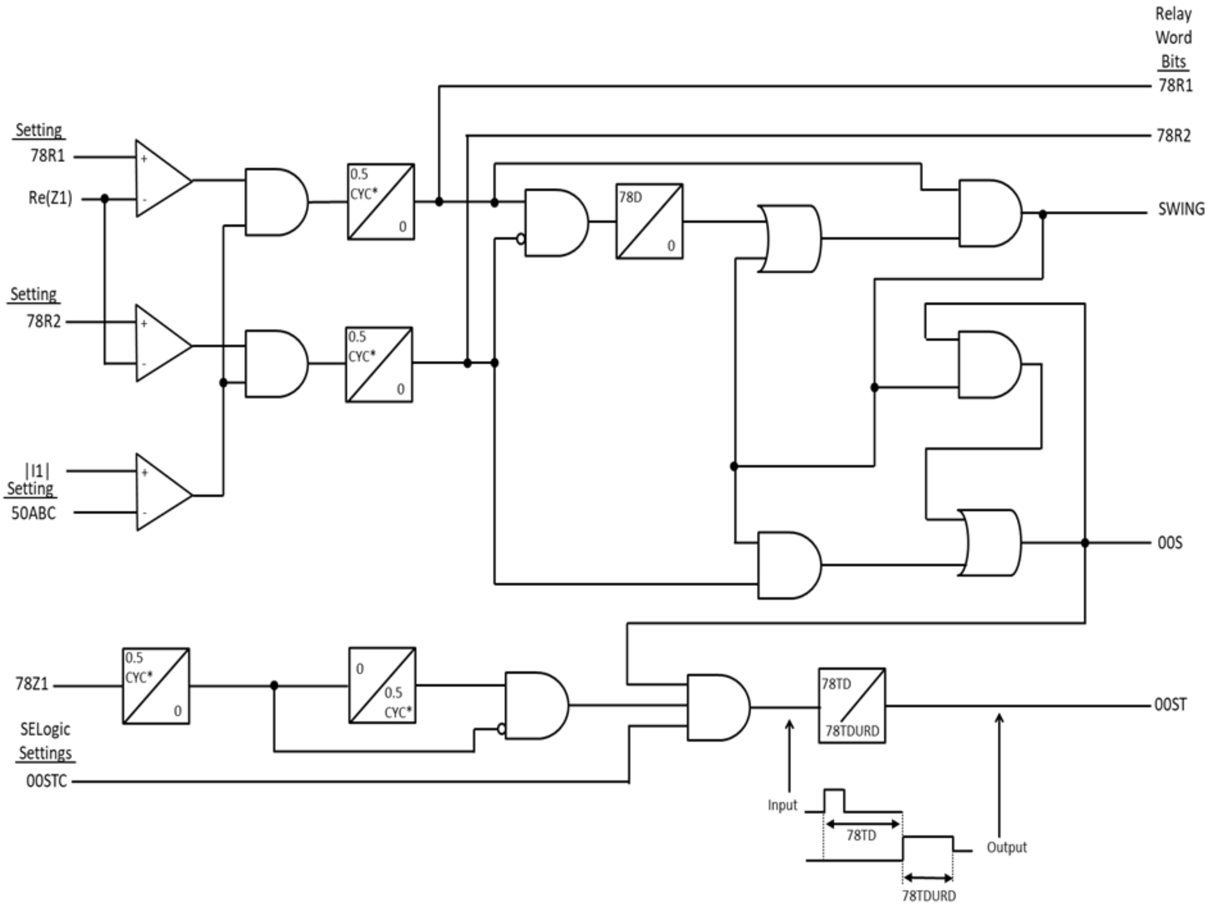

Figure 4.16: Double-Blinder Scheme SEL Logic Diagram (SEL700G IM).

4.7.1.2 OOS Protection Settings for the Double-Blinder Scheme

Forward reach and Reverse reach elements (78FWD and 78REV) have to be configured, the sum of these two quantities has to be 100 ohms or less for relays with 5A CT while they have to be 500 ohms or less for 1A CT relays. The inner blinder 78R2 has to be set such that its setting is greater than or equal to 5% of either forward or reverse reaches, one may choose whichever is greater. The SELogic 78 element torque control equation OOSTC can be left at a default setting 1, as if this setting is at one the out-of-step protection cannot be controlled by any other peripheral conditions.

The scheme includes positive-sequence current supervision 50ABC which contains a setting range of 0.25-3A for 5A relays and 0.05-6A for 1A relays. It should be noted though that this

50ABC settings tends to block the out-of-step function if the positive sequence current levels are below than this current supervision. The trip delay timer also has a 78TDURD (Trip Duration) adjustable dropout delay. If the Relay Word bit OOST is set to directly operate an output contact, the 78TDURD should be set appropriately. Because the Relay Word bit OOST is configured to trip the generator breaker with default trip logic TRX (which includes an identical timer TDURD), the 78TDURD is set to zero by default. If your application requires a different action, the user can change the settings (trip logic and/or 78TDURD).

Lastly the inner resistance blinder should be kept inside the mho circle, whereas the outer resistance blinder must be outside the mho circle in order to achieve a correct and distinctive operation of the scheme logic. When the swing locus first passes the inner blinder characteristic, the relay decides whether to trip. The secure execution of the method depends on the separation angle at this moment. The generator may trip on a recoverable swing if the angle is too small (big blinder setting). For satisfactory relay settings to be confirmed, transient stability studies are typically needed.

4.7.1.3 Settings Calculation for the relay in the system under study

The following system equipment parameters need to be known in order to calculate the response of the IED optimal placed in the system. Moreover, the OOS tripping zone is ought to reach the high-side bushings of the generator step-up transformer from the generator neutral (SEL700G IM).

- Transient reactance of the generator X'_d in secondary ohms.
- Impedance of the generator step-up transformer X_T in secondary ohms.
- Impedance of the line/lines beyond the gen step-up transformers, if necessary.
- All impedances need to be converted to generator base kV.

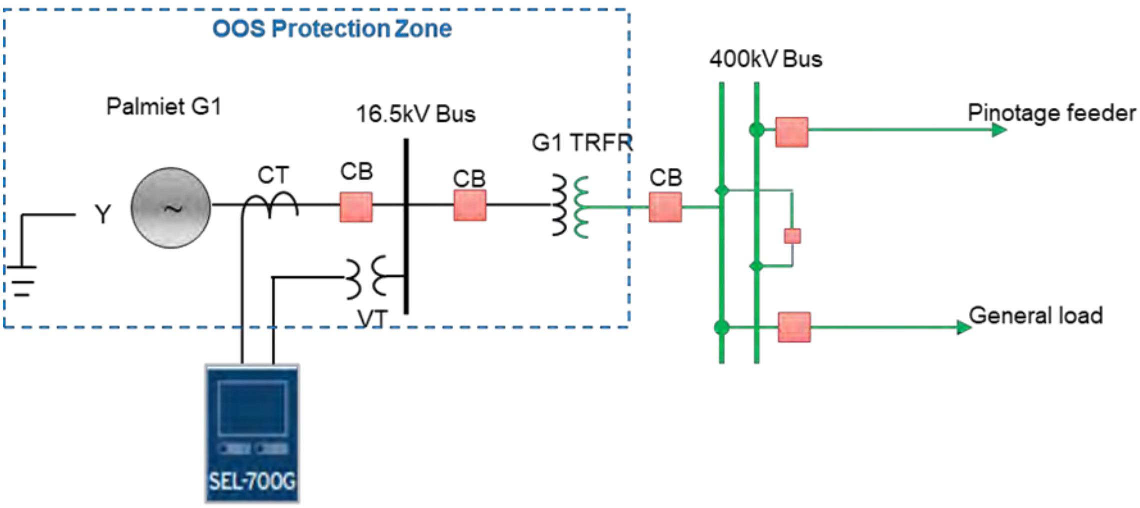

Figure 4.17: Abstract of system for thesis study network depicting the optimal placed SEL-700G relay

Table 4.2:Portion of Palmiet Generator design data

Generator Name Plate Ratings	
Nominal Frequency	50Hz
Capacity	250MVA
Voltage	16.5kV
Power Factor	0.8
Transient reactance X'_d	0.23 p.u
Subtransient reactance X''_d	0.16 p.u

When choosing current transformers for the scheme, the research project used class PX CTs, which state that the maximum design load current should not exceed the Ct rated primary current and the CT ratio should be high enough such that the CT secondary current does not exceed 20 times the rated current under the maximum symmetrical primary fault.

$$\begin{aligned} CT &= I_{FL} \times 120\% \\ &= 6.317kA \times 120\% \\ &= 7.58kA \end{aligned} \tag{4.3}$$

CT is then selected according to first standard rating above 7580A ≈ 7600A

According to IEC 60044-2 standard for voltage transformers, the value of VT rated primary voltage connected between 3-phase system and/or earth must be 1 or √3 times the value of rated system voltage. Then choose the next closest standardized usual value from IEC 60038 standard. A 16500V VT will suffice for this project.

$$CTR = \frac{7600}{1} = 7600 \tag{4.28}$$

$$PTR = \frac{16500}{110} = 150 \tag{4.6}$$

Conversion of impedances to generator base kV is then crucial:

$$V_{base} = 16.5kV \qquad MVA_{base} = 250MVA \qquad Z_{base} = \frac{V_{base}^2}{MVA_{base}} = 1.089\Omega$$

$$\begin{aligned} X'_{dsec} &= X'_d \cdot Z_{base} \cdot \frac{CTR}{PTR} \\ &= 0.23 \times 1.089 \times \frac{7600}{150} = 12.69\Omega \end{aligned} \tag{4.7}$$

Generator fault current level would then be given by:

$$Gen_{Fault} = \frac{Gen_{MVA}}{\sqrt{3} \cdot Gen_V \cdot X_d^{"}} = \frac{250MVA}{\sqrt{3} \times 16.5kV \times 0.16\, p.u} \tag{4.8}$$

$= 54.6kA$ this yields a secondary value of $\frac{54.6kA}{7600} = 7.18\ A$

Transformer reactance is given by where the impedance percentage of TRFR is in the name plate :

$$X_T = \frac{kV^2}{MVA} \times Z_T\% \tag{4.29}$$

$$= \frac{16.5^2}{250} \times 11.8\%$$

$$= \ 0.129\, p.u$$

Then Transformer reactance in secondary ohms will be:

$$X_{T\_sec} = X_T \cdot Z_{base} \cdot \frac{CTR}{PTR} \tag{4.10}$$

$$= \ 0.129 \times 1.089 \times \frac{920}{150}$$

$$= \quad 7.12\ \Omega$$

Protection philosophy calls for a slightly different mho blinder settings for a double blinder scheme compared to that of single blinder scheme, though using the same element names (SEL700G IM). It requires the 78FWD setting to be reduced to establish the outer blinder outside the mho circle. This effort is to ensure that the margin lies below the normal system swing curve, having significant overlap with the loss of field characteristic such that the entire generator impedance is covered:

$$78FWD = \ 2 \times X_d' = 2 \times 12.69 = 25.38\ \Omega \tag{4.11}$$

$$78REV = \ 1.5 \times X_T = 1.5 \times 7.12 = 10.68\ \Omega \tag{4.12}$$

The outer and inner blinders of this relay are made of 78R1 and 78R2 elements, with the blinders on the left and right being mirror images of each other:

$$78R1 = \ {}^{1}\!/_{2}\,(78FWD + 78REV) = {}^{1}\!/_{2}\,(25.38 + 10.68) = 18.03\Omega \tag{4.13}$$

$$78R2 = {}^{1}/_{2}\,(X'_d + X_T)\,tan\left(\theta - \frac{\alpha}{2}\right) \quad (4.14)$$

$$= {}^{1}/_{2}\,(12.69 + 7.12)\,tan\left(90 - \frac{120}{2}\right) = 5.72\Omega$$

The actual setting may be influenced by stability studies, but it will be limited between these boundaries.

When the perceived impedance passes between the outer and inner blinders, the timer setting is calibrated for the generator's maximum swing rate. The occurrence is considered as a fault rather than a swing and the relay OST function is disabled if the system swing locus moves between the blinders faster than the timer setting 78D. This is comparable to how many concentric characteristic schemes operate for both transmission relays and generators.

The outer and inner blinders must be properly separated to ensure that the relay reliably times the out-of-step slip frequency. Assume the largest out-of-step frequency seen is five slip cycles per second, which corresponds to 30 degrees each cycle (50 Hz). Set the blinders to 70° apart. This distance translates to a 2.3-cycle positive-sequence impedance travel time between the two blinders, which should give appropriate timing accuracy. Set the 78D timer to approximately 0.034 seconds (two cycles), ensuring that 78D will detect swings going at 30 degrees or less every cycle (SEL700G IM).

This relay is programmed to always trip after leaving the mho circle. Before issuing the OOS trip, the 78TD timer adds time after entering the mho circle. When exiting to the left, the maximum angle δ = 100.4°, thus additional delay helps ensure that the trip occurs only when the breaker opening is within the circuit breaker rating ($\delta \leq 90°$). In this scenario, with the same mho circle, add some time after the mho exit based on the generator's lowest projected swing rate against the system:

$$78TD = \frac{(\delta - 90°)}{(minimum\ swing\ rate)} \quad (4.15)$$

$$= \frac{(100.4° - 90°)}{(360°/sec)} = 0.02889\ second$$

$$= 1.73\ cycle\ (\ round\ of\ to\ the\ nearest\ 87TD\ half\ cycle = 2.0\ cycles)$$

The minimal amount of time that an OOS trip is held in after it asserts, is often set to be greater than the rated interrupting time of the breaker but less than the breaker failure time by some margin. One can set 78TDURD=3.0 cycles

The OOS characteristic is supervised by this positive sequence current element. It should be configured based on a minimum generation system under stressed conditions (including contingency outages), similar to a fault detector for the farthest-reaching phase distance element in a line protection scheme. It usually doesn't hurt to leave this value at 50ABC = 0.25 amp.

Since no additional supervision will be used for the protection philosophy under study, the OOSTC can be left at a value of 1 which is the default setting of the manufacturer.

Table 4.3: SEL-700G Double Blinder OOS Settings

Relay Element	Typical Value of the Manufacturer	Relay Setting
78REV	1.5-2 times X_T	25.38 Ω-sec
78FWD	2-3 times X'_d	10.68 Ω-sec
78R1	$^1/_2$ (78REV+78FWD)	18.03 Ω-sec
78R2	≥ 5% of MAX(78REV, 78FWD) and ≤$^1/_2$ (X'_d+ X_T) tan($\theta - \frac{\alpha}{2}$) where θ = 90° and α ≈ 120°	5.72 Ω-sec
78D	OOS delay	0.034 sec
78TD	Trip delay timer after mho circle exit	0.028 sec
78TDURD	Minimum trip duration timer	3.0 cycles
50ABC	Positive sequence current supervision for OOS element	0.25 amp
OOSTC	Out-of-step torque control	1

4.7.2 SEL-421 RELAY OOS PROTECTION (GENERATOR BACK-UP)

OOS protection is still a very prolific study subject; while the underlying principle remains the same, an incredible number of scholarly articles address the issue of OOS detection and coordination. The most popular detection approach is impedance-based, and it is followed by the most recent methods studied in literature. Many protection features, such as power swing blocking and out-of-step or pole-slip tripping functions, are built into contemporary distance relays. To distinguish faults from power swings and prevent distance or other relay elements from working during stable or unstable power swings, the power-swing blocking function's primary duty is to distinguish faults from power swings. The majority of power-swing blocking components rely on conventional techniques that track the positive sequence impedance rate. In many situations, especially those where quick swings are likely, it may be challenging to determine the necessary values for the power-swing blocking devices (Gonzalez-Longatt, et al, 2021). This subsection offers a step by-step settings calculations for a the SEL-421 relay optimally placed on the Palmiet-Pinotage transmission line to provide back-up protection to the generator OOS functionality for the Palmiet generating units.

The SEL-421features both an out -of -step tripping OST and out-of-step blocking scheme. Because the operation times of Zones 1 and 2 are often shorter than the times when the impedance of a power swing is present in these protection zones, the OSB logic typically supervises these two zones.

For instance, OSB logic should oversee instantaneous Zone 1 and communications-aided Zone 2 if the period of a swing is 1.5 seconds. Thus, OSB logic will block the phase distance protection during a swing measured within the operating characteristic of the phase impedance elements. It is not required to block all zones in practice, for this study application only Zone 1 and Zone 2 are of interest. Table 4.4 Lists the power system parameters of the line in subject.

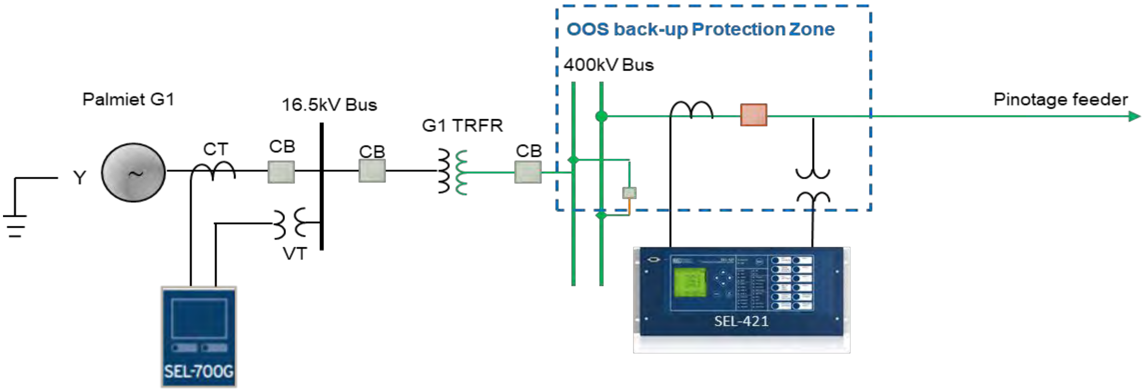

Figure 4.18: 400kV Power System

Table 4.4: Power System parameters data

Parameter	Value
Palmiet_Pinotage Line impedance (Z_1)	$8.032\angle 83.54°\ \Omega$
Zone 2 settings (Z_{2MP})	$9.68\angle 83.54°\ \Omega$
Source Impedance (Z_R)	$3.22\angle 90°\ \Omega$
Receiving end impedance (Z_R)	$3.76\angle 89.5°\Omega$
Current Transformer	600/1 A
Voltage Transformer	400000/110 V
Nominal Frequency	50Hz
Palmiet_Pinotage Line Length	29.6km
Maximum Load current	0.947 secondary

4.7.2.1 Resistive Blinders

The outermost characteristic in this study is Zone 2, therefore a safety margin of 20% is added for this application purpose (SEL-421 IM).

SEL advises assuming that Z1ANG is 90 degrees while setting Zone 6. This enables the user to configure the zone's resistive reach along the x-axis. When the zone setting is applied, the relay will internally modify the setting based on the line angle Z1ANG which then yields the following equation:

$$\begin{aligned} R_{1R6} &= 1.2 \cdot \frac{Z2MP}{2} \\ &= 1.2 \times \frac{9.64}{2} \\ &= 5.78\,\Omega \end{aligned} \tag{4.16}$$

Z2MP depicts the zone 2 phase element reach of the mho characteristic.

The maximum load current, $I_{L(\max)}$, is 0.947A (measured at the secondary of the CT); a power flow study is commonly used to determine this value. When using this information, equation 4.17 can be used to determine the lowest load impedance ($Z_{L(\min)}$) that the relay should measure. The corresponding line-to-neutral voltage when the maximum load is present at the sending generator side is V_{LN} = 63.5. V secondary.

$$\begin{aligned} Z_{L(\min)} &= \frac{V_{LN}}{I_{L(\max)}} \\ &= \frac{63.5\,V}{0.947\,A} \\ &= 67\Omega \end{aligned} \tag{4.17}$$

Assuming that the maximum load angle is 45° the blinder setting R_{1R7} is calculated as follows:

$$\begin{aligned} R_{1R7} &= 0.9 \times Z_{L(\min)} \cdot \cos A \\ &= 0.9 \times 67\Omega \times \cos[45° + (90° - Z1_{ANG})] \\ &= 0.9 \times 67\Omega \times \cos[45° + (90° - 83.54°)] \\ &= 37.57\Omega \end{aligned} \tag{4.18}$$

The inner reactance lines X_{1T6} in Zone 6 should entirely include the outermost zone of phase distance protection that should be prevented from tripping during a power swing. Zones 6 and 7 reactance lines are calculated using equations 4.19 and 4.20 respectively.

$$\begin{aligned} X_{1T6} &= 1.2 \times Z2MP \\ &= 1.2 \times 9.6389 = 11.56\Omega \end{aligned} \tag{4.19}$$

$$X_{1T7} = X_{1T6} + (R_{1R7} - R_{1R6}) \tag{4.20}$$

$$= 11.56 \times (37.57 - 5.78) = 43.35\Omega$$

For OOS blocking delay δ_6 and δ_7 are calculated using the following equations:

$$\delta_6 = 2 \cdot \tan^{-1}\left[\frac{\frac{|Z_T|}{2}}{R_{1R6}}\right] \tag{4.21}$$

$$= 2 \cdot \tan^{-1}\left[\frac{10.18\angle 83.8°}{5.78}\right]$$

$$= 119.7°$$

$$\delta_7 = 2 \cdot \tan^{-1}\left[\frac{\frac{|Z_T|}{2}}{R_{1R7}}\right] \tag{4.22}$$

$$= 2 \cdot \tan^{-1}\left[\frac{10.18\angle 83.8°}{37.57}\right]$$

$$= 66.37°$$

5Hz is a typical stable swing frequency used by this vendor, the value can then be used to acquire OSBD setting:

$$OSBD = \frac{(\delta_6 - \delta_7)50Hz}{\frac{360°}{cycle} \times 5Hz} \tag{4.23}$$

$$= \frac{(119.7° - 66.37°)50Hz}{\frac{360°}{cycle} \times 5Hz}$$

$$= 1.875\ cycles$$

Table 4.5:SEL-421 OOS protection settings for the test system.

Setting	Description	Secondary value entry
R_{1R6}	Zone-6 Resistance	5.78Ω
R_{1R7}	Zone-7 Resistance	37.57Ω
X_{1T6}	Zone-6 Reactance	11.56Ω
X_{1T7}	Zone-7 Reactance	43.35Ω
OSTD	OOS trip delay	1 cycle
50ABC	Positive current supervision	1 A
OSB (1,2,3)	Block Zone	All zones
OSBD	OOS block time delay	1.75 cycles
OOS, no of crossings	Impedance crossing	1

All resistive reach configurations are parallel to the line angle and all reactance reach parameters are perpendicular to the line angle. The following OOS characteristic is then obtained in practice.

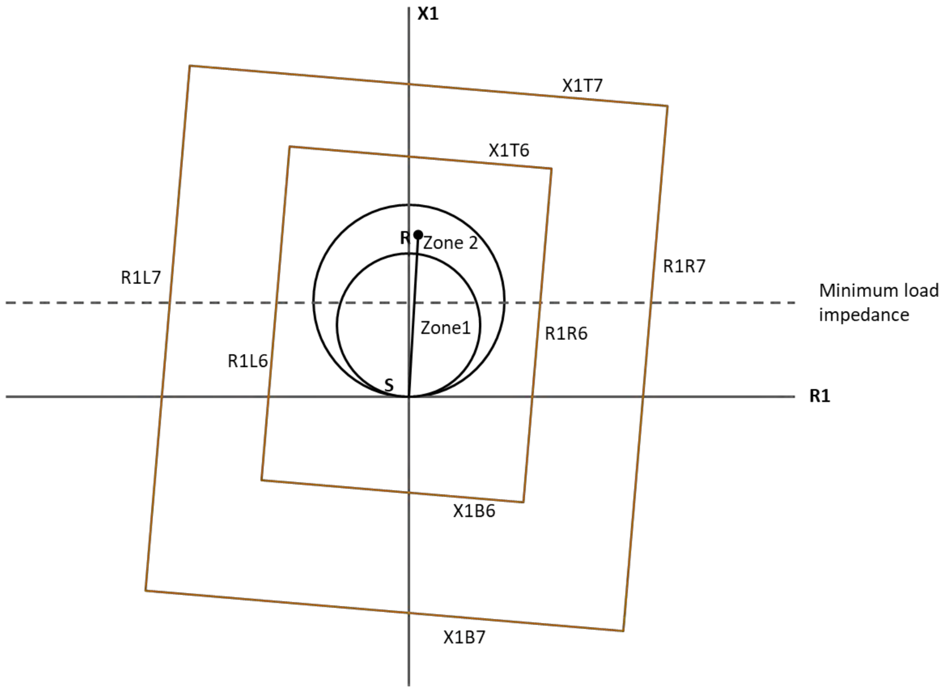

Figure 4.19: OOS settings Characteristic (SEL-421)

4.7.3 Stability Studies

Out-of-step protection settings are calculated by examining the probable range of apparent impedance trajectories in the R-X impedance plane, as well as the related swing rate. Out-of-step protection can be configured using graphical approaches or by conducting transient stability studies (Kundur. P, et al, 2004). While graphical approaches are convenient and straightforward, transient stability studies can be a useful tool for establishing settings or validating the accuracy of settings acquired using a graphical method. The dynamic models of power system elements, specifically rotating machines, and associated control systems, such as the AVR, turbine governor, and Power System Stabilizer (PSS), are studied in transient stability studies.

Graphical techniques are often based on an ideal two-source model with an analogous transmission system model. These models depict a system with two coherent sets of generators swinging against each other, or a generating unit or plant swinging against the rest of the system. These models ease the process of establishing settings, but they have limitations because actual swings are more complex and may display traits that simplified models cannot identify.

Transient stability studies take more time and effort, but they allow you to mimic actual system swings with numerous modes, time-varying voltages, and sudden changes in the apparent impedance trajectory caused by switching events during the swing. Transient stability studies also reveal the position of the electrical centre of potential swings, i.e., whether the swings will travel via the generator or GSU transformer or a transmission line exiting the generating station. Because the apparent impedance locus varies, it is preferable to base out-of-step protection settings on transient stability simulations. Stability studies are used to assess a wide range of operational situations and emergencies. The following issues are addressed in studies:

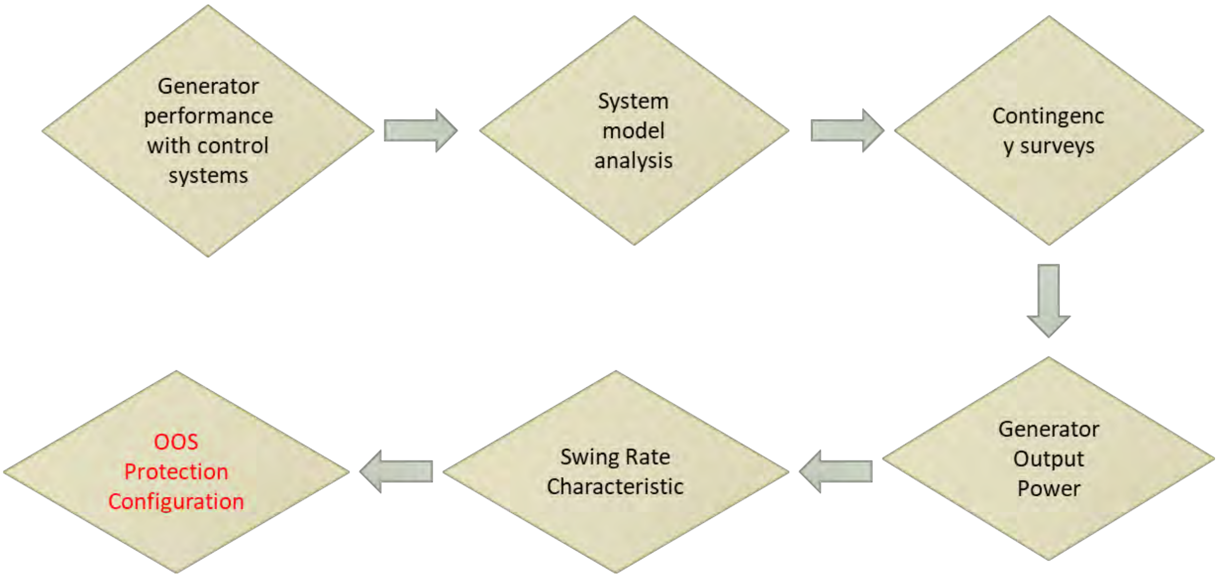

Figure 4.20: OOS Protection Methodology

<u>Generating Unit Models</u>

The generating unit model should contain the excitation system, power system stabilizer (if in service), and governor to accurately reflect generator performance.

<u>System Model</u>

The system model should be precise for the time being of interest, taking present and future initiatives into account.

<u>Contingencies</u>

Typically, surveys are based on significant contingencies identified through planning studies. Planning studies may exclude situations in which the generator loses synchronism, depending on the features of the generator and the system to which it is attached. In such circumstances, providing out-of-step protection may still be desirable, in which case more severe scenarios may be incorporated to the study.

<u>Generator Output</u>

The magnetic field strength created in the air gap by the excitation system determines a generator's stability. The stability margin of a generator is reduced when it works at a leading power factor (i.e., the generator is under-excited and absorbing reactive power). As a result, studies should cover plausible operating situations with the generator at or near its minimal reactive power (maximum absorbing reactive power).

Characteristic of system swing rates

Transient stability simulations are typically used to model system swing conditions. The swing rate (degrees/sec, which is proportional to the slip frequency, Hz) that an OOS relay may undergo is also determined by system stability studies. Several more credible swing rate estimates are available, even in the absence of specific transient stability studies.

- Local oscillations of a generator against the transmission system typically vary from 360 to 720 degrees per second (1-2 Hz).
- For various system settings, several different generalized estimates of transmission system swing rates point to a maximum value of 2.5 Hz (900°/sec).
- System oscillations (many generator plants in each area) rarely surpass 1 Hz (360°/sec) and can be as low as 0.2–0.3 Hz.

The characteristics of variations of the generator swing locus, which are typically circles on the positive sequence impedance plane, rely on the ratio of the system impedances and the Thevenin equivalent voltages of the generator and transmission system. The swing locus tends to "push" toward the transmission system (+X direction) and curve upward due to a decreased Thevenin equivalent voltage when transmission components are open, such as after clearing faulty elements and applying stress to the system. Additionally, in the typical situation where the automatic voltage regulator is in use, the generator voltage during a disturbance is initially not constrained by the excitation limiters, surpassing the equivalent voltage of the transmission system, and "pushing" the swing locus toward the transmission system.

The system conditions mentioned above serve as a general boundary for the swing locus range. System errors, fault clearing, and other system switching events all influence the apparent impedance at the generator relay.

4.8 CONCLUSION

The basic operating principles of protective relaying systems, as well as their functional properties, have been examined in this chapter. Relaying principles of synchronous machine has been conferred in detail to provide understanding of the generator behaviour during transient faults. The research system under study on which the OOS protective functions are based was addressed, taking into account all the essential calculations and power swing/pole slip effects on the OOST element, and any assumptions made were explicitly mentioned. Furthermore, settings calculations for OOS protection relating to SEL700G and SEL-421 relays have been implemented.

Transmission operators seek to preserve the machine from damage after an OOS occurrence so that the system can be restored to normal operation as soon as possible. The transmission operator also wants to trip the fewest components possible to prevent an increasing system disruption, thus does not want to rely on sympathetic tripping of nearby transmission elements to provide this protection. Both generator owners and transmission operators want the OOS system to be secure so that the generator is not taken out of service unnecessarily. By doing stability studies with adequate modelling of the system and the machine to establish swing characteristics for different circumstances, proper use of the relay scheme (either setting the relay or confirming the setting found by graphical methods) can be enhanced. The extensive stability studies issues have also been addressed which will be essential function later in the research study. Similarly, the performance of the element will then be of aid in predictive system analysis.

The next chapter seek to provide non-real time simulations to validate the reliability of the proposed adaptive scheme in DigSilent PowerFactory® simulation platform

5 CHAPTER FIVE

DIgSILENT system modelling, simulation, and results for OOS protection analysis of Pump Storage Plant.

5.1 INTRODUCTION

Beyond 2050, the complications for dependable and secure operation and planning of sustainable electrical networks will skyrocket. The combined effects of transnational grids and increased market pressures, the transition of generation technology to fulfil environmental standards, and changes in predicted future energy use are the causes of these difficulties (F. Gonzalez-Longatt, et al, 2018). Building a smarter grid is at the heart of the big changes in the way we supply and use energy. The capacity to accept considerable volumes of decentralized and highly variable renewable production necessitates upgrading network infrastructure to enable smart operation. Dynamically intelligent applications and solutions are being developed as dependable and sophisticated solutions to the anticipated problems of the future networks are being implemented during the gradual process of establishing the smarter grid. Additionally, the distinctions between transmission and distribution, which have been essential to the organization of the power sector and its engineering support groups, will become ambiguous and eventually vanish. In order to meet the economic, technical, and security requirements of upcoming smart grids, it is obvious that we need to rethink how we currently operate the power systems.

This chapter aims to develop a framework to investigate the power system rotor angle stability during steady state and transient stability occurrence in DIgSILENT PowerFactory® software. This is realised through performing root-mean square (RMS) and electromagnetic transients (EMT) simulations for the Eskom Western Grid that is adopted as the testing network. In completion of simulating the system behaviour analysis a protective relaying for generator out-of-step protection for Palmiet parallel generators will be implemented using SEL-700G in the DIgSILENT environment. In aid to predict the future system variations and planned outages impact on the system for a solid protection design; a Quasi-Dynamic simulation tool is also incorporated to fully run a simulation scan for designing critical clearing times of the protective equipment.

The Generators under study are outfitted with a variety of control systems, including speed governors (GOVs), automated voltage controllers (AVRs), and power system stabilizers (PSS) which form a composite frame for executing the RMS/ EMT simulations. The automatic voltage controller is in charge of controlling the excitation of the generator, and the power system stabilizers are an extra control loop to the AVR for the stability of both the rotor angle and the voltage at the generator's stator terminals. The active power is controlled by the speed governor. Its responsibility is to balance the active power between the generations' loads. The performance of the generator protection relay is studied through short-circuit events conditions injected on the station busbars supplied by these generators considering only the double blinder impedance scheme of the SEL-700G.

The adopted ESKOM test network is made up of the interrelated components listed below:

- 8 synchronous generators
- PV panel
- Wind turbine
- 16 transformers
- 9 overhead lines
- 7 loads
- 19 buses

The modified network is a multi-level voltage grid with 400kV running through the transmission lines and voltages of 132kV, 110kV,50kV,33kV,24kV and 16.5kV being the voltages available at the generating station buses. The system comprises of 2 independent power plant (IPPs) of renewable energy supplying the grid when necessary. The grid modelled in compliance with the national regulating standard (NERSA) which allows a per unit deviation of up to 10% from the standard 1.0 p.u in voltages across all buses in the grid. Furthermore, The South African grid code's network section 7.6.5 refers to the integration of new power stations and stipulates that transient stability must be maintained under the following conditions:

- A three-phase line or busbar fault cleared during regular protection periods, with the system healthy and the most demanding power station loading situation.
- A single-phase fault that is quickly resolved, leaving the system stable and;
- The toughest loading condition for power plants.
- A single-phase breakdown that was repaired during regular protection periods but left any one line unusable and the power plant loaded to its average availability.

Taking into account the grid code requirement indicated above, a series of case studies involving dynamic studies is constructed in the DIgSILENT platform with a nominal frequency of 50Hz . A visual representation of this test model showing a graphical network in a de-energised state can be seen in the figure below.

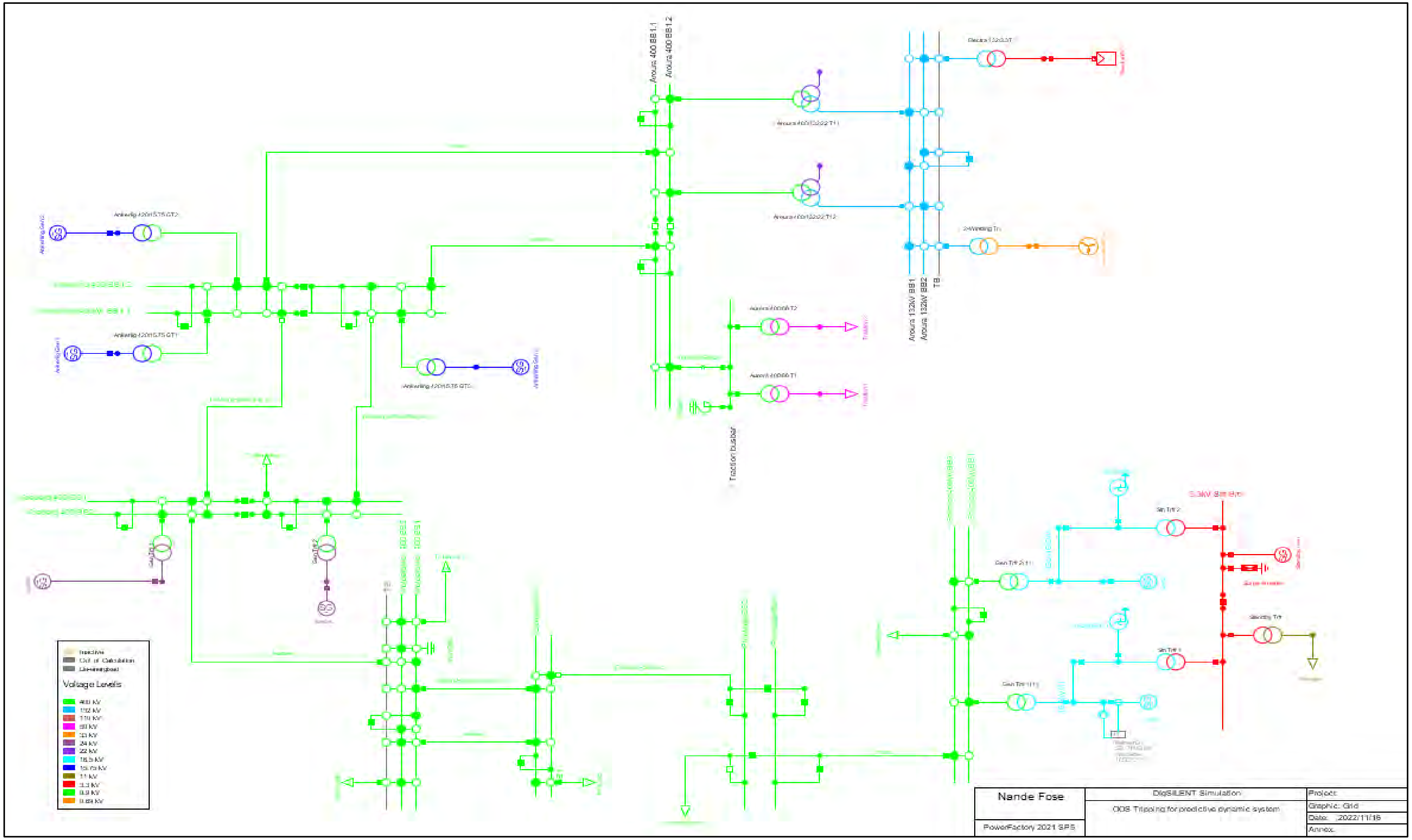

Figure 5.1: Modified Eskom West grid graphical representation in de-energised state

The network parameters used in the modified adopted test system are given in Tables below, with Table 5.1 presenting Bus data, which entails the voltage ratings in real and per unit values, voltage phi angle, also the active and reactive power of the load demand at the bus are given.

Table 5.1: Data for busbar parameters

Bus Data						
Bus Name	**Usage**	**V (p.u)**	**V_{rated} (kV)**	**Voltage Ø**	**P_{load} (MW)**	**Q_{load} (MVar)**
Palmiet Gen 1 B/B	Busbar	1.3	16.5	28.3°	200	108
Palmiet Gen 2 B/B	Busbar	1.3	16.5	28.3°	200	108
Palmiet 3.3kV Stn Brd	Busbar	1.0	3.3	152.3°	-	-
Palmiet 400kV B/B	Busbar	1.25	400	-108.8°	28.2	3.5
Pinotage B/B	Busbar	1.25	400	-108.4°	233.6	121.5
Stikland B/B	Busbar	1.46	400	-146.5 °	-	-
Muldersvlei B/B	Busbar	1.46	400	-146.5°	-102.2	-41.6
Koeberg B/B	Busbar	1.46	400	-146.5°	106	186.4
Ankerling B/B	Busbar	1.01	400	24.6 °	-	-
Aroura 132kV B/B	Busbar	1.02	132	25.3°	-	-
Aroura 400 B/B	Busbar	1.02	400	24.6°	-	-
Traction B/B	Busbar	1.02	400	24.8°°	-	-
Electra IPP	Junction Node	1	3.3	-24.4°	0.8	0.4
Fransvlei IPP	Junction Node	1.04	33	19.5°	47	16.7
Koeberg 1	Junction Node	1	24	169.3°	-866	163.4
Koeberg 2	Junction Node	1	24	15.78°	900	254.5
Ankerling Gen 1	Junction Node	0.96	15.75	0.469°	148.8	-1.2
Ankerling Gen 2	Junction Node	0.94	15.75	-197.8°	-345.2	-1.2
Ankerling Gen 3	Junction Node	0.96	15.75	0.469°	148.8	-1.2

Table 5.2 illustrates the data for each generator situated at each generating station with which the electrical ratings, plant category and dynamic controller models are specified.

Table 5.2: Generator data

Generator Data							
Generator					**Dynamic Controller Models**		
Name	**Type**	**MVA_{rated}**	**PF**	**Plant Category**	**Automatic voltage regulator**	**Governor**	**Power system stabiliser**
Ankerling Gen 1	P-V	186	0.8	Diesel	IEEET1	TGOV1	STAB1
Ankerling Gen 2	P-V	186	0.8	Diesel	IEEET1	TGOV1	STAB3
Ankerling Gen 3	P-V	186	0.8	Diesel	IEEET1	TGOV1	STAB3
Koeberg Gen1	Slack	1072	0.9	Nuclear	EXST2	GAST	STAB1
Koeberg Gen2	P-V	1072	0.9	Nuclear	EXST2	GAST	STAB1
Palmiet Gen 1	P-V	250	0.8	Pump storage	IEEET1	TGOV2	STAB1
Palmiet Gen2	P-V	250	0.8	Pump storage	IEEET1	TGOV2	STAB3

Standby Gen	P-V	250	0.9	Hydro	IEEET1	TGOV1	STAB3
Electra PV	P-Q	0.91	1	PV	-	-	-
Fransvlei	P-Q	2	0.8	Wind	-	-	-

Table 5.3 summarizes the transmission line data. These impedance parameters are shown as rectangular impedances. The rated line voltage of all the lines is 400 kV and line lengths are also provided in km. In Table 5.4 the load demand is presented where load classification and actual load demand at each station are stipulated.

Table 5.3: Transmission line data

Transmission Line Data			
Line Name	**Length**	**Line Impedance**	
		R in Ω	**X in Ω**
Ankerling-Aroura 400_1	82	1.921832	26.3643
Ankerling-Aroura 400_2	82	1.921832	26.3643
Koeberg-Ankerling 400_1	29.6	0.6937345	9.516869
Koeberg-Ankerling 400_2	29.6	0.6937345	9.516869
Muldersvlei-Koeberg 400	27.2	0.3815796	5.240827
Palmiet-Pinotage 400	29.6	0.9031993	7.981514
Pinotage – Stikland	20.7	0.6322947	5.927394
Stikland-Muldersvlei- 400_1	16.3	0.3797413	5.311185
Stikland-Muldersvlei- 400_2	16.3	0.3797413	5.311185

Table 5.4: Load data

Load demand			
Name	**Load Classification**	**P in MW**	**Q in Mvar**
Palmiet Storage 1	Agricultural	10	50
Palmiet load	Commercial	18	2
Pinotage load	Commercial	150	78
Stikland load	Domestic	150	0
Muldersvlei MV load	Industrial	6.1	2.95
Muldersvlei_kappa load	Domestic	-51	-21
Koeberg_Sterrekus 1	Commercial	50	87.9

The transformer information is also crucial for network modeling. Understanding the power flow through the transformer and computing protection settings are made possible by transformer data such as impedances and transformer ratio. Table 5.5 below contains this important information about electrical parameters of transformer, resistance is normally negligible since its approximately 0.0 p.u value. Reactance's are computed from 1000MVA base as the highest MVA rating transformer is 1050MVA . Included are the transformer's voltage rating (LV and HV).

Table 5.5: Transformer data

Transformer data					
Name	**MVA**	**HV (kV)**	**LV (kV)**	**R (p.u)**	**X (p.u)**
Standby Trfr	2	11	3.3	0.01	0.199
Stn board Trfr 1	10	16.5	3.3	0.002	0.15
Stn board Trfr 2	10	16.5	3.3	0.002	0.2
Palmiet Gen Trfr 1	260	400	16.5	0	0.118
Palmiet Gen Trfr 2	260	400	16.5	0	0.118
Koeberg Gen Trfr 1	1050	420	24	0	0.118
Koeberg Gen Trfr 2	1050	420	24	0	0.147
Ankerling Gen Trfr 1	186	420	15.75	0	0.11
Ankerling Gen Trfr 2	186	420	15.75	0	0.109
Ankerling Gen Trfr 3	186	420	15.75	0	0.109
Aurora Trfr 1	500	400	132	0.002	0.137
Aurora Trfr 2	500	400	132	0	0.136
Electra 132/3.3T	90	132	3.3	0.003	0.12
Fransvlei Trfr	80	132	33	0	0.108
Traction Trfr 1	40	400	50	0	0
Traction Trfr 2	40	400	50	0	0

5.2 WEST GRID TRANSMISSION SYSTEM MODELLING AND RELATIVE DYNAMIC CONTROLLER MODELS

Generators, transmission lines, composite load, and reactive power compensators are all part of the power system. Depending on the application, the configuration of these components may alter. The network is simulated using DIgSILENT simulation software, and all the parameters are shown in Tables 5.1 to table 5.5 above. Because the present Eskom west grid network model is generic and unsuitable for predictive dynamic stability research, the generator modeling had to be altered and plant models made from composite models in the software had to be added in each synchronous generator to meet the study's objectives. Dynamic models must be incorporated in the power system simulation tool in order to measure the contribution of the dynamic features of the components of a power system. For example, to simulate synchronous and asynchronous machines, the control systems of the voltage regulator and the speed governor must be included. The power system stabilizer must be incorporated in the synchronous generator model for further research, such as tiny signal stability. This is carried out to investigate the pole slipping of the 2 parallel generators at Palmiet pump storage when the system is presented with various contingencies. To optimize the generator OOS protection settings (SEL700G and SEL-421) the time varying transients presented on the system will be determined.

5.2.1 Model parameters for synchronous generators

In Figure 5.2 the input settings configured on the Koeberg synchronous generator 1 model in DIgSILENT are depicted. The data is captured in the manner shown in Table 5.2 above. The data capturing procedure is the same for all other 7 generators. Because it is a slack generator, this sort of generator is designated as the "reference machine." To view the generator's parameters, double-click it and select load flow.

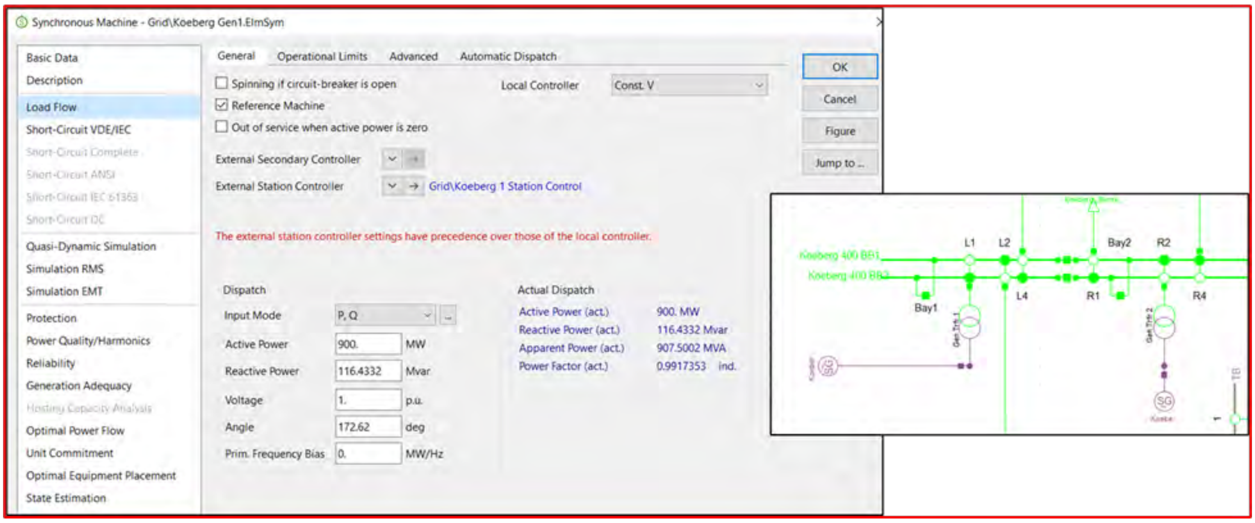

Figure 5.2: Koeberg Gen 1 parameters

5.2.2 Generation dynamic controllers

The generation plant has a control system that includes a power system stabilizer (PSS), automatic voltage regulator (AVR), and speed governing system (GOV).The controlling system's function is to control the active power flowing between the load and the generator. For the valve positions to adjust appropriately in response to the error signal supplied by the governor, feedback is employed to transmit the error signal to the turbine. Primary active power control is the name given to this process. To keep the power system voltage at the busbars, the reactive power is managed by AVRs and power system stabilizers. According to Figure 5.3 below, the three control systems are installed in traditional generation systems.

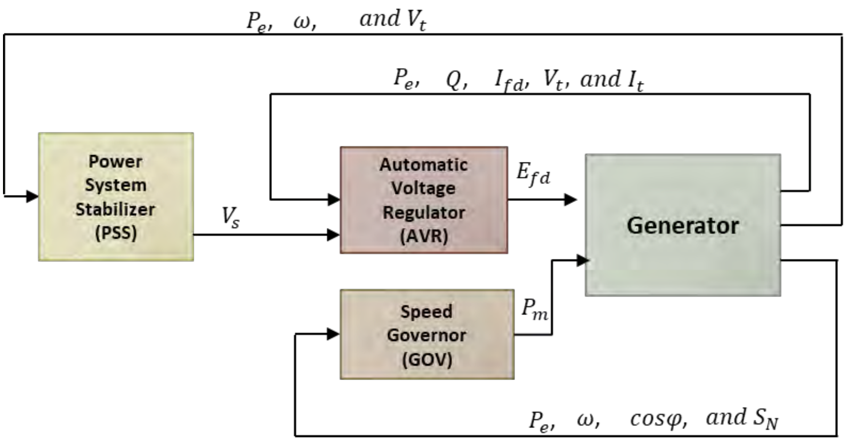

Figure 5.3: Model Frame structure for Generation system (Zhao et al., 2013).

In Figure 5.3 block diagram, V_s is the power system stabilizer's output voltage signal, E_{fd} and I_{fd} are the excitation voltage and current, P_m is the governor's mechanical power signal, P_e and Q are active and reactive power, V_t and I_t are the voltage and current at bus terminals, $cos\varphi$ is the power factor, and S_N is the nominal apparent power (Zhao et al., 2013).

The generation control system is critical in ensuring that power remains within limits even when there is a disturbance. This can only be accomplished by properly integrating the generation control system. The absenteeism or incorrect integration of the generation control system might result in power system instability. During dynamic analysis, the control systems within the generation plant must be modeled in order to meet the grid code requirement. Figure 5.4 below presents a snapshot of a typical dynamic frame model for Palmiet Gen 1 generation.

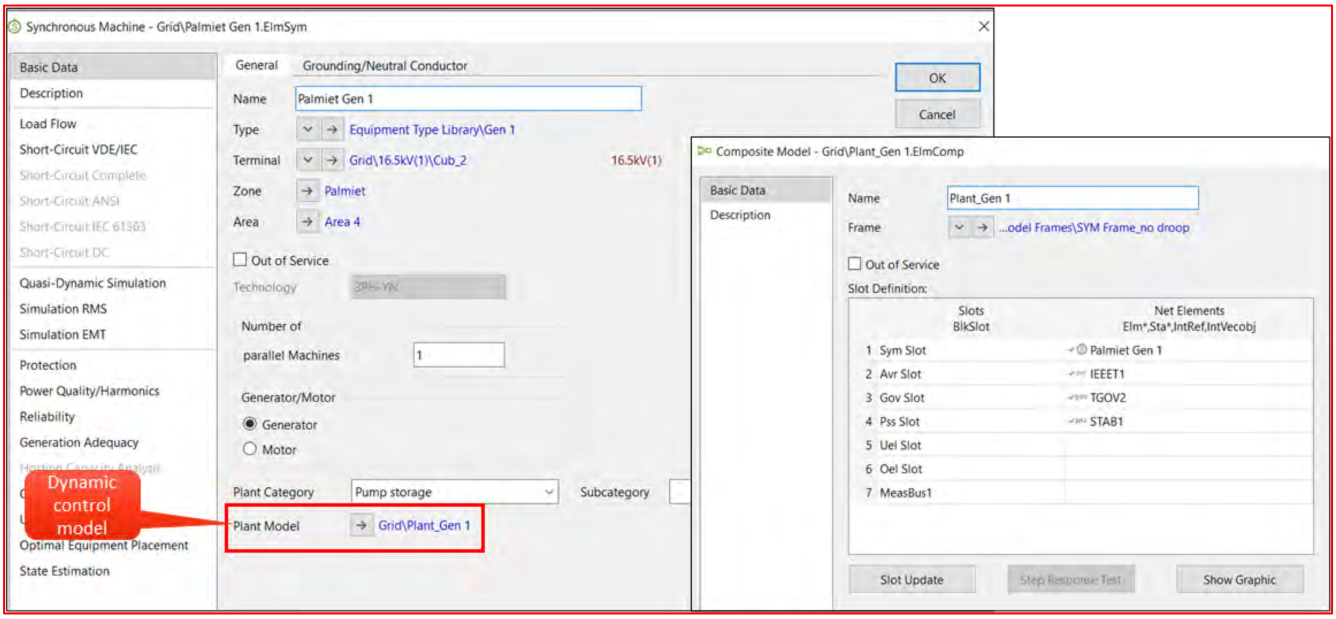

Figure 5.4: Dynamic frame modelled n DIgSILENT platform

5.2.2.1 Automatic voltage regulator

As previously mentioned in Chapter 3.4.2 it can be claimed that the purpose of the excitation system should be to maintain the terminal voltage under both normal and abnormal network disturbance conditions by automatically changing the excitation field. For this dissertation an IEEET1 model is implemented for Palmiet generators (1 and 2), according to DIgSILENT PowerFactory® 2021 manual; this model is frequently used to describe systems that have uncontrolled shaft-mounted rectifier bridges, alternator exciters, and shunt dc exciters. Internally, the AVR is adjusted for the dynamic response either by a lead lag filter in the direct path $\frac{1+sT_1}{1+sT_2}$ or a derivative in the feedback path $\frac{sT_f}{1+sT_f}$.

For the purpose of completeness, the over and under excitation limitations will now be covered since the summation point of an AVR comprises of these two parameters . The OEL limiter's job is to prevent the excitation system from supplying too much field current. When the system voltage abruptly drops and when the machine itself develops a problem, the field current may exceed the full load level. To avoid a voltage collapse, the field current must be increased for an extended period of time in order to maintain grid voltage until the fault is repaired. The job of the under-excitation limiter (UEL) on the other hand is to ensure that the field current does not go below a certain threshold or that the reactive power falls below a certain threshold. Excitation loss and asynchronous operation can occur if the UEL limitations are not maintained. Nonetheless for this investigation these two slots are not of utmost importance since the focus of the study isn’t on voltage stability studies as they affect mainly the voltage stability in the system.

A visual representation of the AVR model implemented for the Palmiet pump storage power plants can be seen in the Figure 5.5 below.

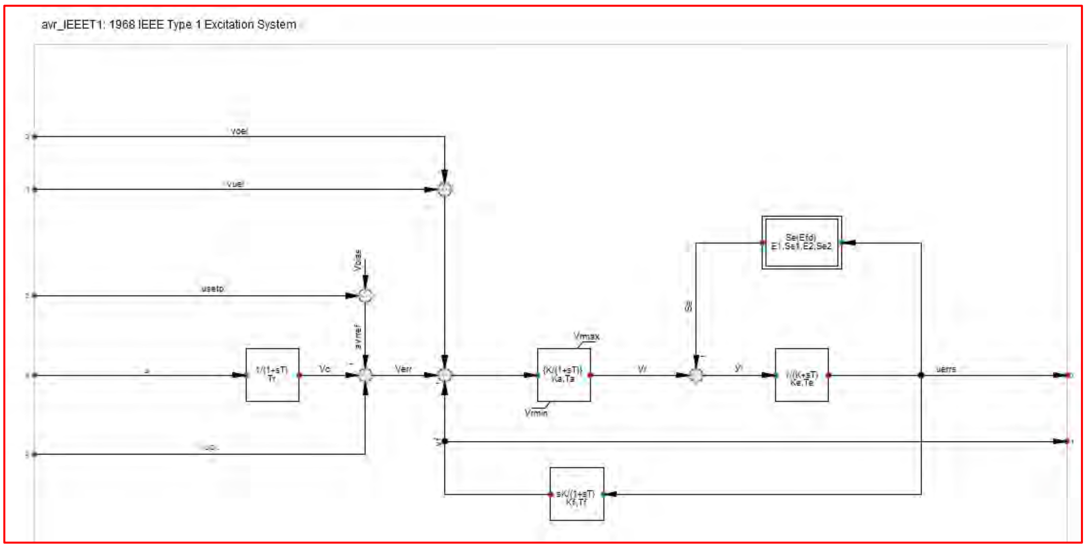

Figure 5.5: Palmiet plant AVR implemented in DigSilent PowerFactory

5.2.2.2 Speed / Turbine governor

Governors are not examined during first swing transient stability investigations, mostly because the governor's responses during these events are ignored. In essence governors are neglected if the duration of the dynamic study is less than 10 seconds. Their main purpose is to control turbine speed and/or load as previously cited in chapter 3.4.2 The governor slots implemented for Palmiet generators is TGOV2 type which provides a very convenient way to monitor the speed after the first swing transient stabilities and finds many applications in steam turbine generators as they comprise of fast-valving models. According to DigSilent user manual this governor represents governor action, a reheating time constant and the effects of fast valve closing to condense mechanical power. For illustrative purposes the applied governor slot is shown below in Figure 5.6.

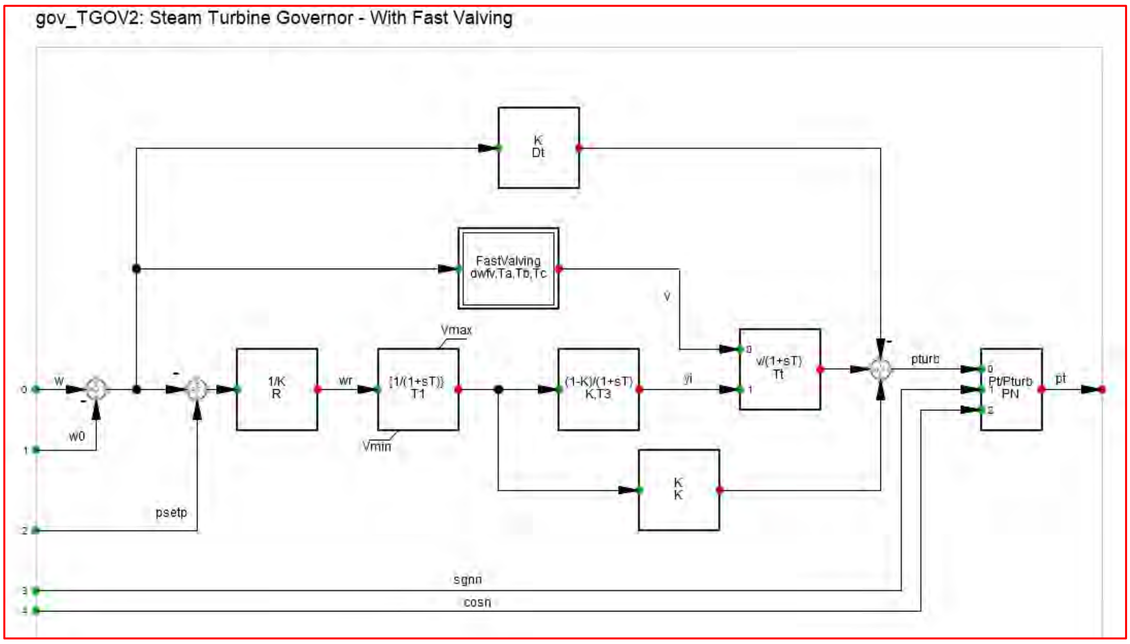

Figure 5.6: Speed governor implemented in Palmiet generating units

5.2.2.3 Power System Stabilizer

The power system stabilizer model, which is also discussed in Chapter 3 is necessary to stabilize the dynamic response induced by the high loop gain that is required for static accuracy. The model implemented for Palmiet generating units is the STAB1 and STAB3 for generator 1 and 2 respectively. STAB1 is referred to as a model type that is speed sensitive as it takes its sole input from the shaft speed of its specified generator. Meanwhile The STAB3 is power sensitive type model, this model is a specific representation of supplemental stabilizing units. It generates a supplementary signal by adding phase-lead into a signal proportional to the generator terminals' electrical power output (DigSilent user manual 2021).

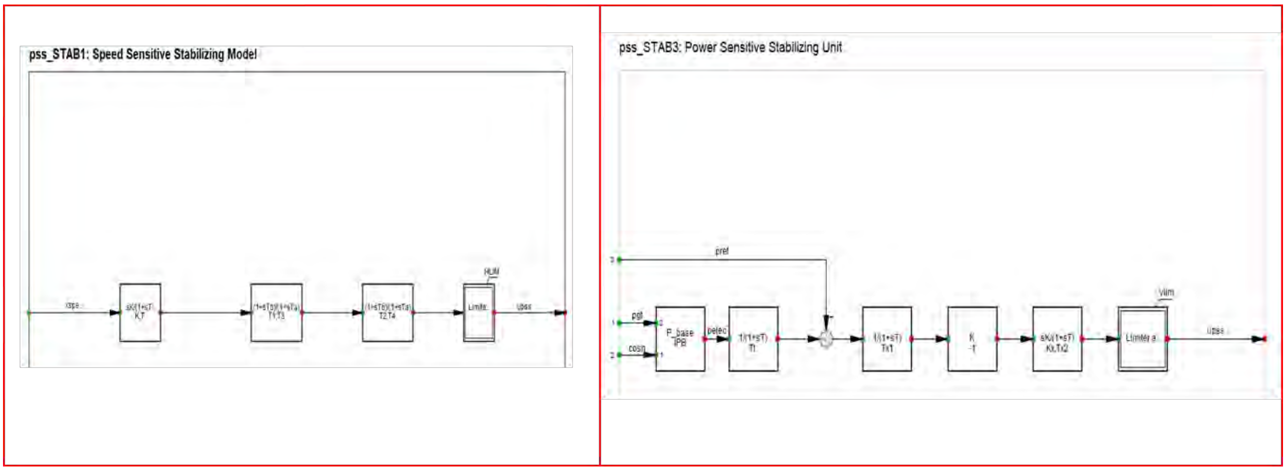

Figure 5.7: Power system stabilizers implemented at Palmiet generating units.

All other dynamic models optimally placed in the network generating units as stated in Table 5.2; their type of description and figure illustrations can be found in Appendices.

5.2.3 Model parameters for power transformer

The use of Palmiet Gen 1 in the model is to step-up voltage from generator terminals 16.5kV to 400kV bus for transmission to various parts of the grid. Double-click on the elements to bring up the element window and view the transformer's data. The transformer data will appear when you click the right-pointing direction under basic data-general, under type. This procedure is repeated for all the transformers in the test network. Figure 5.8 below shows such a window.

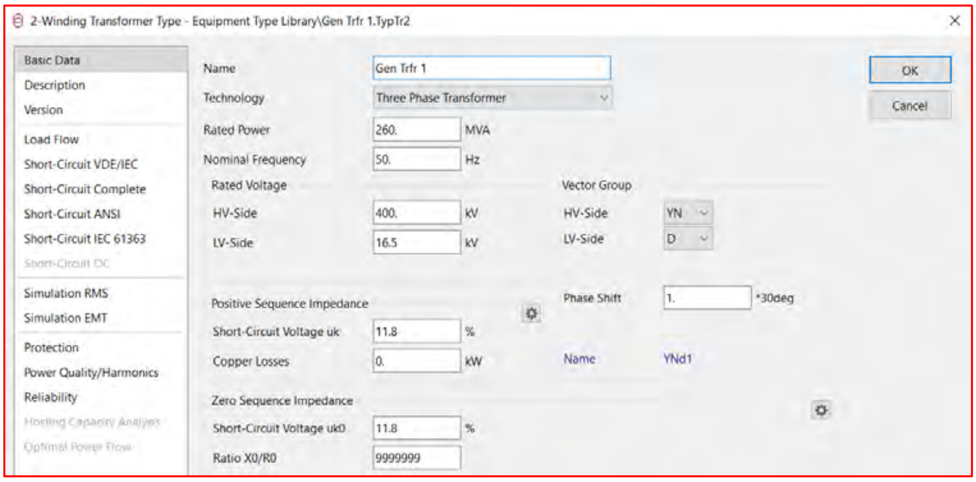

Figure 5.8: Transformer parameters

5.2.4 Model parameters for transmission line

The model of each line will differ since their parameters are different for the transmission line equivalent circuit data shown in Table 5.3 earlier. The line data for the Palmiet_Pinotage transmission line, transmitting from Palmiet 400kV bus is shown in Figure 5.9. Other transmission lines' data capturing processes won't be displayed because the parameter capture on DIgSILENT for those lines will be the same as that for Palmiet_Pinotage line.

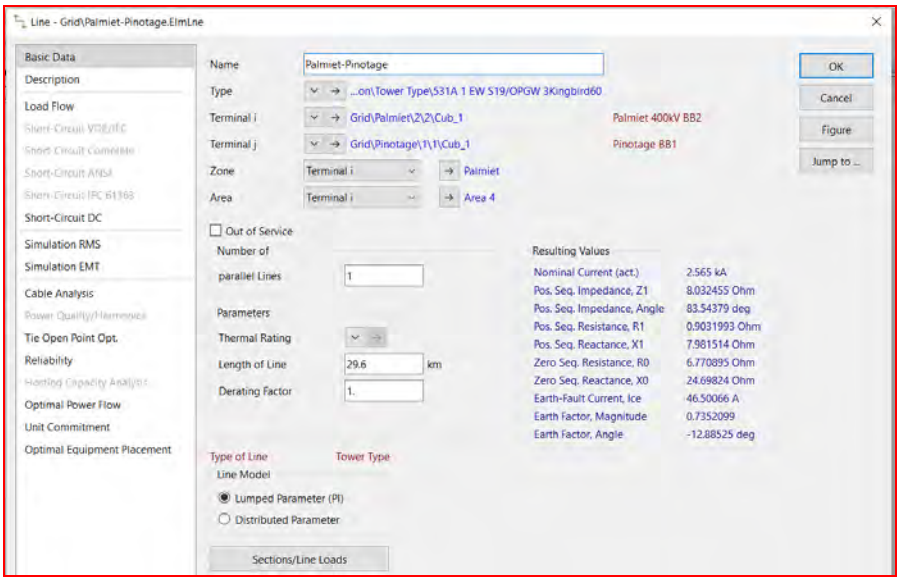

Figure 5.9: Palmiet_Pinotage transmission line data

5.2.5 Dynamic load parameters

Major voltage collapse accidents have demonstrated that the kind of load can significantly affect a power system stability. Given the variety of load types present on a single network, load modeling can be challenging. As a result, it is frequently preferable to classify the loads roughly into the following groups:

- Domestic.
- Industrial.
- Commercial; and
- Agricultural.

Loads are intricate because they do not behave as continual admittances; rather, most loads tend to restore their pre-disturbance power level following a system incidence. The table below adapted from (Van Cutsem, 2017) shows the recovery times for dynamic loads.

Table 5.6: Dynamic load response following system disturbance

Component	Time Scale	Internal Variable	Equilibrium Condition
Induction motor	$\sim 1\ second$	Motor speed	Mechanical torque = electromagnetic torque
Load tap changer	$\sim few\ minutes$	Transformer ratio	Control the voltage within a death band

Thermostatically controlled load	$\sim few\ minutes\ to\ tens\ of\ minutes$	Amount of connected load	Temperature within dead band

To be able to observe the behavior under network disturbances, loads in a simulation environment should be defined as belonging to a specific class. Only P_0 and Q_0 need to be specified for balanced load flow analyses, as executed in this dissertation. Equation (5.1), which has three polynomial terms, is used by DigSilent PowerFactory® to express how voltage-dependent the loads are (DIgSILENT, Technical Reference, 2020).

$$P = P_0(aP.\left(\frac{v}{v_0}\right)^{e-aP} + bP.\left(\frac{v}{v_0}\right)^{e-bP} + (1 - aP - bP).\left(\frac{v}{v_0}\right)^{e-cP}) \qquad (5.30)$$

where P_0 is the initial active power flow, v is the busbar voltage in per unit, and $1 - aP - bP = cP$ (DIgSILENT, Technical Reference, 2020). Information on the selection for the various load types is provided in Table 5.7.

Table 5.7: Different types of loads exponent selection

Exponential Constant	Constant
0	Power
1	Current
2	Impedance

A list of the various sorts of loads can be defined:

- Constant impedance: In this static load model, also known as a constant admittance, the power directly fluctuates with the square of the voltage magnitude (IEEE Task Force on Load Representation for Dynamic Performance, 1993).
- Constant current: In this static load model, the power directly fluctuates with the magnitude of the voltage.
- Constant power: This static load model, also known as a constant MVA model, does not modify its power in response to variations in voltage magnitude. Although this model is occasionally thought of as a conservative representation for induction motor loads, care should be taken when applying it (Rust. J. H, 1979). Only the active portion of the load and voltage levels between 80 and 90% have the constant MVA feature. As the voltage lowers past a certain amount, it is predicted that the reactive portion of an induction motor load will grow.

Many load models in power system modeling software give users the option to switch from constant MVA to constant impedance without tripping the load below a predetermined voltage in an effort to address shortcomings. The linear load (constant power) and the non-linear load (constant impedance) are the two types of loads that are modeled in this study for various load data models given in Table 5.4. RMS/EMT was simulated using DigSilent PowerFactory® software to show the differences in reaction to a trip at the HV busbar of the relative load demand. See Appendix B for load characteristic modelling of Palmiet s/s load.

5.3 Load flow analysis of the west grid network

The power system analysis is a thorough investigation that focuses on how different parameters affect the stability of the network. The steady-state and dynamic states of the analysis must both be evaluated. When the power system is working without interruptions, the steady-state analysis is conducted. As a result, the system's frequency is at its nominal value of 50Hz in steady state, when the generated active power equals the total of active load power demand and system power losses. The power flow analysis is the technique utilized to carry out this state of analysis (Tomsovic & Venkatasubramanian, 2005).

When assessing the performance and control of power systems, the electrical engineer frequently faces inquiries like:

- Are the voltages of each busbar in the power system acceptable?
- How is the various equipment in the power system loaded? (Generators, transmission lines, transformers, etc.
- How can I make the electricity system run as efficiently as possible?
- Is there a vulnerability (or vulnerabilities) in the power system? If so, where are they and how can I take precautions against them?

Although we may believe that the above questions would only arise when analyzing the behavior of "existing" power systems, the same questions can be posed when the task relates to the analysis of "future" systems or "expansion stages" of an already existing power system; for example, evaluating the impact of commissioning a transmission line or a power plant, or the impact of refurbishment or decommissioning of equipment (for example, shutting down a power plant).

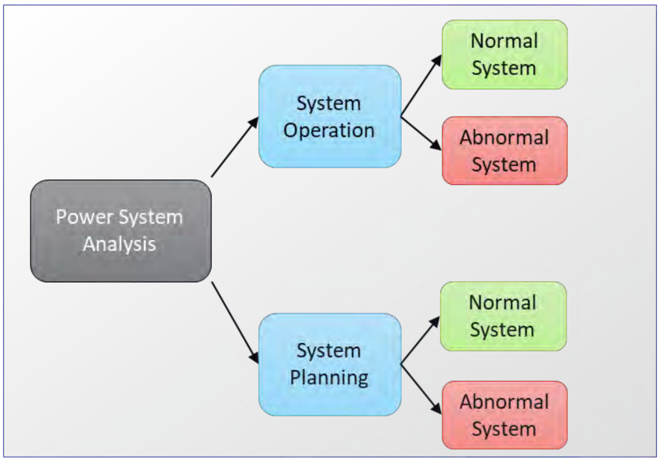

Figure 5.10: Consideration for power system analysis (DigSilent PowerFactory® 2020 user manual)

In a simulation environment a load flow is stated to be a steady-state analysis since it reflects the conditions of the system for a certain time stamp. For the purpose of the study, the active and reactive power flows for all branches, as well as the voltage magnitude and phase for all nodes, will be determined by a load flow calculation.

5.3.1 Load Flow Method

Newton-Raphson (Power Equations, classical) algorithm is calculated in the study owing to large transmission heavily loaded lines. Iterative techniques is used to solve the resulting nonlinear equation systems. This type of formulation converges best when the subject network is of large transmission grid, Figure 5.11 below shows the iterative method used to execute load flow studies of the modified Eskom West grid in DigSilent PowerFactory® environment.

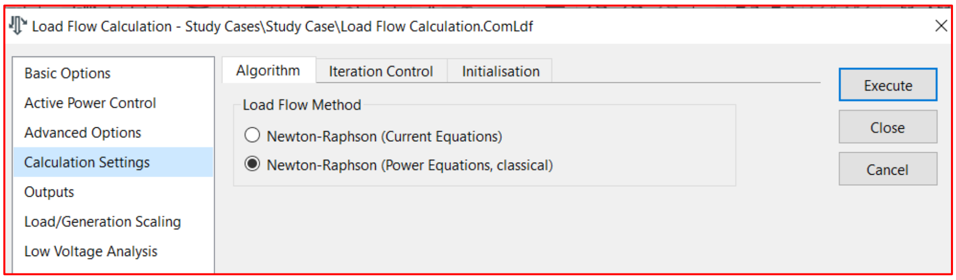

Figure 5.11: Applicable load flow method for the West grid

Incompletion of the load flow execution a complete system report denoting all the system parameters in-a steady state can be drawn out. This report includes but not limited to; installed generation loading capacity, busbar voltage profiles with tolerable normal operating deviation range of +/- 10%. Protection devices installed in the network, Area zone summaries. Snapshots depicting bus voltage profile results and grid summary are illustrated in Figure 5.12 and 5.13 respectively.

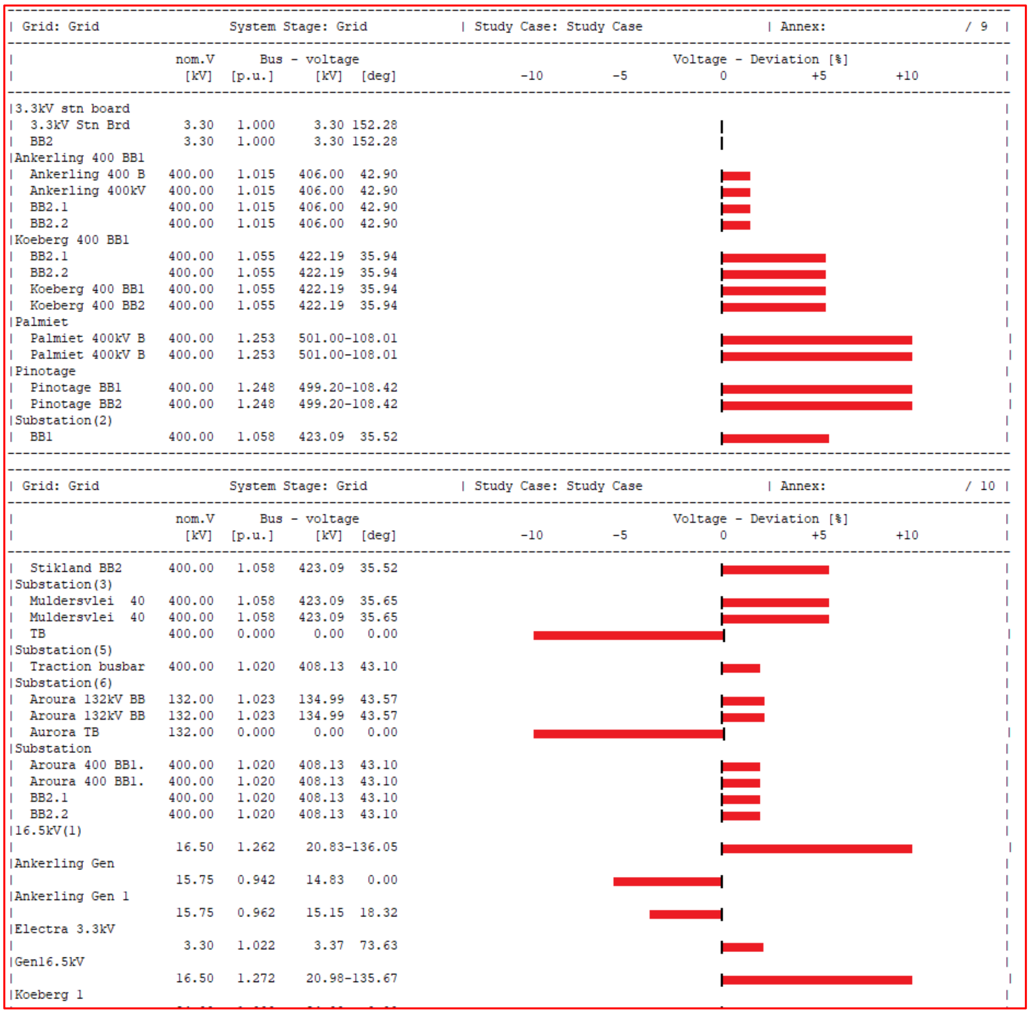

Grid: Grid	System Stage: Grid	Study Case: Study Case	Annex:	/ 9

	nom.V [kV]	Bus - voltage [p.u.]	[kV]	[deg]
3.3kV stn board				
3.3kV Stn Brd	3.30	1.000	3.30	152.28
BB2	3.30	1.000	3.30	152.28
Ankerling 400 BB1				
Ankerling 400 B	400.00	1.015	406.00	42.90
Ankerling 400kV	400.00	1.015	406.00	42.90
BB2.1	400.00	1.015	406.00	42.90
BB2.2	400.00	1.015	406.00	42.90
Koeberg 400 BB1				
BB2.1	400.00	1.055	422.19	35.94
BB2.2	400.00	1.055	422.19	35.94
Koeberg 400 BB1	400.00	1.055	422.19	35.94
Koeberg 400 BB2	400.00	1.055	422.19	35.94
Palmiet				
Palmiet 400kV B	400.00	1.253	501.00	-108.01
Palmiet 400kV B	400.00	1.253	501.00	-108.01
Pinotage				
Pinotage BB1	400.00	1.248	499.20	-108.42
Pinotage BB2	400.00	1.248	499.20	-108.42
Substation(2)				
BB1	400.00	1.058	423.09	35.52

Grid: Grid	System Stage: Grid	Study Case: Study Case	Annex:	/ 10

	nom.V [kV]	Bus - voltage [p.u.]	[kV]	[deg]
Stikland BB2	400.00	1.058	423.09	35.52
Substation(3)				
Muldersvlei 40	400.00	1.058	423.09	35.65
Muldersvlei 40	400.00	1.058	423.09	35.65
TB	400.00	0.000	0.00	0.00
Substation(5)				
Traction busbar	400.00	1.020	408.13	43.10
Substation(6)				
Aroura 132kV BB	132.00	1.023	134.99	43.57
Aroura 132kV BB	132.00	1.023	134.99	43.57
Aurora TB	132.00	0.000	0.00	0.00
Substation				
Aroura 400 BB1.	400.00	1.020	408.13	43.10
Aroura 400 BB1.	400.00	1.020	408.13	43.10
BB2.1	400.00	1.020	408.13	43.10
BB2.2	400.00	1.020	408.13	43.10
16.5kV(1)	16.50	1.262	20.83	-136.05
Ankerling Gen	15.75	0.942	14.83	0.00
Ankerling Gen 1	15.75	0.962	15.15	18.32
Electra 3.3kV	3.30	1.022	3.37	73.63
Gen16.5kV	16.50	1.272	20.98	-135.67
Koeberg 1				

Voltage - Deviation [%]: -10, -5, 0, +5, +10

Figure 5.12:Busbar voltage deviation profiles

	DIgSILENT PowerFactory 2021 SP5	Project: Date: 2022/11/23

Load Flow Calculation — Grid Summary

AC Load Flow, balanced, positive sequence		Automatic Model Adaptation for Convergence		Yes
Automatic tap adjustment of transformers	Yes	Max. Acceptable Load Flow Error		
Consider reactive power limits	Yes	Bus Equations(HV)		1.00 kVA
		Model Equations		0.10 %

Grid: Grid | System Stage: Grid | Study Case: Study Case | Annex: | / 1

Grid: Grid Summary

No. of Substations	10	No. of Busbars	37	No. of Terminals	208	No. of Lines	9
No. of 2-w Trfs.	12	No. of 3-w Trfs.	2	No. of syn. Machines	8	No. of asyn.Machines	0
No. of Loads	9	No. of Shunts/Filters	2	No. of SVS	0		

Generation =	420.35 MW	507.86 Mvar	659.25 MVA
External Infeed =	0.00 MW	0.00 Mvar	0.00 MVA
Inter Grid Flow =	0.00 MW	0.00 Mvar	
Load P(U) =	416.85 MW	203.24 Mvar	463.76 MVA
Load P(Un) =	333.10 MW	199.85 Mvar	388.46 MVA
Load P(Un-U) =	-83.75 MW	-3.38 Mvar	
Motor Load =	0.00 MW	0.00 Mvar	0.00 MVA
Grid Losses =	3.50 MW	427.65 Mvar	
Line Charging =		-226.81 Mvar	
Compensation ind. =		0.00 Mvar	
Compensation cap. =		-2.12 Mvar	
Installed Capacity =	3052.11 MW		
Spinning Reserve =	2603.45 MW		

Total Power Factor:
Generation = 0.64 [-]
Load/Motor = 0.90 / 0.00 [-]

Figure 5.13: System grid summary

Figure 5.13 above displays the modified Eskom West Grid network grid summary findings for operating with steady-state load flow. There is also an indication of the overall number of power system components employed in the network, the no of busbars used shows a vast number of buses as compared to the ones mentioned earlier in the chapter; this is due to the busbar topologies employed at each of the stations, for instance at Muldersvlei s/s we have a double busbar with a transfer bus topology. The entire load demand is displayed as 416.85MW, the operational installed generating active power capacity is shown as 3052.11MW, the grid power losses are shown as 3.50MW, and the generation active power is shown as 420.35MW. The generation spinning reserves, which are stated to be 2603.45MW, are used when the load demand changes. The spinning reserves demonstrates a huge amount of unused generating capacity owing to the fact that Koeberg power station is a national generating unit but for the purpose of the study only the modified regional loads are of interest.

Two protection devices SEL-700G and SEL-421are placed on the Palmiet parallel generators and Palmiet outgoing feeder for OOS tripping during pole slipping of these generators. A predefined Load-flow analysis report also comprises of relays optimally placed in the network along with their measuring devices, current transformers and voltage transformers see Figure 5.14 below.

```
----------------------------------------------------------------------------------------------------------------------------------
| Relay Model                          Relay Type : SEL 421-1A                                                                    |
|   Ct     : Current Transformer       Location   : Busbar         : Palmiet 400kV BB2    /Palmiet           Ratio        : 600A/1A     |
|                                                   Branch         : Palmiet-Pinotage                        Connection   : Y           |
|                                                                  :                                                                 |
|   Vt     : Voltage Transformer       Location   : Busbar         : Palmiet 400kV BB2    /Palmiet           Ratio        : 400000V/1V  |
|                                                   Branch         : Palmiet-Pinotage                                     :   - Y       |
|   Polarizing Z1    : Polarizing Z1                                  Line-Line Impedances                     Impedances              |
|     Polarisation Unit    : Phase-Phase/Phase-Earth          [pri.Ohm]     [sec.Ohm]     [deg]        [pri.Ohm]     [sec.Ohm]     [deg]  |
|     Polarisation Method : Positive Sequence            A :    495.652         0.743      8.95          494.359         0.742      8.79  |
|     Earth Factor,       k0 :    0.735                  B :    497.233         0.746      8.85          497.530         0.746      8.90  |
|     Earth Factor, Angle : -12.88  deg                  C :    495.702         0.744      8.74          496.708         0.745      8.86  |
|   Polarizing Z     : Polarizing Z                                   Line-Line Impedances                     Impedances              |
|     Polarisation Unit    : Phase-Phase/Phase-Earth          [pri.Ohm]     [sec.Ohm]     [deg]        [pri.Ohm]     [sec.Ohm]     [deg]  |
|     Polarisation Method : Positive Sequence            A :    495.652         0.743      8.95          494.359         0.742      8.79  |
|     Earth Factor,       k0 :    0.735                  B :    497.233         0.746      8.85          497.530         0.746      8.90  |
|     Earth Factor, Angle : -12.88  deg                  C :    495.702         0.744      8.74          496.708         0.745      8.86  |
|   Z1MP     : Z1MP                      ( IEC: Z>>    ANSI: 21    )     Unit     : Phase-Phase      Zone: 1                          |
|     Characteristic          :    Mho                     Tripping Direction   : Forward          Tripping Time        Total Tripping Time |
|     Replica Impedance       :    6.450 sec.Ohm   Reach Multiplier100.00  %                   A :      0.015 s             0.015 s     |
|     Relay Angle             :   83.54  deg       Max. Reach   :       6.450 sec.Ohm          B :      0.015 s                         |
|     Character. Angle        :   90.00  deg                         4300.000 pri.Ohm          C :      0.015 s                         |
|     Offset                  :    0.00  sec.Ohm   0.00 deg                                                                         |
----------------------------------------------------------------------------------------------------------------------------------

----------------------------------------------------------------------------------------------------------------------------------
| Grid: Grid                   System Stage: Grid              | Study Case: Study Case                  | Annex:                  / 8  |
----------------------------------------------------------------------------------------------------------------------------------

----------------------------------------------------------------------------------------------------------------------------------
|   Z2MP     : Z2MP                      ( IEC: Z>>    ANSI: 21    )     Unit     : Phase-Phase      Zone: 2                          |
|     Characteristic          :    Mho                     Tripping Direction   : Forward          Tripping Time        Total Tripping Time |
|     Replica Impedance       :    9.650 sec.Ohm   Reach Multiplier100.00  %                   A :      0.015 s             0.415 s     |
|     Relay Angle             :   83.54  deg       Max. Reach   :       9.650 sec.Ohm          B :      0.015 s                         |
|     Character. Angle        :   90.00  deg                         6433.333 pri.Ohm          C :      0.015 s                         |
|     Offset                  :    0.00  sec.Ohm   0.00 deg                                                                         |
|   Logic       : Logic                                                                  yout                :  9999.999 s            |
|     Breaker              Cubicle       Branch                   Busbar               / Substation       Fault Clearing Time          |
|      CB2                 Cubicle_S0.1.1B2                       T2.2                 /  Palmiet                 9999.999 s          |
----------------------------------------------------------------------------------------------------------------------------------
| Palmiet G1                           Relay Type : SEL 700G 1A                                                                   |
|   Ct  X   : Palmiet G1 CT X          Location   : Busbar         : 16.5kV(1)            /                  Ratio        : 7600A/1A    |
|                                                   Branch         : Palmiet Gen 1                           Connection   : Y           |
|                                                                  :                                                                 |
|   Ct  Y   : Palmiet G1 CT X          Location   : Busbar         : 16.5kV(1)            /                  Ratio        : 7600A/1A    |
|                                                   Branch         : Palmiet Gen 1                           Connection   : Y           |
|                                                                  :                                                                 |
|   Ct  In  : Palmiet G1 CT X          Location   : Busbar         : 16.5kV(1)            /                  Ratio        : 7600A/1A    |
|                                                   Branch         : Palmiet Gen 1                           Connection   : Y           |
|                                                                  :                                                                 |
|   Vt  X   : Voltage Transformer      Location   : Busbar         : 16.5kV(1)            /                  Ratio        : 16500V/110V |
|                                                   Branch         : Palmiet Gen 1                                         :   - Y       |
|   Vt  Y   : Voltage Transformer      Location   : Busbar         : 16.5kV(1)            /                  Ratio        : 16500V/110V |
|                                                   Branch         : Palmiet Gen 1                                         :   - Y       |
|   OutputLogic OutputLogic                                                              yout                :  9999.999 s            |
|     Breaker              Cubicle       Branch                   Busbar               / Substation       Fault Clearing Time          |
|      Switch              Cub_2          Palmiet Gen 1            16.5kV(1)            /                          9999.999 s          |
----------------------------------------------------------------------------------------------------------------------------------
```

Figure 5.14: Protection relays details.

It is highly helpful to colour the single line-diagram while completing load flow calculations so that you can quickly see the results, for instance, if elements have a loading percentage above 90% or if the voltages of the busbars are beyond the allowed range. PowerFactory offers the possibility to choose several colouring modes based on the computation done. If a certain calculation is correct, the chosen colouring for this calculation is shown. For the simulation study the no calculation mode presents various voltage topologies as seen Figure 5.1 when the system is de-energised, however when performing load-flow calculation the colouring provides grouping according to generating area zones. It is also possible to define a protection path through colouring when executing load flow calculations. Figure 5.15 and 5.16 illustrates the typical colouring diagrams to denote OOS tripping zone and load flow calculation results respectively. For the OOS tripping zone it can be seen that the path is from the synchronous generator up to the HV side of the generator transformer terminal busbar as previously discussed in chapter 4 when setting the tripping zone of the out-of-step element.

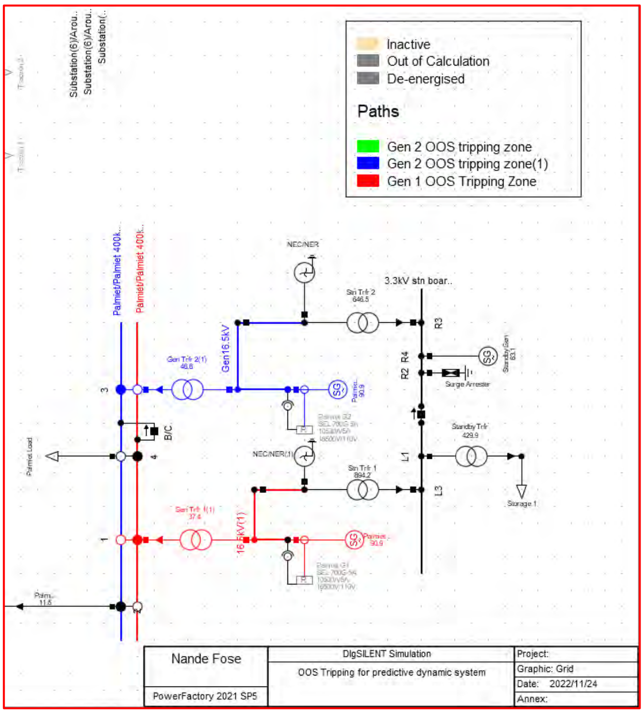

Figure 5.15: Abstract of the test system depicting OOS tripping path

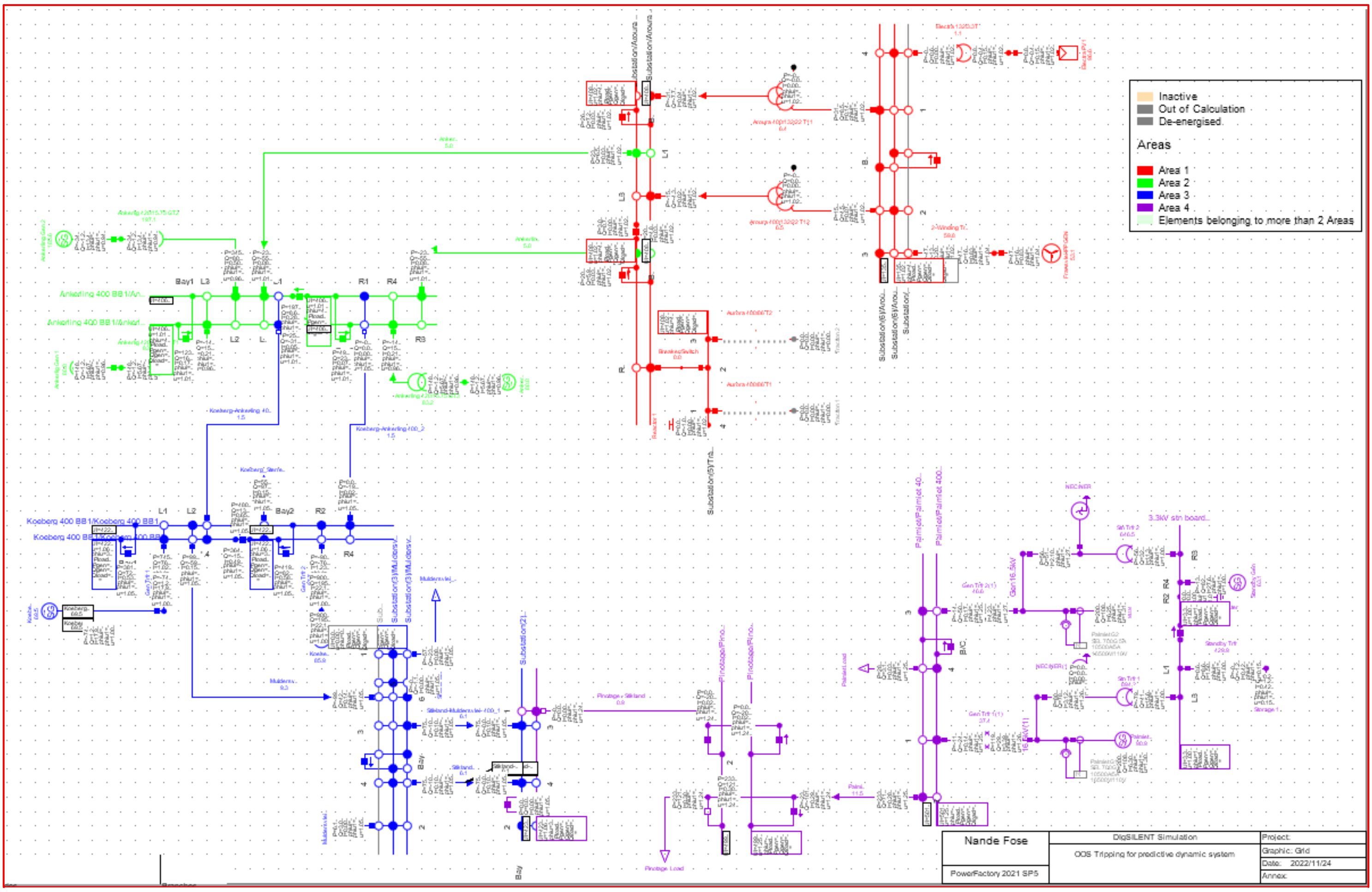

Figure 5.16: Test system during load flow calculation

On successful load flow calculation, the monitored variables such as active and reactive power of the generating units along with current and voltage magnitudes on the buses can be computed. The system is deemed stable when all these parameters are within the rated value of the system components, Figures 5.17 and 5.18 provide bar graphs for electrical quantities seen by the generators and buses during steady-state analysis.

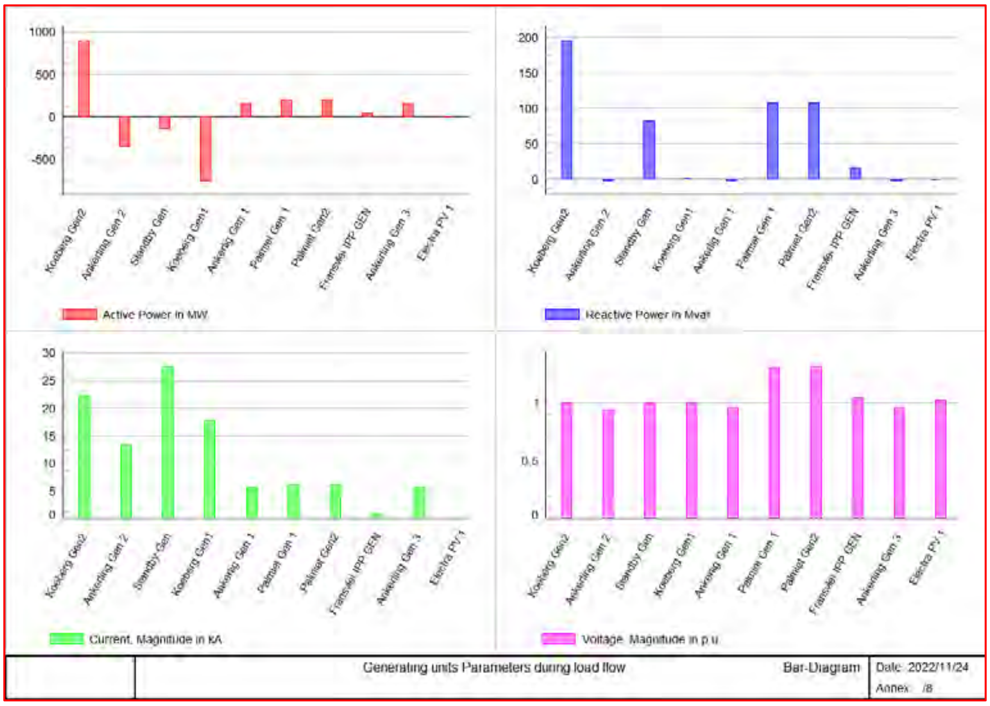

Figure 5.17: Generating capacity capabilities during load flow

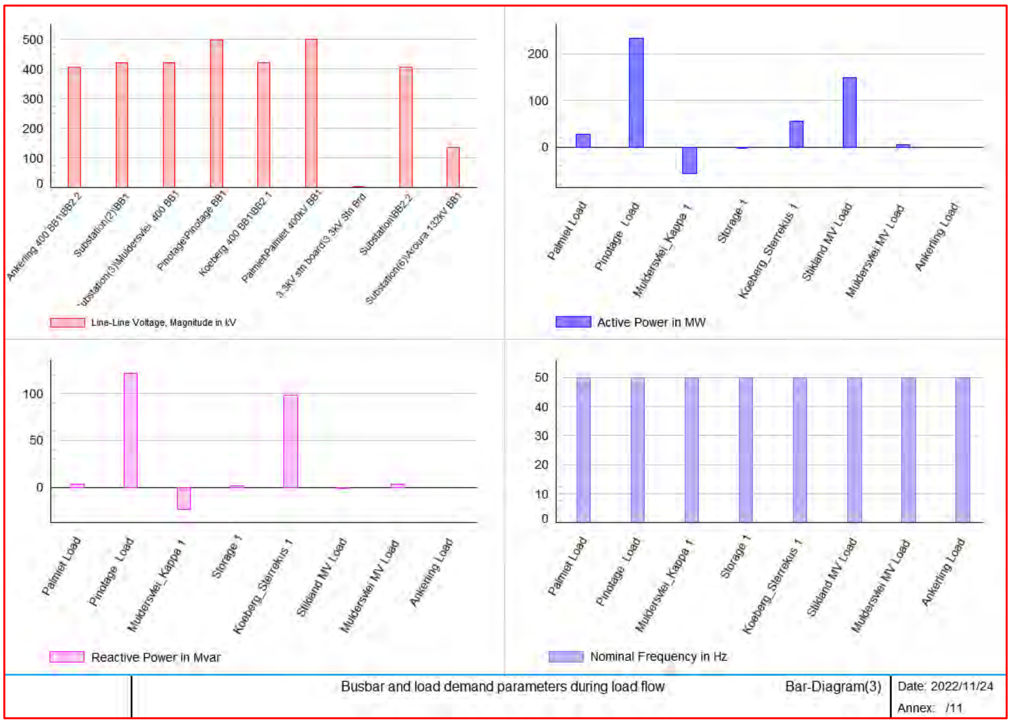

Figure 5.18: Busbar loading capacity during load flow

The system nominal frequency is yet another important factor to consider during the steady-state analysis, as this variable is expected to be the same throughout the network. Figure 5.18 above explains this phenomenon as it is visible that the frequency across all loads is a uniform 50Hz that is injected by the generating units supplying the load demand. The system voltages should fall within the nominal value's +/- 10% tolerance range. In Figure 5.17 shows that the minimum measured p.u voltage is 0.99 p.u and the maximum voltage is 1.25 p.u (which is above the 1.1 p.u tolerance limit). As a result, the control operator may get a warning signal and take appropriate action.

5.4 PROTECTION DEVICE CONFIGURATION

PowerFactory® allows the user to design a protection scheme by incorporating protective devices into the system provided by the network model of a project. The software can be used to help with protective device coordination and to provide graphical representations of protection system features. A relay model library is included in the DIgSILENT library's "Protection Devices" section, which comprises models of both generic and manufacturer-specific relays. PowerFactory® supports the following plot types to aid in the visualization of protection system performance. The SEL-700G OOS mho is configured for the simulation of stable and unstable power swing, two relays are used situated at the Palmiet parallel generating units for pole slipping illustration purposes. The input connection between a relay element and the electrical network is made up of the CT and VT models. A tripping signal is provided from the relay element to a network relative circuit breaker for the relay output. With the newer versions of DigSilent you can actually draw in the graphical representation of this devices and connect the elements to the desired branch and/or busbar. In completion of adding these devises one needs to configure protection settings for the device, for illustrative purposes one SEL relay installed on Palmiet 1 Gen is shown below:

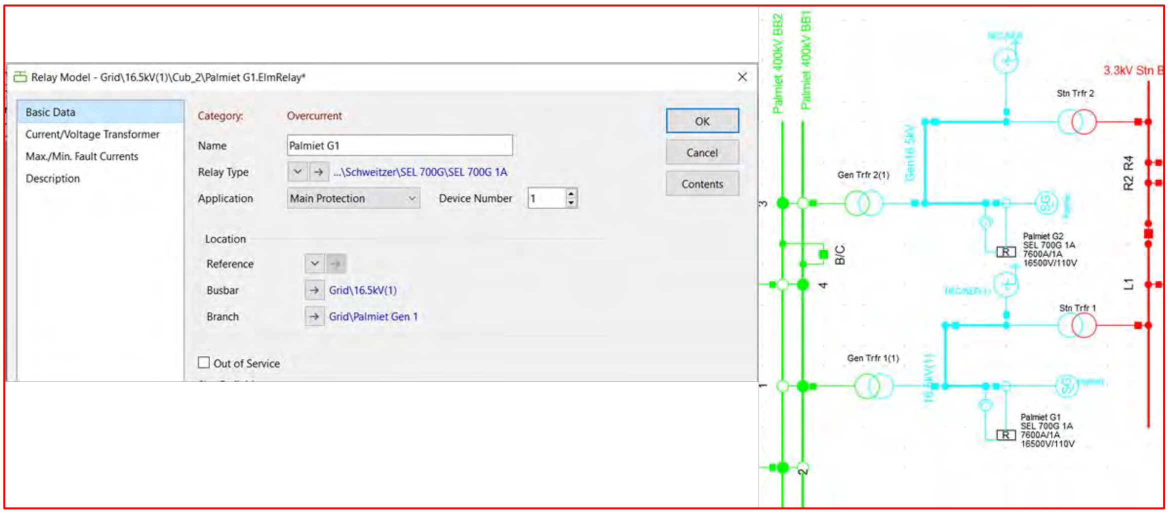

Figure 5.19: SEL-700G for generator OOS protection tripping

The current transformer and voltage transformer ratios are 7600/1A and 16500/110V respectively as given in Table 5.8. The SEL-700G PowerFactory® relay model has two available model versions: SEL-700G-1A and SEL-700G-5A. It also includes the main model and a sub-relay hosting the OOS relay. The SEL-700G-1A model is utilized in this thesis. The measurements units: X-side and Y-side measurements are fed by this CT and VT measurements instruments. On the other hand, the SEL-421-1A measurements are fed through W&Y winding with CTR=600 and PTR=6363 respectively, Table 5.9 provides SEL-421-1A relay settings as configured in simulation platform. The OOS relays consists of power swing detection through polarizing distance logic, two inner and outer blinders defining the power swing detection area, positive sequence current supervision block for minimum current activation threshold and one timer associated with the out-of-step trip signal (OOS Delay block). The interface between the relay and the system model is the output logic. The user has access to a set of various relay output signals that can be tuned to implement any control logic, but this dissertation only focuses on OOS tripping output.

The power swing block in PowerFactory® can be configured to initiate power swing blocking of distance zones and to trip the relay when out of step situations are detected. In this block, one or both of these functions can be enabled. When the impedance trajectory crosses an outside mho blinder characteristic, a timer is started to detect a power swing blocking condition. If a specified duration (typically two to three cycles) elapses before the trajectory reaches a second inner mho blinder characteristic zone, a power swing is declared, and the relay sends a blocking instruction to the relay's elements. The power swing block's second purpose is to detect unstable power swings and issue a trip command - this is known as out of step or loss of synchronism protection. Figure 5.20 and 5.21 illustrates the function block diagram of the SEL-700G and SEL-421 impedance elements in DigSilent.

Table 5.8: SEL-700G Out-Of-Step relay settings

Description					
Impedance Element setting	**Zone 1**	**Zone 2**	**Z1 time delay**	**Z2 time delay**	**Direction**
	6.42Ω	9.64Ω	0 seconds	0.4 seconds	Forward
Out-of-step Mho settings	**Outer blinder**	**Inner blinder**	**OOS delay**	**OOS trip delay**	**OOS trip DUR**
	18.03Ω.sec	5.72Ω.sec	0.04 seconds	0.04 seconds	0.06 s
Current transformer	**Ct X**	**Ct Y**	**Ct In**	**Connection**	
	7600/1A	7600/1A	7600/1A	Y	
Voltage transformer	**Vt X**	**Vt Y**	**Vt open delta**	**Connection**	
	16500/110V	16500/110V	16500/110V	Y	

Table 5.9: SEL-421 Out-Of-Step relay settings

Description					
Impedance Element setting	**Zone 1**	**Zone 2**	**Z1 time delay**	**Z2 time delay**	**Direction**
	6.42Ω	9.64Ω	0 seconds	0.4 seconds	Forward
Out-of-step Mho settings	**Zone 5 R-X reaches**	**Zone 6 R-X reaches**	**OOS delay**	**OOS trip delay**	**OSBD**
	5.82-11.56Ω.sec	37.57-43.35Ω.sec		0.02 seconds	0.035 seconds
Current transformer	600/1A				
Voltage transformer	400000/110V				

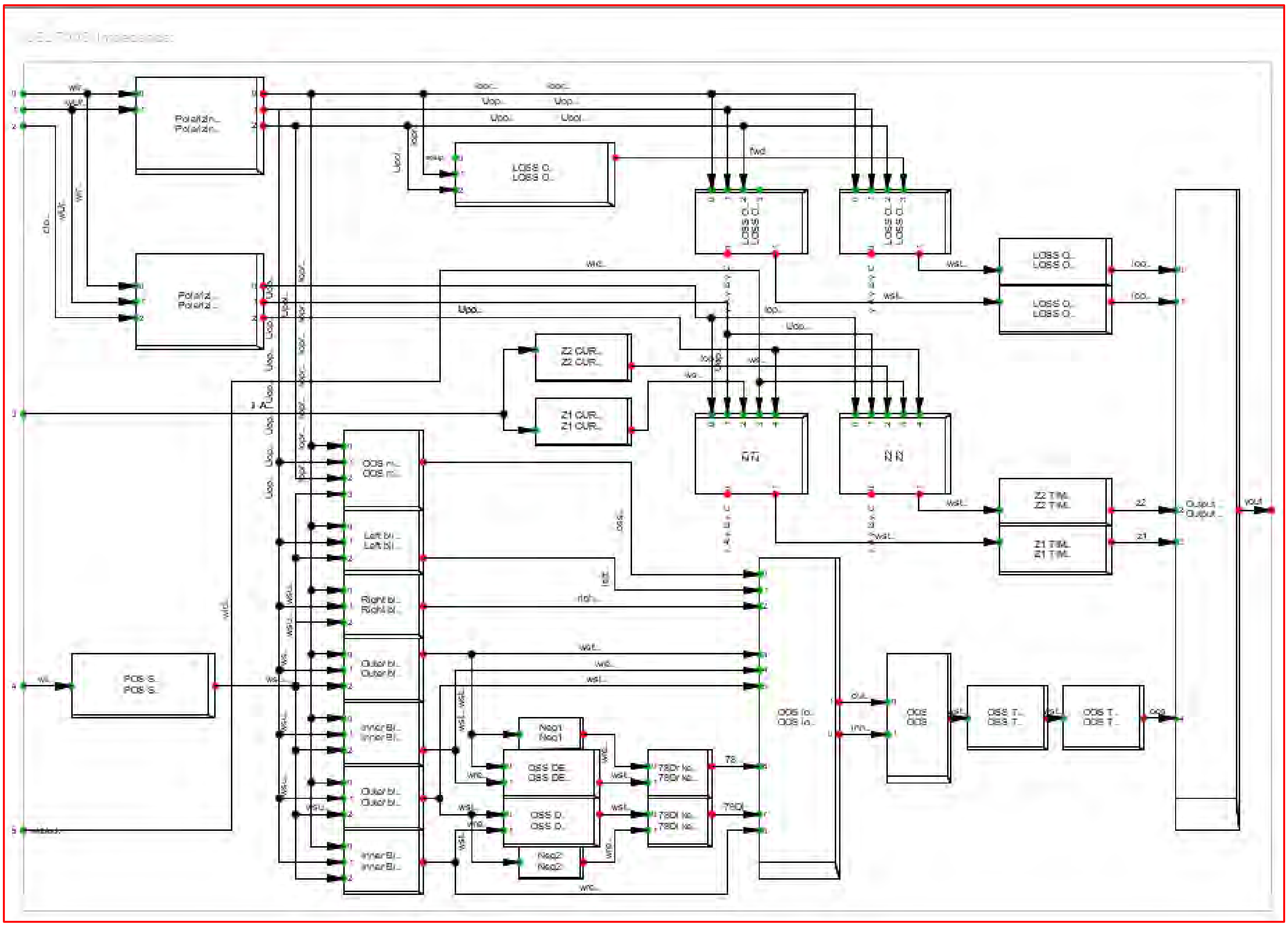

Figure 5.20: SEL-700G Block diagram of PowerFactory® model implementation for OOS

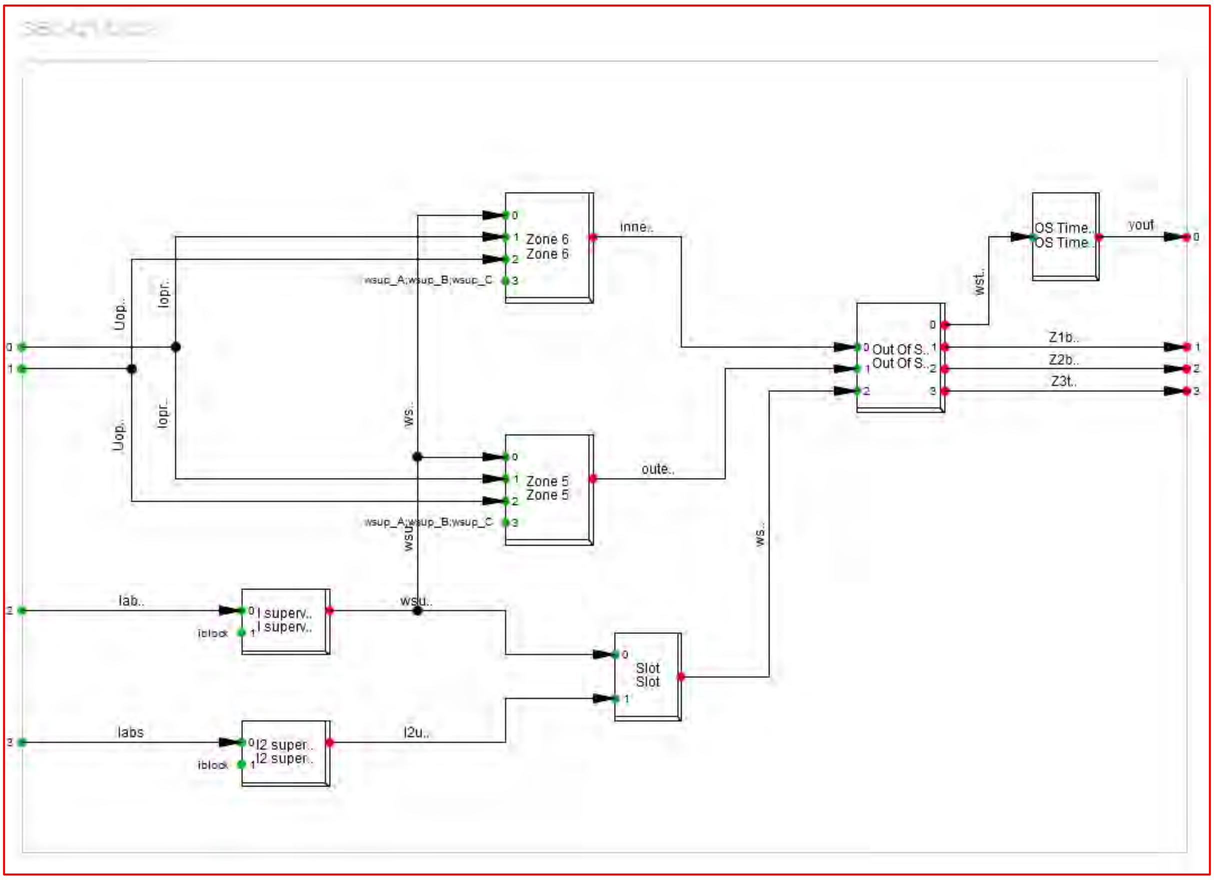

Figure 5.21: SEL-421 Block diagram of PowerFactory® model implementation for OOS

5.5 DYNAMIC STABILITY SIMULATION

The study of the electromechanical oscillations inherent in the power system is referred to as rotor angle stability. The key question to be answered is how the rotor angle varies in response to a change in power output, because under normal stable operation, the rotor angle does not change:

- The network's synchronous machines all run at 2πf electrical speed.
- The phase angle between all machines' internal electro-magnetic forces is constant, hence the term synchronism; and
- All mechanical and electromagnetic torques operating on the spinning masses of the synchronous machine are equal.

The primary considerations in rotor angle stability studies are to ensure that synchronous generators are in synchronism, that all generators' electrical speeds are similar, and that appropriate damping is available if oscillation occurs. The rotor speed is investigated to see if there is an imbalance between the mechanical and electromagnetic torques. An imbalance is common in the event of a disturbance and, if not resolved promptly, might cause the synchronous machine to overspeed. When a disturbance is present, oscillation can be reduced by reducing active power generation, providing dynamic brake resistance when power supply is abundant, or shedding a load when power supply is scarce (Gustafsson. M. & Krantz N. 1995).

As briefly covered above, dynamic resistance braking, excitation, fast valving (i.e., reducing the mechanical torque as quickly as possible), a power system stabilizer, generation tripping, and load shedding are some of the control techniques needed to stabilize a power system for transient or small-signal stability (Gustafsson. M. & Krantz N. 1995).

According to its subcategories, the typical time scale for rotor angle stability is as follows:

- Small (signal rotor angle stability): 10–20 seconds following the observation of the disruption. The appropriate equation (5.2) is provided below so as to visualise these consequences.

$$\Delta T_c = K_s \Delta\delta + K_d \Delta\omega \qquad (5.2)$$

  Where;

$$\Delta T_c = \textit{electromagnetic torque}$$
$$K_s\Delta\delta = \textit{synchronizing torque}$$
$$K_d\Delta\omega = \textit{damping torque}$$

  It is possible to see a decrease in synchronizing torque, which causes the machine to move out of step, as well as a decrease in damping torque, which might result in expanding oscillations, during small-signal stability events.

- Large (disturbance rotor angle stability or transient angle stability): 3 to 5 seconds following the disruption. What is noticeable during these events is that voltage-sensitive consumers may be impacted by generators that desynchronize and huge angle swings that cause voltage dips.

To monitor the above-mentioned variables (rotor angle stability, generator speed and output power) DigSilent simulation make use of RMS/EMT simulation studies as well as Quasi-Dynamic simulation to profile the dynamic past and/or future events. RMS is an electromechanical transient analysis tool, whereas EMT is an electromagnetic transient analysis tool for short- to medium-term dynamic analysis (DigSilent PowerFactory® 2021).

5.5.1 RMS/EMT simulations

The dynamic behaviour of both small and big power systems can be examined using the RMS/EMT simulation features offered by DIgSILENT PowerFactory. The fundamental framework enables the modelling of a wide range of complex systems while accounting for electrical, mechanical, and control aspects, including massive transmission grids, renewable energy facilities, and industrial networks. By implantation of the flow chart shown in Figure 5. 22 below a successful RMS/EMT event can be executed.

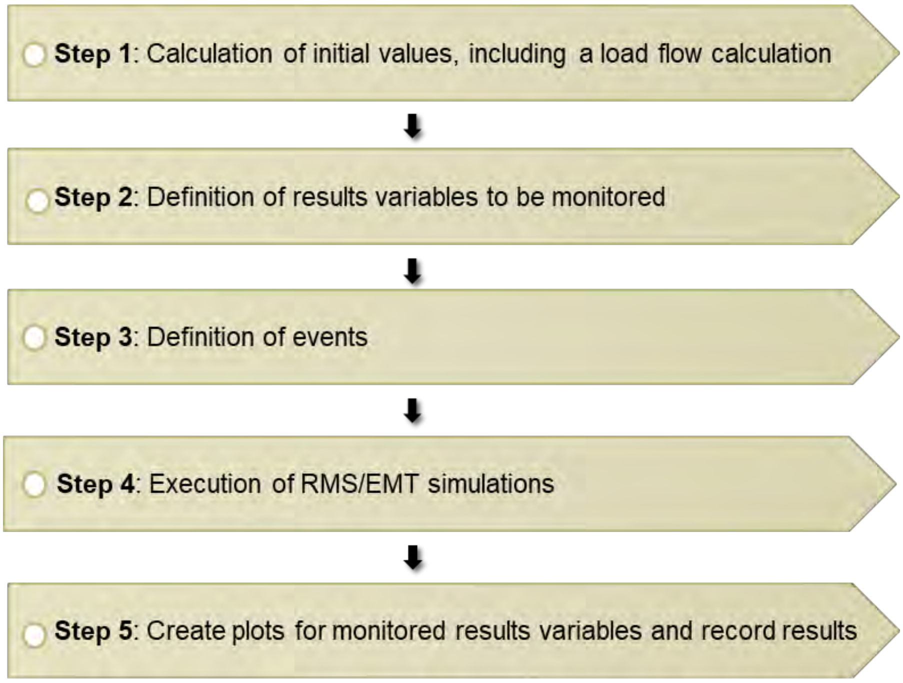

Figure 5.22: RMS/EMT simulation flowchart

The main objective of the case studies is to analyse the out-of-step detection based on the angle $firel$ (rotor angle of the synchronous machine with respect to the rotor angle of the local reference). When the rotor angle $firel$ reaches the detection angle, out of step is detected, whereby the detection angle is set by the user and for this dissertation a value 360° is selected in reference to the relay settings $\alpha = 120°$ which is the separator angle between generator and the system.

5.5.1.1 Case Study 1- Stable power swing

Other simulations in other parts of the system were performed as part of the overall system protection coordination research. It was discovered that some Out-Of-Step circumstances are not recognized by the relays under investigation because the electric centre of the oscillations is not located in the generator under investigation. For instance, an RMS/EMT event that doesn't define any switch event or short-circuit event across the transmission system has been executed for a period of 15s which is the adequate time to detect any rotor instabilities has been executed. In this case the power swing does not enter in the mho characteristics of the devices under study for which all the system generators experience a stable power swing. This process is observed in the Figures to follow:

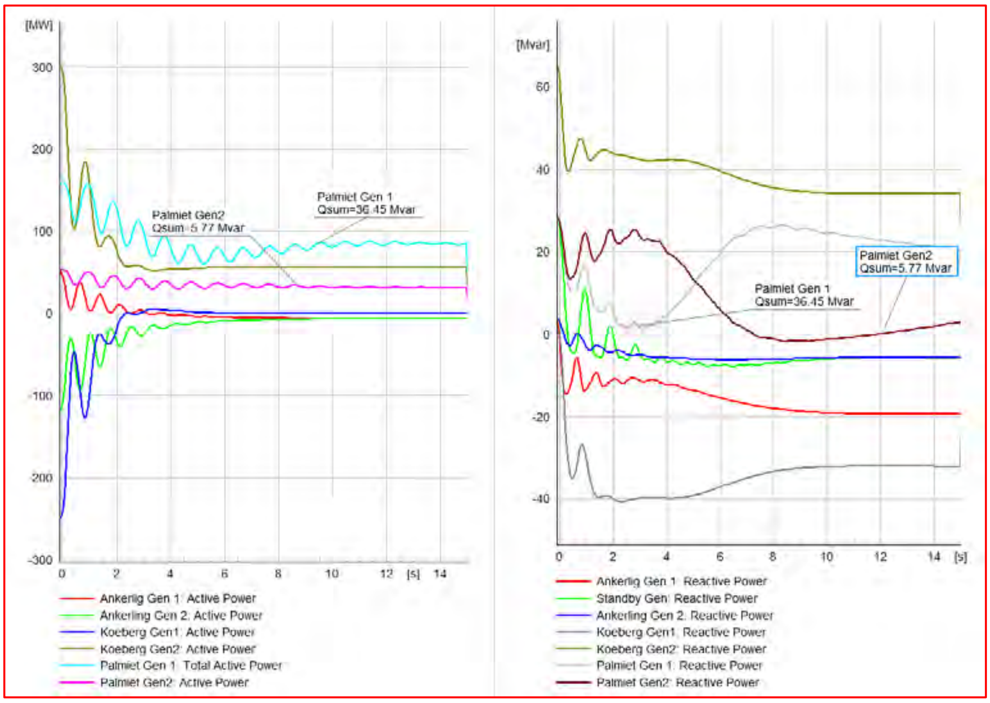

Figure 5.23: Transmission Generators safely distributing MW and Mvar power to designated loads.

From the waveforms it can be seen that Ankerling Generators absorb active power from the system, this is a curtesy of the renewable power plants at Aurora substation. The Palmiet parallel generators both supply equal active power to the system. For this evaluation Koeberg gen1 also supplies negative active power this is due to the spinning reserves which then flows back to the source since the load demand is relatively small than the intended national demand.

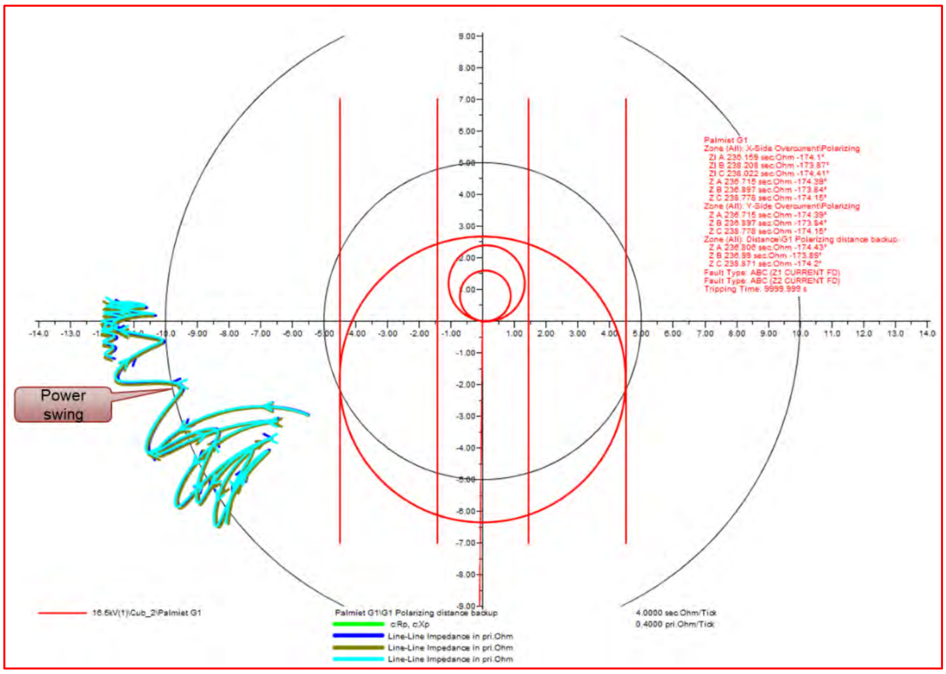

Figure 5.24: Power swing measured from Palmiet Gen 1 (SEL-700G) terminal during the simulation.

Unlike the power-swing impedance from the two-machine systems, the power swing impedance does not follow the traditional circle trajectory since the system under test is a multimachine system. The oscillation slightly crosses from the 3rd quadrant to the 2nd one in this case it is not possible to detect OOS condition as this swing does not cross the relay's OOS blinder only PSB may be applicable in a protection device situated on the Palmiet_Pinotage line.

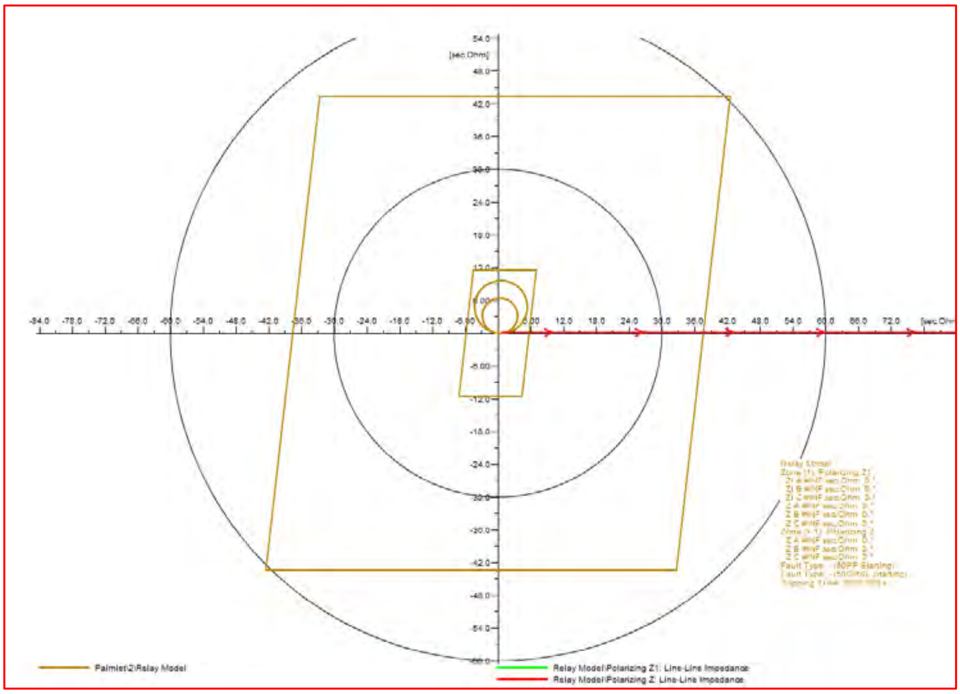

Figure 5.25: Power swing measured from Palmiet line (SEL-421) during the simulation.

The swing trajectory seen by this protection device (Figure 5.25 above) is of a stable nature as it enters and leaves on the right side of the relay characteristic, in a practical environment the relay would issue OSB in this instance.

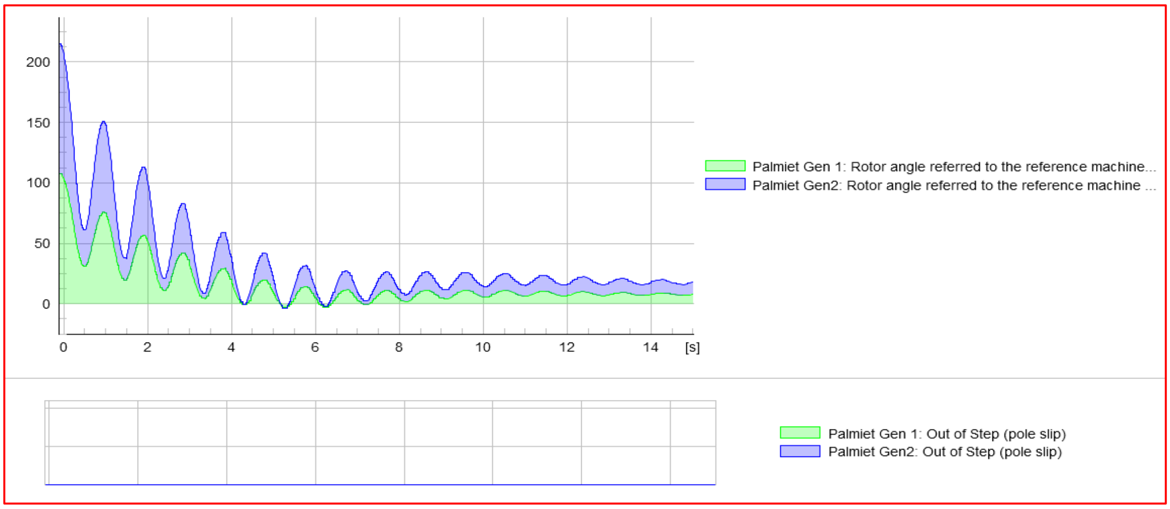

Figure 5.26: Rotor angle stability of the Palmiet Gens binary plot during the case study

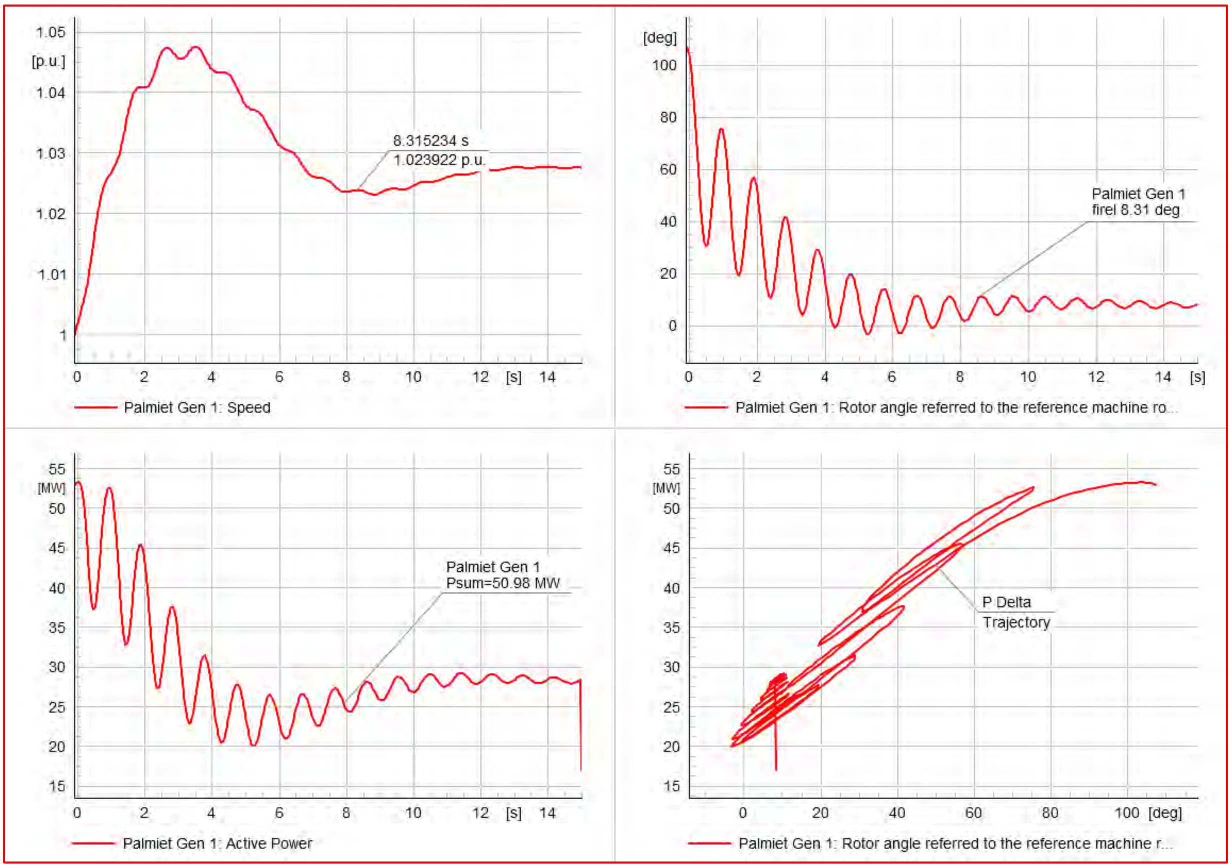

Figure 5.27: Generator parameters on Gen 1 during the stable RMS/EMT simulation.

It can be seen that the machines rotor angle deaccelerates smoothly along with the supplied active power as the rotor speed oscillates to an equilibrium point to gain stable operating point. The P-delta curve provides a graphical representation of the generator electrical output with respect to the load angle at the run time of the simulation. This is a very important feature for power transfer capability limit as a user shouldn't overload the generator otherwise it will lose synchronism, in this case Palmiet Gen 1 is still within safe operating limits.

5.5.1.2 Case study 2- Power swing due to power transfer capability limit

The purpose of this case study is to examine and evaluate the performance of OOS protection scheme and how the entire network behaves when a serious contingency arises in the system. The disturbance used is a 3 bolted short circuit in at Palmiet 400kV busbar in order to detect a pole slipping situation of the Palmiet generators carrying over their loading capability limit. In a steady state operation both generators were loading 72.1% and supplying 158.4MW and 86.0Mvar to the system through Palmiet busbar with rotor angle of 107.2°. Immediately after the simulation at t=1s the generators 1 and 2 supplied 37.9MW, 1193.1Mvar with a loading of 477.5% and -4.2MW, 522Mvar with loading of 209.0% respectively to the station transformers and storage load. From these parameter results reading it is already suspicious that the machines are not in synchronism with the system and each other, however plots of the simulation results are to follow in the diagrams to follow. Consequently, an unstable power swing is also experienced at the station stand by generator.

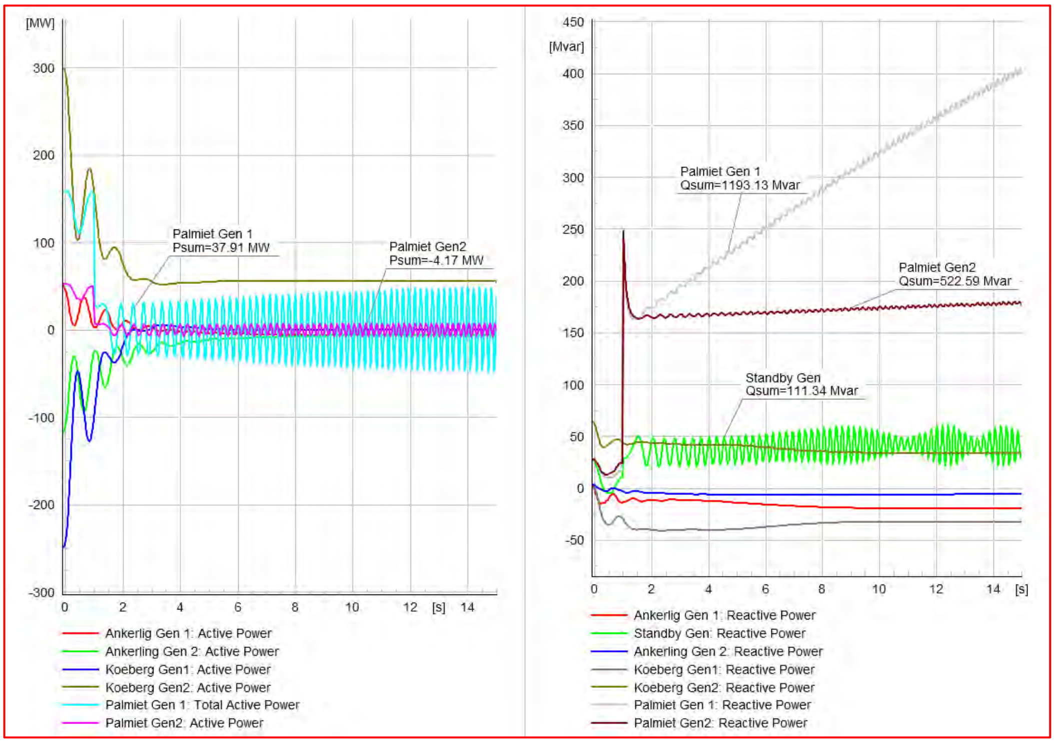

Figure 5.28: Generating profiles during unstable power swing.

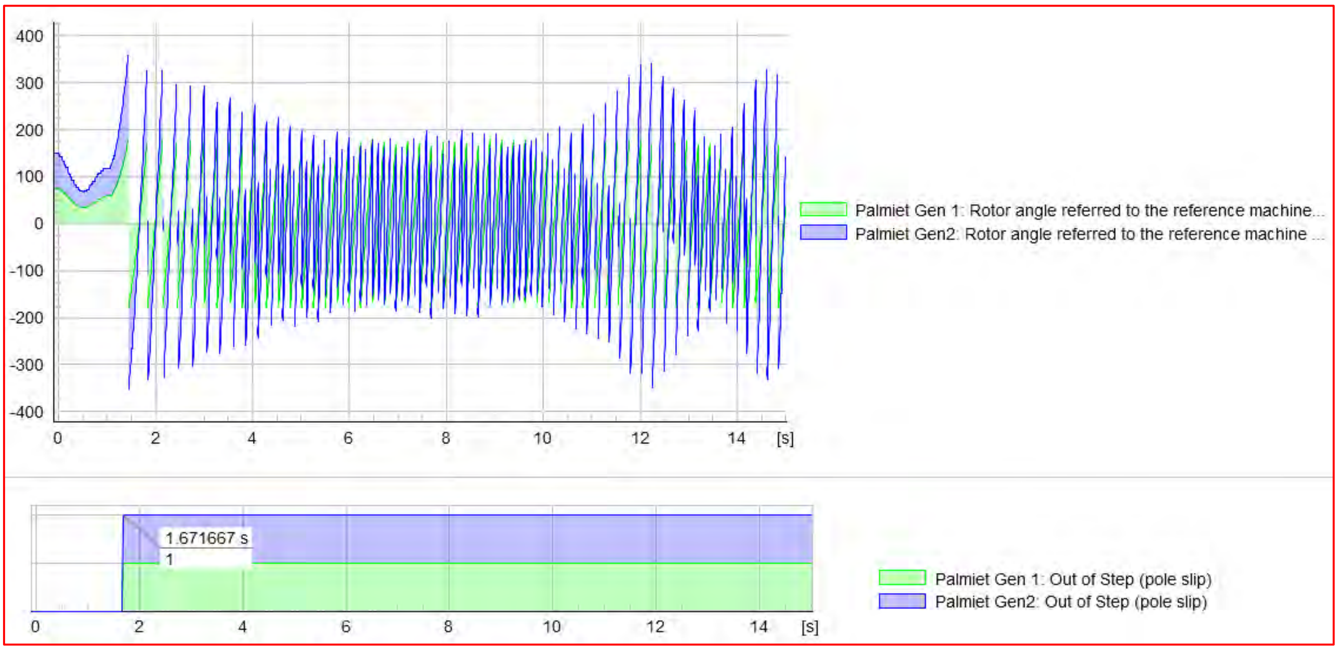

Figure 5.29: Palmiet generators pole slipping detected by DigSilent PowerFactory® simulation

At $t = 1.672s$ the parallel generators lost synchronism with the system. The machine's rotor angle was gradually increased over the course of the simulation window of 15 s to reach 180°, which prevents the parallel generators from staying in synchronism. Figure 5.30 illustrates the effect of this contingency on Palmiet Gen 1 speed and rotor angle.

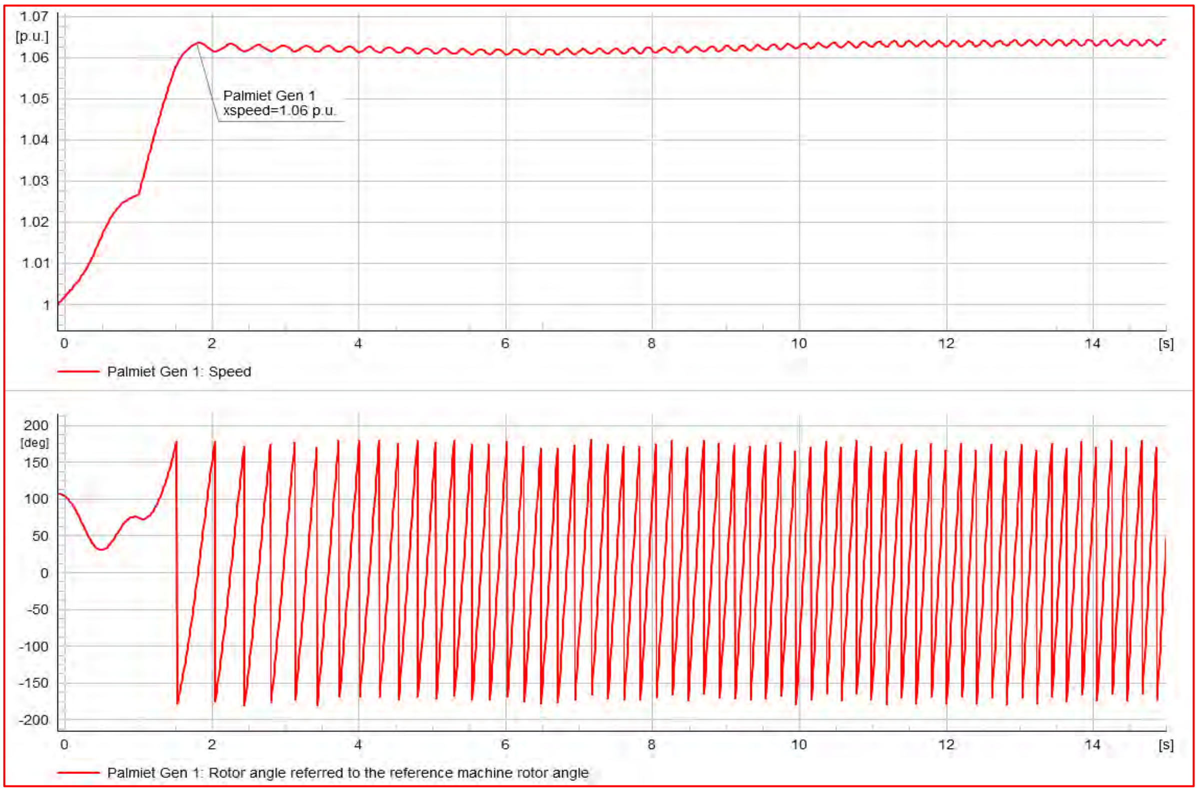

Figure 5.30: Rotor angle Gen behaviour influenced by accelerating Gen speed.

From this analysis it can be observed that before the contingency we have an internal rotor angle in the synchronous machine (as previously discussed in chapter 3 on generator modelling), now that a fault is produced at the Palmiet_400kV busbar there is no active power supplied by the 2 parallel generators going to the other parts of the system as there's zero voltage present. As a consequent there is no electrical power in the machines their rotors are purely driven by the mechanical power with which in turn this mechanical power is used to accelerate the speed of the generators. As the rotor increases the speed, PowerFactory® creates a plot where a rotor angle is defined from 180° to -180° although it is also oscillating in an accelerated direction. These software limitations create a saw teeth like graph as seen above.

```
(t=01:672 s) --------------------------------------------------------------
(t=01:672 s) 'Grid\Palmiet Gen 1.ElmSym':
(t=01:672 s) Generator out of step (pole slip).
(t=01:672 s) --------------------------------------------------------------
(t=01:672 s) 'Grid\Palmiet Gen2.ElmSym':
(t=01:672 s) Generator out of step (pole slip).
```

Figure 5.31:Abstract of RMS/EMT result output window for this simulation

During this incident, protection devices under study can now see this impedance trajectory as it enters the mho blinders of the protected area. For illustrative purposes the relay has been set not trip (trip logic set to out of service) although a fault is detected shown in Figure 5.32 below.

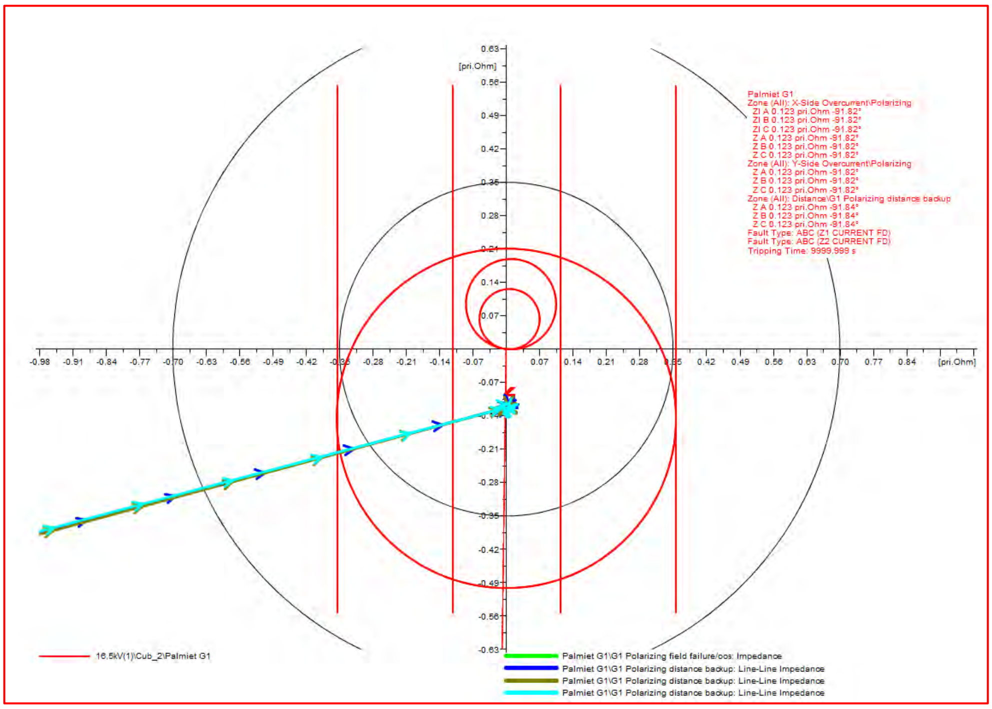

Figure 5.32: SEL-700G with OOS condition detected

The next simulation event aims to illustrate the generator response when OOS trip logic is activated in the protection relay. Subsequent to a successful trip signal the relay sends an output logic to generator to open its relative breaker at approximately 2s. However, the relay binary contact takes about 1s to clear (DigSilent relay technical reference, 2021).

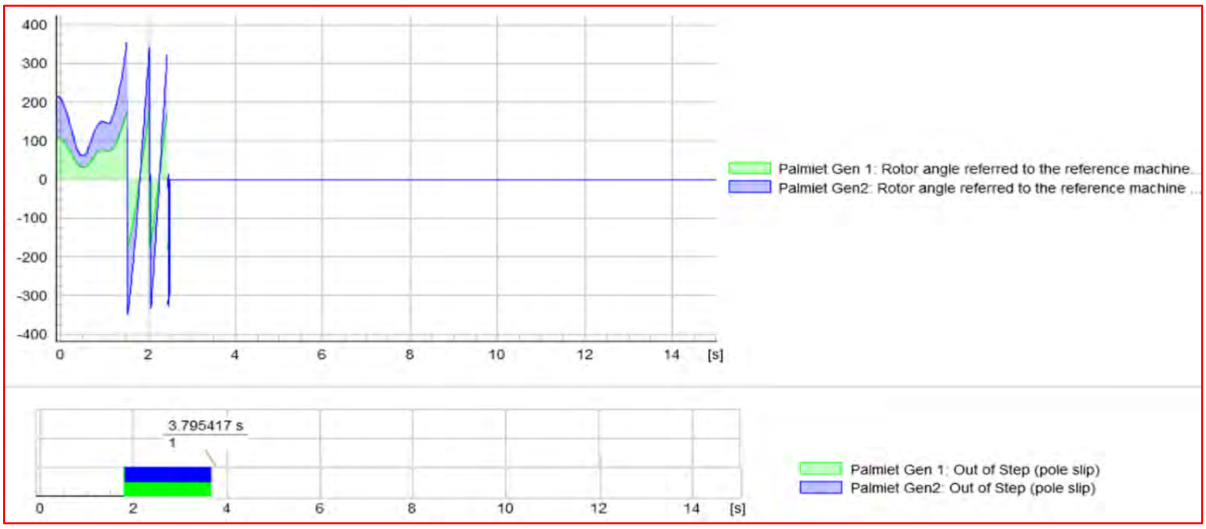

Figure 5.33: Palmiet generators pole slipping cleared in DigSilent PowerFactory® simulation.

The rotor speed then oscillates to try and regain equilibrium, it is important to note that the rotor is full of kinetic energy it will decelerate. Since the system under study is not a classical 2 synchronous generator machine system, the system inertia needs damping hence the not so smooth curve results. As the generator breaker opens and will remain open until the fault on the busbar is fixed, the rotor angle $firel$ decelerates to zero so is the output power of the machine. Figure 5.34 illustrates this process.

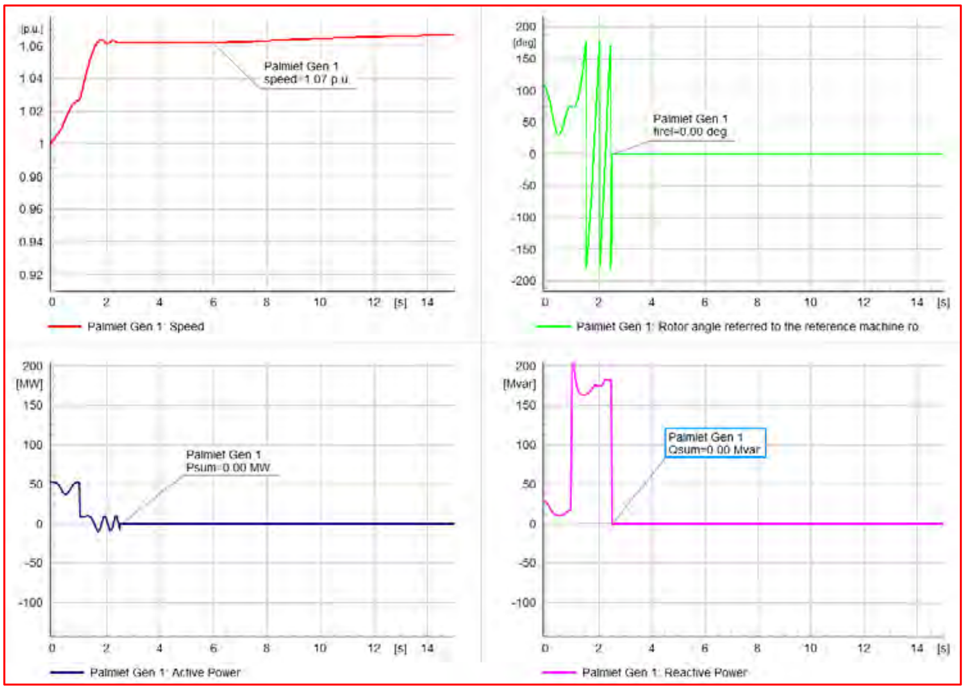

Figure 5.34: Generator parameters on Gen 1 with OOS protection active and fault cleared

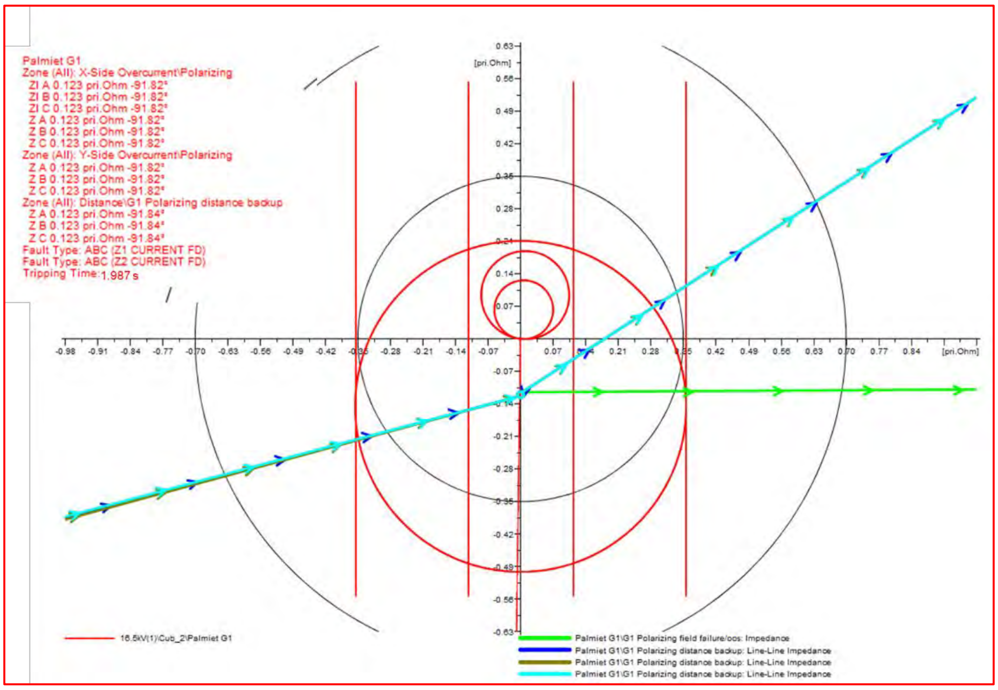

Figure 5.35: R-X plot of the SEL-700G clearing OOS

The SEL-421 relay can also detect OOS condition during this incident, however the relay is time delayed and placed as a back-up protection to the SEL-700G relay, so it won't trip unless the main generator protection is out of service. For illustrative purposes the SEL-421 response is shown in the following Figures for when the SEL-700G is in-service and when it is out of service respectively.

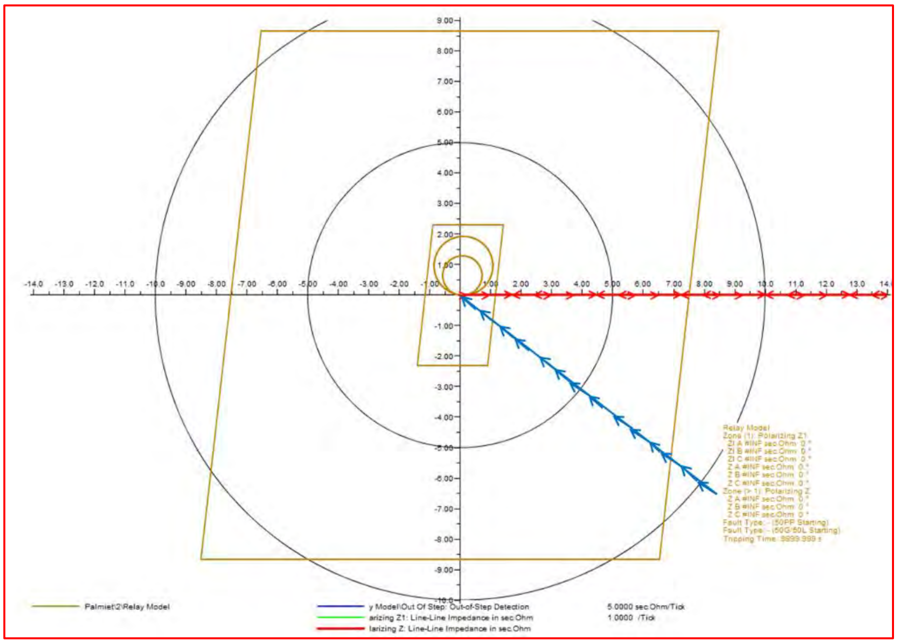

Figure 5.36: SEL-421 detecting OOS with SEL700G in-service

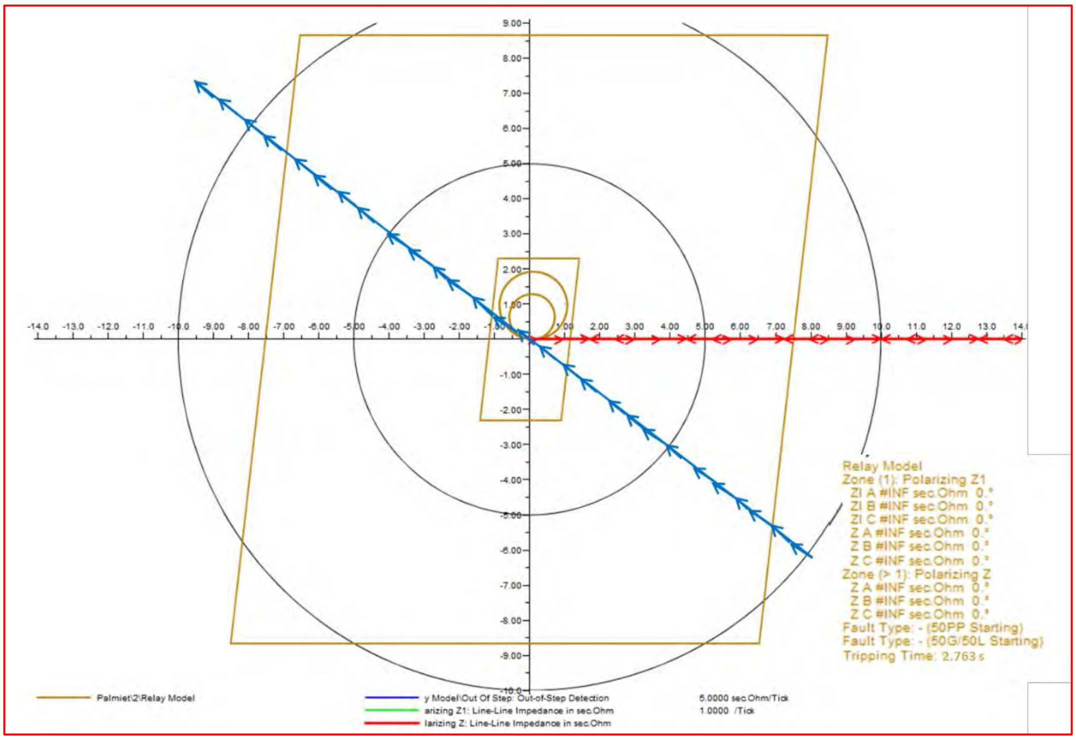

Figure 5.37: SEL-421 clearing OOS with SEL700G out-of-service

5.5.1.3 Simulation Scan-Critical Clearing time

This case study focuses on defining the appropriate protection relay tripping time with reference to the system under study. The existing OOS protection fault clearing time is based on the relay element functionality settings tests. A simulation scan needs to be performed to acquire the exact safe operating time before the generators experience severe damage. The critical clearing time is the most important variable in a protection view for the utility as it tells the exposition of equipment to short-circuit faults etc.

PowerFactory allows you to define some simulation indicators that one can control during the simulation window, for this case DigSilent will create an object that is scanning the internal variable OOS which also internally consist of a binary variable 1 and 0 (becomes 1 if OOS is detected and 0 if stable). For this simulation the scan is defined to stop if OOS condition is detected. To perform this a short circuit event that defines clear short circuit event needs to be defined in the same busbar that a 3-phase bolted fault was defined, then perform trial and error time domain simulation to acquire the exact point where the fault can be cleared before the machines lose synchronism by decreasing event time to be just less that the point where the OOS is detected by the machines.

The following steps can be executed to assess the simulation scan:

- Click on edit simulation tab, a drop-down selection of element variables will appear select 'Loss of Synchronism Scan Module (ScnSync)' and click OK. A case study will then be added into the simulation Scan tab

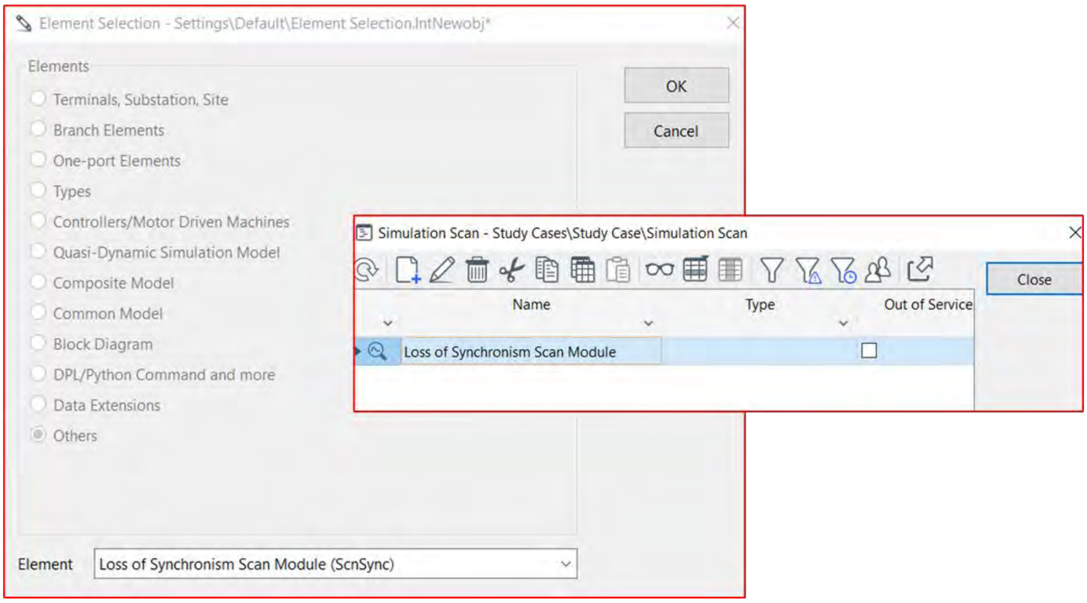

Figure 5.38: Loss of synchronism scan module case study

- User defined settings can be defined inside the case study with which a stop simulation action is selected. One needs to make sure that a scan simulation is also active under initial conditions of an RMS/EMT calculation simulation. When all desired conditions are met the RMS/EMT simulation can be run.

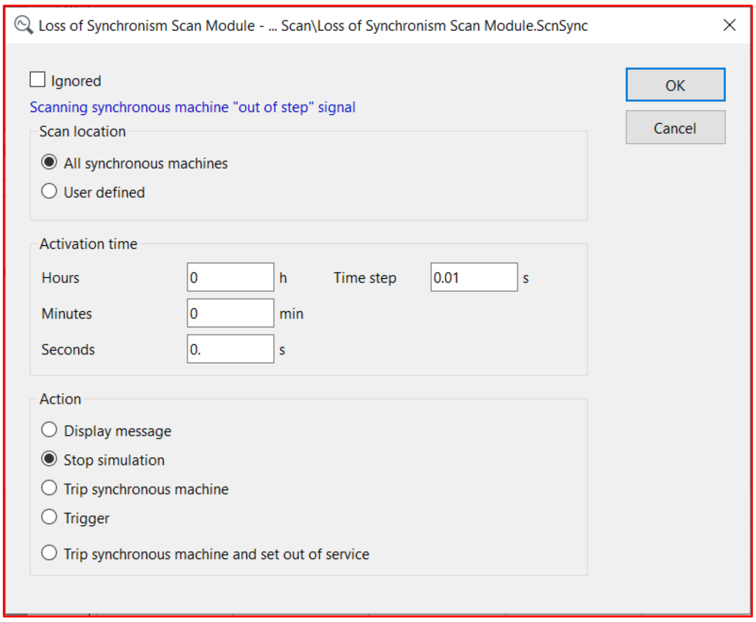

Figure 5.39: Loss of synchronism scan module settings.

DigSilent defines a time stamp where an OOS condition is detected by the machines on the output window results after a successful RMS/EMT event the critical clearing time needs to be less than this time stamp. Snapshot of this can be seen below:

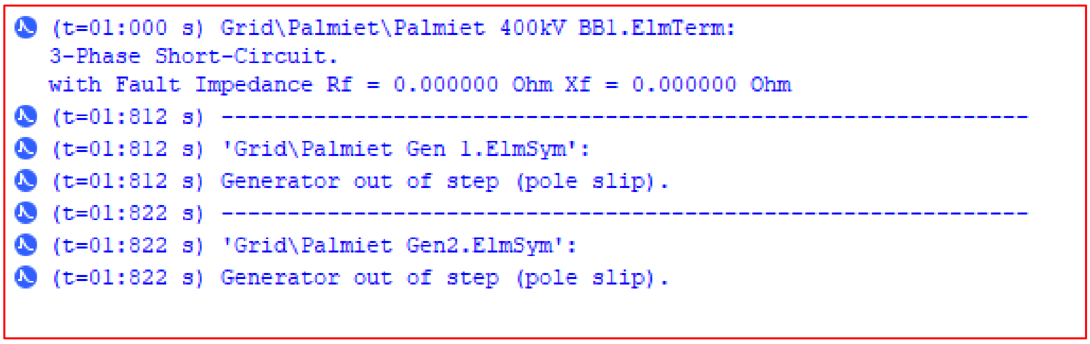

Figure 5.40: Abstract of output window events results in DigSilent during simulation scan.

At t=1.33s the machines seem to be stable even if the short circuit is presented in the busbar, a time stamp of t=1.34s was also performed but the machines loss synchronism with the system at this point. So, the critical clearing time from a protection point of view should be set to **330ms** since the machine is stable only at t=1.33s however it should be noted that the short circuit event was presented to the busbar at t=1s. The plots to follow depict the results of the simulation scan.

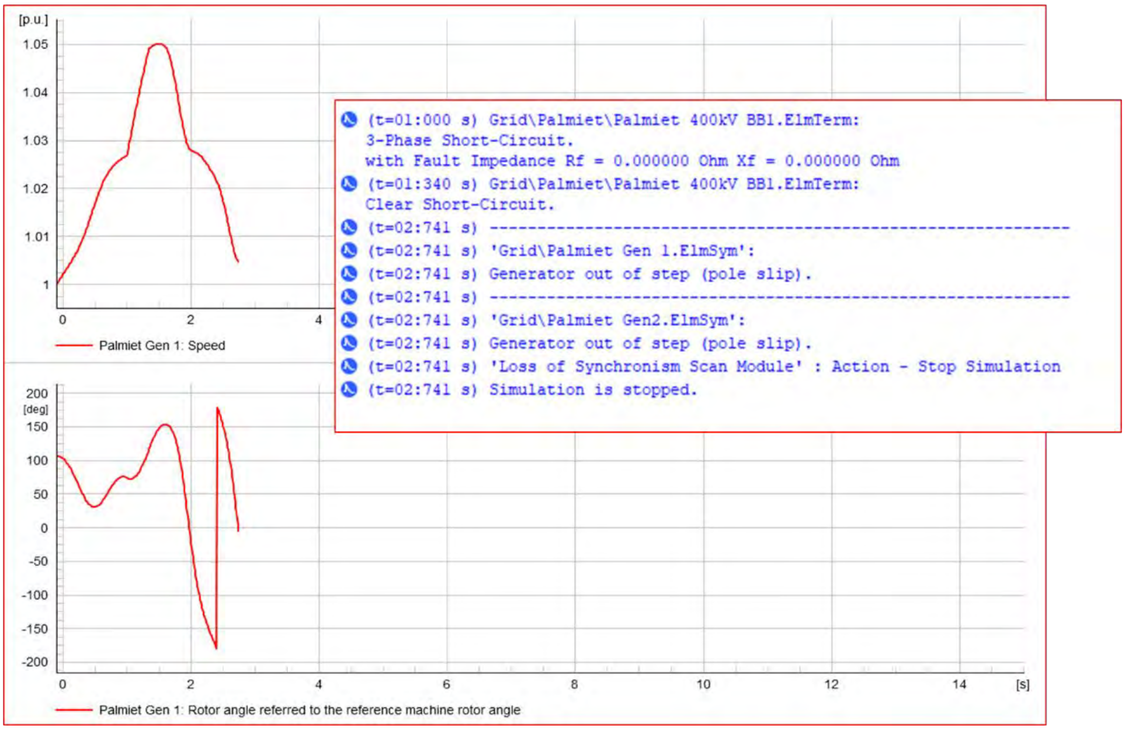

Figure 5.41: Synchronous of synchronism detected and simulation scan stopped.

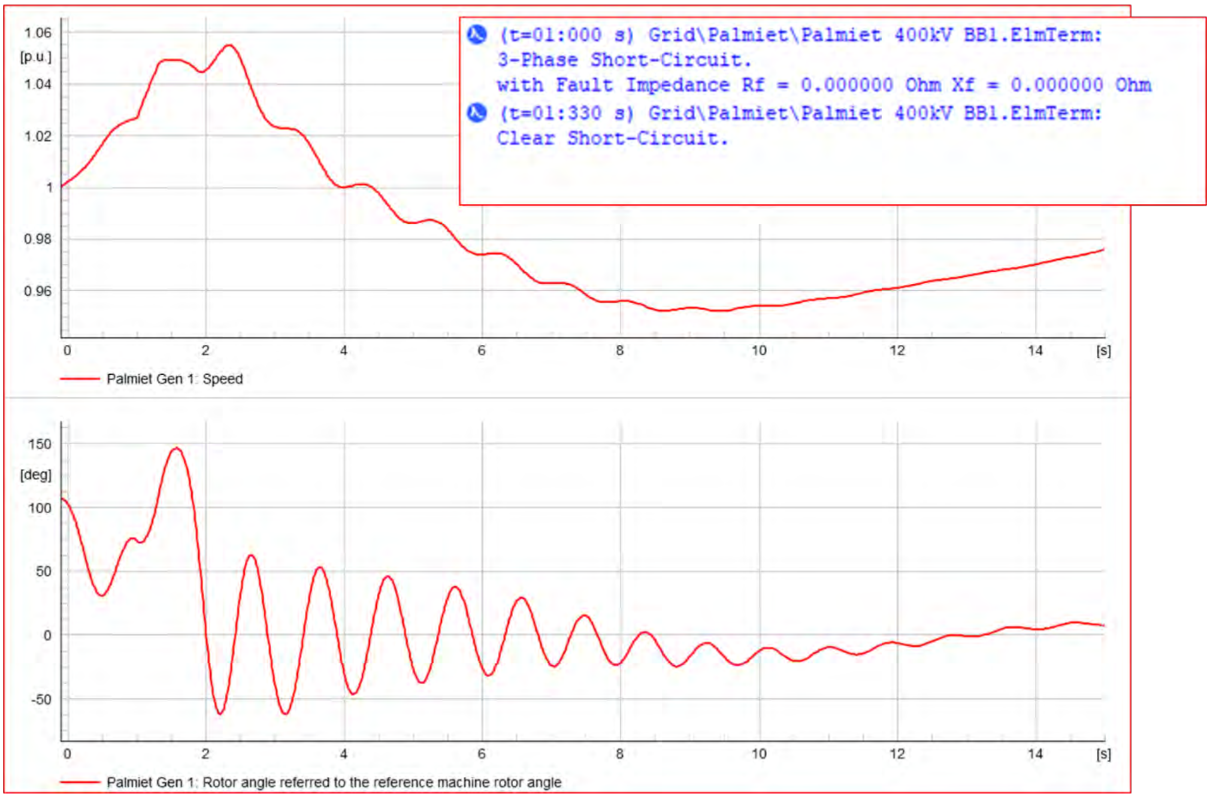

Figure 5.42: Machines remain stable in synch when the fault cleared at 330ms.

5.5.2 Quasi-Dynamic simulation

The idea of this type of simulation study is to calculate the steady state of the electrical power test system but considering the time dependence as the transmission system carries various complex loads which leads the system to be heavily loaded sometimes. The load flow computation calculated earlier in the chapter considers a single set of operating conditions. Engineers in most electrical systems are interested in the system's performance under worst-case operational scenarios. However, because of the network's complexity, it may be difficult to intuitively comprehend which operational situations and network states produce such problems (DigSilent PowerFactory® user manual, 2021).

As a result, engineers must frequently run several distinct load-flow simulations using a variety of operating parameters to find the worst-case operating conditions. Because most operational parameters have an underlying time dependence, this is commonly accomplished by modelling the network dependence on time. As an example:

- Due to daily and seasonal cyclic load variation, load is time dependent.
- The output of renewable energy sources, such as solar and wind power, varies with time-dependent factors such as wind speed and sun insolation.
- Time dependence for network variations, maintenance outages, and contingencies.
- The influences of wind and temperature can also affect equipment ratings.

It is frequently not the variations on a timeline of seconds (power system transients) that are of interest when evaluating load flow variation over time, but rather the behaviour of a network in timescales of minutes/hours up to months/years. For this dissertation weekly Load profiles acquired from Eskom NetOps department are analysed. To achieve the quasi-dynamic simulation, a new time characteristic on each load on the system needs to be defined. The load was scaled to reflect the loading on January 2021 evaluation. These values are given in Table 5.10.

Table 5.10: January, Week 4, 2021, 400kV loads evaluated in Quasi-Dynamic studies

Weekly load demand						
	Muldersvlei Load	**Storage load**	**Palmiet Load**	**Pinotage load**	**Stikland Load**	**Sterrekus load**
Days	**MW loading**					
Monday	557	0.3	122	214	138	19
Tuesday	135	5	32	68	122	8
Wednesday	270	8	114	115	53.8	-14
Thursday	318.5	4.5	3.5	36	90	122
Friday	79	9	80	120	76	32
Saturday	249	9	14.5	145	87.6	14.5
Sunday	360	9.8	58	150	145	100

A screen shot for defining Load time characteristic is given below:

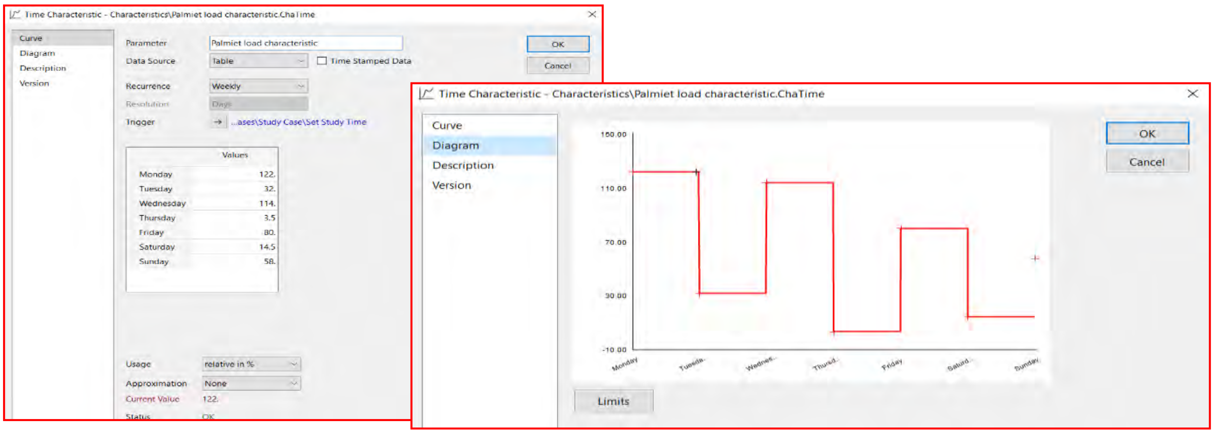

Figure 5.43: Load profile window to define load variables.

Quasi-dynamic simulation is performed with above mentioned events to determine if whether the 400kv network needs improvements and expansions or not.

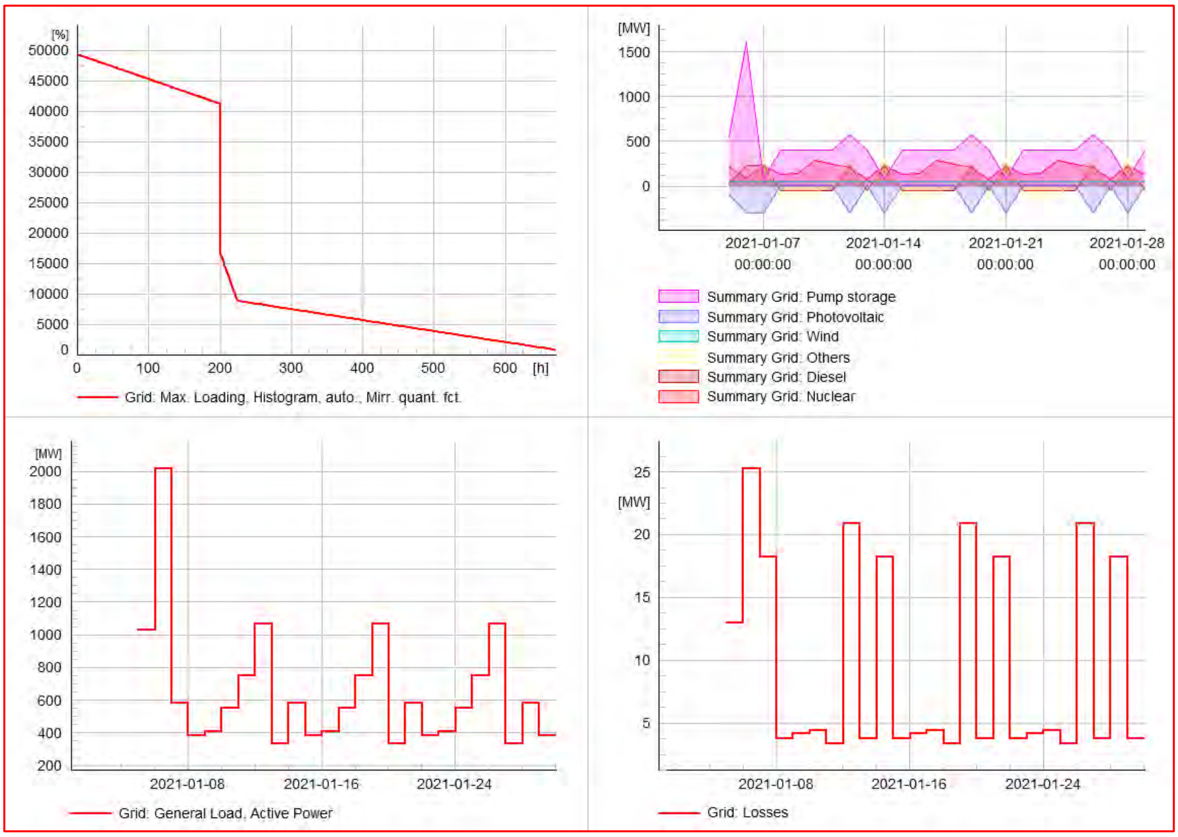

Figure 5.44: Quasi-Dynamic simulation of Generation plant categories and Loading demands for January 2021.

On protection aspect these dynamic trends helps with configuring protection co-ordination for the power system to cater for all system states i.e., for seasonal change (people consume less electricity in summer than in winter) this might force network planners to swing certain points in the system to add or deduct generating supplies, when necessary, thus protection system should withstand all these varieties posed by the power system (Protection reliability comes in play in these situations). The following figure provides an illustration of weekly load trends in the West Grid region:

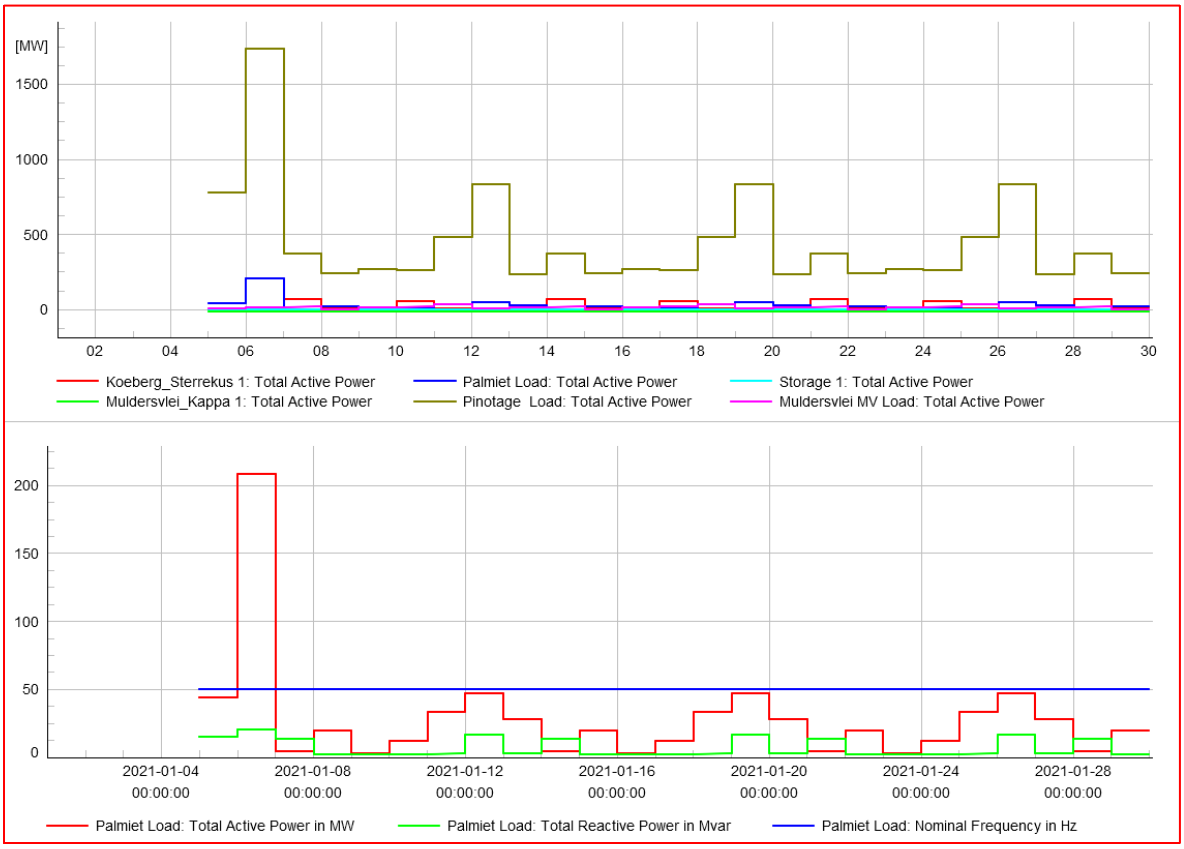

Figure 5.45: Weekly load demand in the West Grid seen from Quasi-dynamic simulation.

5.6 DISCUSSION OF RESULTS

The protection devices that are optimally placed in the system operate efficiently for OOS and PSB conditions. However, the results cannot be claimed to universally be the case for all generating units in the system owing to its dynamic loads though a similar approach may be applicable. From these simulation results it is clear that a critical clearing angle/ time plays a critical part in mitigating OOS conditions and thereby saving the generators from wearing out. The generator speed quickly accelerates to regain stability once the pole slipping is cleared for continuation of smooth operation. In the above results this is not quite clear owing to the time stamp of the simulation being limited to 15 seconds for clear view of graphs. As mentioned before the system under test is not a classical two-machine system so it might take a while for the speed to regain its operating equilibrium as seen in the following Figure.

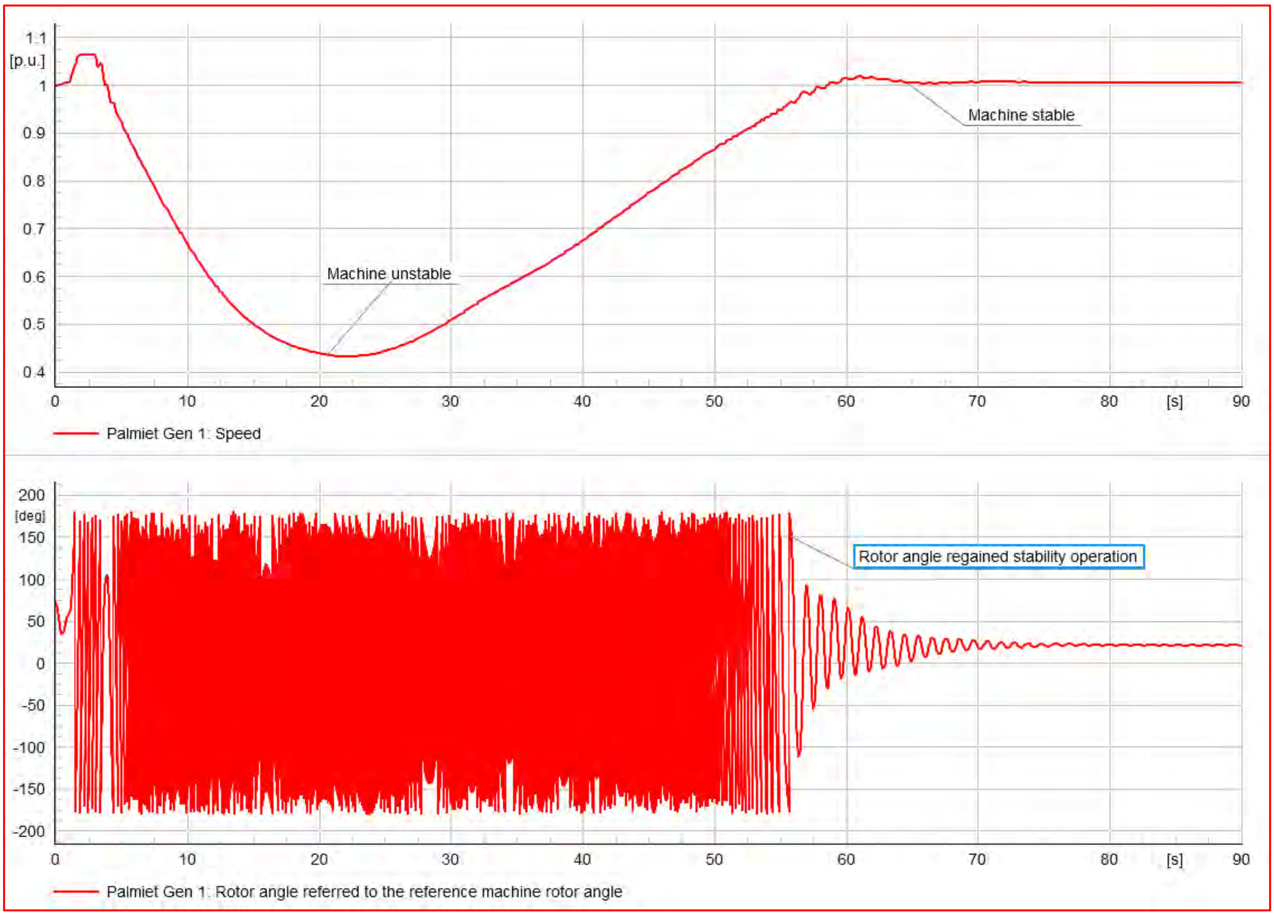

Figure 5.46: RMS/EMT simulation for OOS tripping with a longer timestamp.

5.7 CONCLUSION

This chapter described how to implement a generator main and back-up protection for out-of-step tripping in a DIgSILENT simulation environment. The DIgSILENT software package is used to simulate the stable and unstable power swing in modified Eskom west grid transmission system. Stable load flow was simulated and resulted were computed as this is the initial phase of developing and designing any protection scheme. Dynamic state simulation was performed for various system contingencies and switching using RMS/EMT simulation event to investigate the response of the protection relays deployed for out-of-step protection.

From the simulation results it is apparent that the protection relaying designed to monitor rotor angle stability is reliable as it would trip for unstable power swing and remain stable for instances of stable power swing as it would block out-of-step tripping for faults on the transmission line. In the next chapter the same test system will be implanted on RSCAD-FX to be used later in the thesis for real-time simulations.

6 CHAPTER SIX

POWER SYSTEM NETWORK MODELING AND SIMULATION ON RSCAD

6.1 INTRODUCTION

Power systems use a variety of simulation tools for modelling and simulation research. These technologies enable more efficient than traditional ways for solving mathematical computations. The process of predicting a physical system's behaviour through simulation, as opposed to actual measurements of the system, can be conceived of as simulation. The creation of mathematical models to depict the system's behaviour is the initial step in this approach. The mathematical models that represent the dynamic behaviour of individual system components (generators, transformers, transmission lines, loads, etc.) are typically well-known and their validity and scope are accepted in the field of power systems. In order to create a simulation model of a power system, these existing models of the different components are typically connected to create a model of the power system as a whole. A power system's dynamic model is presented as a set of differential and algebraic equations.

In this chapter, the Real-time Simulator Computer-Aided Design (RSCAD) software is used to construct the power system network and generator control scheme modes, that were developed in DigSilent are further implemented for RTDS which serves as the basis for research into rotor angle stability issues and later protection studies. In order to account for eventualities (such as an increase in load demand), active power versus voltage (PV) and voltage over reactive power (QV) statistical analyses are performed.

6.2 WEST GRID POWER SYSTEM MODELLING IN RSCAD-FX

The RSCAD-FX software suite of RTDS uses a sophisticated and simple graphical user interface. A user can create, simulate, and analyze the simulation output of the real-time digital simulator using the program, which is made up of a number of modules. The components found in the power and control system library can be used by users to model the power system, and the Real-Time Digital Simulator can be used to simulate it. The 'Draft', 'Runtime', 'Multiplot', 'Cable', 'T-Line', 'Help', 'Convert', and 'Manuals' menus are available in the RSCAD's file manager window. The 'Draft' option in RSCAD-FX is used to model the power system, and there is a drag-and-drop interface available to model the necessary components. The 'Runtime' option allows users to view the simulation results when the RSCAD-FX simulation model has been correctly compiled. The RSCAD-FX program has a great graphical user interface that makes it easy to define in detail the parameters of the power system components. The user can prioritize the components using the RSCAD-FX software package of RTDS to ensure that the processor utilization is evenly spread without overwhelming any one processor (RSCAD-FX 1.1 manual).

The RSCAD-FX draft of RTDS was used to build the network diagram in Figure 6.1. The same dynamic network utilized in chapters five was used to the network diagrams to assess the effectiveness of the autonomous generation control and assess the rotor angle stability of Palmiet pump storage generating units.

Areas 1, 2, and 3 are the groupings given to the three subsystems in Figure 6.1. The multi-generation system is a mesh system with n/o points in a practical aspect so subsystem needed to be constructed to cater for these scenarios. Power for Area 1 is being generated from Ankerling generators and sometimes export power to Area 2. Ankerling 3 generating units' apparent power is 148.8 MW each which is sufficient enough to cater for load demand in other parts of the system when required to. Koeberg parallel T-lines are used to export this power to Area 2.

Likewise, Area 2 power is being generated from Koeberg generators and often export power to Area 1 and Area 3 as this is the primary source of National Grid supply. Koeberg T-lines and Muldersvlei T-line are the ones responsible for this power transfer to the relative areas. The 2 generating units at Koeberg station have an apparent power of 900MW each. Whereas Area 3 is fed from Palmiet generators, this power is never exported to any other parts of the system unless there's contingency as it a peaking station supply. Palmiet storage generators each generates an apparent power of 200MW to be distributed to various loads in Area 3.

The nominal frequency of 50Hz is kept constant throughout the system for simulation results in this test platform. Figure 6.1 provides an overview of the test system modelled in RSCAD-FX draft.

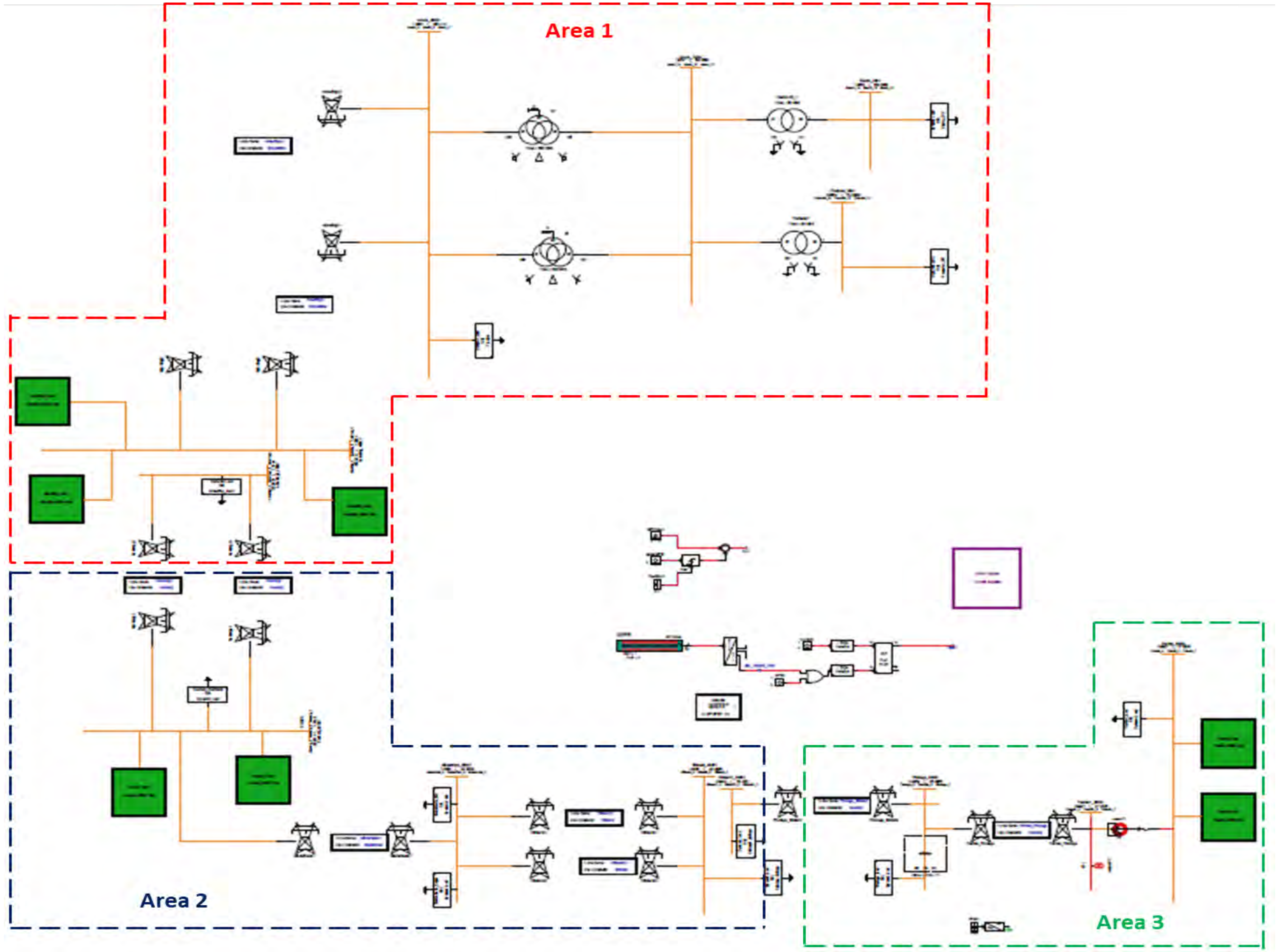

Figure 6.1:Modified West Grid Transmission network system model in RSCAD-FX

6.3 GENERATOR DYNAMIC CONTROLS

Control elements are obtained from the library of RSCAD/Draft controls. Using the "Save Tab As" option, the library window can be modified and saved as a user library. The COMPONENT>ADD function can be used to add specific components to a library. To store the recently added component in the library, the library must first be saved (RSCAD-FX CC-manual). For generator control the following controls will be implemented in the study simulation:

- Powers system stabilizer
- Excitation sytem
- Speed governor

Power system stabilizer

The research uses STAB1 from the controls library which incorporates a single speed sensitive input. Figure 6.2 shows the control logic inside a STAB1 model in RSCAD-FX.

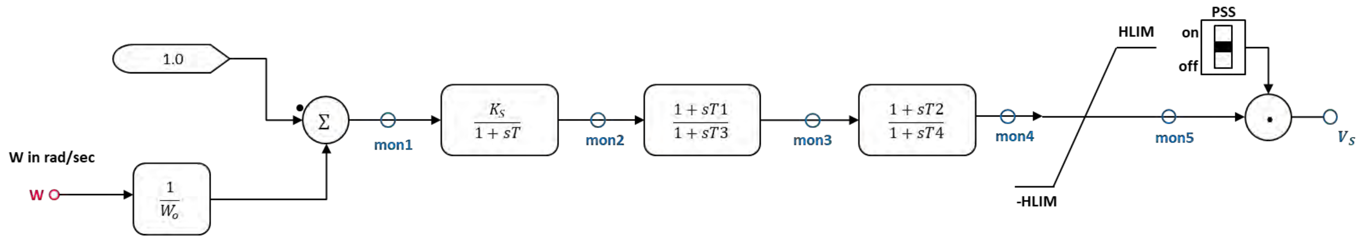

Figure 6.2: STAB1 control logic model in RSCAD simulation platform (RSCAD-FX CC-manual).

The snaps to follow show configuration and parameters of the stabilizer respectively:

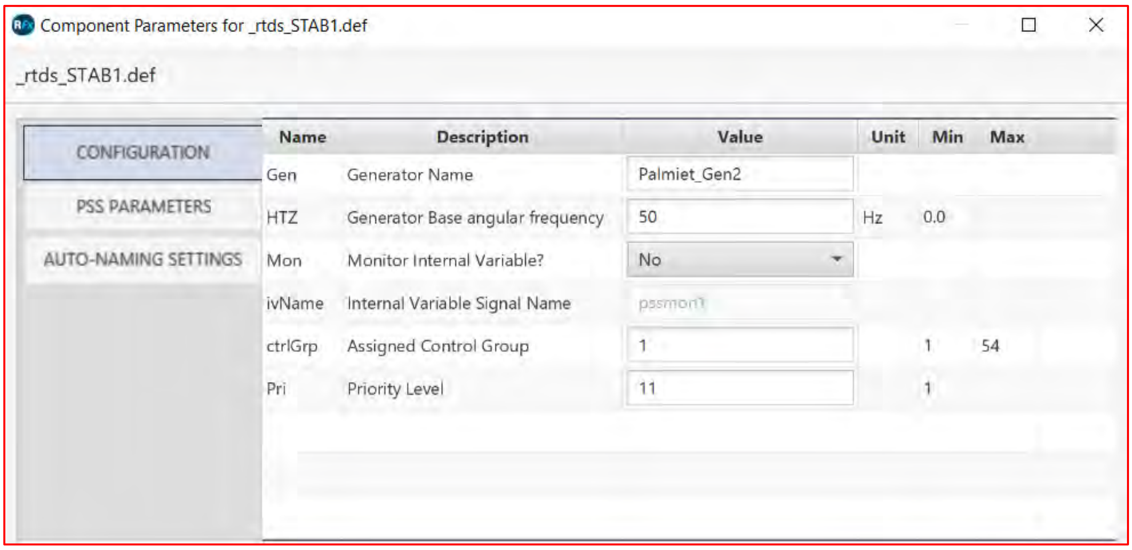

Name	Description	Value	Unit	Min	Max
Gen	Generator Name	Palmiet_Gen2			
HTZ	Generator Base angular frequency	50	Hz	0.0	
Mon	Monitor Internal Variable?	No			
ivName	Internal Variable Signal Name	pssmon1			
ctrlGrp	Assigned Control Group	1		1	54
Pri	Priority Level	11		1	

Figure 6.3: Configuration of STAB1.

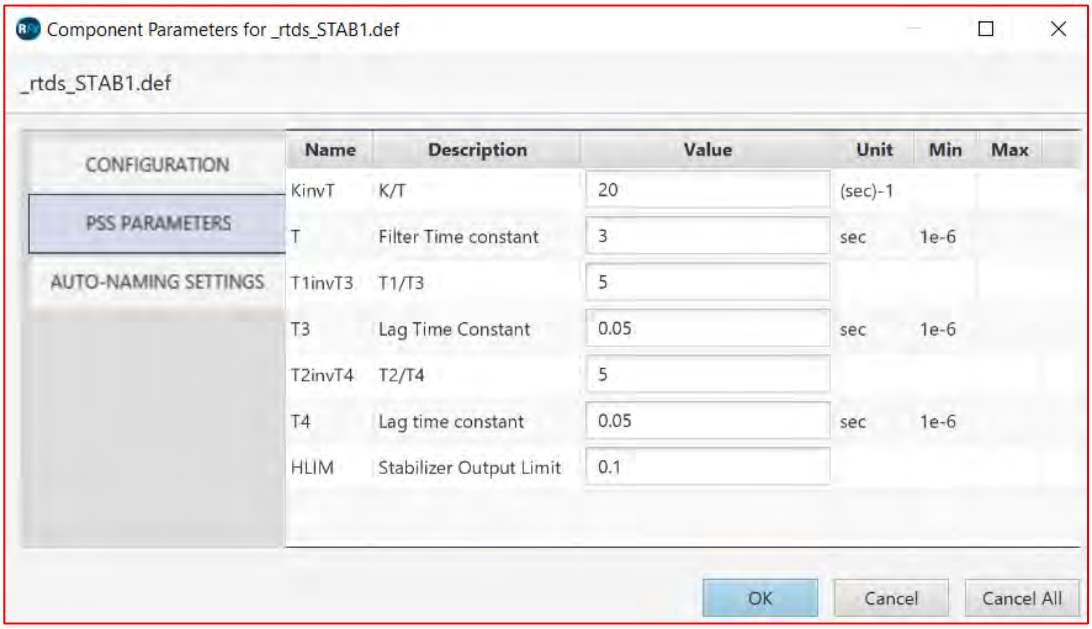

Figure 6.4: Parameters of PSS STAB1.

Excitation System

The DC exciters are represented by the IEEE Type Excitation System in the simulation platform. The field voltage and current for DC exciters are provided by a dc generator, which is frequently affixed to the main generator shaft. Although some older producing plants still employ DC exciters, many have been replaced by contemporary static excitation systems (RSCAD-FX CC-manual) . Figure 6.5 provides an illustration of the control logic inside the AVR.

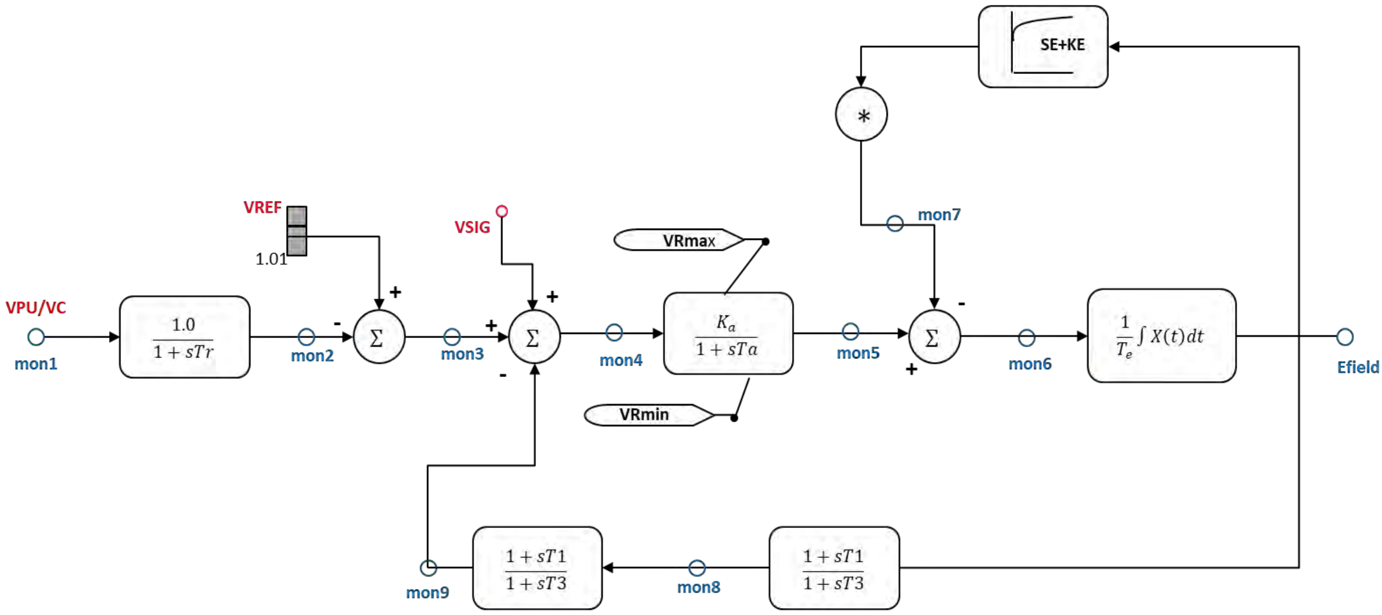

Figure 6.5: IEEET logic diagram for exciter in RSCAD (RSCAD-FX CC-manual).

The exciter quantities and parameters are configured according to the following Figures:

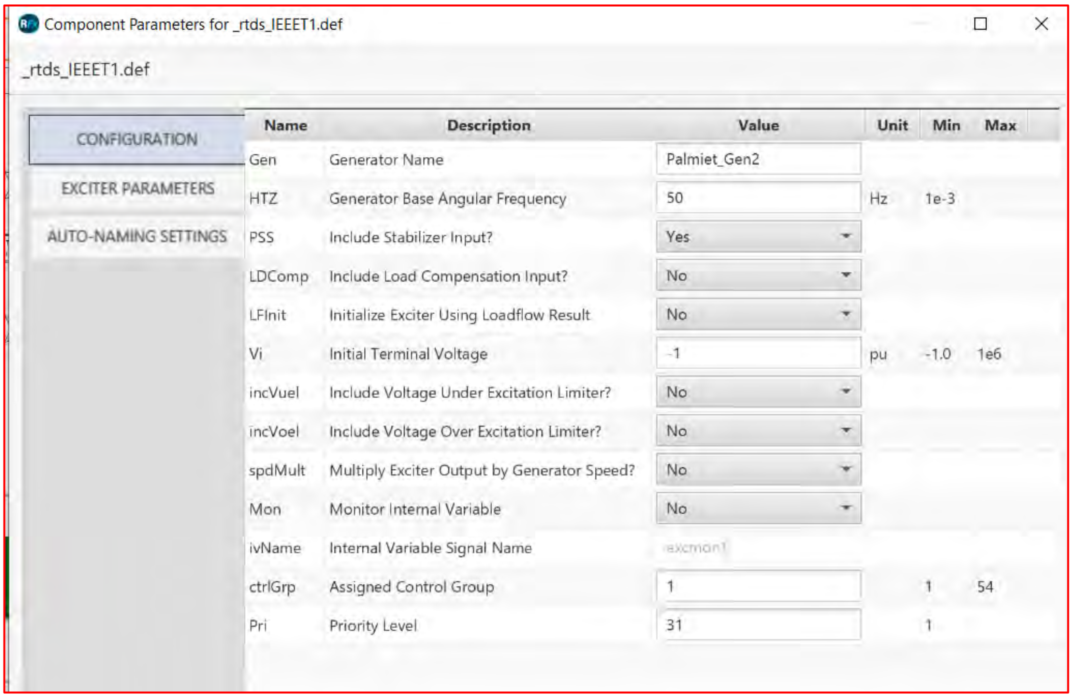

Component Parameters for _rtds_IEEET1.def

_rtds_IEEET1.def

CONFIGURATION | EXCITER PARAMETERS | AUTO-NAMING SETTINGS

Name	Description	Value	Unit	Min	Max
Gen	Generator Name	Palmiet_Gen2			
HTZ	Generator Base Angular Frequency	50	Hz	1e-3	
PSS	Include Stabilizer Input?	Yes			
LDComp	Include Load Compensation Input?	No			
LFInit	Initialize Exciter Using Loadflow Result	No			
Vi	Initial Terminal Voltage	-1	pu	-1.0	1e6
incVuel	Include Voltage Under Excitation Limiter?	No			
incVoel	Include Voltage Over Excitation Limiter?	No			
spdMult	Multiply Exciter Output by Generator Speed?	No			
Mon	Monitor Internal Variable	No			
ivName	Internal Variable Signal Name	excmon1			
ctrlGrp	Assigned Control Group	1		1	54
Pri	Priority Level	31		1	

Figure 6.6: IEEET AVR configuration.

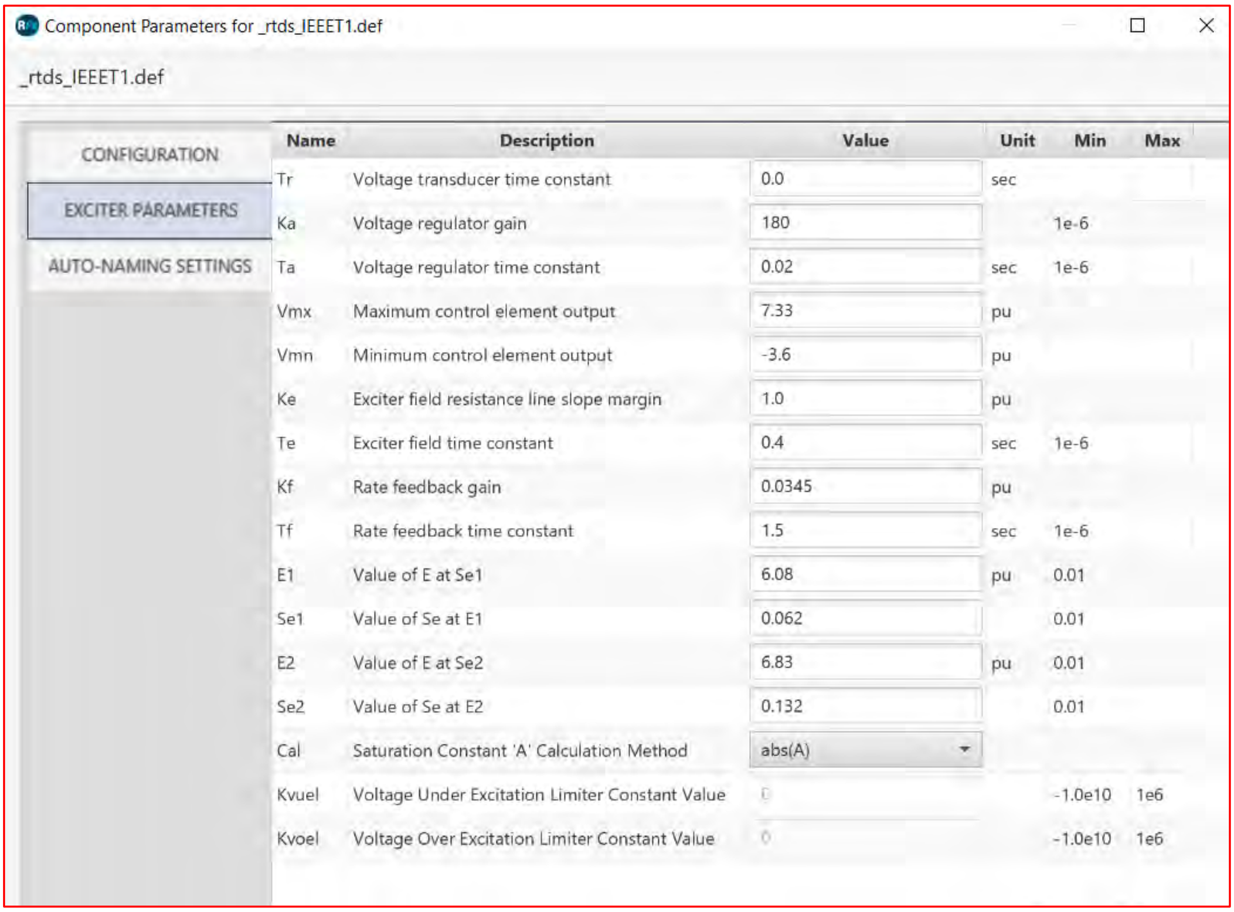

Component Parameters for _rtds_IEEET1.def

_rtds_IEEET1.def

CONFIGURATION | EXCITER PARAMETERS | AUTO-NAMING SETTINGS

Name	Description	Value	Unit	Min	Max
Tr	Voltage transducer time constant	0.0	sec		
Ka	Voltage regulator gain	180		1e-6	
Ta	Voltage regulator time constant	0.02	sec	1e-6	
Vmx	Maximum control element output	7.33	pu		
Vmn	Minimum control element output	-3.6	pu		
Ke	Exciter field resistance line slope margin	1.0	pu		
Te	Exciter field time constant	0.4	sec	1e-6	
Kf	Rate feedback gain	0.0345	pu		
Tf	Rate feedback time constant	1.5	sec	1e-6	
E1	Value of E at Se1	6.08	pu	0.01	
Se1	Value of Se at E1	0.062		0.01	
E2	Value of E at Se2	6.83	pu	0.01	
Se2	Value of Se at E2	0.132		0.01	
Cal	Saturation Constant 'A' Calculation Method	abs(A)			
Kvuel	Voltage Under Excitation Limiter Constant Value	0		-1.0e10	1e6
Kvoel	Voltage Over Excitation Limiter Constant Value	0		-1.0e10	1e6

Figure 6.7: IEEET type exciter parameters.

Speed Governor

For the study a TGOV1 from the controls library which is made from a simple steam model is used. Figure 6.8 shows the control logic inside aTGOV1 model in RSCAD-FX.

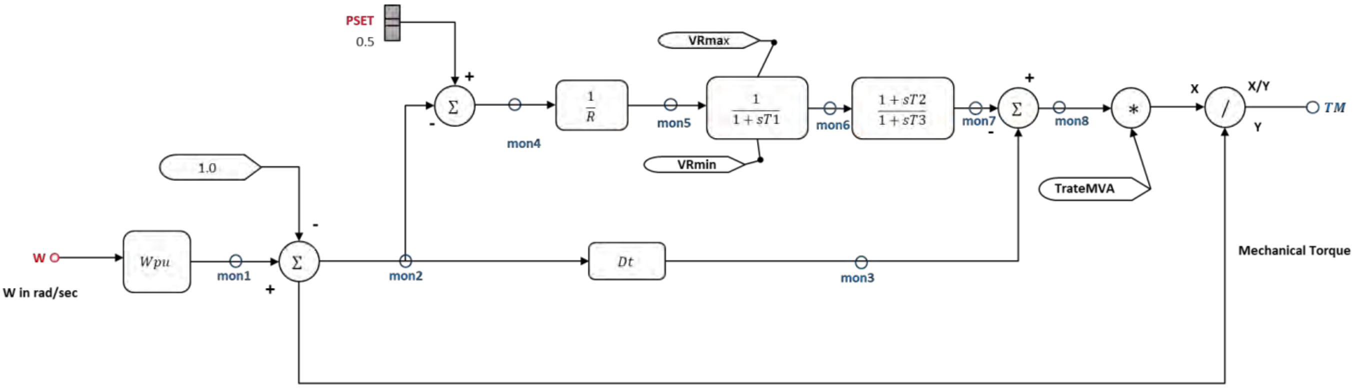

Figure 6.8: Control logic for governor in RSCAD interface (RSCAD-FX CC-manual).

The parameters and configuration settings for the governor are defined as follows:

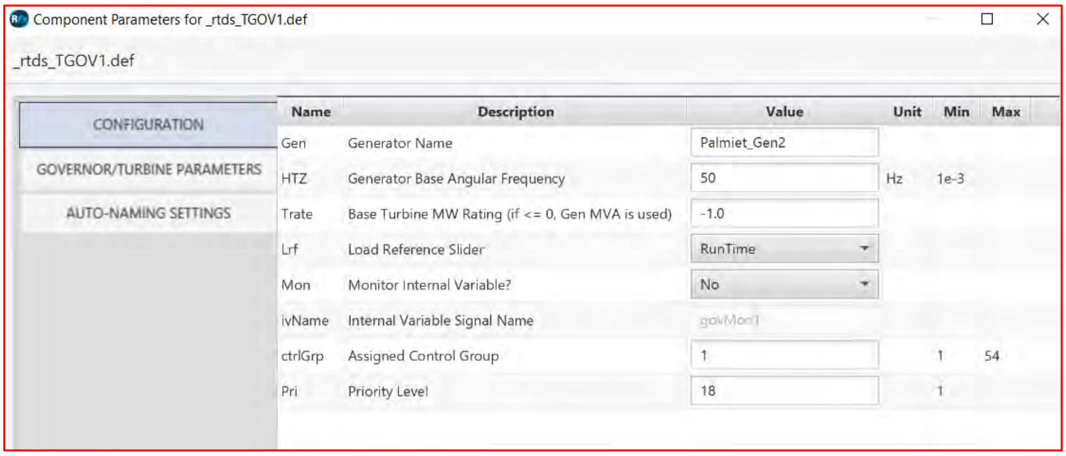

Component Parameters for _rtds_TGOV1.def

_rtds_TGOV1.def

CONFIGURATION
GOVERNOR/TURBINE PARAMETERS
AUTO-NAMING SETTINGS

Name	Description	Value	Unit	Min	Max
Gen	Generator Name	Palmiet_Gen2			
HTZ	Generator Base Angular Frequency	50	Hz	1e-3	
Trate	Base Turbine MW Rating (if <= 0, Gen MVA is used)	-1.0			
Lrf	Load Reference Slider	RunTime			
Mon	Monitor Internal Variable?	No			
ivName	Internal Variable Signal Name	govMon1			
ctrlGrp	Assigned Control Group	1		1	54
Pri	Priority Level	18		1	

Figure 6.9: Configuration for governor.

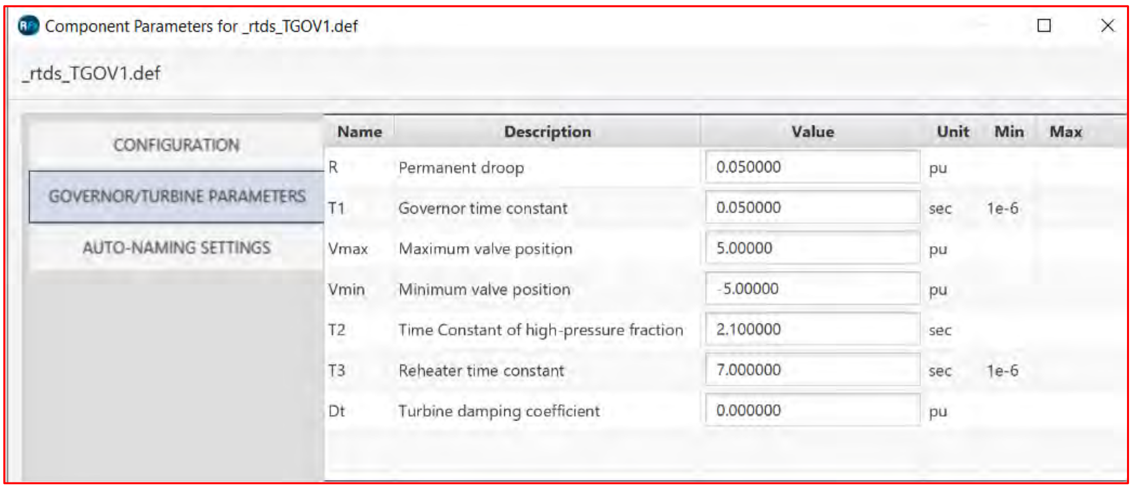

Component Parameters for _rtds_TGOV1.def

_rtds_TGOV1.def

CONFIGURATION
GOVERNOR/TURBINE PARAMETERS
AUTO-NAMING SETTINGS

Name	Description	Value	Unit	Min	Max
R	Permanent droop	0.050000	pu		
T1	Governor time constant	0.050000	sec	1e-6	
Vmax	Maximum valve position	5.00000	pu		
Vmin	Minimum valve position	-5.00000	pu		
T2	Time Constant of high-pressure fraction	2.100000	sec		
T3	Reheater time constant	7.000000	sec	1e-6	
Dt	Turbine damping coefficient	0.000000	pu		

Figure 6.10: Parameter settings for governor at Palmiet_Gen2.

6.3.1 Synchronous machine with its controls attached

Generalized machine theory-based synchronous machine models for the RTDS hardware may be coupled to the user-defined power system network in RSCAD / Draft. Network nodes that were modelled using the Real-Time Network Solution can be joined to this model (RSCAD-FX CC-manual). An optional Y-Δ generator unit transformer with separately specified zero sequence settings is included in the model. The model also simulates the three nodes between the transformer and the generator if the transformer option is enabled. As a result, more nodes can be efficiently described in a single lumped network.

Instead of currents, the model employs flux connections as state variables. A new approach of estimating winding currents based on winding fluxes has allowed the resistance drop in the windings to be applied without a one-step delay in the integration of fluxes. This will improve damping accuracy at higher frequencies. Furthermore, in practice voltage projection techniques are used to remove delay from the machine and main network closed loop as effectively as possible. For this study the RMS voltage signal output from the per-unit value, is acquired from the high side of the step-up transformer at Palmiet-Gen 2.

Palmiet_Gen2_P and Palmiet_Gen2_Q are the active and reactive power names used for monitoring signals of the generator. Figure 6.11 illustrates this phenomena:

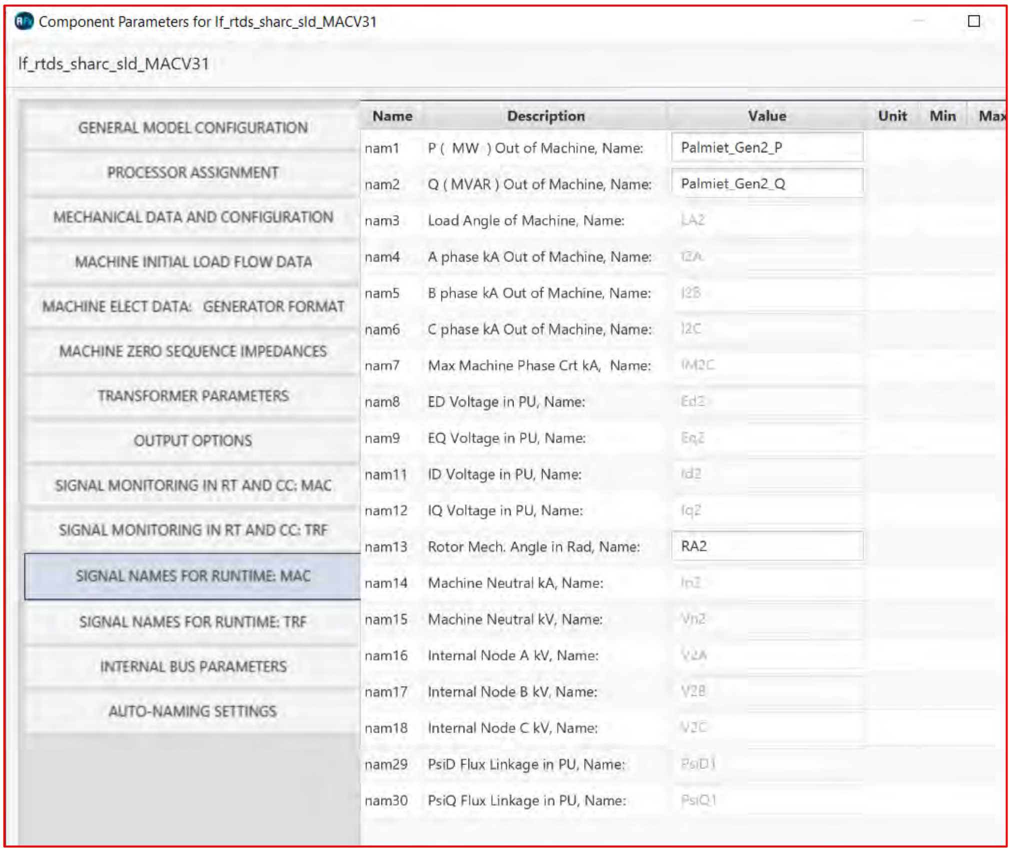

Figure 6.11: Synchronous machine monitored signals for run time.

Palmiet-Gen 2's output voltage and current have been set up for monitoring. However, only current signals are monitored because the simulation cases in this part are based on the high voltage transmission side of the network model. For the remaining system generators, the same components and configurations are used.

In Figure 6.12 below, the controls for the generator are displayed. The governor/turbine receives the W1 angular speed signal, which is monitored from the generator. W1 is the angular rotational speed measured in rad/sec, therefore a conversion component from radians to degrees is needed for runtime simulation. The governor/mechanical torque signal, or TM1, serves as an input to the synchronous generator.

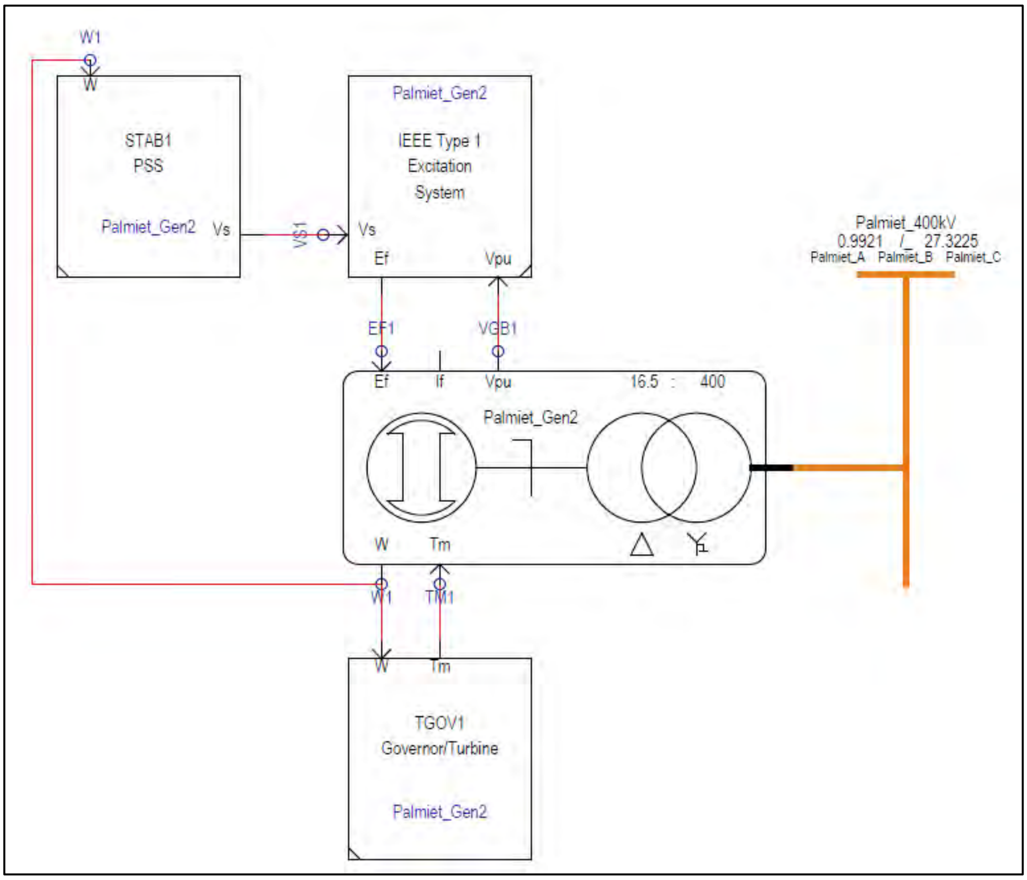

Figure 6.12: Synchronous machine and its controls in RSCAD-FX interface.

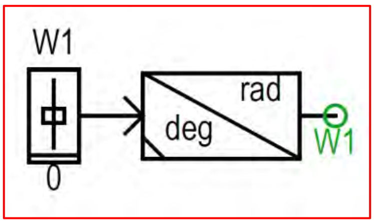

Figure 6.13: Conversion component for monitored speed.

6.4 T-LINE MODELS

The Unified T-line Model can be used to integrate a transmission line model in a simulation. It can simulate a variety of transmission line types, as the name suggests. Although either of these models can be condensed into a simpler PI representation of a line, when necessary, it is primarily employed to model a Bergeron or Frequency Dependent Phase model (RSCAD-FX CC-manual).

Three different icons make up the unified t-line model. A calculation box, a sending end terminal, and a receiving end terminal. Figure 6.14 displays the three necessary elements for Palmiet_Pinotage 400kV transmission line.

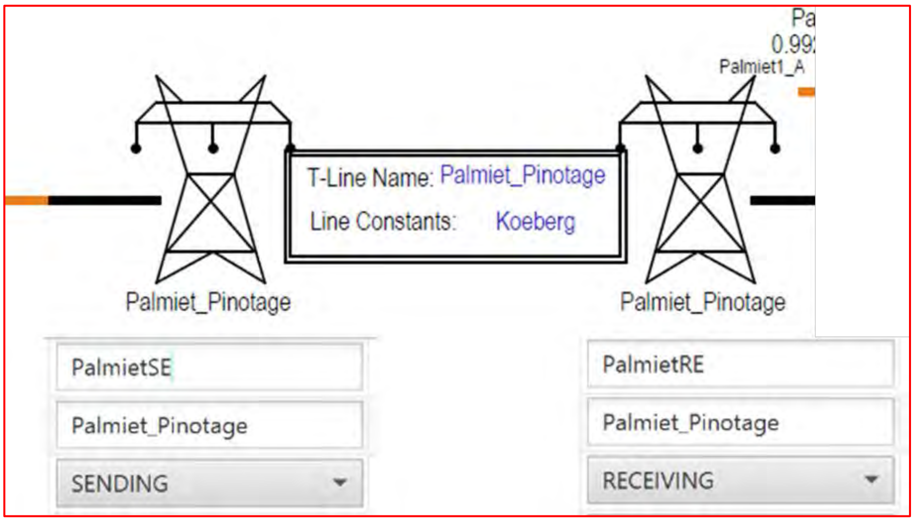

Figure 6.14: Elements required for transmission line model.

These three symbols are solely used to connect the transmission line to the rest of the simulated electrical network. The physical characteristics of the line are accessed through an external file rather than being directly provided inside any of the icons. RSCAD's T-line Module is typically used to generate this external file. This module specifies the physical properties of the Bergeron line model and the frequency dependent phase model. When applicable, the Bergeron T-line output of the T-line Module is also used to derive analogous PI section models. For further information on the T-line module, the user is directed to the t-line script in the RSCAD interface. A screen capture of the T-line Module is seen in Figure 6.15. By selecting the "edit" button on the component this configuration can be accessed.

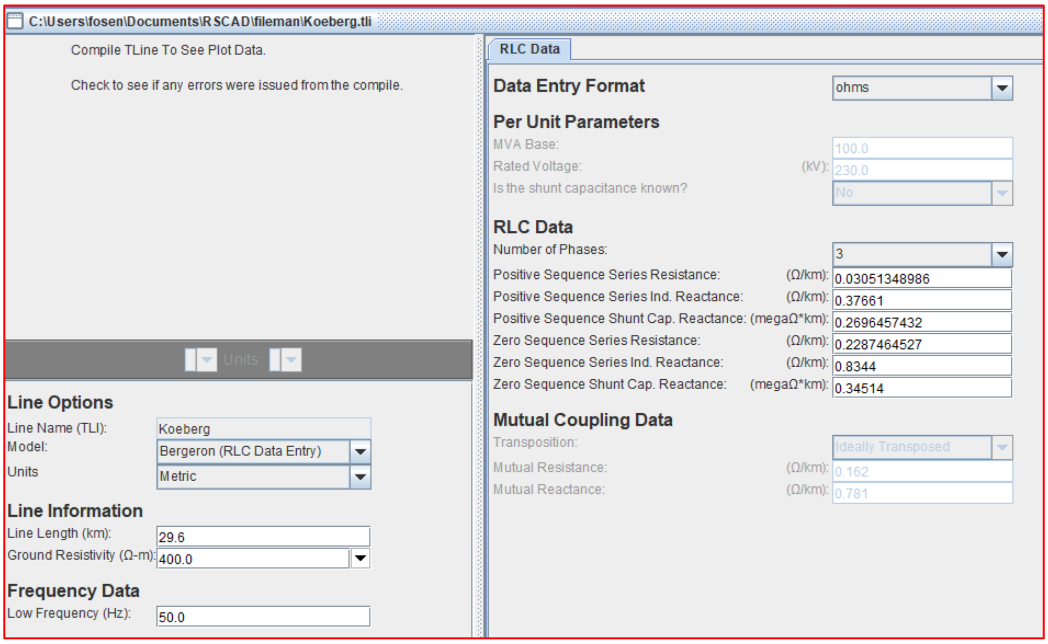

Figure 6.15: T-line RLC Data and line information.

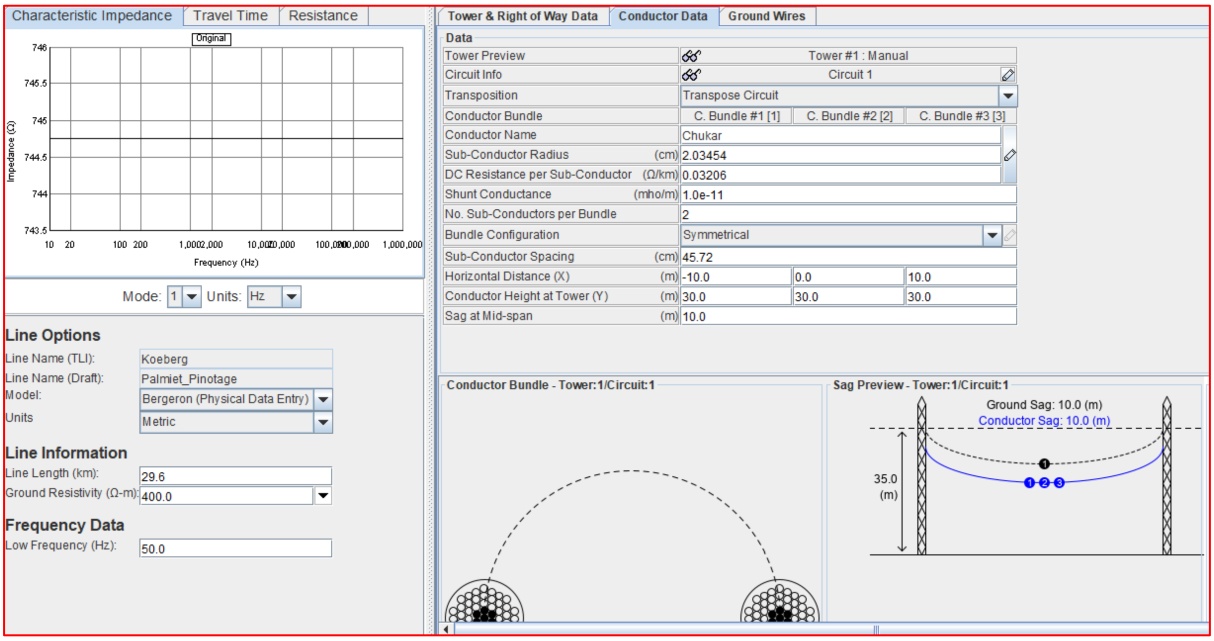

Figure 6.16: T-line physical data entry in the .tlo file.

Dependent Phase t-line it is essential to restore the .tlo file containing the t-line data in order to alter the line length , this will be available upon successful compilation of the T-line.

For monitoring in runtime platform all the transmission lines in the test system are given signal names with current and power inputs specified for each line, Figure 6.17 shows a signalling parameter at one of the Palmiet_Pinotage line.

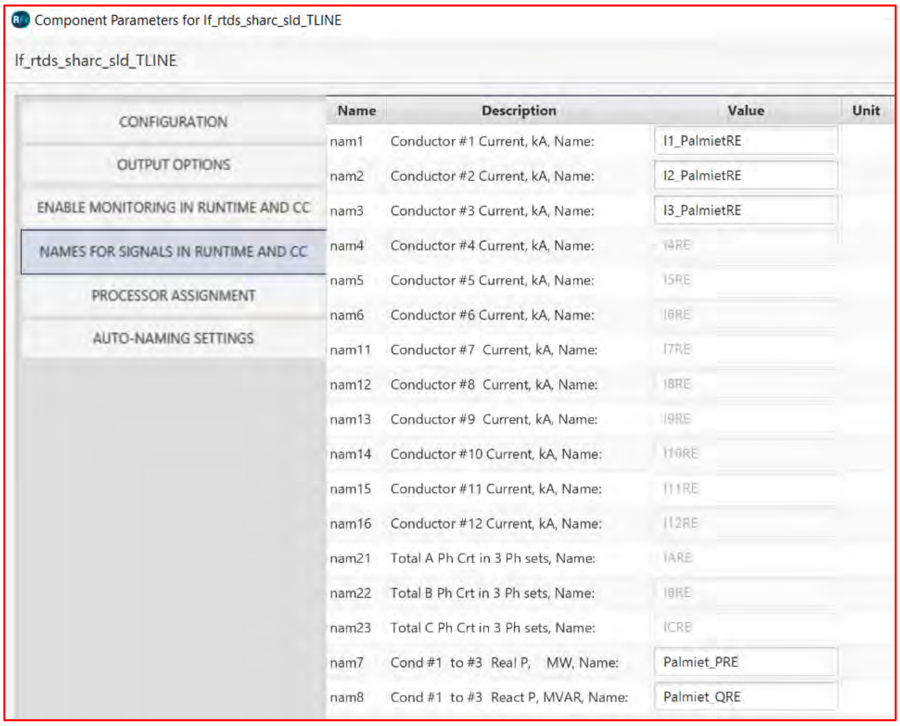

Figure 6.17: Signal Parameters for runtime module.

6.5 DYNAMIC LOADS

In RSCAD-FX the load model is be used to dynamically alter the load in order to keep the P and Q set points constant. This is accomplished by the use of variable conductance.

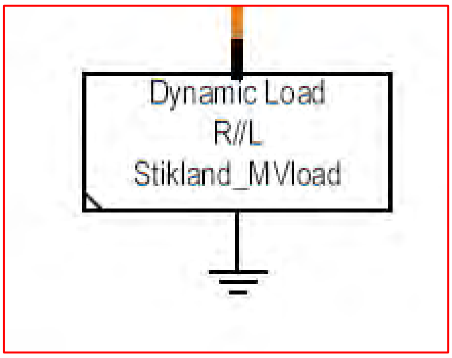

Figure 6.18: Stikland dynamic load.

Each monitored current signal name is enabled according to the load name as shown in Figure 6.18. Loadshedding settings are also available for dynamic loads, the function allows you to alter the P and Q set points by a factor. For example, if it is necessary to shed 20% of the load, the NmLoadShed parameter can be set to 20%. This is especially handy if a large number of dynamic loads need to be adjusted. In this case, setting one parameter is preferable to modifying all of the controllers for each individual dynamic load as shown in Figure 6.19.

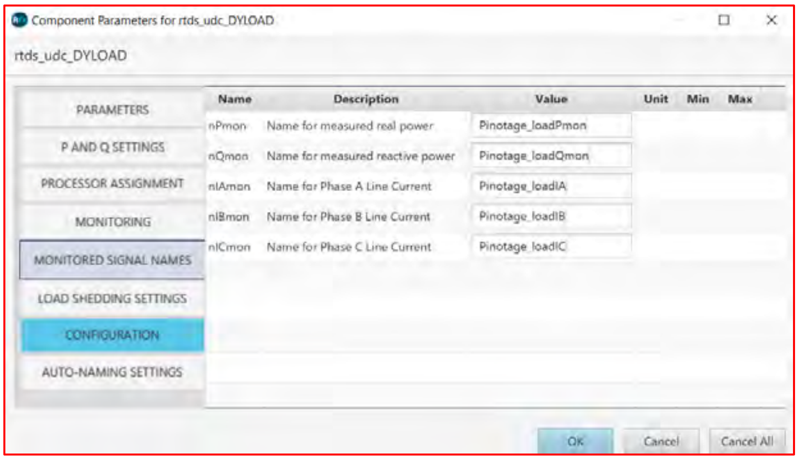

Figure 6.19: Monitored variables in dynamic load.

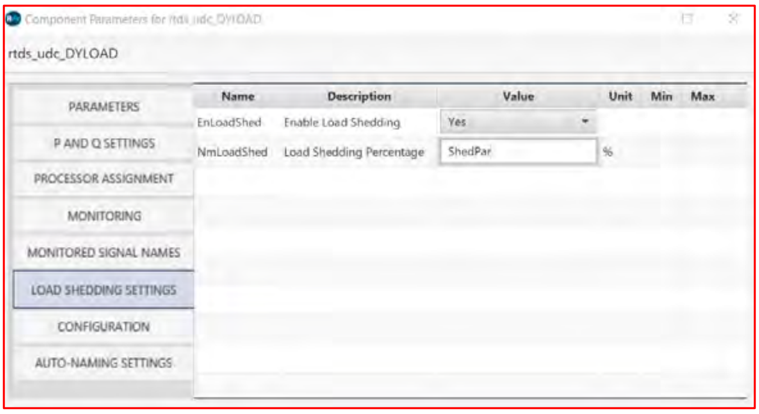

Figure 6.20: Menu for load shedding settings

6.6 Monitoring of Bus Quantities

The bus label component is made up of three node icons. To use the load flow analysis, each bus must have a bus label. Each bus must be uniquely labeled using a bus label component in order for the load flow to execute effectively. Figure 6.21 depicts the bus label parameters.

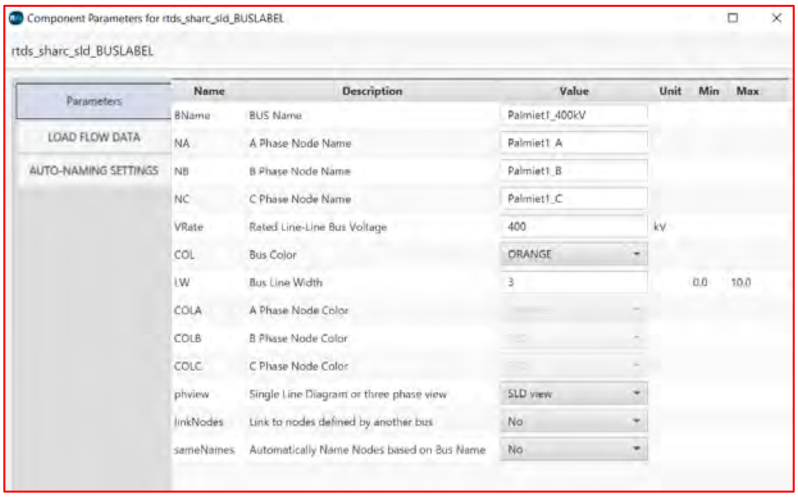

Figure 6.21: Busbar parameters in RSCAD draft.

Initial bus voltage and angle can be entered as fixed values (Real or Integer) or as draft variable names with the $ prefix (for example, $var). The parameter receives the value from a draft variable slider. This value can be automatically modified using a script command from RunTime, and load flows can be executed with various initial values.

From the drop-down option for the "Type" parameter, you can choose the bus type. There are three different bus types: SLACK, PQ, and PV Bus. A minimum of one SLACK bus must be present in the simulation case in order for a load flow computation to be successful. Voltage and angle parameters "Vd" and "Ad" are automatically adjusted whenever the load flow converges.

The user must build additional logic to determine the difference between the sending-end or generated and receiving/consumed power when active power losses and reactive power absorption in the system are necessary for monitoring. This is based on the idea that the difference between the active or reactive power generated, and the active or reactive power consumed by the load is what is known as the active or reactive power lost or absorbed on the transmission. Table 6.3 provides list of monitored quantities for the test system with monitored variables marked with “X” and “grey” for non-monitored.

Table 6.1: System monitored variables

Parameter	Busbars	Generators	Dynamic Loads
Frequency		X	X
Rotor Angle		X	
Angular speed		X	
Torque		X	
Voltage	X	X	X
Power Factor	X	X	X
Apparent Power	X	X	X
Active Power	X	X	X
Current	X	X	X
Reactive Power	X	X	X

Generators can be operated in either the lock mode or the free mode. In the lock mode, the generators generate power based on the prime mover's rotational speed. In the free mode, the generator's operation is determined by the mechanical torque applied to it.

The angular velocity of the generator, which fluctuates depending on how loaded it is, can be used to measure the frequency in the generators.

6.7 LOAD FLOW ANALYSIS

Verifying the stability of the busbar or node voltages is one of the fundamental jobs in examining power system network issues. The load flow at constant frequency of 50Hz was simulated with 3 AC subnetworks denoting areas of generation, the results given in Figure 6.22.

```
RSCAD LOAD FLOW Version 1.053
===========================

There Are 3 AC Sub Networks:

There Are 3 AC Sub Networks:

Sub-Network #1 -
     Slack Bus 'Koeberg_Gen1'
--------------------------------------------------

ITER     DELTAP      BUS     DELTAQ      BUS
 0    220.04307574    5    47.97358108    2
 1     85.96506418    2    23.07910229    2
 2     15.61893149    2     0.69858534    2
 3      0.07994434    5     0.00637527    5
 4      0.00106794    2     0.00009528    2
 5      0.00004182    2     0.00000225    2
Specified tolerance reached in  5 iterations.
```

```
Sub-Network #2 -
No Slack Bus Identified
--------------------------------------------------

Notice: BUS Ankerling_Gen1 (3) is automatically assigned as a slack bus.

ITER     DELTAP      BUS     DELTAQ      BUS
 0    40.04282058    1    50.06448432    1
 1    22.15490288    1    15.86111912    1
 2    30.39574738    1    27.93059389    1
 3    20.09398712    1     8.86666620    1
 4     1.57722725    1     0.09549582   10
 5     0.02531292    5     0.00664661   10
 6     0.00080891    5     0.00038206   10
 7     0.00004346    5     0.00002207   10
Specified tolerance reached in  7 iterations.
```

```
Sub-Network #3 -
     Slack Bus 'Palmiet_Gen1'
--------------------------------------------------

ITER     DELTAP      BUS     DELTAQ      BUS
 0    21.74536679    1    10.35797946    5
 1     0.57788689    4     0.03656901    4
 2     0.00600099    4     0.00041560    4
 3     0.00005898    4     0.00000390    4
Specified tolerance reached in  3 iterations.

RSCAD Loadflow finished successfully.
exit code = 0
```

Figure 6.22: RSCAD-FX draft load flow simulation results in offline mode.

When the draft load flow simulation is run, the busbar voltages, real and reactive power generated and consumed on the draft network simulated in subsystems can be read.

The results are shown in Table 6.2, where P_G and Q_G represent the active and reactive power generated during the draft load flow in megawatts (MW) and megavars (MVARs), respectively, and P_L and Q_L represent the active and reactive power demanded by the loads during the draft load flow in megawatts (MW) and megavars (MVARs) (MVARs). After the RSCAD draft load flow computation is completed, the per-unit busbar voltage magnitudes and phase-shifts are recorded.

Table 6.2: Load flow results in RSCAD-FX draft

Bus bar	Type	V(p.u)	$P_G(MW)$	$Q_G(MVar)$	$P_L(MW)$	$Q_L(MVar)$
Palmiet_Gen 1	Slack	$1.0\angle 0°$	191.43	40.26	-	-
Palmiet_Gen 2	PV	$1.0\angle 0°$	191.43	40.26	-	-
Palmiet_400kV	PQ	$0.99\angle 27.33°$	-	-	391.43	60.71
Pinotage_400kV	PQ	$0.99\angle 27.10°$			-370.09	-59.91
Stikland_400kV	PQ	$1.0\angle -32.39°$	-	-	-150	-0.1
Muldersvlei_400kV	PQ	$1.0\angle -32.26°$	-	-	-806.82	-159.92
Koeberg_400kV	PQ	$1.01\angle -29.19°$	-	-	10.6	97.7
Koeberg_Gen1	Slack	$1.0\angle 0°$	-700	-250.01	-	-

Koeberg_Gen2	PV	$1.0\angle 3.26^\circ$	900	587.13	-	-
Ankerling_400kV	PQ	$1.0\angle 160.02^\circ$	-	-	349.76	150
Ankerling_Gen 1	Slack	$1.0\angle -170.0^\circ$	-1.43	-19.19	-	-
Ankerling_Gen 2	PV	$1.0\angle 132.87^\circ$	148.8	-15.5	-	-
Ankerling_Gen 3	PV	$1.0\angle 132.80^\circ$	148.8	-15.5	-	-
Aurora_400kV	PQ	$1.0\angle 158.41^\circ$	-	-	145.74	150
Aurora_132kV	PV	$1.0\angle 158.35^\circ$	-	-	47.8	33.8
Fransvlei_33kV	PQ	$0.96\angle 154.87^\circ$	-	-	47.0	33.4
Electra_33kV	PQ	$1.0\angle 158.30^\circ$	-	-	0.8	0.4
Total			2308.24	967.85	2248.08	816.23

In order for the load flow to successfully converge at least1 slack bus for each AC subsystem needs to be specified in the transmission test system e. Koeberg_Gen1, Palmiet_Gen1 and Aurora_Gen1.

6.8 CONCLUSION

In this chapter the same test system simulated in DigSilent chapter is developed with the goal of performing steady-state simulation analysis in RTDS's offline mode (non-real time). The goal of developing this network model was to successfully verify whether the load flow converges before commencing on developing a hardware-in-the-loop test bench for live simulation results of RTDS, which is the first prerequisite in any protection technique design (Awareness of stable power flow is principal).

The next chapter will look at implementation of the hardware-in-the-loop test bench incorporating the virtual system of RSCAD implemented in this chapter for hard wired protection scheme.

7 CHAPTER SEVEN

HARDWARE-IN-THE-LOOP TESTING OF OUT-STEP-PROTECTION WITH RTDS

7.1 INTRODUCTION

The RTDS simulator is a software application for modeling and simulating real-time simulations of power and control systems (Ouellette, et al., 2004). The dynamic behavior of a power system is examined in real-time using RTDS. When studying the behavior of a power system under transient conditions and dynamically changing conditions, real-time simulation is critical. It is necessary to simulate various fault circumstances on a power system in order to assess the reliability of the protection system in use. Simulating fault conditions in real time enhances observational accuracy because simulations are closer to real-world settings. This contributes to the enhancement of the protection strategy as well as the protective system models (McLaren, et al, 1992).

The hardware design for the parallel processing used by the RTDS is unique and is organized into rack-like components. Triple Processor Cards (3PC), Giga Processor Cards (GPC), Twelve Channel Analogue Output Card (GTAO), and other cards make up the RTDS. The power system test case can be modeled using the 3PC card. Each 3PC card of the RTDS hardware has an analog device called the ADSP21062 (SHARC) digital signal processors (DSP) (RTDS Instruction manual, 2020). The analogue channel outputs offered by the 3PC cards can be used to connect external devices and carry out hardware-in-the-loop (HIL) testing.

In this chapter simulation of the test system modelled in chapter 6 will be carried out with which real-time fault simulations in out-of-step zone and external zone will be analyzed for Palmiet-Gen1 unit. The Real-Time Digital Simulator is coupled in a closed-loop mode with an external physical IED SEL-421 optimally placed in Palmiet_Pinotage 400kV line. A power swing trip or blocking signal is sent by the SEL-421 IED to the trip logic configured in RSCAD-FX for RTDS. The simulation results are further analyzed using SEL-SynchroWave disturbance record analyzer to investigate if either the protection for the generator is reliable or not.

7.2 DIFFERENCES BETWEEN REAL-TIME AND NON-REAL-TIME SIMULATION

The obvious distinction between real-time and non-real-time simulation is, as the names imply, the rate at which the simulations are carried out. In both instances, a power-law mathematical model of the state (or behavior) of the system is ascertained from the solution at each time step of a system that is solved at regular intervals, or time steps. Traditional simulations require longer than real time to calculate the system's state at each interval; in other words, it takes the simulator much longer than 10 seconds to determine how a given system would behave in practice throughout that time period (Rigby, 2012). Contrarily, in a real-time simulation, the simulator determines the behavior of the system in precisely real time. It computes the system's state and outputs it at the exact same rate as the system's actual behavior occurs.

A real-time simulator, however, is considerably more than just a quick simulation of a conventional power system. A real-time simulator's main function is to connect with and afterwards test the ever-sophisticated machinery utilized to safeguard and manage contemporary power systems.

Examples of research that have been conducted with a real-time simulator include the following:

- Protection relays closed-loop testing.
- Power system controllers closed-loop testing.
- Studies on power swing and power system damping.
- Studies on how a system and a controller interact.
- Rapid evaluation of numerous scenarios and contingencies (owing to real-time operation and the possibility for automated batch-mode operation of the simulator).

A real-time simulator opens up the possibility for doing a variety of advanced tests and system studies that would otherwise be impossible or impracticable since it enables physical equipment to be linked to and interact live with a simulation of a power system running in real time.

7.2.1 Traditional (non-real time) simulation

A traditional, non-real time simulator's structure and organization are depicted diagrammatically in Figure 7.1 below. Any traditional non-real time power system simulator (such as DIgSILENT, PSCAD, EMTP/ATP, PSS/E, etc.) would have a structure and organization similar to what is illustrated below. The diagram shows that all the tasks necessary to simulate the behavior of the to-be-studied power system are performed by a single computer (and a single processor on that computer).

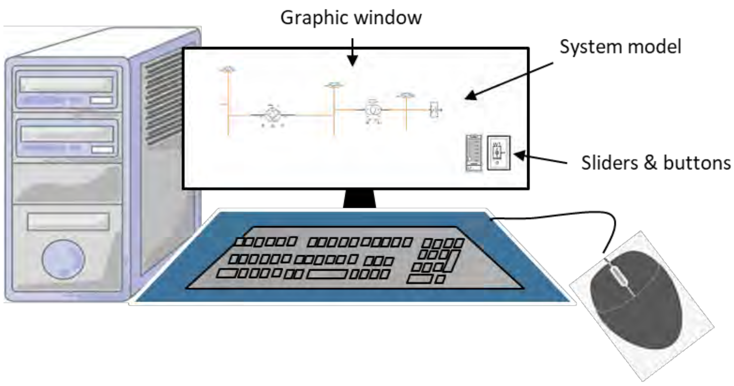

Figure 7.1: Organisation of a non-real time simulation.

Depending on the simulation environment, the user may be able to view simulation results as they are calculated and interact with the simulation while it is running using the keyboard and/or mouse. However, the following characteristics distinguish this form of simulation:

- The simulation's beginning and ending times are fixed.
- The system's simulation model is created, assembled, solved, and shown by the same computer and on a single processor.
- The system model's solution takes much longer than real time to finish.
- There are no connections (either input or output) to external power system components because they are always simulated as part of the software simulation using mathematical models, even though it may be feasible to interact with the simulation throughout the solution.

The non-real time simulations have been dealt with in chapter 5 (DigSilent) & chapter 6 (RSCAD-FX) of the dissertation, however it is utmost important to make comparison with real-time simulation for the research objectives and interest's sake.

7.2.2 Real-time simulation (as executed by RTDS hardware)

In Figure 7.2 an illustration of an organization of real-time simulation as conducted by RTDS is shown. The diagram demonstrates that the most obvious difference from a conventional simulation is that the actual solution of the system model is carried out on a specialized, multi-processor computing platform (the RTDS rack), whereas the software suite required by the user to prepare and manage the real-time simulation is ho (a standard personal computer).

The real-time simulation's subtasks are distributed among a number of specialized pieces of equipment on the rack itself. The rack includes a number of different processor cards, specialized input and output cards (both digital and analogue), and a workstation interface (either WIF or GTWIF) card to handle communications with the host PC. The GTWIF cards, are also used to handle communications between the racks itself in multi-rack simulator configurations.

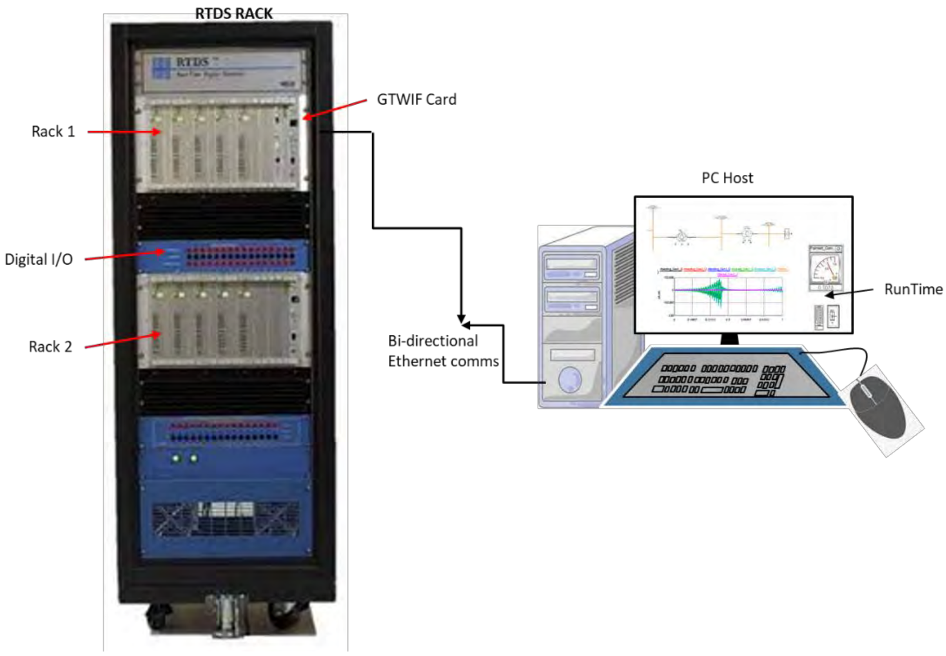

Figure 7.2: Real-time simulation in RTDS.

The user can alter certain elements of the system model while the simulation is running, comparable to several non-real time simulators. For instance, it is possible to alter the system inputs, open and close circuit breakers, apply and remove faults, adjust controller gains, etc. Through the host computer's runtime interface, these online modifications to the simulation model are made while the simulation is running.

At each time step of the simulation, user-specified variables from the simulation model can be delivered to analog and digital output ports for measurement or for connection to external devices like relays and controllers. Relays and controllers, for example, can produce outputs that can be fed back into the simulation to modify the model as it operates in real time.

The following but not limited to processor cards are accessible in the RTDS modules offered at Cape Peninsula University of Technology's Centre for Substation Automation and Energy Management Systems (CSAEMS).

- Digital I/O panel
- Gigabit Transceiver Analogue Output Card (GTAO)
- Gigabit Transceiver Analogue Input Card (GTAI)
- Gigabit Transceiver Workstation Interface (GTWIF)
- Gigabit Processor Card (GPC)
- The GYSYNC card is utilized to synchronize the RTDS simulation time step with an external synchronize time reference GPS clock as well as devices under test.
- HV patch panel

7.3 HARDWARE-IN-THE-LOOP (HIL) FOR PROTECTION RELAYING SYSTEM

Closed-loop analysis of protection systems is desired because it allows for the prediction and understanding of interactions between relays and the power system. The standard method for analyzing closed-loop interactions between different components of a power system is to employ time-domain simulations, which are often run in non-real time. In the case of the given example of a protection system, this technique would necessitate the use of mathematical models to represent the protective relay (or relays) in the simulation.

However, a modern protection relay is typically a highly-complex system in its own right; developing a mathematical model to faithfully reproduce the behavior of a relay for all possible electrical inputs to the relay, and for all possible permutations of user-selectable features and protection settings is a daunting task, even for a single type of relay supplied by a single manufacturer. Given the complex nature of protection relays, and the significant number of different such devices in use, this approach is not feasible for closed-loop analysis in cases where a high degree of confidence is required in the results. Therefore, hardware-in-the-loop loop testing is necessary for such instances as it incorporates the actual physical relay in its set-up.

The Hardware-In-The-Loop (HIL) testing technique is one of the most significant approaches as it is used to analyze the nonlinear and dynamic behavior of the physical device and aids in the construction and validation of a model to govern the physical devices. In the creation and testing of sophisticated real-time systems, the HIL simulation is used. The major goal of the HIL simulation is to provide a helpful platform for developing the test-bed to test the protective relay in real-time simulation. Electrical emulation of sensors and actuators for the communication interface between a protective relay and the simulator must be included in the HIL simulation.

For this study, protection system is concentrated at generating station in Area 3 the Palmiet synchronous generators. However, due to limited cards and licensing on the SEL700GT available at the CSAEMS the OOS protection is not available in this IED such that only the SEL-421 relay which provides back-up OOS to the generating units is tested for practicality with HIL testing. The relay is virtually placed on the Palmiet_Pinotage 400kV line in the system under test on RSACD-FX. Figure 7.3 Shows a schematic diagram of Area 3 with the protection relay installed on RSCAD-FX interface.

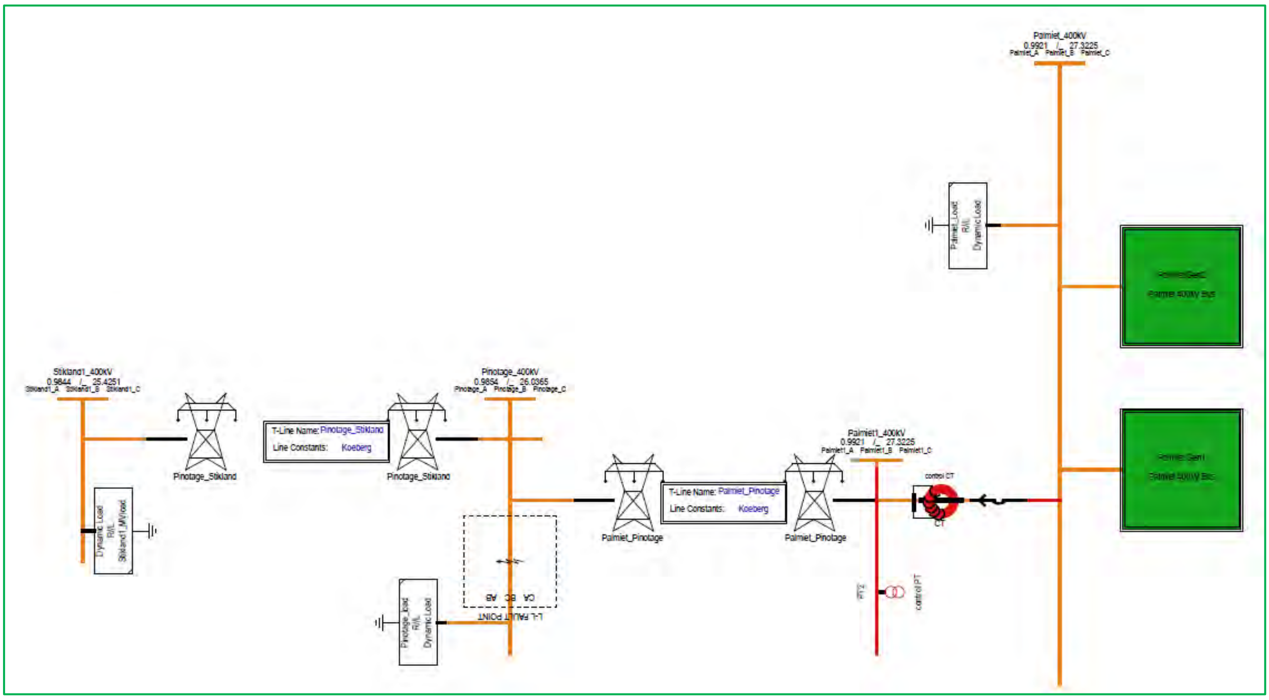

Figure 7.3: Area 3 portion of test system in RSCAD-FX interface.

7.3.1 HIL test bed implementation for OOS protection scheme

Real-time power system simulators are appealing because they enable the integration of both analytical methods—hardware performance evaluation of the actual protection relay and extensive simulation modeling of interactions with the power system—into a single closed-loop analysis tool. Using a real-time simulator, it is possible to feed the protection relay (or relays) under investigation with pertinent outputs from a power system simulation model that is running in real time, and the relay's response to these outputs is then sent back into the power system simulation live (Rigby, 2012).

This method combines the benefits of the two analytical approaches as follows: the analysis is closed-loop in nature because the inputs and outputs of the relay are connected to a precise simulation of the power system in the same way that they would be connected to the actual power system; a high level of confidence can be placed in the results because the actual relay, with its intended settings, is used in the analysis.

Figure 7.4 provides an illustrative diagram of the implemented test bed for out-of-step protection scheme. The currents detected by the CTs are transferred to the protective relay equipment using the • Gigabit Transceiver Analogue Output Card (GTAO) component found in the RSCAD-FX simulation environment, as shown in Figure 7.4. IBURA, IBURB, and IBURC are the currents measured by the CT, whereas VBURA, VBURB, and VBURC are the respective voltages measured by the PT. The input signals are sent to the GTAO high precision analogue output board by the GTAO component, as it is known in the RSCAD library.

The 12-channel GTAO board is a part of the RTDS hardware. Real input signals are taken in by the GTAO. Through the optical port of the RTDS hardware, the component transforms the input signals, scales them to 16-bit resolution, and writes them to the GTAO card. The GTAO produces an output in the 10 V range. Figure 7.4 depicts the GTAO card that served as the interface between the RTDS rack and the Omicron amplifiers. The floating communication signals are connected through a centered ethernet port which is locked by GPS clock to acquire constant comms between the test bed components.

The trip signals are defined to be sent via the feedback link from the SEL-421 hardware relay to the Digital, I/O port of the front panel of the RTDS, as shown in Figure 7.4. The SEL-421 hardware relay's analogue signals are continuously tracked and updated. Amplification is used to feed the SEL-421 hardware relay with the digital current signals from the RTDS GTAO card.

The SEL-421 distance relay is designed to send trip signals in response to internal occurrences in the generator protected zone. The SEL-421 relay is set up using AcSELerator Quickset engineering setup software. The location of the equipment to be protected and the connection of its circuit breakers serve as the foundation for the zone definition. All the monitoring is performed through RSCAD-FX draft with host PC. Communication between RTDS rack 1 and host PC is acquired through Gigabit Transceiver Workstation Interface (GTWIF), thus physically completing the hardware-in -the-loop protocol.

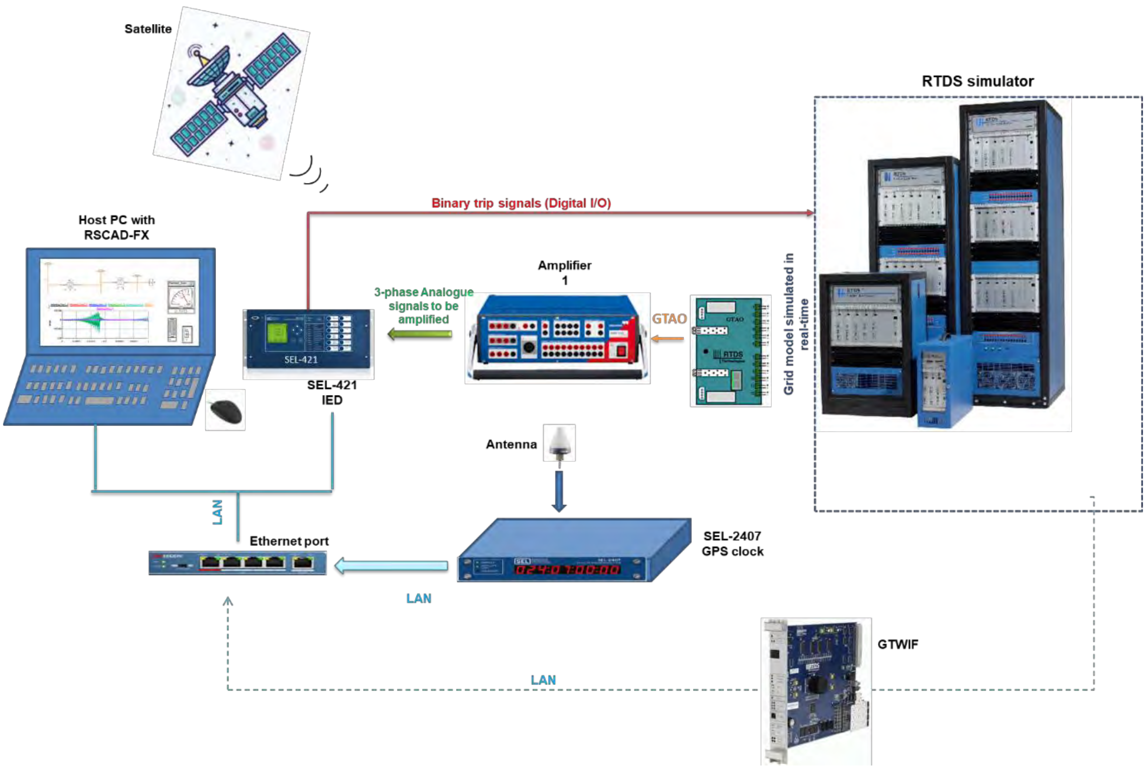

Figure 7.4: OOS protection scheme setup in RTDS hardware-In-the-loop.

7.3.2 Steady-state simulation results in RunTime

On the runtime module, there are many monitoring options, including RMS meters and graphs. RMS meters, for instance, can be used to examine the system's power flow in steady-state conditions. The plots are employed in disturbance (or transient) analysis. This analysis is done to demonstrate that the network is stable before the contingencies are implemented. Monitoring is done for bus voltages, generator supply, load demand, and system frequency. Results for the total generating supply, total system load demand, bus voltages, Palmiet_Gen1 speed (W3) and network frequency during steady-state analysis are shown in the RMS meters of Figure 7.5 below. Figures 7.6, 7.7, 7.8 and 7.9 further provide plot diagrams for system quantities in a stable state. The power system voltage is steady at 396.6kV and according to the data gathered. Palmiet_400kV bus was used to measure the system frequency, which was found to be steady at 50Hz.

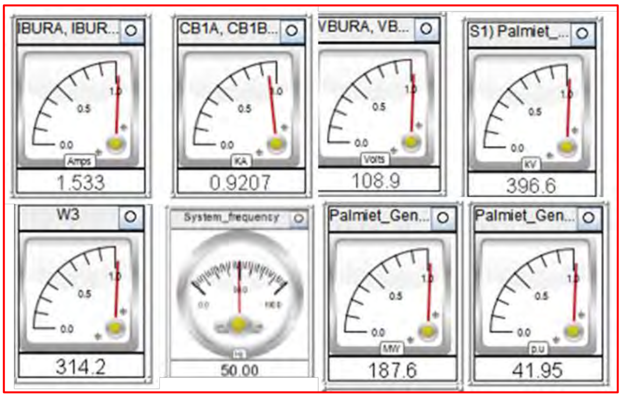

Figure 7.5: RMS meter reading for steady state system quantities in Area 3.

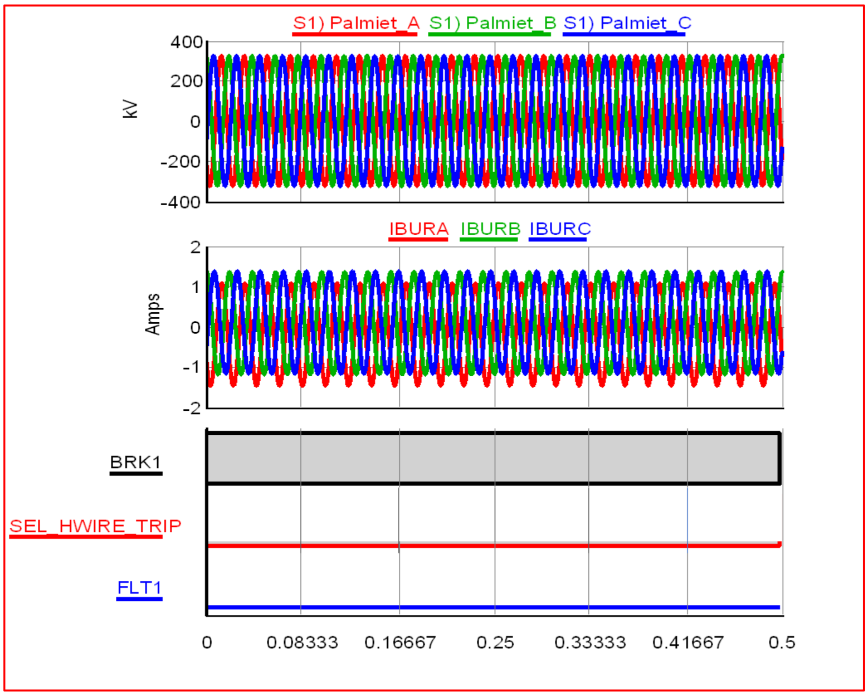

Figure 7.6: Steady state currents and voltages with circuit breaker closed at Palmiet_400kV busbar.

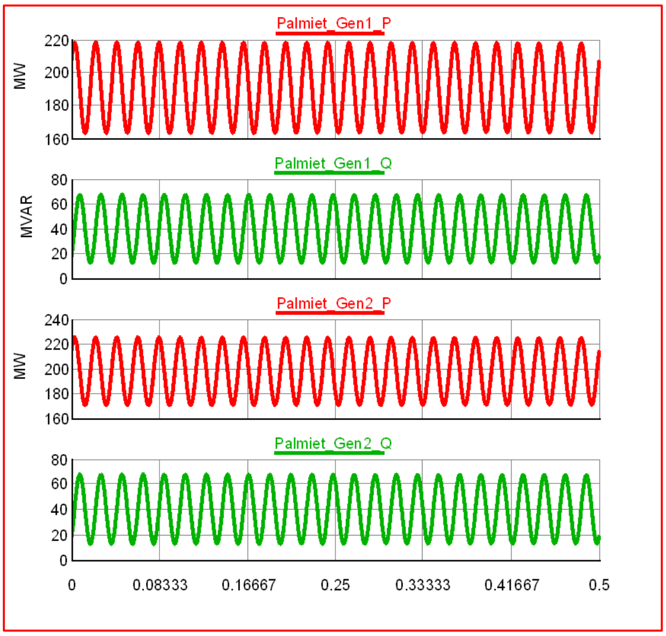

Figure 7.7: Palmiet generating units power supply.

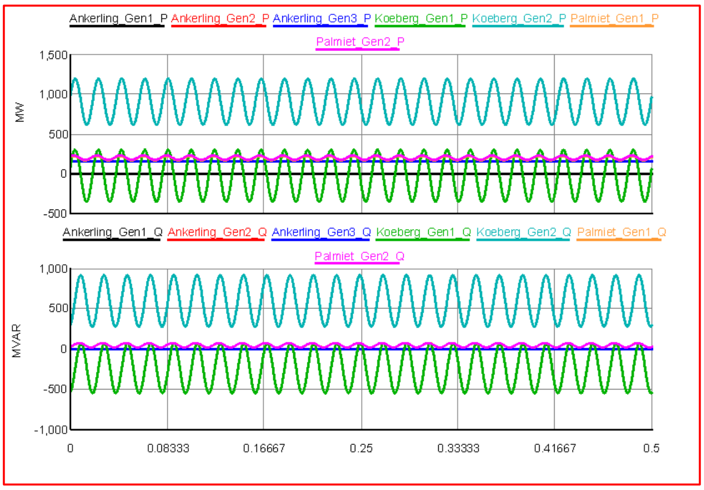

Figure 7.8: Steady state complete system power supply.

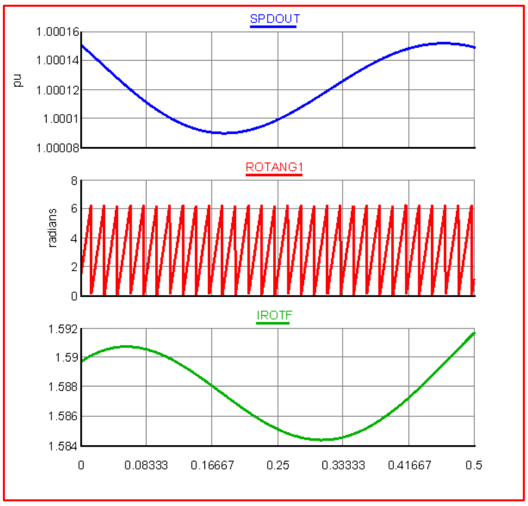

Figure 7.9: Palmiet_Gen1 rotor speed, angle and current in steady state.

By deducting the load demand power from the total generation supply, the power loss may be calculated. 60.16 MW are the power losses result computed.

7.3.3 Protection configuration

For any protection scheme the fundamental purpose is to safeguard the power system, in order to do so system analogue measurements needs to be converted to considerable smaller quantities that will be able to be read by the protection relay. In RTDS simulation platform this is carried out through digital to analogue converter (DAC) which enables current and voltage signals measured by the CT and PT configured in RSCAD draft to be sent to the physical hardware protection relay device. GTAO card component as referred to in RSCAD library is responsible for this high precision signal processing as mentioned earlier in the chapter. Figure 7.10 provides a channel link performed internally by RTDS between GTA card and analogue signals configured in the CT and PT of RSCAD-FX draft model.

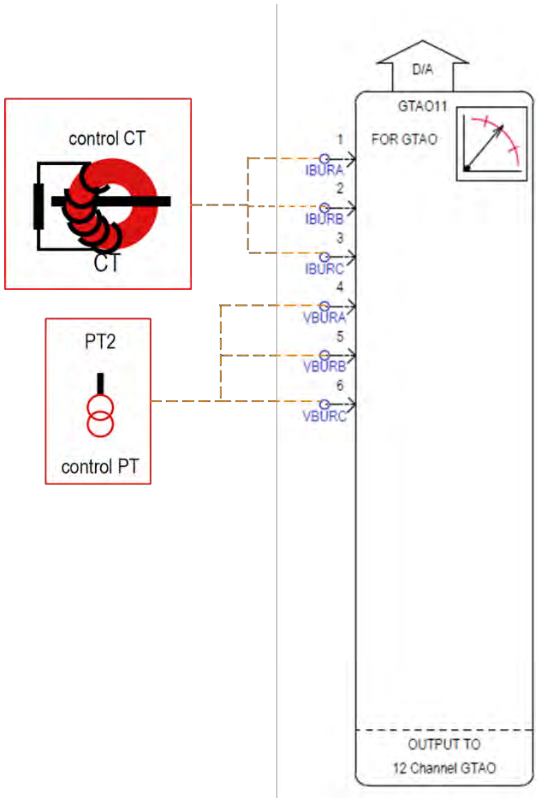

Figure 7.10 Analogue signals from instrument transformers to DAC component in RSCAD.

It is necessary to provide an initial output advance parameter in time steps. This option sets the output signal's starting point for the following time step. In an effort to reduce time delays brought on by interfaces with external equipment, the GTAO output signal can be advanced using the advance factor. The advance factor should be set to 1.0 if no advance is required. The most recent information is being used when the advance factor is set to 1.0. The GTAO's input and output will be one time step delayed if the advance factor is set to 0.0.

7.3.3.1 Breaker control logic modelling

Circuit breaker has a crucial role in protection system as it is expected to rapidly disconnect the fault currents when commanded to do so by protection relay. The most important component in studies on protection is time. Practically, the time delay in power systems occurs while the circuit breakers are operating. Typically, the circuit breaker operation in high-voltage transmission networks takes between 0.2 and 0.3 seconds (Sakthivel & Dhivya, 2018).To demonstrate this phenomena in RTDS, a circuit breaker control logic is developed. Opening the breaker will de-energise the Palmiet_400kV bus which will subsequently lead to zero power supply being transferred to the other ends of buses in Area 3.

It is advisable to focus on the time parameter in protection studies in order to validate the conclusions and make the simulation studies realistic. For this reason, timers are employed in the developed logic to account for delays in circuit breaker activation when integrating the physical device with the RTDS devices. The connection between the GTFPI model and the circuit breaker control logic is shown in Figure 7.11 below.

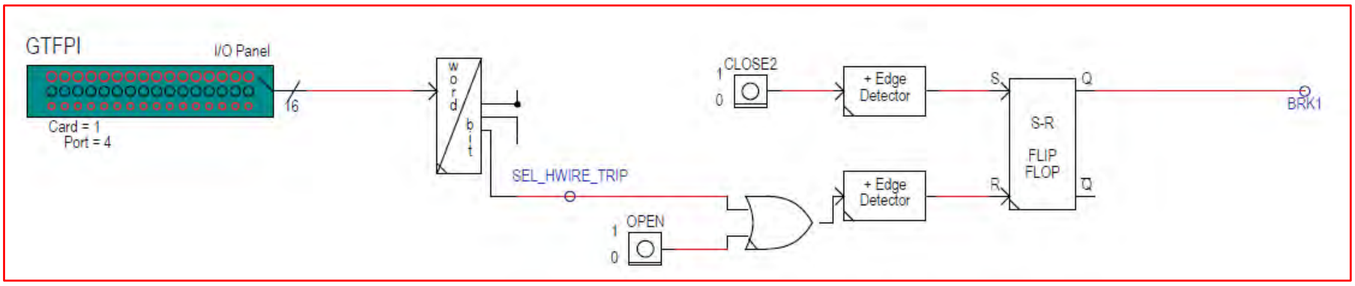

Figure 7.11: GTFPI (I/O panel) connected to CB control logic.

The GTFPI component can write to and read from GTFPI cards in binary integer format. The RTDS front panel is physically attached to a GTFPI card. Word bit convertor block is responsible for conversion of relay word bit to digital input of RTDS in RSCAD simulation environment, in turn hardwire output trip signal from the relay data is read through this block. The 16-bit data is read via the digital input port and returned as an INTEGER, which is subsequently sent as a trip signal from SEL-421 relay to the network to trip and open the relative virtual circuit breaker. Edge detectors are the logics used trigger and disable the SEL-421 relay's trip command.

Three supply branches link to Palmiet_400kV bus in the integrated system. If a failure occurs, the entire busbar section must be disconnected from the system by disconnecting all supplying branches. This function is represented by three-phase circuit breakers CB1A, CB1B, and CB1C modelled in one breaker. These circuit breakers are controlled by the BRK1. Figure 7.12 illustrates an example of this settings configuration as developed in RSCAD-FX.

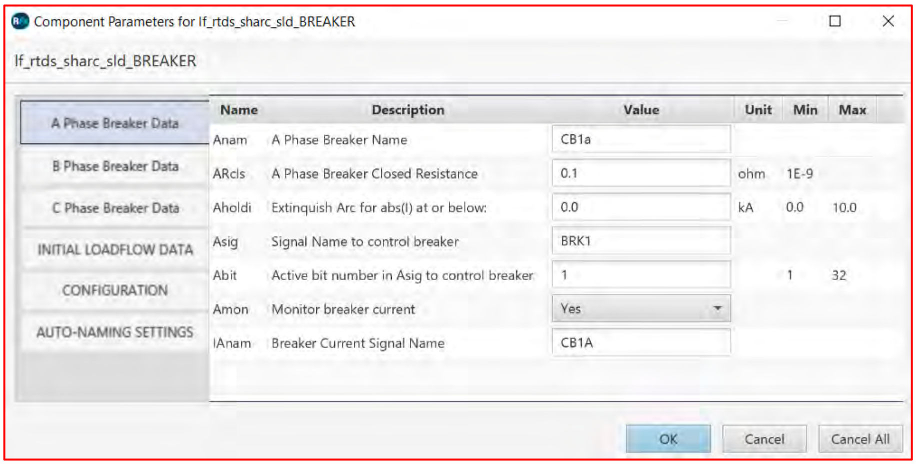

Figure 7.12: Signal name configuration for BRK1 in RSCAD-FX.

7.3.3.2 Modelling of Fault control logic

The fault control logic that regulates the kind, duration, position on the wave, and location of the fault is built using controls components from the RSCAD library. In the RTDS runtime environment, the fault can be managed, and it's used to examine how the relay operates when there are high voltage side faults, low voltage side faults, and internal failures.

The majority of power system faults are single-line to ground faults, however in addition to single-line to ground problems, three-phase faults are also simulated for the protection scheme phase parts. The fault simulation logic is defined and configured in RSCAD-FX as seen in Figure7.13.

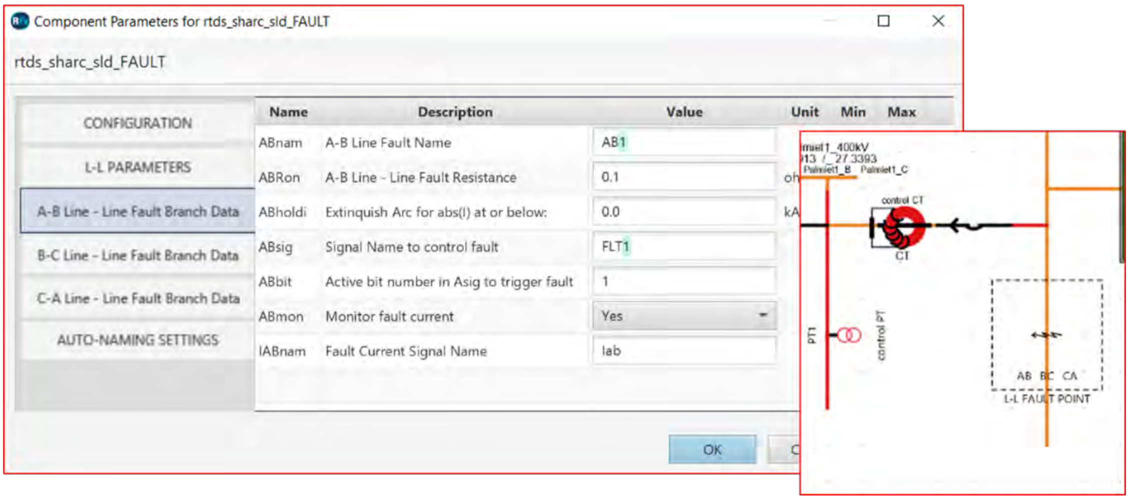

Figure 7.13: Signal names to define fault control in RSCAD-FX.

Figure 7.14 depicts the fault control logic that is intended to initiate a single-line-to-ground, a double-line-to-ground, and a triple-line-to-ground. In zone and out of zone faults to OOS tripping zone can occur for the Palmiet_Gen1, which is protected by the relay hardware SEL-421.

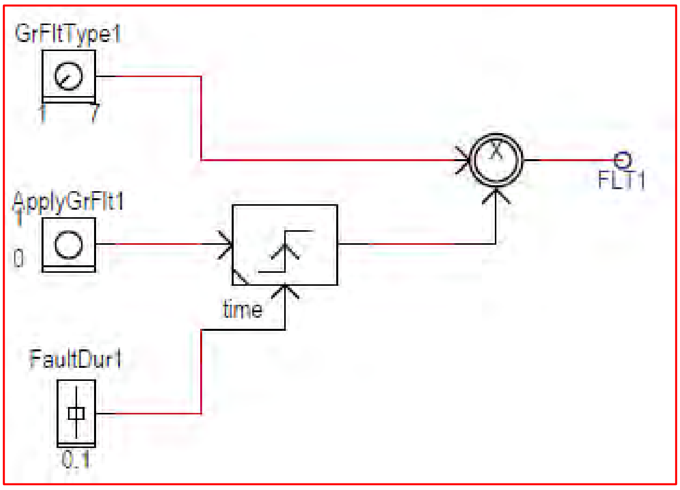

Figure 7.14: Fault inception control logic as defined in RSCAD-FX.

Fault inception is based upon the node voltages of the faulted part in the system as the fault will be moved to different zones (zone1 and zone2) of the line owing to distance protection (SEL-421). Due to its ability to start a defect that will eventually be discovered by the hardware relay, the fault inception logic (GrFltType1) is a crucial component of the hardware in the loop testing. The protected equipment voltage is used by the fault inception logic as a reference point for the point on wave delay. As soon as the FLT button is pressed in runtime interface the ApplyGrFlt1 button in the logic produces a signal bit “1” which initiates fault sequence to the pulse duration timer. The output of the duration timer is set to logic one when the pulse rises to logic one, which is equivalent to the amount of time needed to rotate the number of degrees away from the zero-crossing detection. When this happens the multiplication junction integer produces the final out signal of the logic i.e., FLT1.

7.3.3.3 IED configuration

In this sub-section, the AcSELerator Quickset is used to finish configuring the SEL-421 Protection Automation Control device.

Both of the functioning conditions of the interconnected resultant system are satisfied after this scheme has been configured. Consequently, the device's settings are split into two groups to accommodate the power swing blocking and out-of-step trip. The configuration process will be done according to calculations settings done previously in chapter 4.

The general global settings of the out-of-step scheme relay are shown in Figure 7.15, which includes station identifier, SEL-421 relay identifier, 50Hz nominal system frequency and fault condition equation for an ABC system phase rotation with 120 ° phase shift.

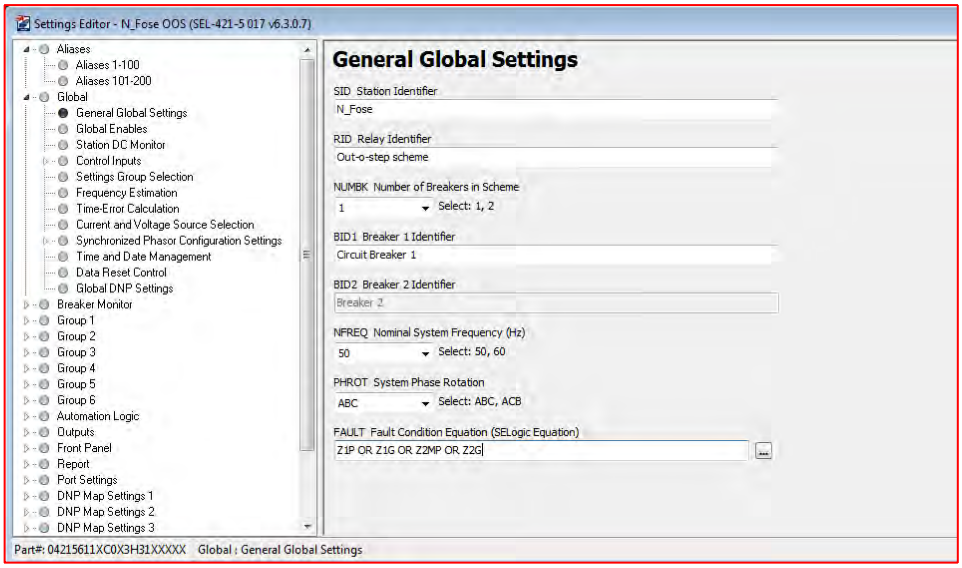

Figure 7.15: General global settings for SEL-421 IED.

Next important step is to configure the instrument transformer settings. The settings are the same as those entered during the configuration of the signaling devices and RSCAD-FX modeling for the scheme in chapter 6. However, only turns ratio settings are applicable on the relay not necessarily primary and secondary windings Figure 7.16 below provide an illustration of the Line configuration with W and Y winding inputs selected on the relay.

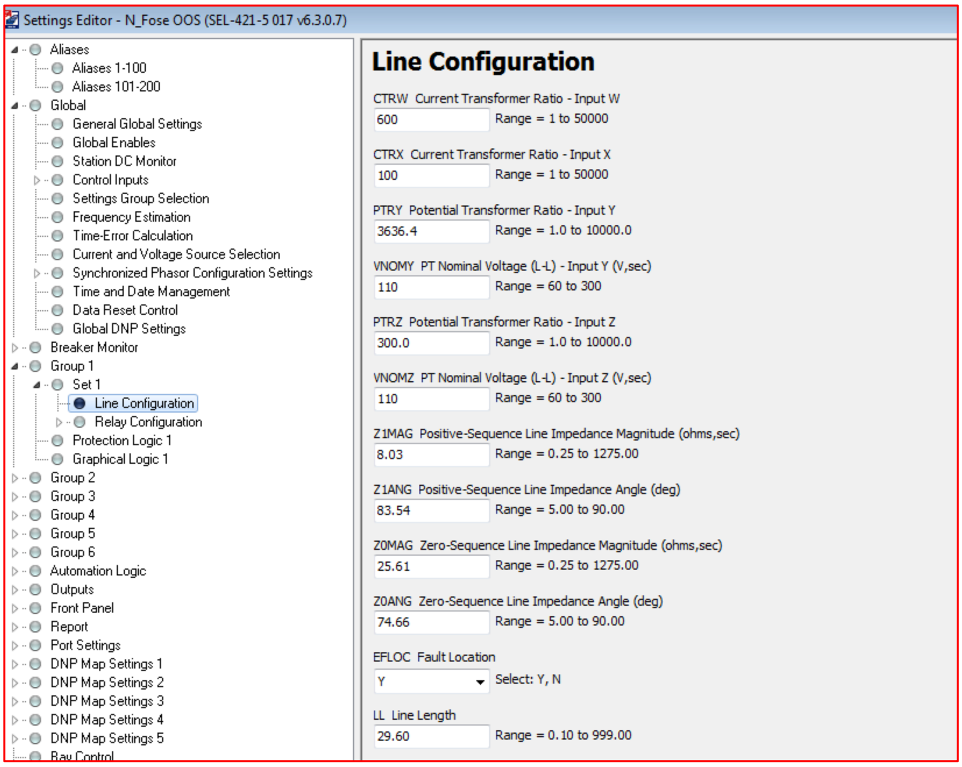

Figure 7.16: Line configuration settings as configured in SEL-421 relay.

Protection philosophy calls for out-of-step protection tripping to be made available from the relay, this is achieved by enabling mho distance characteristics for zone 1 and zone 2 and there by activating out-of-step enable to yes (Y) as shown in Figure 7.17 below.

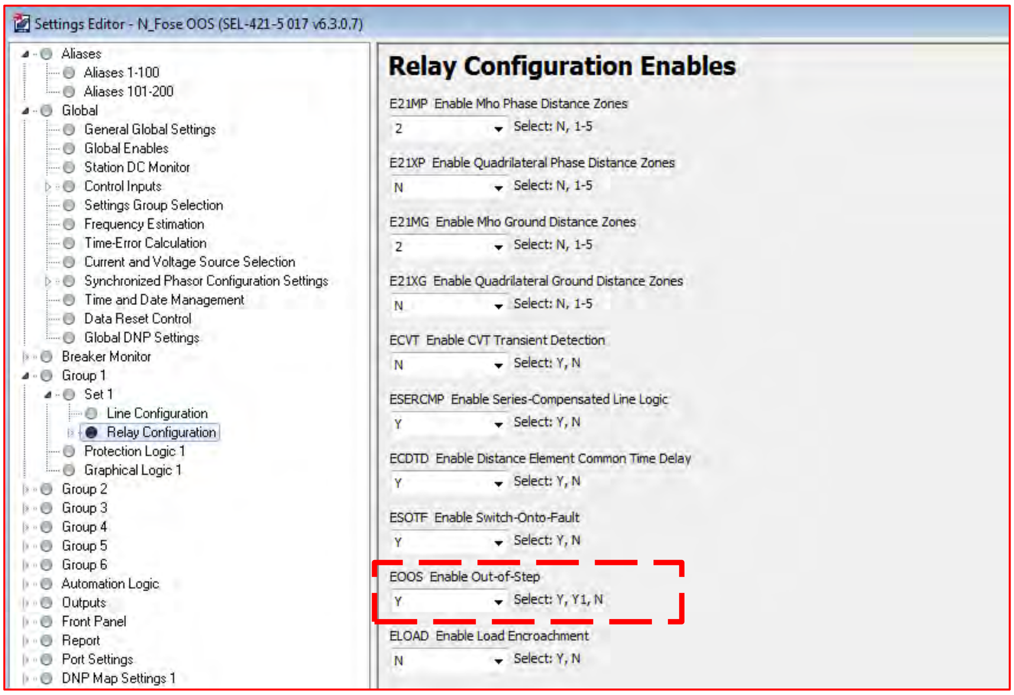

Figure 7.17: SEL-421 relay configuration settings.

Mho distance element reach is set to be 80%of the line for zone 1 and 120% of the line for zone 2.

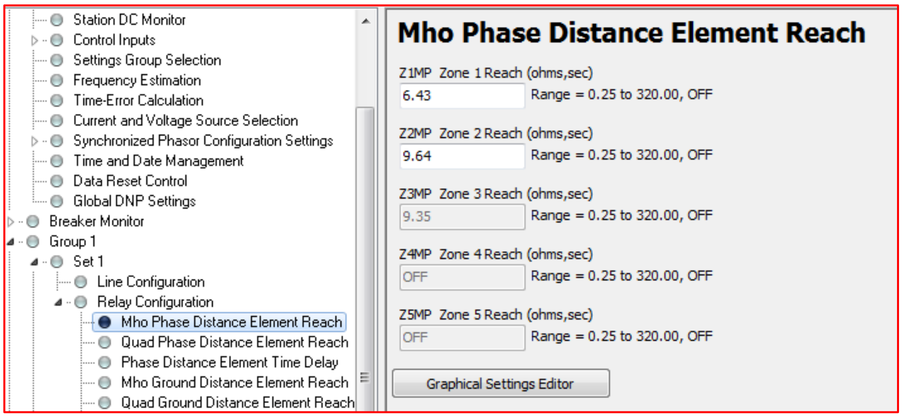

Figure 7.18: Distance mho element reach settings.

Out-of-step blocking (OSB) for zone 1 and zone 2 faults need to be defined to avoid the protection device from tripping on OOS for faults on the line downstream. It is also important to note that out-of-step tripping is set to operate when the power swing leaves the second outer blinder hence the setting “O” is selected. Blinder settings are configured according to settings calculated in chapter 4 for this device shown in Figure 7.19 on the next page.

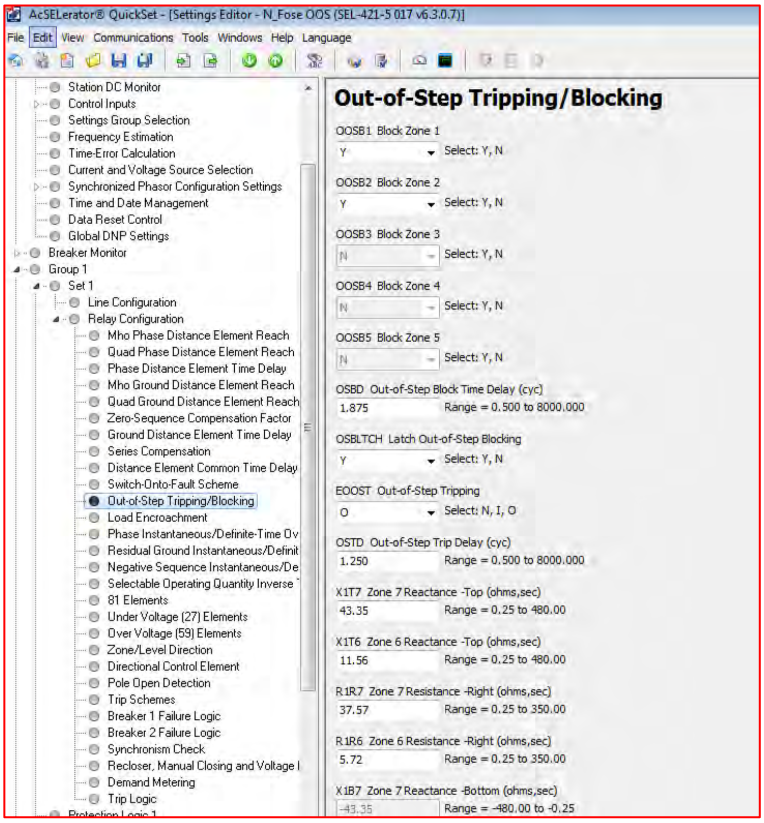

Figure 7.19: SEL-421 OOS tripping and blocking settings.

For local OOS tripping, the relay is configured to include OST and OSB relay word bits for tripping output on the existing distance trip logic to monitor the out-of-step tripping signal (Figure 7.20). A control output for notification of the out-of-step tripping condition is set on OUT105 (Figure 7.21).

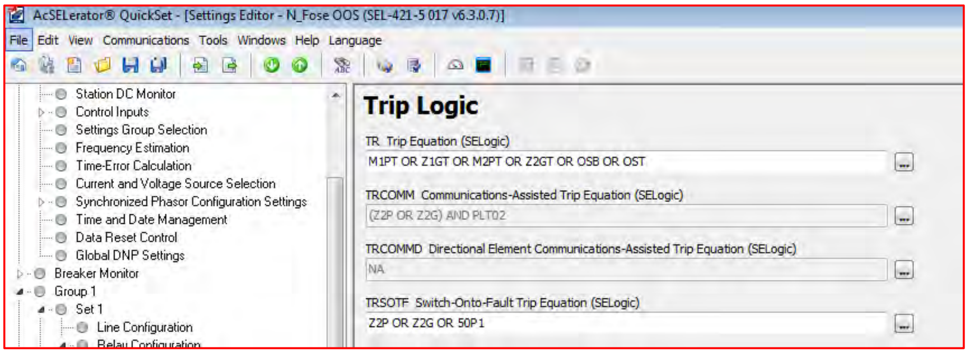

Figure 7.20: SELogic trip equation for the SEL-421 relay.

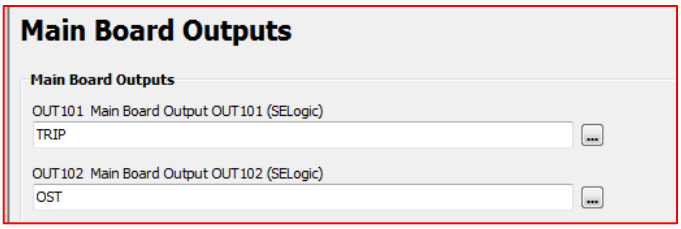

Figure 7.21: Trip output settings for out-of-step tripping.

7.3.4 Analysis of the results from dynamic state simulation

Unlike DIgSILENT PowerFactory®, the load contingency or RMS/EMT events on RSCAD is implemented by incepting a fault on the system or opening of the breaker related to the generator on runtime module while the system is running. Case studies for monitoring zone 1 and zone 2 faults have been executed for which the relay is expected to issue power swing blocking when the fault is in these areas and trip on OOS for the generator protection when the fault is at the closest bus to the Palmiet_Gen1 synchronous machine.

The TLINE CALCULATION BLOCK line length calculation options (pp var)% and (100 - pp var)% are specifically provided to allow a pair of series lines to have their individual lengths adjusted together by a single pre-processor slider, while keeping their combined series lengths at 100% of the true value (as defined in their *.tlb files). This method is highly beneficial when doing fault investigations with the real-time simulator, where faults are routinely applied at varied places along a fixed-length transmission line for comparative study as shown in Figure 7.22 (Rigby, 2012).

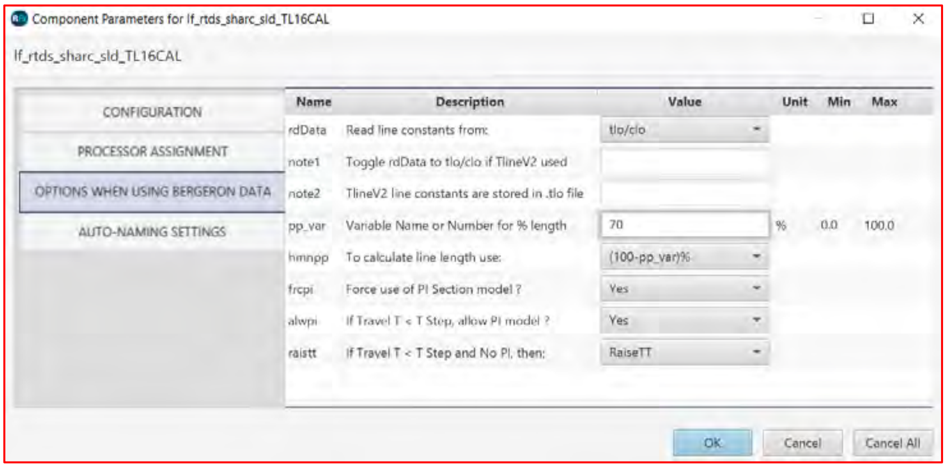

Figure 7.22: Fault location example calculation for 30% of line length in zone 1.

7.3.4.1 Case study 1- Zone 1 bolted fault

The developed out-of-step protection scheme need to tested stability against stable power swing scenarios which in this case can be produced by injecting a zone1 line-ground fault (C-G). For generator protection to be stable only zone 1 trip should occur in the relay and PSB as it will be clearing fault on the downstream of Palmiet_Pinotage 400kV line and not on the generator OOS protection zone. The physical positioning of the fault on RSCAD is not paramount as the fault location is defined exclusively on the T-Line calculation block of the relative transmission line. Figure 7.23 provides a diagrammatically expression of the OOS protection zone to be able to distinguish when the fault is in zone or out of zone.

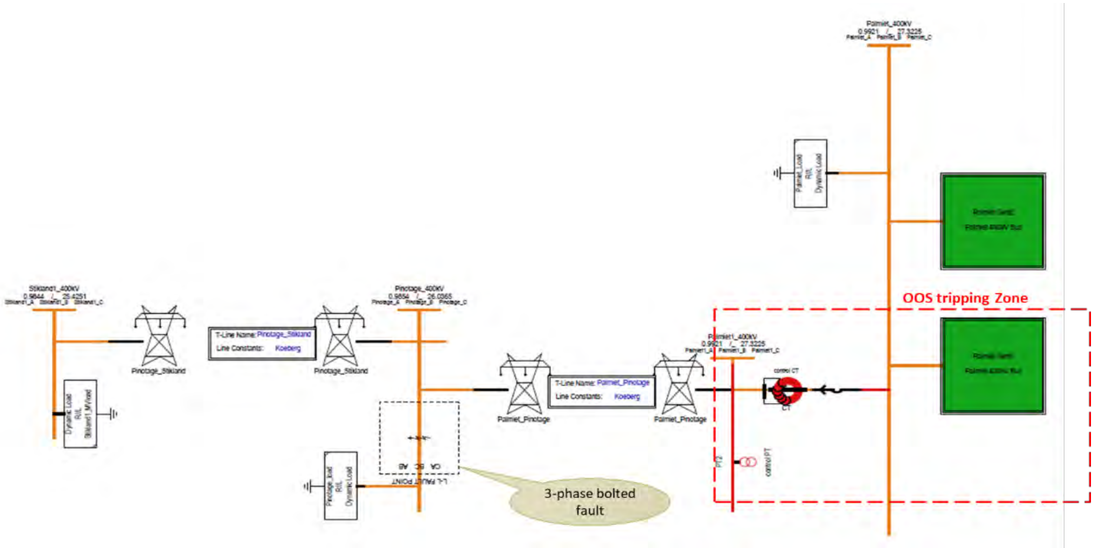

Figure 7.23: Area 3 network system depicting OOS tripping zone for case studies.

In Figure 7.24 the RMS values of current and voltage signals seen by the relay when the zone 1 fault disturbance are shown. The SEL-hardwire trip does not assert as the relay is till starting to see the zone 1 trip with the circuit breaker still closed at the fault inception.

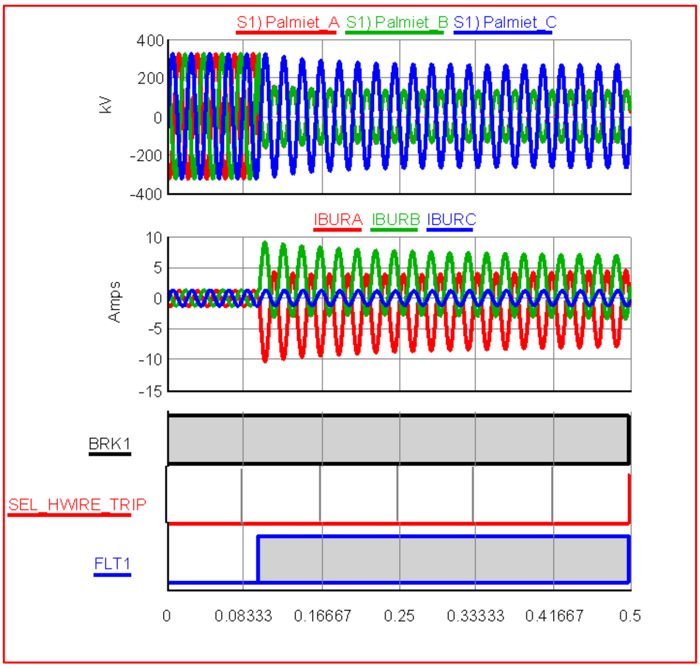

Figure 7.24: Zone 1 3-phase stater plot diagrams on RSCAD-FX.

As the fault is incepted in the system the power supply from Palmiet generating units start to fluctuate in a stable state manor not necessarily getting out of slip as the load in Palmiet_Pinotage 400KV declines. The speed output of Palmiet_Gen1 also decreases as the machine deaccelerates so is the rotor angle. The resultant plots on RunTime simulation platform are shown in the following Figures:

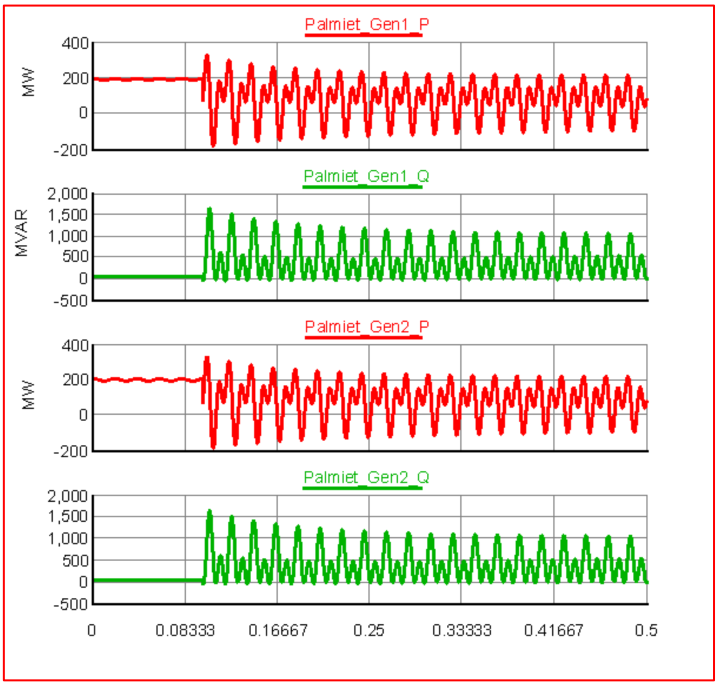

Figure 7.25: Palmiet generating units capacity during fault starter.

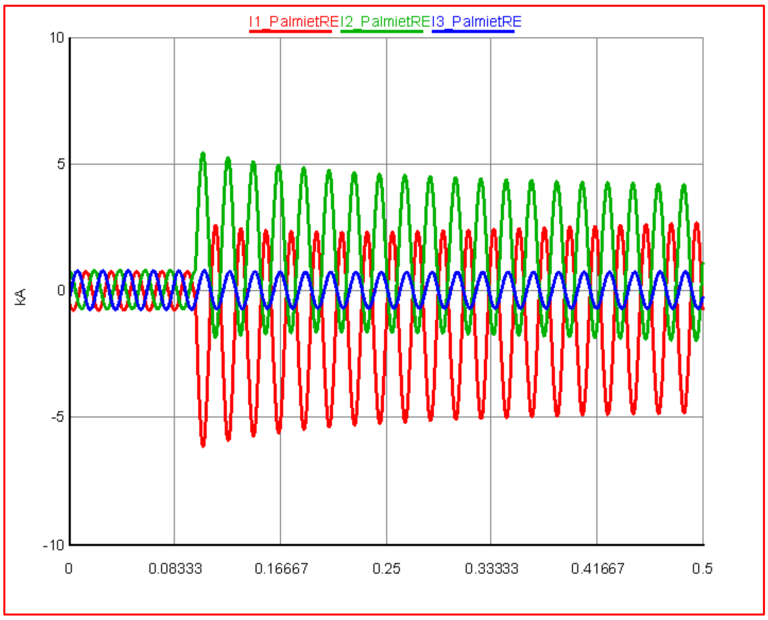

Figure 7.26: Currents seen by the transmission line at fault inception.

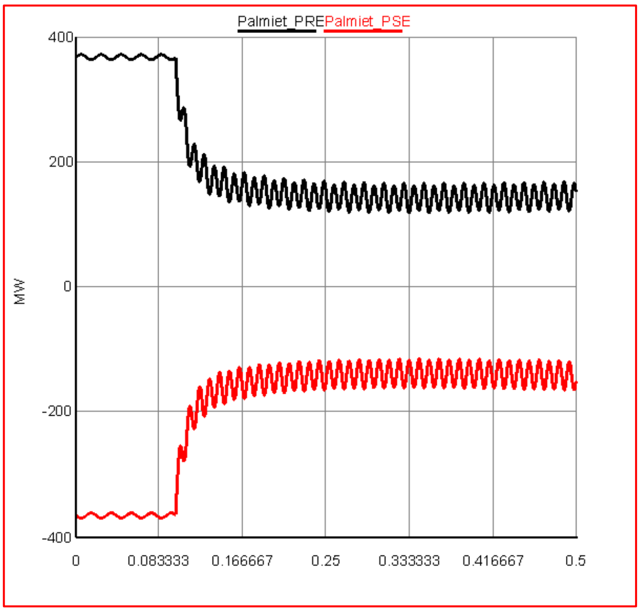

Figure 7.27: Transmission line load at fault inception.

When the zone 1 fault clears (which happens rapidly) the circuit breaker opens and the system the relevant system quantities decline approaching zero magnitudes as shown in the Figures to follow:

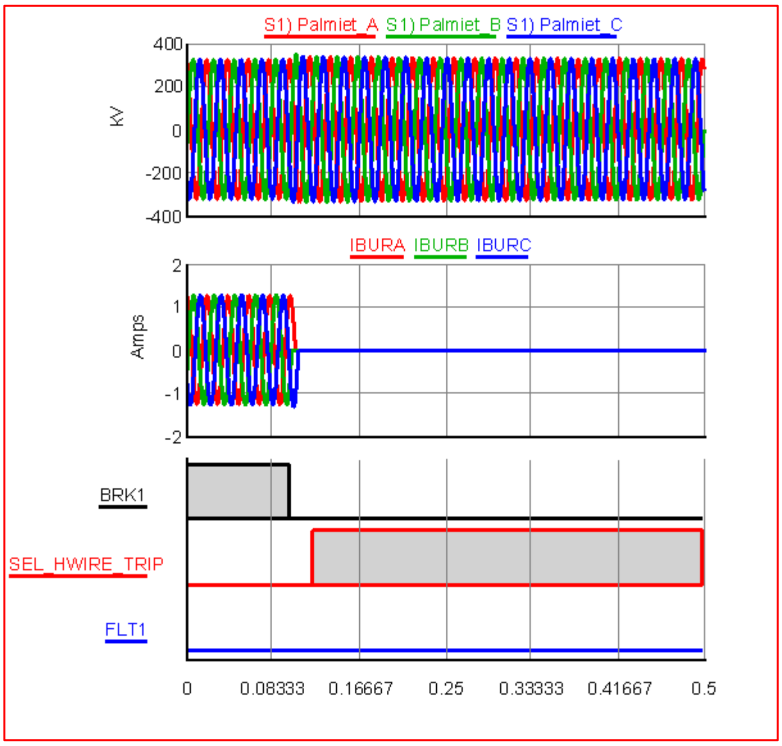

Figure 7.28: RMS meter readings and SEL-hardwire asserted.

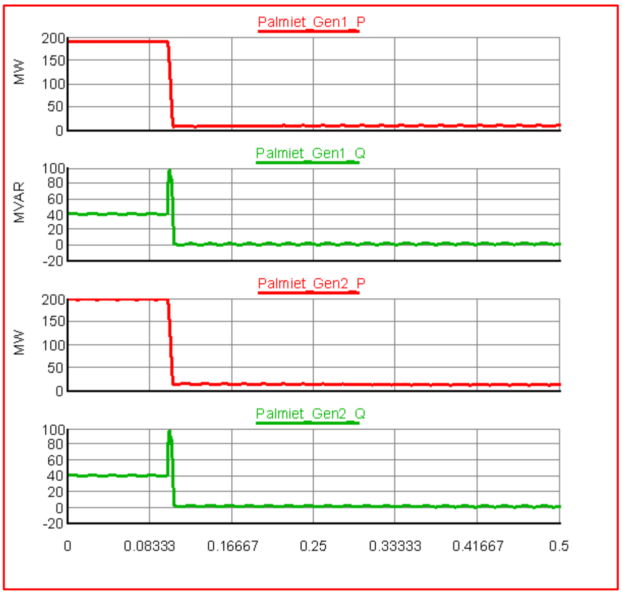

Figure 7.29: Palmiet Generating capacity declining to zero.

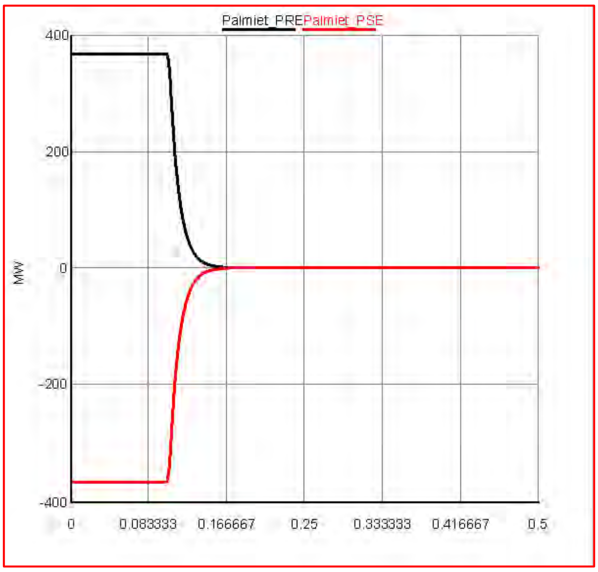

Figure 7.30: Palmiet transmission Load reduced to zero.

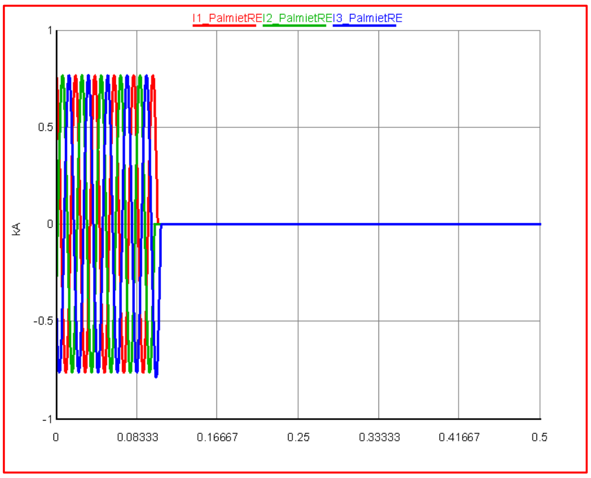

Figure 7.31: Transmission line current readings.

During this event the relay is set to be able to distinguish between stable power swing of zone 1 and zone 2 faults, as a result the rotor machine speed of Pamiet_Gen1 decreases so as the rotor angle. In this case besides Zone 1 trip target the protection relay also asserts OSB alarm as seen in the following Figures:

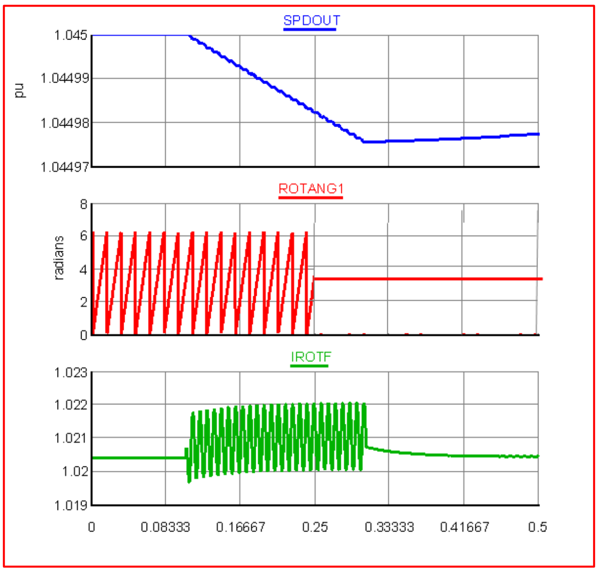

Figure 7.32: Rotor machine control variables during zone 1 fault.

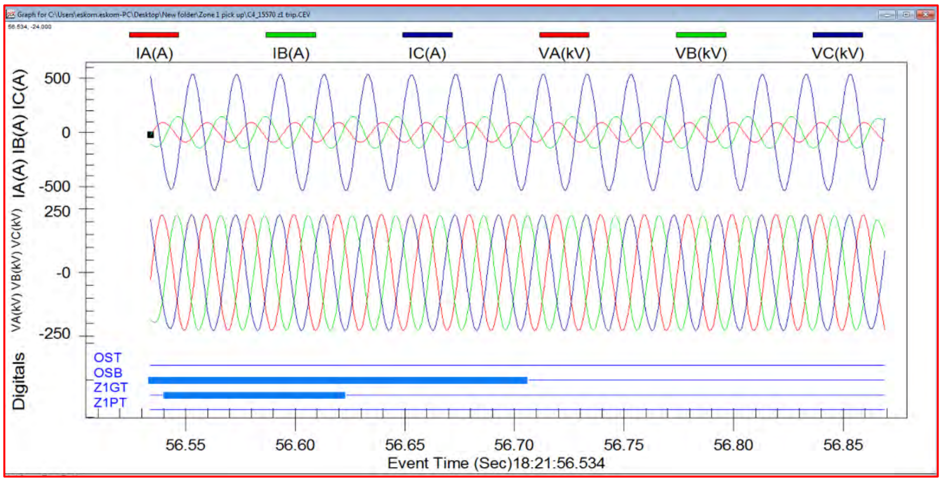

Figure 7.33: Relay Disturbance record as viewed from ACSELarator analytical assistant software.

7.3.4.2 Case study 2- Zone 2 bolted fault

When another zone 2 line-line fault (B-C) is injected in RSCAD-FX run time, at point of inception the system quantities are the same as that of Zone 1 stater fault as the faults are seen in the same direction by the protection although it is now further downstream in the line. What is further exclusive about this nature of fault is the time it takes the relay to clear such a fault will be now longer than the fault in zone 1. However, the synchronous machines still observe this disruption as a stable power swing, hence again the OSB alarm to block out-of-step tripping will again assert with zone 2 trip in the SEL-421 relay. Resultant graph plots on runtime interface as the zone 2 fault clears are shown in the following Figures:

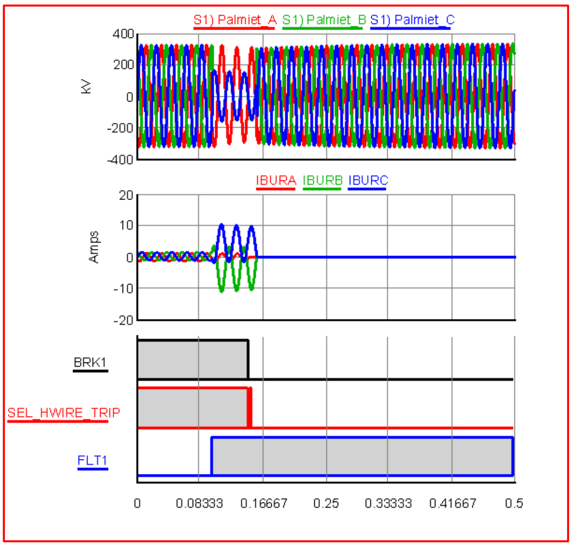

Figure 7.34: Analogue signal during Zone 2 fault disturbance.

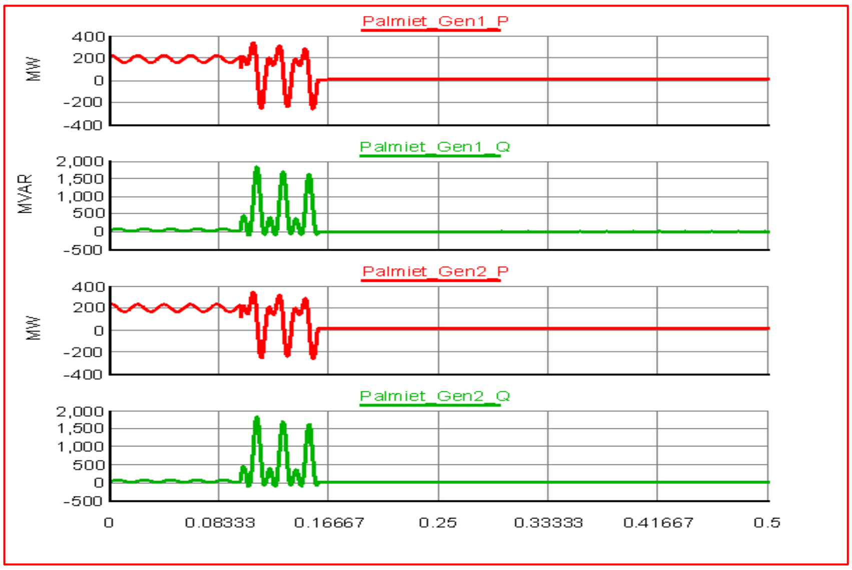

Figure 7.35: Palmiet synchronous machine generating capacity in zone 2 fault.

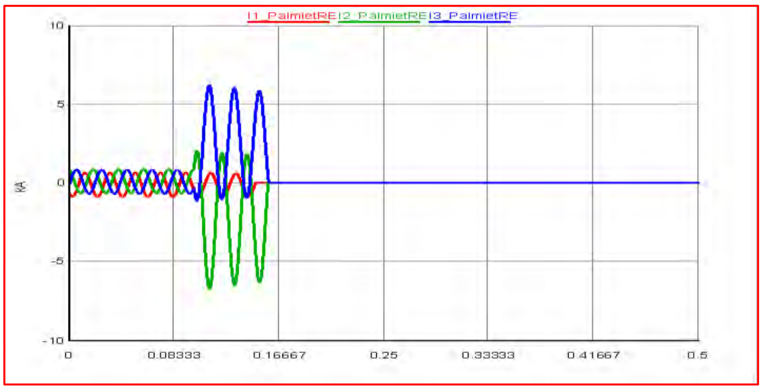

Figure 7.36: Palmiet_Pinotage transmission line current reading.

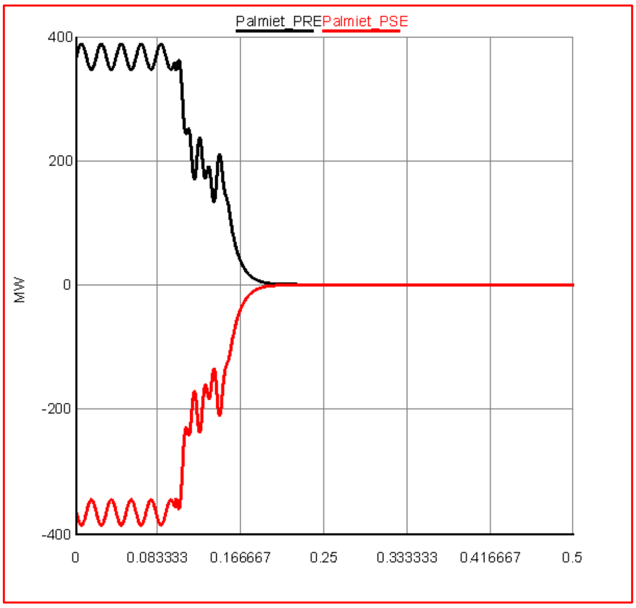

Figure 7.37: Transmission line loading.

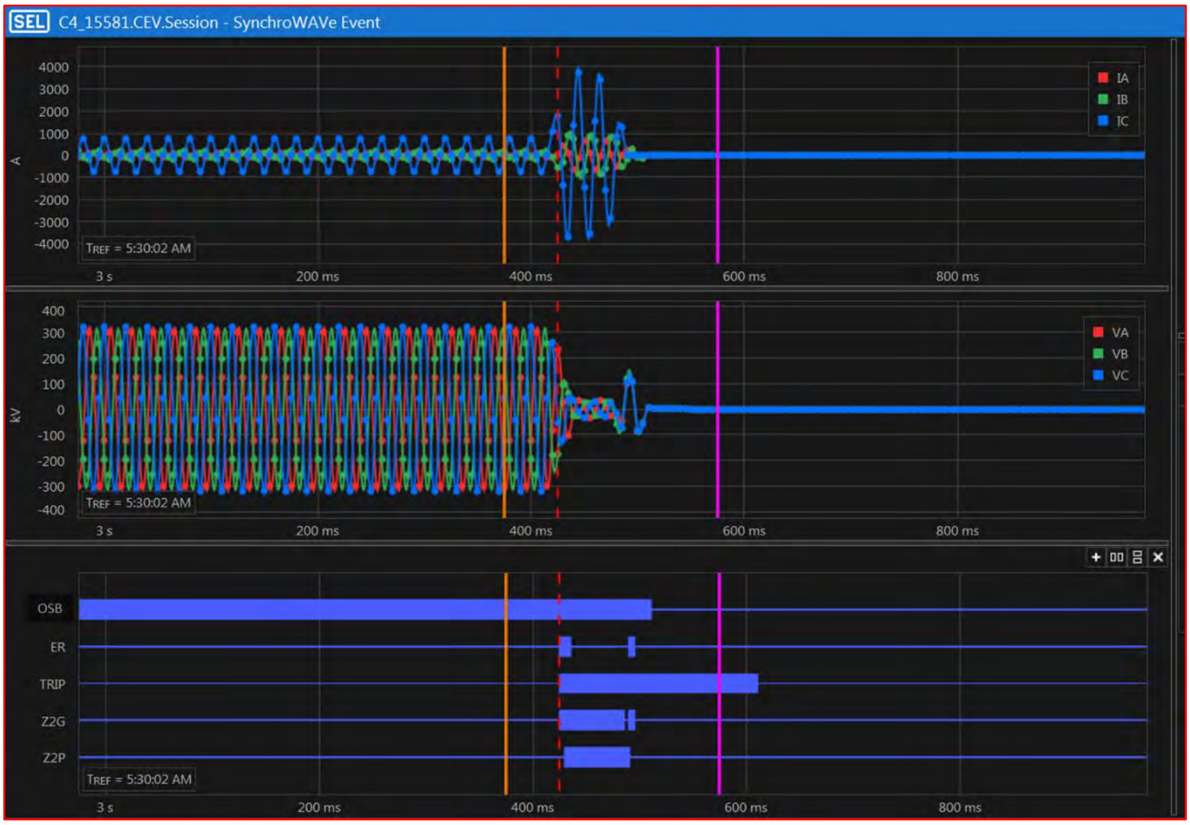

Figure 7.38:Relay Disturbance record as viewed from SEL Synchrowave Event software.

The relay remains stable and block power swing seen by the system during zone 1 and zone 2 disturbances. Now a case of pole slipping needs to be simulated to see the protection relay response in hardware-in-the-loop testing environment. The next case study looks at this kind of scenario.

7.3.4.3 Case study 3- Busbar fault

Simulating a short-circuit event on the Palmiet_400kV bus will be sufficient for pole slipping operation of Palmiet generating units as this was evident in DigSilent chapter. When the bus experiences a fault, the synchronous machines will experience power transfer capability limit, thus the electrical torque produced by the rotor will divert to mechanical torque. As soon as this situation occur the machines rotor speed accelerate rapidly which in turn causes the rotor angle to lose stability. When the rotor angle is gradually increased, the synchronous machine is bound to lose synchronism with the rest of the system, therefore an out-of-step trip will be triggered in the SEL-421 relay.

For this particular case study, a 3-phase to ground fault is injected in the OOS tripping zone at the back of SEL-421 relay such that the protection won't think it's the distance fault but rather a pole slipping occurrence and provide back-up tripping to the generator. It is important to note even though the device is solely used for simulation it is still intended for providing back-up OOS to the Palmiet generating units. The Figures to follow show graph plots resulting in runtime during this fault execution and further a resultant disturbance record from the relay is also provided in Figure 7.43 :

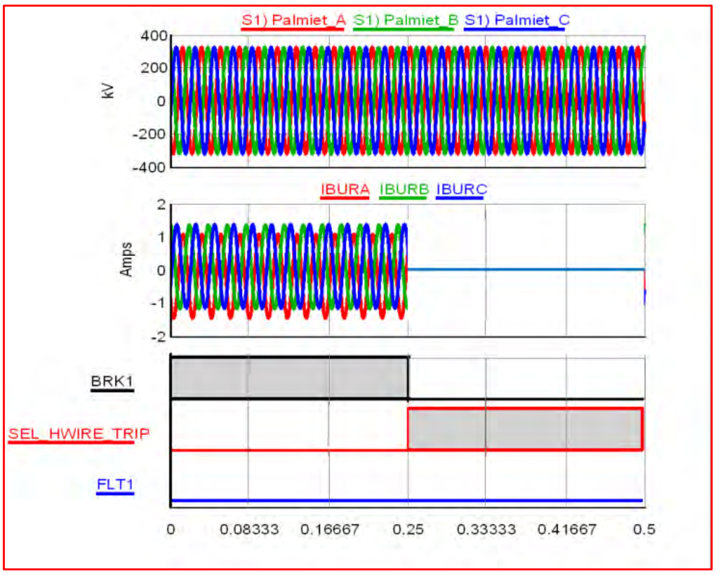

Figure 7.39: Analogue signals seen by the relay during fault on the bus.

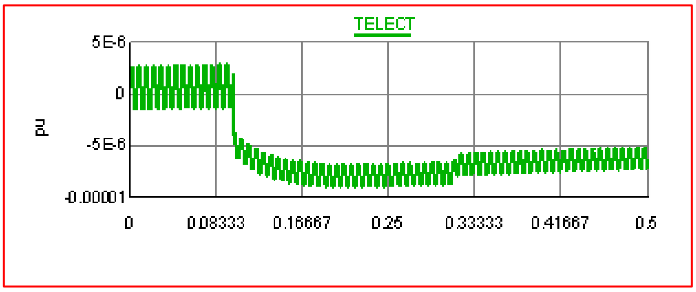

Figure 7.40: Palmiet_Gen1 electrical torque during bus fault.

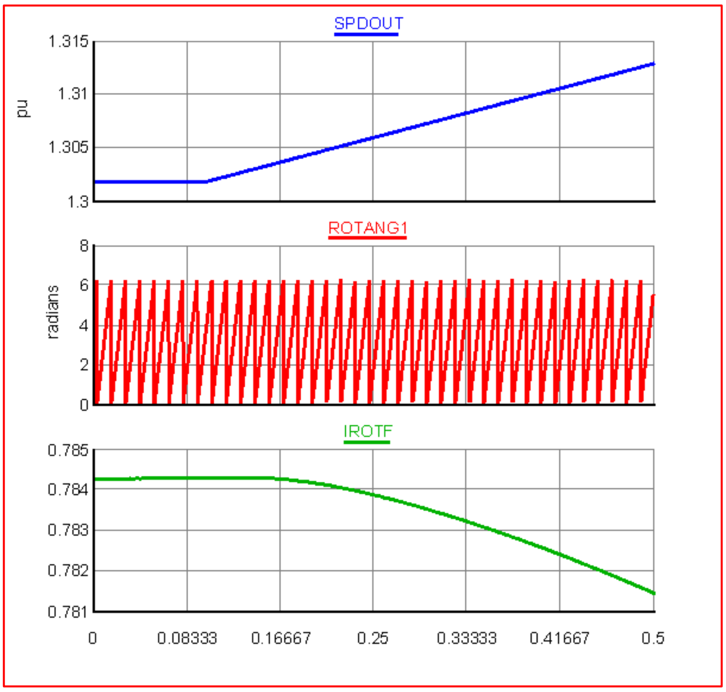

Figure 7.41: Rotor control variables during this disturbance.

In the above Figure, as speed of the rotor increases the current in the rotor (IROTF) declines as the machine is now converting electrical power to mechanical power due to limited power transfer at the fault location frequently referred to as zero-voltage crossing point.

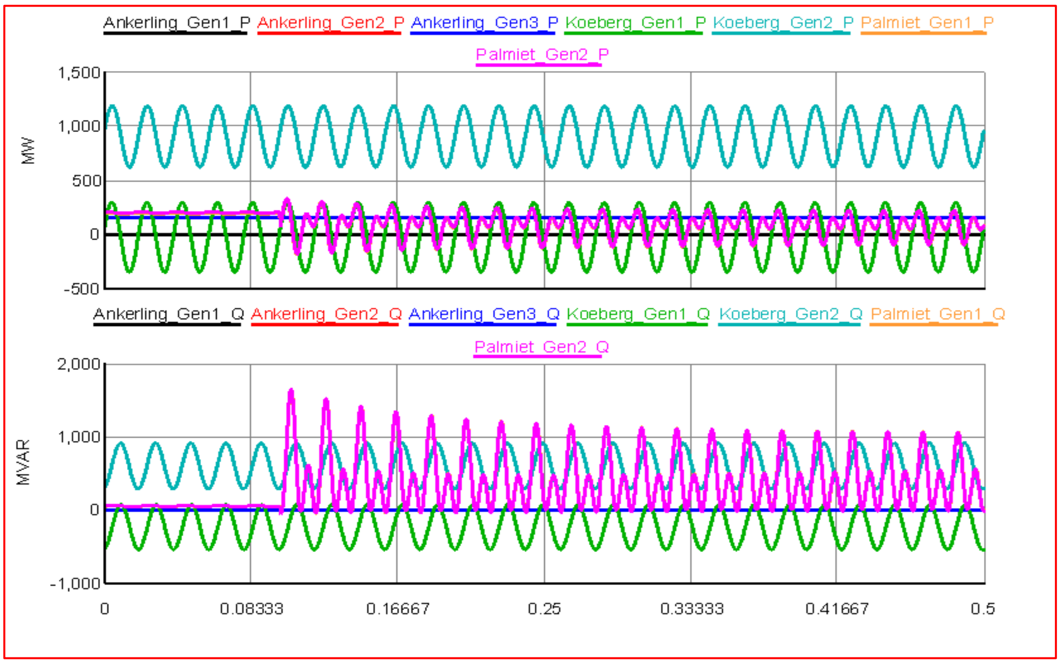

Figure 7.42: System power transfer capabilities with Palmiet generating units losing synchronism with the rest of the system.

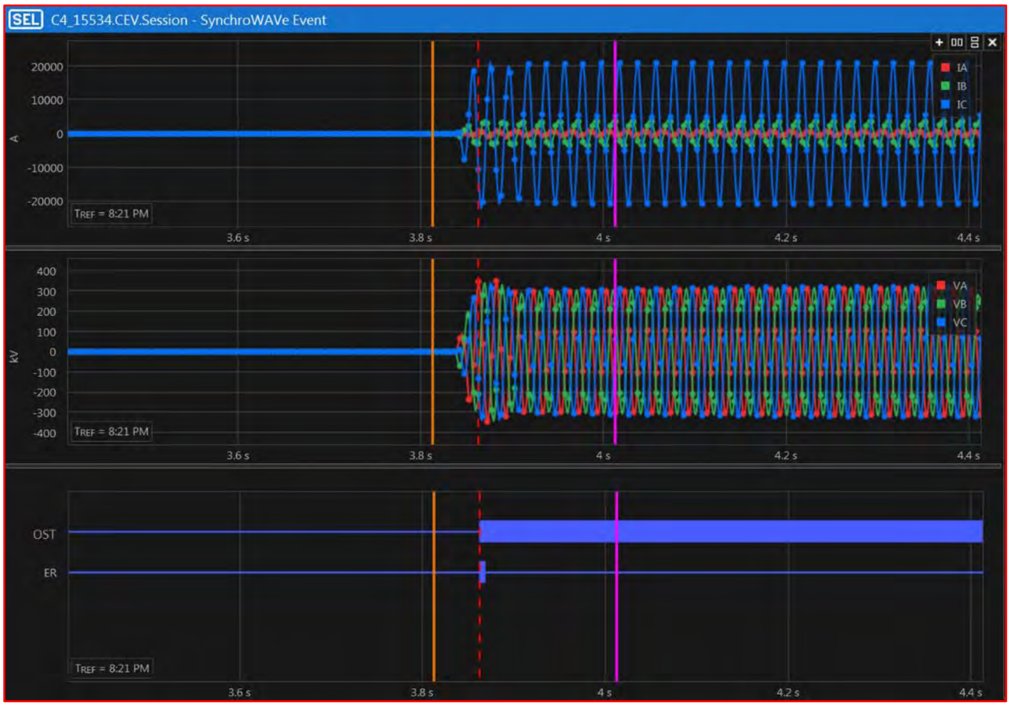

Figure 7.43: SEL-421 disturbance record with OST triggered as seen from SEL Synchrowave Event software.

7.4 Discussion of results

This section provides a summary of fault event results which were obtained during the real-time simulation in RTDS platform. Table 7. Below provides tabulated fault event list.

Table 7.1: Summary of fault events

Fault location	Fault type	Relay operation	Fault duration	Relay Targets
Zone 1	Blue-Ground	80ms	500ms	Z1GT, OSB
Zone 2	White-Ground	400ms	1.5s	Z2G,Z2P,OSB
Palmiet_Bus	3-phase	25ms	417ms	OST

The above table proves the reliability of the scheme employed in the test system as it is discreet in distinguishing the type of fault and fault location and operate accordingly. The physical device produced event reports containing monitored currents, voltages, and operated and non-operated binary signals to provide thorough event analysis.

The results cannot be claimed to universally be the case for all the other generators in the system as the test was concentrated locally only on Area 3, of which all results are relay specific and system quantity dependent for instance protection for Koeberg generators might require different settings configuration for the same scheme. Hence it is crucial to perform system studies before partaking on any protection design.

7.5 CONCLUSION

A hardware-in-the-loop test bench was implemented for the test system in this chapter using a SEL-421 protection physical relay in the loop. The design of the adaptive scheme was presented and tested through hard wire protection protocols. When a fault downstream the transmission line was injected, the relay remain stable for out-of-step tripping as this would be blocked by the configured OSB settings to accommodate impedance protection of the designated line. However, when the disturbance was injected to the bus closer to the running Palmiet generating unit, a rotor angle stability issue arises then the designed protection philosophy called for out-of-step tripping in such scenario.

The chapter also presented the differences between non-real time and real time simulation with real time simulation being the obvious choice amongst most protection design engineers as this type of simulation allows analysis of power system quantities and disturbances in real time stamp. Furthermore, the main function of real-time simulator is to connect with and afterwards test the ever-sophisticated machinery utilized to safeguard and manage contemporary power systems.

This means that the created protection scheme is adaptable, even though it employs the standard method of protection, which consists of hard-wired binary outputs to the circuit breakers. In a real-world scenario, these cables would be significantly longer, raising the expense of labour and expensive copper. Furthermore, commissioning hard-wired binary outputs takes time.

The next chapter presents an innovative IEC-61850-90-5 communication standard for predictive maintaining stability system with perception to reduce or eliminate the hardwired outputs from the protection device, as the system analogues will be transmitted by virtual PMU to the relay for proper tripping decision.

8 CHAPTER EIGHT

IEC-61850-90-5 STANDARD IMPLEMENTATION FOR A PREDICTIVE DYNAMIC STABILITY SYSTEM IN HARDWARE-IN-THE-LOOP

8.1 INTRODUCTION

The introduction of IEC-61850-90-5 has gained enormous interest amongst protection engineers as it has made it possible to locally measure both magnitude and phase electrical quantities since it incorporates phasor measurement units (PMUs) that can be optimally placed in the power system. A more systematic and theoretical examination of the IEC TR 61850-90-5 standard have been studied in literature. Where they searched for a suitable indicator that would indicate the occurrence of a disruption with a slow onset of 5 s to 10 if an out-of-step condition emerges in a loop or a mesh network connecting two or major power systems. When an OOS is detected, the program can prevent the OST situation from occurring by separating the system at a specific point. An out-of-step state can be established, and the out-of-step can be avoided by eventually separating the system at a specific moment.

The current timing capabilities of the recently installed global positioning system (GPS) offer a realistic solution for accurately time stamping geographically dispersed data. This means that measurements made, or phasors computed using a time reference at one site are globally valid and can be utilized in local computation (resulting in globally valid results) or in conjunction with data gathered or computed at different locations.

Given the current state of computing and communication, as well as the distributed nature of the method, this model may now incorporate the system's dynamic behaviour. In this chapter a practical implementation of the standard is proposed making use of a virtually placed PMU in RSCAD-FX to create an out-of-step protection scheme in RTDS for hardware-in-the-loop testing.

The phasor measurement unit (PMU) is configured to transmit voltage and current signal angles to the SEL-421 protection device for it’s own local portion of the power system (Area 3). If the angles seen by PMU surpass a pre-defined value, the IED will decide that there’s an out-of-step-condition and thereby triggering the relevant circuit breaker. However, it is important to note that remote area monitoring, and testing is not possible for this study as the practical testing involves a lab scale test bench as wide area networking involves multiple stations to be tested that may be only possible practically in an industrial applications where remote sites are available for commissioning and testing.

8.2 TEST BENCH DEVELOPMENT FOR IMPLEMENTATION OF HARDWARE-IN-THE-LOOP TESTING

Some of the hardware requirements and the hardware-in-loop (HIL) test have previously been built in Chapter 7. Additionally, the chapter included configuration of the protection scheme settings, with relay word bits designed in accordance with the American National Standards Institute (ANSI). The protection technique discussed in Chapter 7's relay word bits was utilized to define hardwire connection of the relay for OOS protection scheme control.

In this chapter, the developed test bed is configured to integrate the PMU for system OOS tripping control. The analogue signals transmitted to the phasor measurement unit are measured at the Palmiet_400kV busbar. The signals are then transported through communication medium using ethernet switch and via GPS clock. The Giga-Transceiver Network (GTNET) Communication Card is installed on RTDS, allowing signal transmission and reception from the virtual device (PMU) specified in the testbed. The PMU also requires GTSNC card to operate which is connected to port 7 of the GTWIF card. In Figure 8.1 below, the developed test-bed configuration is displayed. The communication link between the agents is indicated by the blue arrows on the lines.

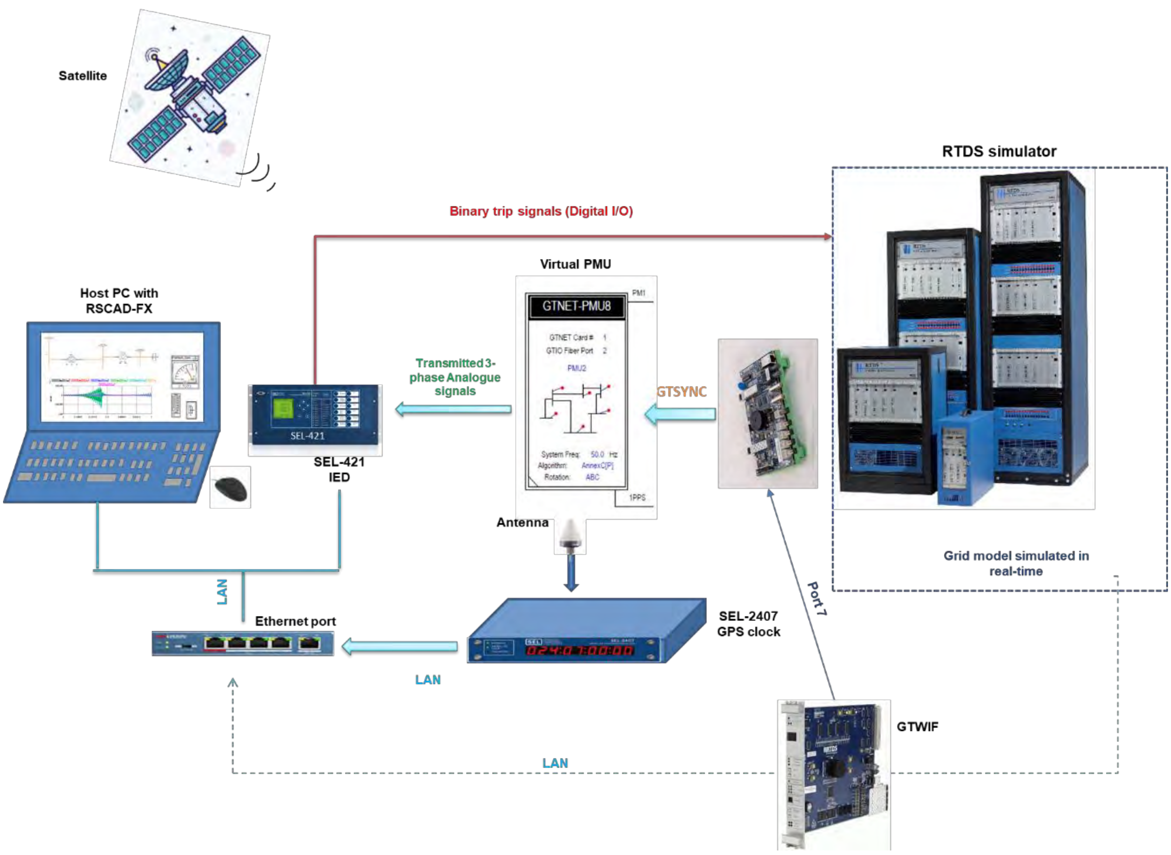

Figure 8.1: Hardware-in-the-loop test bench setup fully integrated with virtual PMU.

8.2.1 PMU configuration on RSCAD-FX simulation environment

When it comes to 3-phase sets of instantaneous voltage and current values, the phasor measurement (PMU) component is suited for delivering the symmetrical component information. One component contains eight PMUs that each function individually. The measurement loops supply the voltage, current, positive, negative, and zero phasor information (voltage and current). These plot signals come in magnitude and angle values as well as real and imaginary ones. Each PMU will deliver a total of 12 phasors, the measured frequency, and the rate of frequency change if all signals are chosen. However, to reduce backplane transfers and improve the simulation time-step, the frequency plot signal outputs will be disabled on RunTime since they are of less interest to the study as the system frequency is ran at constant value of 50Hz.

Each PMU is coupled to the voltage and current signals via six signal name inputs found in the component menus. This component supports two PMU algorithms; the option "pmutype" adjusts the algorithm from Annex C of the IEEE C37.118.1TM2011 standard to P or M class. The angle difference can be detected and monitored, with the output in degrees.

The usual processes taken by the PMU to process the input signals are shown in Figure 7.2. The component does not include the anti-aliasing LP filter, a GTNET card supplies the absolute time reference, and the simulation data is sampled at a pre-set sample rate. When the timestamp at the window's centre is used, the phasor estimate at its centre is unaffected by the real system frequency and does not need additional phase correction.

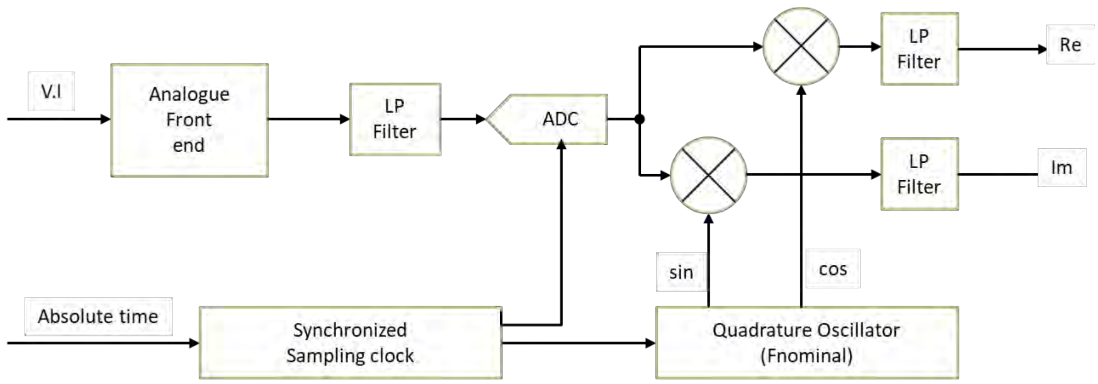

Figure 8.2: Model for PMU Phasor Signal Processing: Single Phase Section (RSCAD-FX CC-manual).

The snapshot of configuration of PMU in RSCAD-FX for acquiring stable communication and reliable operation is given in Figure 8.3 with the angle difference setting set to “0” which is the common offset applied to all PMU inputs generally. To delay voltage input signals by 1 timestamp against the current inputs, ADV setting needs to be yes. Monitored AC signal names are also provided in Figure 8.4.

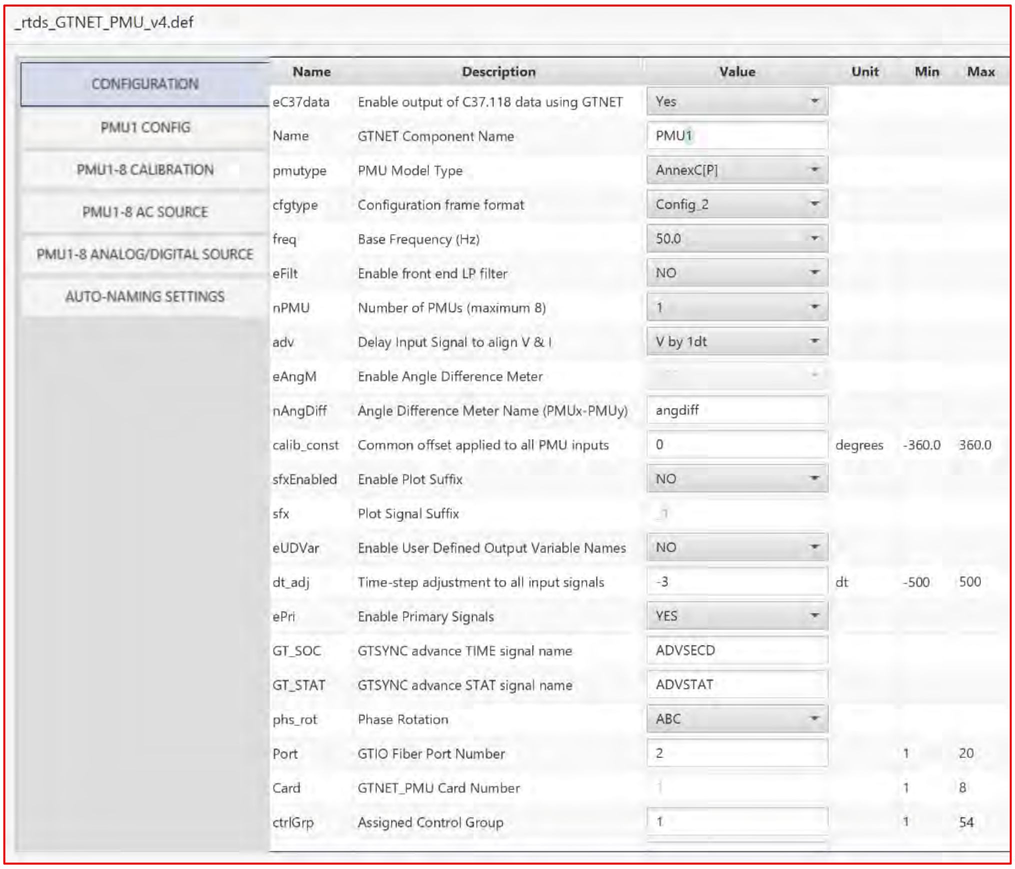

_rtds_GTNET_PMU_v4.def

CONFIGURATION | PMU1 CONFIG | PMU1-8 CALIBRATION | PMU1-8 AC SOURCE | PMU1-8 ANALOG/DIGITAL SOURCE | AUTO-NAMING SETTINGS

Name	Description	Value	Unit	Min	Max
eC37data	Enable output of C37.118 data using GTNET	Yes			
Name	GTNET Component Name	PMU1			
pmutype	PMU Model Type	AnnexC[P]			
cfgtype	Configuration frame format	Config 2			
freq	Base Frequency (Hz)	50.0			
eFilt	Enable front end LP filter	NO			
nPMU	Number of PMUs (maximum 8)	1			
adv	Delay Input Signal to align V & I	V by 1dt			
eAngM	Enable Angle Difference Meter				
nAngDiff	Angle Difference Meter Name (PMUx-PMUy)	angdiff			
calib_const	Common offset applied to all PMU inputs	0	degrees	-360.0	360.0
sfxEnabled	Enable Plot Suffix	NO			
sfx	Plot Signal Suffix	1			
eUDVar	Enable User Defined Output Variable Names	NO			
dt_adj	Time-step adjustment to all input signals	-3	dt	-500	500
ePri	Enable Primary Signals	YES			
GT_SOC	GTSYNC advance TIME signal name	ADVSECD			
GT_STAT	GTSYNC advance STAT signal name	ADVSTAT			
phs_rot	Phase Rotation	ABC			
Port	GTIO Fiber Port Number	2		1	20
Card	GTNET_PMU Card Number	1		1	8
ctrlGrp	Assigned Control Group	1		1	54

Figure 8.3: PMU configuration settings on RSCAD-FX interface.

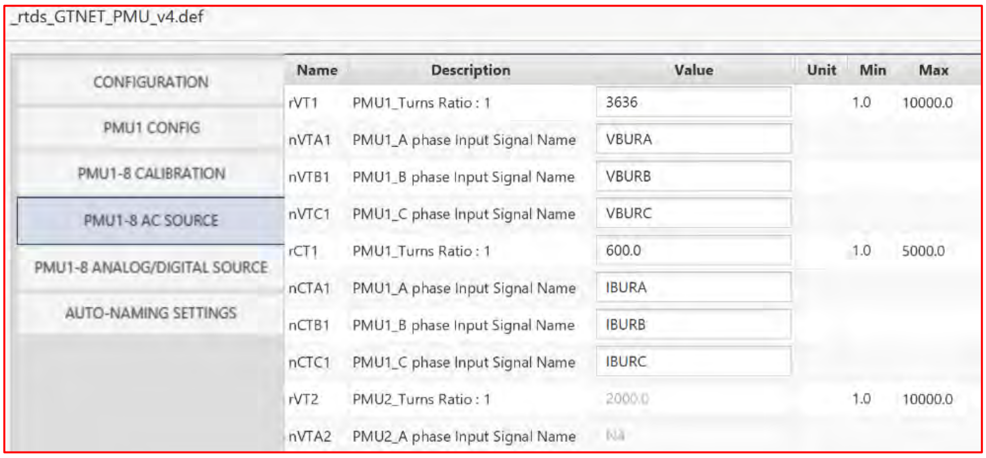

_rtds_GTNET_PMU_v4.def

CONFIGURATION | PMU1 CONFIG | PMU1-8 CALIBRATION | PMU1-8 AC SOURCE | PMU1-8 ANALOG/DIGITAL SOURCE | AUTO-NAMING SETTINGS

Name	Description	Value	Unit	Min	Max
rVT1	PMU1_Turns Ratio : 1	3636		1.0	10000.0
nVTA1	PMU1_A phase Input Signal Name	VBURA			
nVTB1	PMU1_B phase Input Signal Name	VBURB			
nVTC1	PMU1_C phase Input Signal Name	VBURC			
rCT1	PMU1_Turns Ratio : 1	600.0		1.0	5000.0
nCTA1	PMU1_A phase Input Signal Name	IBURA			
nCTB1	PMU1_B phase Input Signal Name	IBURB			
nCTC1	PMU1_C phase Input Signal Name	IBURC			
rVT2	PMU2_Turns Ratio : 1	2000.0		1.0	10000.0
nVTA2	PMU2_A phase Input Signal Name	NA			

Figure 8.4: AC signals of PMU as configured in RSCAD-FX.

The PMU used for the case study is the GNET-PMU8 which is already interface with the GNET card through RSCAD internal programming, the component can be found in RSCAD-FX library is designed to perform lab bench studies, otherwise for utility testing there is another one available i.e., PMU utility test that is interfaced with PMU wave control for industrial practicality.

8.2.2 PMU configuration on SEL-421 protection relay

For the case study the same line configuration settings parameters that were entered in chapter 7 are still valid and will be of aid even in this instance. However, the PMU communication protocol needs to be configured in the protection relay to achieve a stable gateway for transmitting the analogue signals seen by the PMU into the relay for it to subsequently make sound decision thereof.

First step is to enable phasor measurement unit element on the device's global enables settings as shown in Figure 8.5 below.

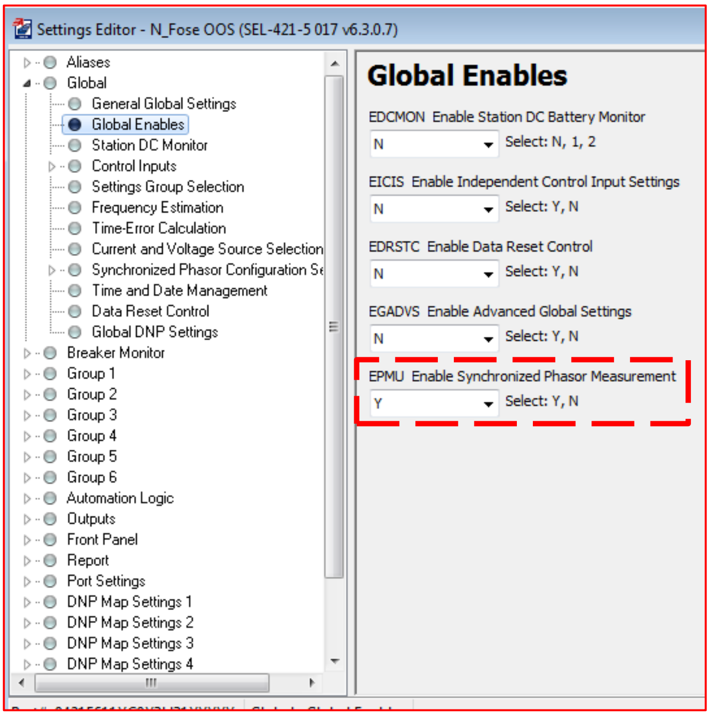

Figure 8.5: PMU setting selection on SEL-421 relay.

When the phasor measurement unit is enabled configuration settings linked to the device needs to be applied. Programme the IED such that it recognises PMU message format, this process is done under synchronised phasor configuration settings as shown in Figure 8.6 below. It is paramount to note that the C37.118 data enetered for GNET usage on RSCAD-FX PMU is configured as the same value even on the SEL-421 IED for correct synchronisation of the devices (MFRMT meesage format on the SEL-421).

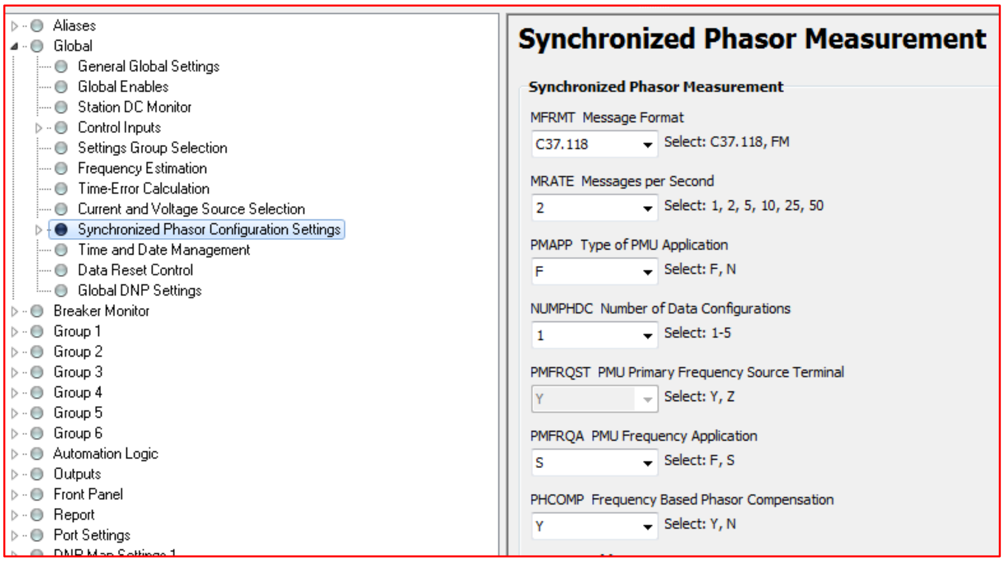

Figure 8.6: Synchronised phasor configuration on SEL AcSeLarator Quickset software.

Phasors included in the data transmission need to match the relay's CTR and PTR input contact windings for current and voltage signals with which for this specific relay input-W for currents is used and input-Y for voltage signals is used as illustrated in Figure 8.7.

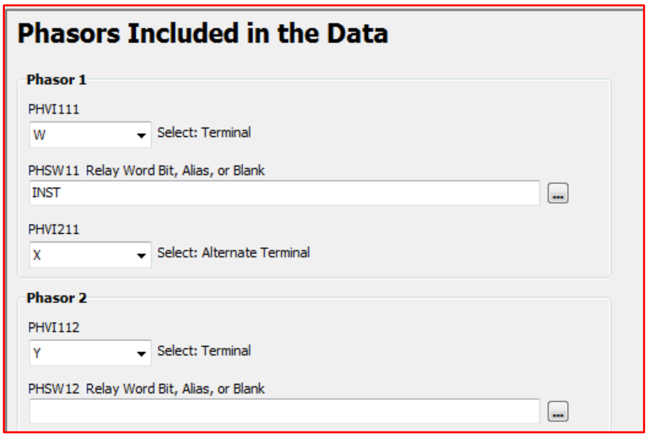

Figure 8.7: Input phasors data configuration.

For time synchronization to be successful, the time and date of the relay needs to correspond to the coordinated universal time UTC, such that the IRIG-B control bits definition will always be true.

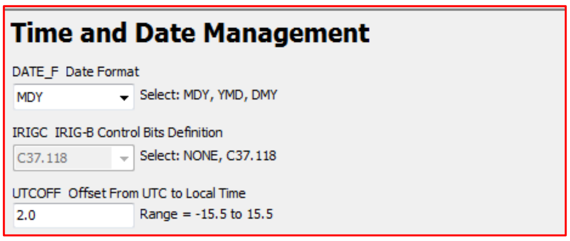

Figure 8.8: Time and date settings configuration in SEL-421.

To create the link with the PMU the SEL-421 IEDs, the device communication port must be properly configured as depicted in Figure 8.9. Phasor measurement communication settings are available under port 5 of the SEL relay communication ports. The IP address domain used to configure the contact port of the device must match the PMU client IP address domain. Once a communication link is successfully established, transmitting, and receiving signals can be achieved seamlessly.

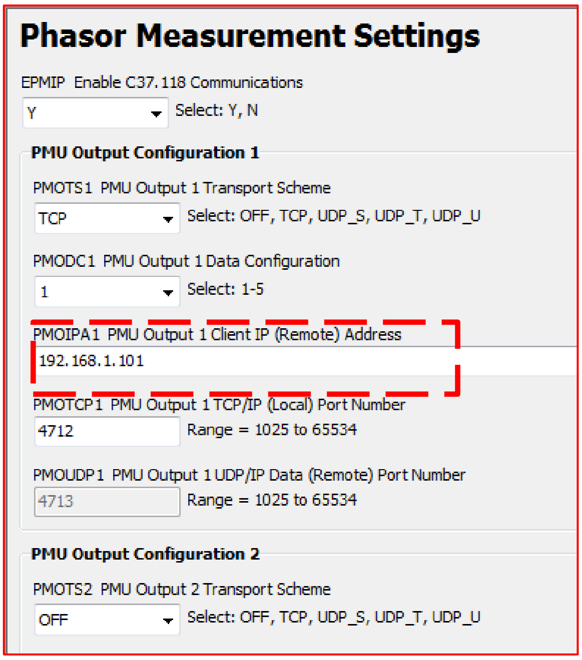

Figure 8.9: PMU communication settings in port 5 of the SEL-421 relay.

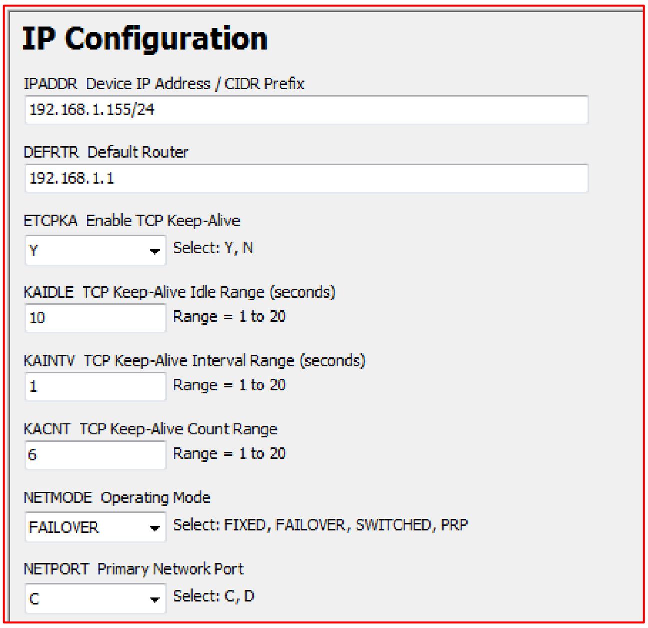

Figure 8.10: PMU IP configuration settings in AcSeLarator Quickset software.

When the settings are completed and sent to the physical device successfully. The metering values of the phasor measurement units can be viewed on the relay's human machine interface (HMI) provided that the HIL test is running on RSCAD-FX RunTime. Figure 8.11 below provides a screen capture of the test system metering values seen by the PMU in steady-state load flow.

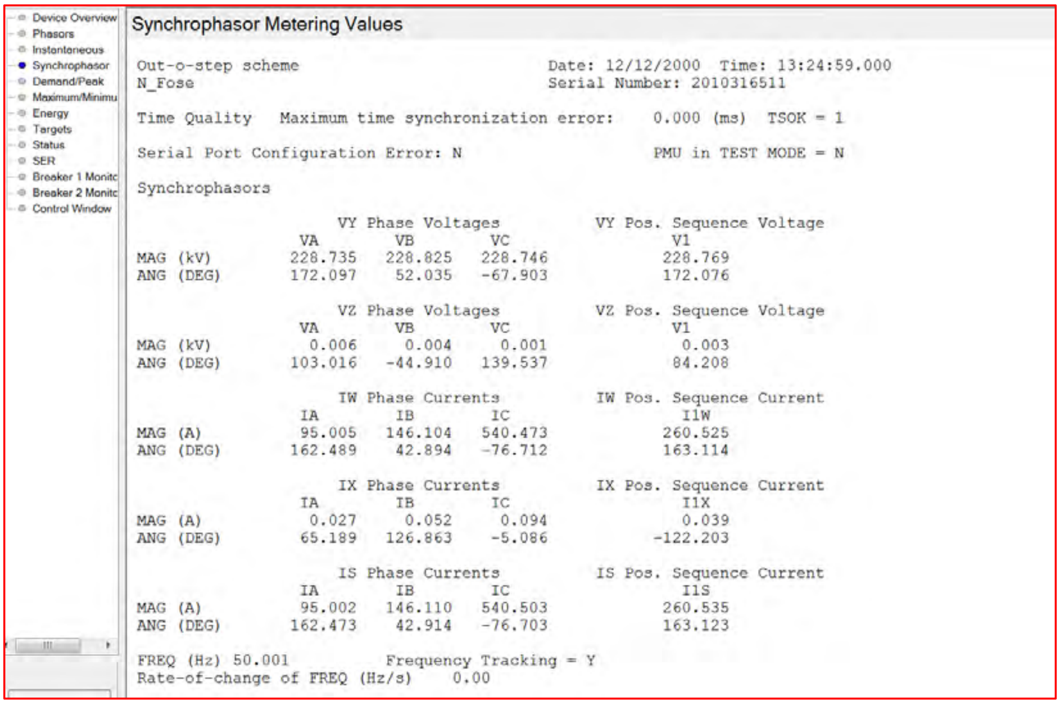

Figure 8.11:PMU metering values received by the relay.

On successful GPS time synchronization between the agents in the hardware-in-the-loop test bed the PMU status will be TSOK thereby locking IRIG on the relay front panel. This can also be viewed from the SEL-421 HMI device overview along with the phasors seen by the relay as depicted in Figure 8.12 and 8.13 respectively.

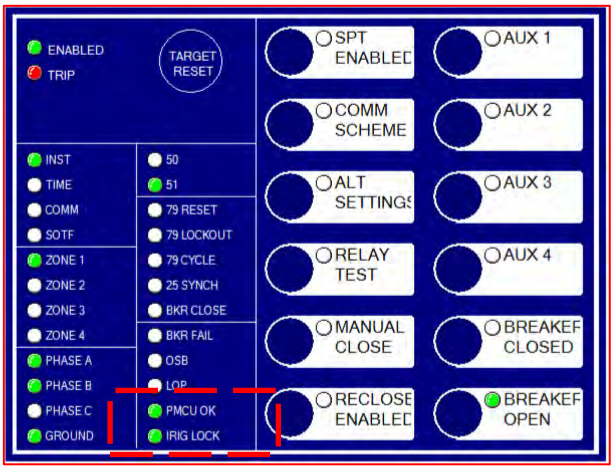

Figure 8.12: PMU status as viewed from SEL relay HMI.

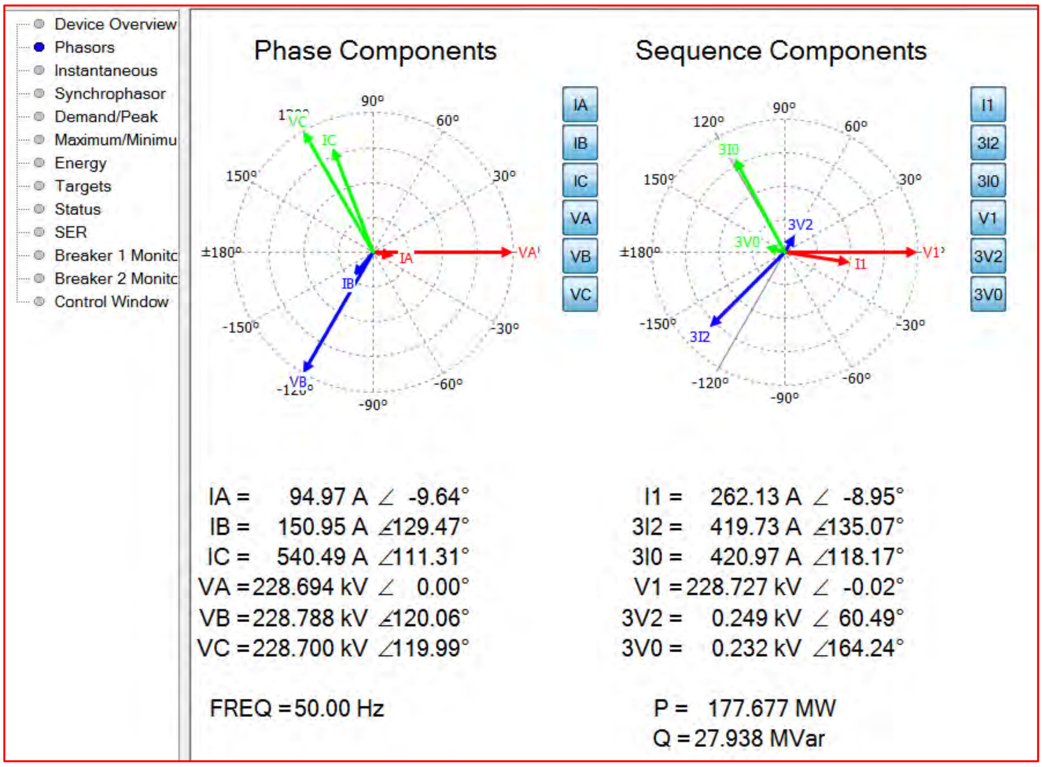

Figure 8.13: System under test electrical quantities as seen by the SEL-421 relay.

8.2.3 GOOSE message engineering configuration for SEL-421 IED

The relay word bits that were defined earlier chapter 4 for the SEL-421 relay tripping functionality on RTDS simulated network namely; Trip (for zone tripping), OSB (out-of-step blocking) and OST (out-of-step trip). Will now be defined by corresponding logical node PRO for GOOSE message to be successfully published via the Ethernet network. The available LN's corresponding to ANSI relay word bits in the device are listed in Table 8.1 below.

Table 8.1: List of relay word bit to logical device PRO for SEL-421

Relay word bit	Description	Logical Node	Status
TRIP	General trip (Z1&Z2)	TRIPPTRC1	Tr.general
OSB	Out-of-step block	OSB1RPSB2	Str.general
OST	Out-of-step trip	OSTRPSB1	Op.general

The logical device nodes described in the above table are utilised to configure data sets for GOOSE messaging in AcSELerator Architect software, the initial configured file in the software is the substation configuration language (SCL) it hosts the CID file and all the information relevant to the substation. The key parts of the configuration tool for AcSELerator Architect are shown in Figure 8.14 below with IP address of the IED specified in order to acquire communication when the configured IED description (CID) needs to be sent to the physical relay. CID file is responsible for publishing data sets from relay to hardware-in-the-loop test bench via the Ethernet to issue trip to the relevant circuit breaker in real-time simulation.

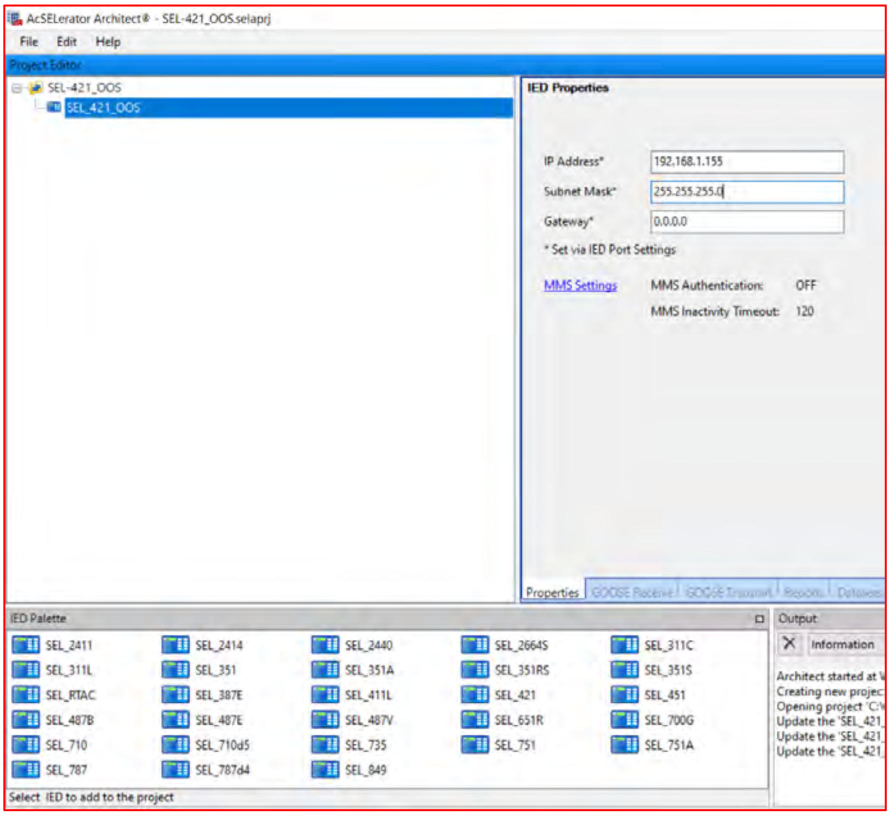

Figure 8.14: IEC 61850 configuration tool for SCL files.

As shown in the preceding Figure 8.14, the project editor, IED palette, and IED configurations tab are the main sections of the configuration tool. The IED Palette is a list of all IEC 61850 compliant SEL relays. A device is selected from the IED palette to start a new project and dragged into the editor of the project. The IED configuration window will appear when a system has been successfully added to the project editor. The IED configuration windows include the IED property, GOOSE receives configuration, and GOOSE transmits configuration, Reports and Dead configuration tabs.

New datasets for the SEL-421 are defined, under the Dataset configuration tab. There are 14 predefined datasets available that the user can choose from, however, for this application, the rest is deleted of the data sets are deleted to create room for the three logical devices assigned the names TRIP, GOOSE_OST and OSB_GOOSE. The names are chosen, such that they help the user to easily identify the GOOSE message from the list of many other data sets has been published. Subsequently to the datasets created, a functional constraint that incorporates the required logical nodes needs to be assigned to it, the data attributes of the protection needs to be published to the real-time-simulator as mentioned earlier. An example of the configured data for GOOSE_OST sets is shown in Figure 8.15. on the next page, the process is also the same for the other 2 data sets.

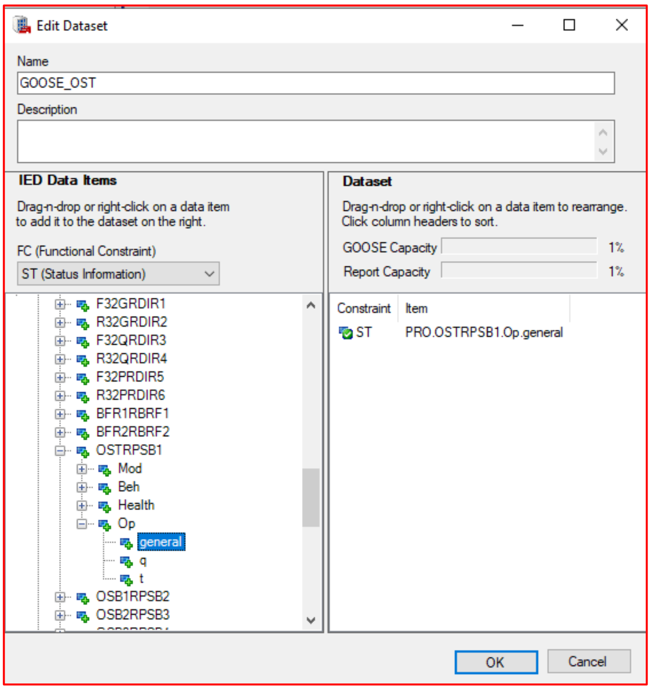

Figure 8.15: Configure data set for OOS tripping.

When data sets configuration is done the GOOSE transmission mapping is done with MAC address and complete names defined to be sent to the receiver agent as illustrated in Figure 8.16.

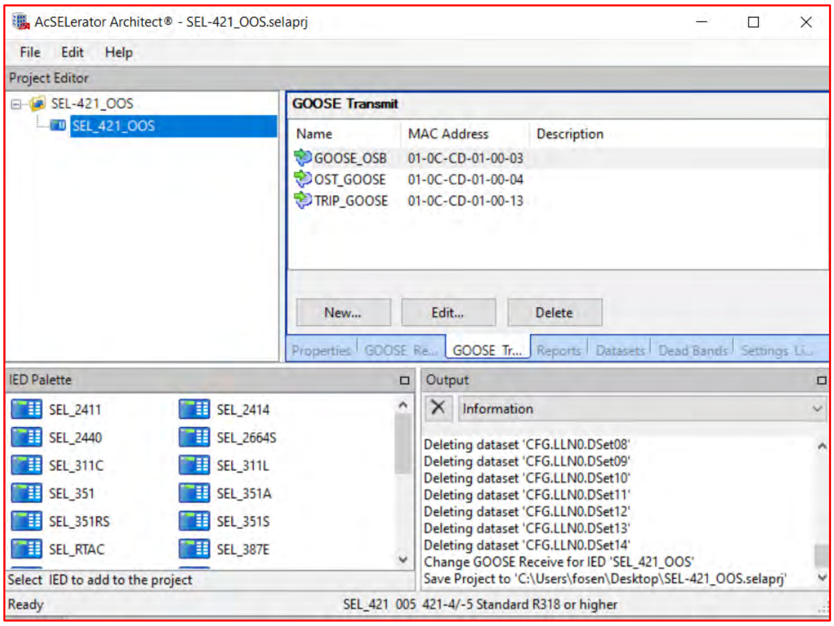

Figure 8.16: Finalization of the logical node's transport to sent to the IED as CID file.

The RTDS GTnet GSE card is set up for mapping the datasets to the virtual system circuit breakers in RTDS for trip commands when GOOSE is successfully configured for a protection relay. This is discussed in the next subsection.

8.2.4 RTDS GTnet GSE configuration for GOOSE message status event

This section breaks down the procedures involved in configuring GTnet for GOOSE message posting. But first, a description of the connection between the SEL-421 physical device and the GTnet component is given. The protection device is connected to the three-phase circuit breaker RTDS virtual simulation power system network. The internal IEDs of the GTnet, a virtual device in the RTDS simulation, are used to carry out its operations.

The GGIOs that make up the IEDs in the GTnet component. The purpose of a GTnet is to subscribe to GSSE/GOOSE messages generated by protection devices and utilize those messages to activate virtual system breakers for fault isolation at the busbar. The RTDS GSE component is then exported from the component library and included to the RTDS draft with which can be placed anywhere in the available space of the draft. A typical GTNET-GSE component can be seen in the following Figure 8.17 with the SCD file inputs required for GOOSE message configured in the template. The SCD file created during IED configuration is where these are imported from.

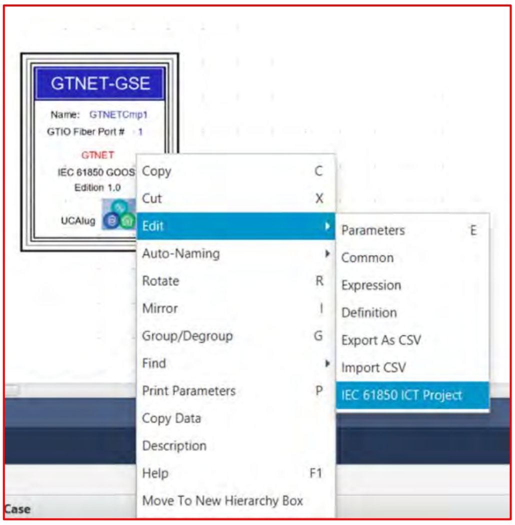

Figure 8.17: IEC 61850 GOOSE GSE card in RSCAD-FX.

The imported CID file can then be selected and edited as the external IED publisher in IEC 61850 ICT tool of RSCAD-FX as can be seen in Figure 8.18 below.

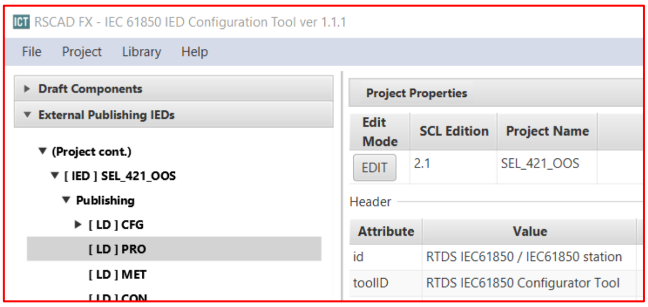

Figure 8.18: SEL-421 CID file as an external publishing IED in ICT tool.

In order for the circuit breakers to detect the command and respond appropriately when the status event is communicated by the GOOSE publishing IED, the GTnet component attempts to link the physical device with the RTDS virtual circuit breakers. For successful linking, the GOOSE configuration of GTNET-GSE component needs to configured and enabled to output YES as depicted in Figure 8.18.

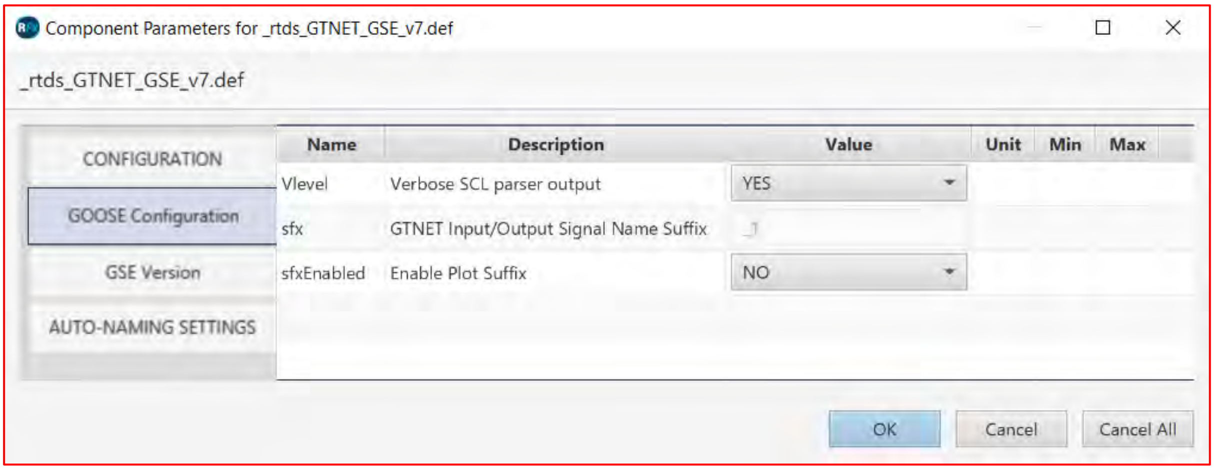

Figure 8.19: GNET-GSE GOOSE configuration.

Incompletion of GNET-GSE component configuration, a new circuit breaker logic that is an extension to the one created in chapter 7, that will incorporate the IEC 61850 GOOSE messaging needs to be defined for complete implementation of the communication standard, Figure 8.20 provides a schematic of this control logic.

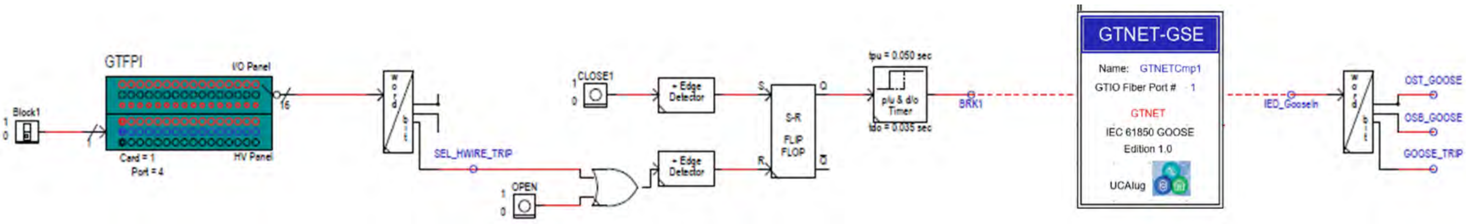

Figure 8.20: GOOSE tripping circuit breaker control logic in RSCAD-FX draft.

In the above Figure, the GOOSE trip signals are perceived by the circuit breakers via the word to bit conversion block with the OST_GOOSE, OSB_GOOSE and GOOSE_TRIP being the signal attributes published by the SEL-421 external IED to be transmitted to the real-time-simulator by the GNET-GSE component.

Smart circuit breakers typically operate in 40 millisecond gusts. This delay is taken into account by the pickup/dropdown timer that is displayed in the circuit breaker logic in the above Figure as its set to pick up in 50ms and drop in 35ms. Following this configuration, the RTDS draft file is saved and assembled together with the updated RTDS SCD file.

8.3 DYNAMIC STATE SIMULATION

To test the effectiveness of the predictive scheme, the PMU is incorporated on the RSCAD-FX draft in Area 3 which is solely optimally placed to perform ITR IEC-61850-90-5 protocol. A schematic diagram with GNET-PMU in Area 3 is illustrated in Figure 8.21 below.

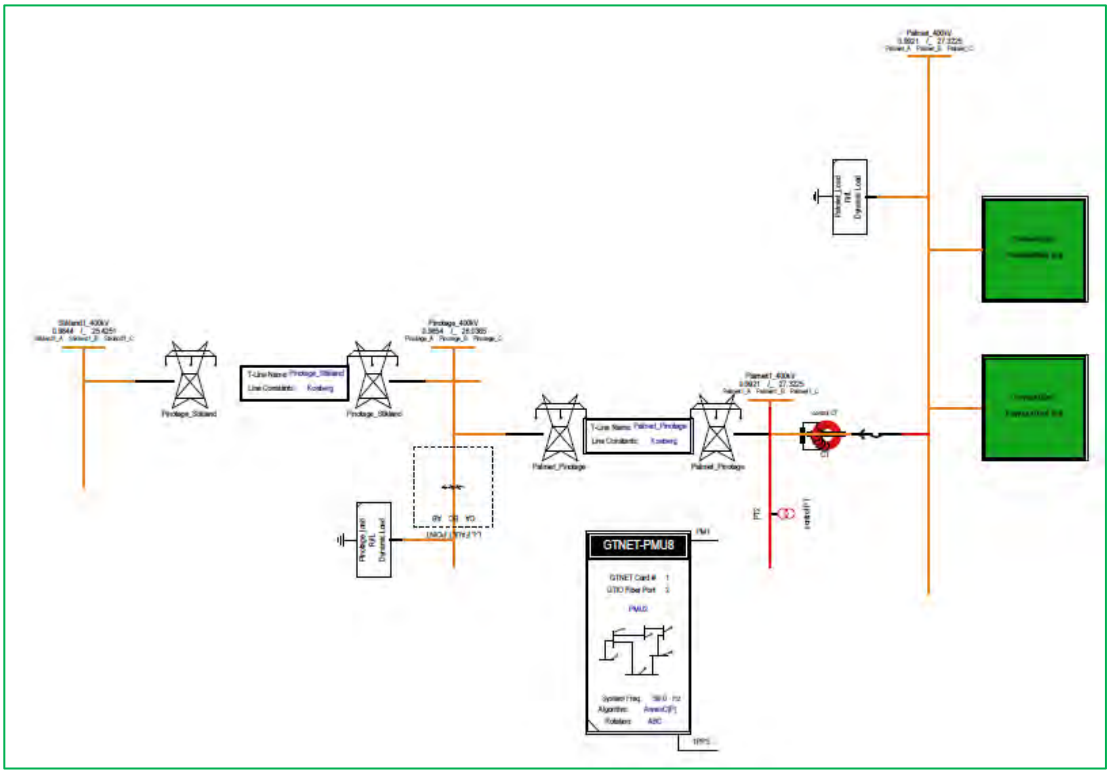

Figure 8.21: Area 3 network with PMU integrated on RSCAD-FX draft.

As previously discussed in literature the virtual PMU can be employed in the test methodology. For power transmission networks, each bus is linked to a limited number of lines. There are a sufficient number of channels in existing phasor measurement instruments. It is therefore reasonable to consider that the installed system not only records the complex bus voltage, but also the complex currents flowing along all the lines that exist on this bus, once the bus is chosen for PMU instrumentation. Each generating source will be placed with a PMU to detect OSS and subsequently isolate its pre-determined protected area to obtain optimal full device isolation.

For the identification of the most susceptible load buses with respect to voltage stability for a study case , modal analysis of the reduced system matrix and calculation of the bus participation factors will be used. The following flow chart in Figure 8.15 presents the PMU algorithm data origination and sending steps from PMU to SEL-421 IED.

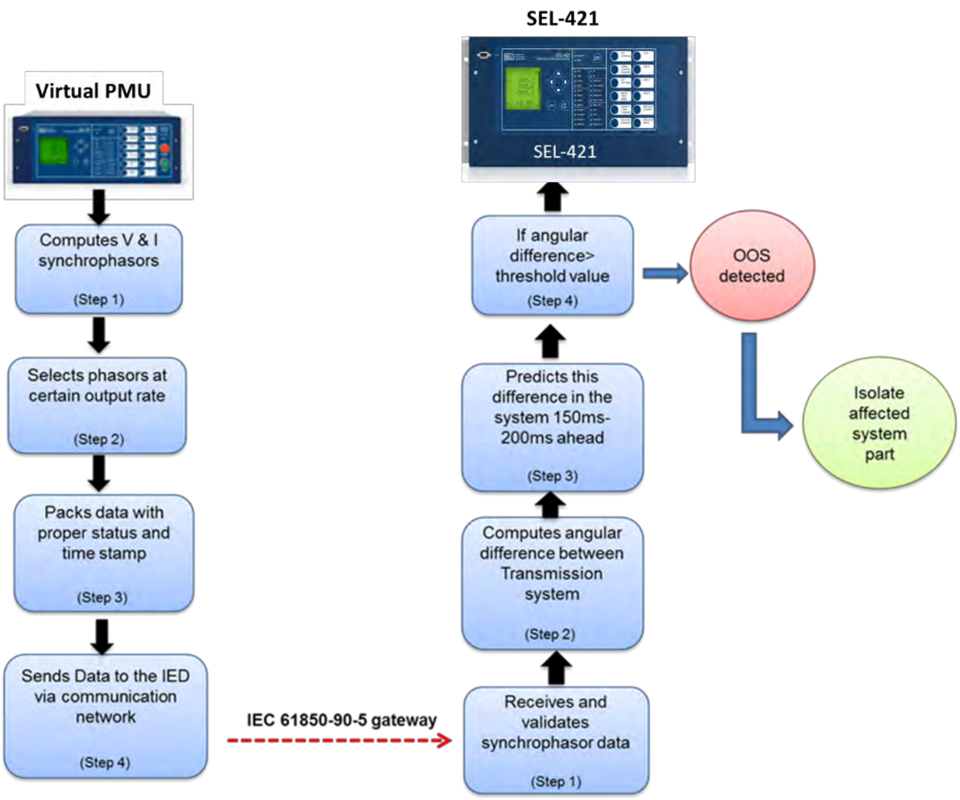

Figure 8.22: Flow chart for PMU algorithm execution.

Out-of-step protection testing can now be done effortlessly and precisely without the worry of misconnection of wires for analogue signals nor hardwired trip signals as these signals are being published by the GNET-PMU8 to be subscribed in RTDS hardware interface.

8.3.1 Case study 1- Zone 1 fault on Palmiet_Pinotage 400kV line

For this study only a zone 1 fault will be simulated on the line as its qualities and effects on protection are the similar to that of zone 2 fault (just that zone 2 is further on the line). For completeness an out-of-step blocking needs to be verified hence only one impedance fault will be injected to confirm the OSB functionality through PMU detection and GOOSE messaging. It is also important to note that IEC 61850-90-5 standard often specifies a Routable-GOOSE for its desired operation, however for the study this is not necessary as the hardware-in-the-loop test bed is housed on one location at the CSAEMS for a limited period of time no cyber-attacks may arise in the scenario. Cyber security as defined by Routable-GOOSE may be applicable in an industrial network that is always running live conditions.

A 3-phase bolted fault is injected similar to that simulated in hardwire study of chapter 7. The figures to follow illustrate the resulting plots of RSCAD RunTime as the GOOSE trip assert with OSB data set blocking the zone 1 fault:

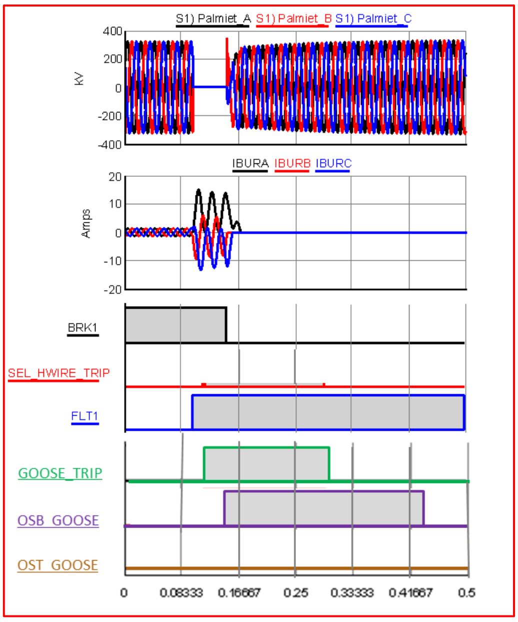

Figure 8.23: Current and Voltage signals with GOOSE digital outputs.

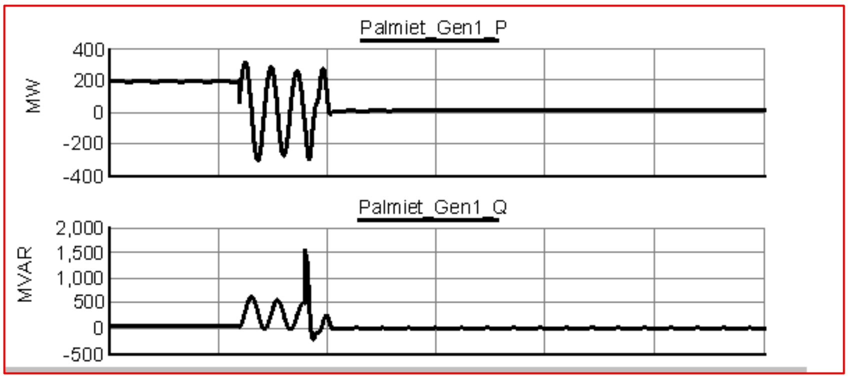

Figure 8.24: Palmiet generating units supply with zone 1 fault cleared.

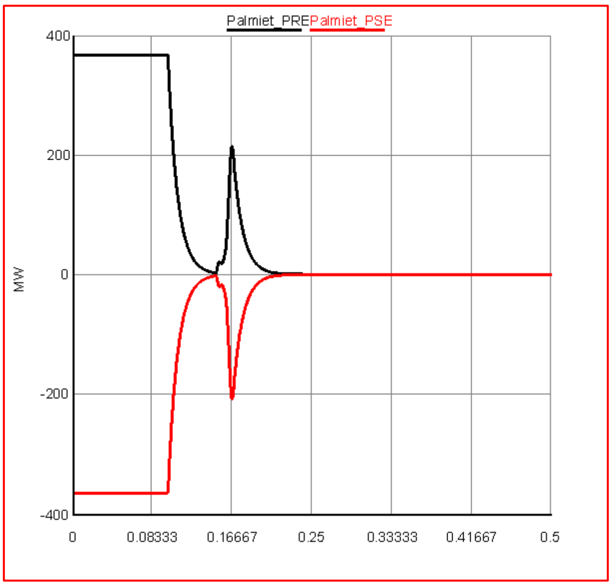

Figure 8.25: Palmiet transmission line load during the disturbance.

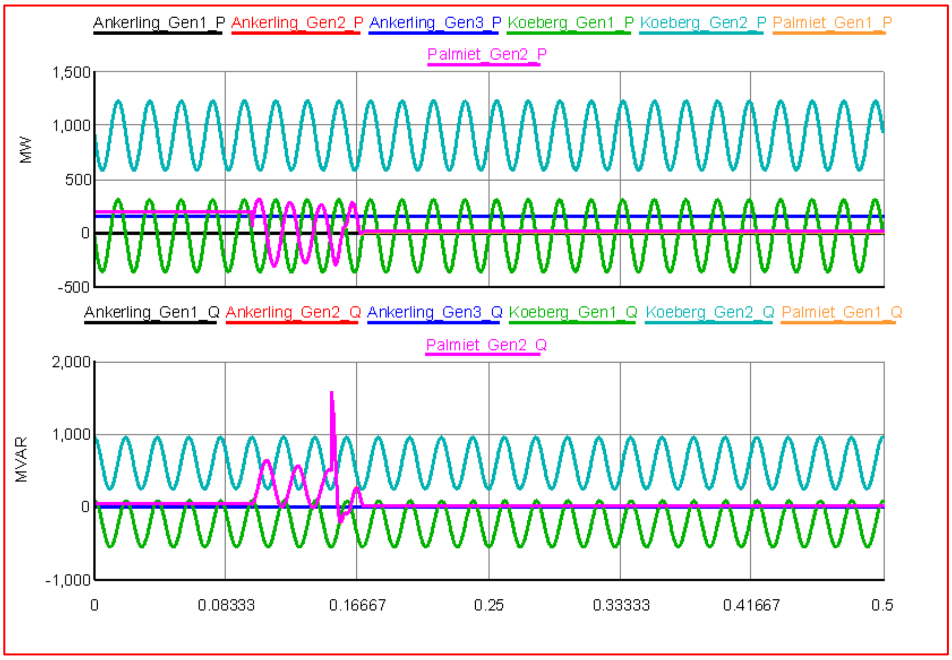

Figure 8.26: Complete system generating supply during zone 1 fault.

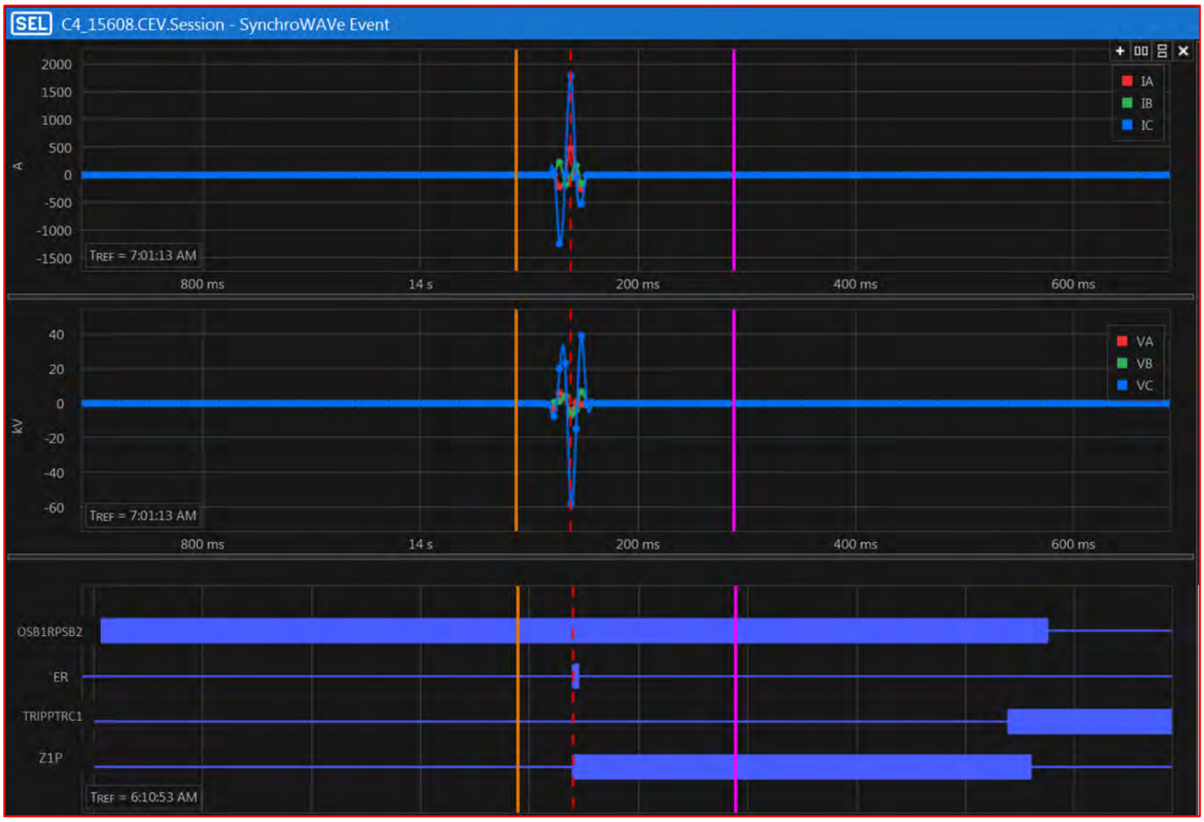

Figure 8.27: Logical nodes trip signals of SEL-421 as viewed from SynchroWave software.

It can be seen the relay remains stable and block power swing seen by the system during zone 1 disturbances as the power swing blocking (OSB1RPSB2) and trip output (TRIPPTRC1) elements are asserted as soon as relay clears the injected fault.

8.3.2 Case study 2: Busbar Fault on Palmiet_400kV bus

Analysing a pole slipping condition through the adaptive scheme is also of interest to the dissertation study. Now a 3-phase bolted similarly to the one previously injected in hardwired real-time simulation study is injected to investigate the reliability of the published data sets to virtual circuit breakers in the test system. Protection philosophy calls for only out-of-step tripping when generator pole slipping arises, hence only OSTRPSB1 logical node signal should be seen from SEL-421 relay's response (on the event report). The Figures to follow show graph plots resulting in runtime during this occurrence in the test system.

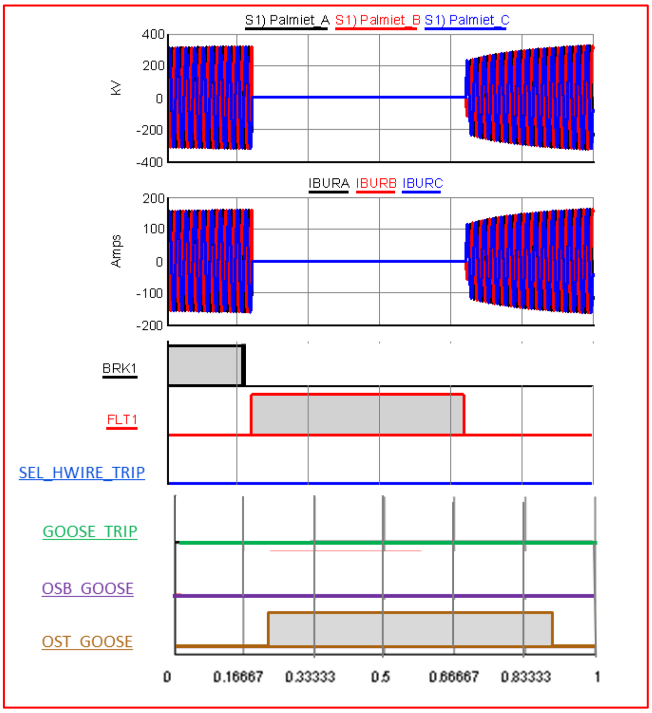

Figure 8.28: CT & PT analogues along with GOOSE data sets for out-of-step condition.

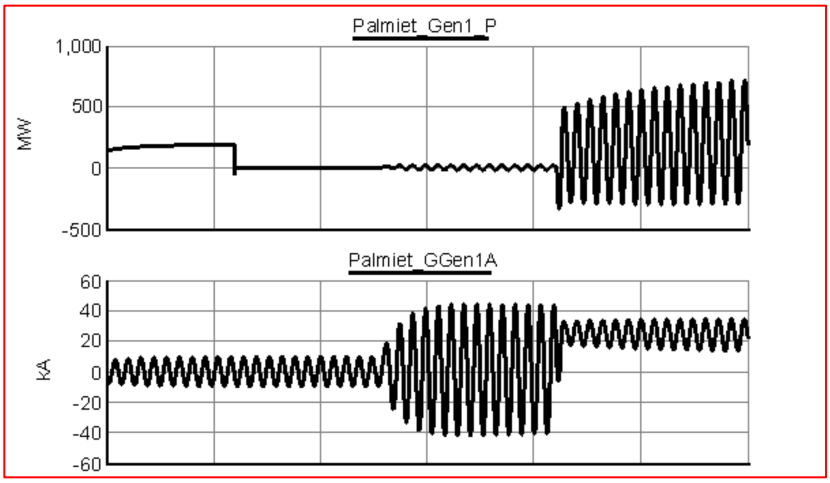

Figure 8.29: Palmiet generating supply during pole slipping.

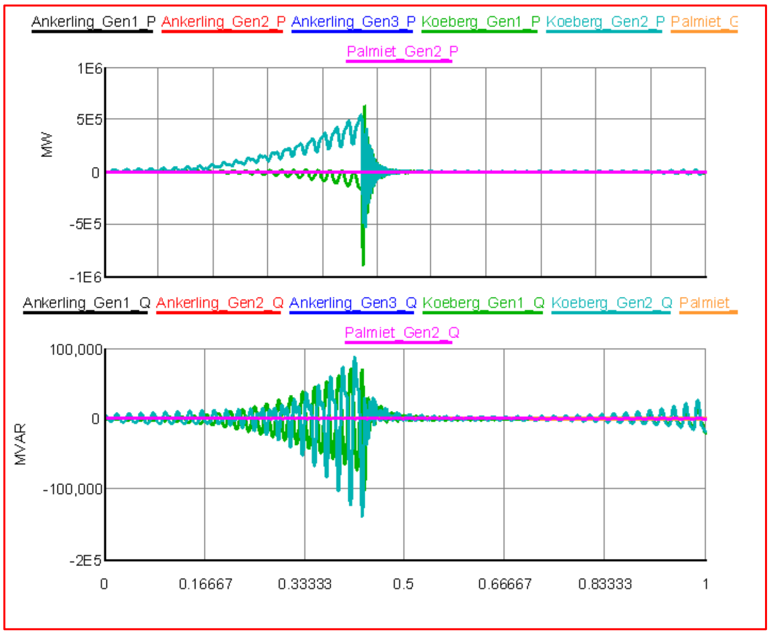

Figure 8.30:Complete system supply during out-of-step occurrence.

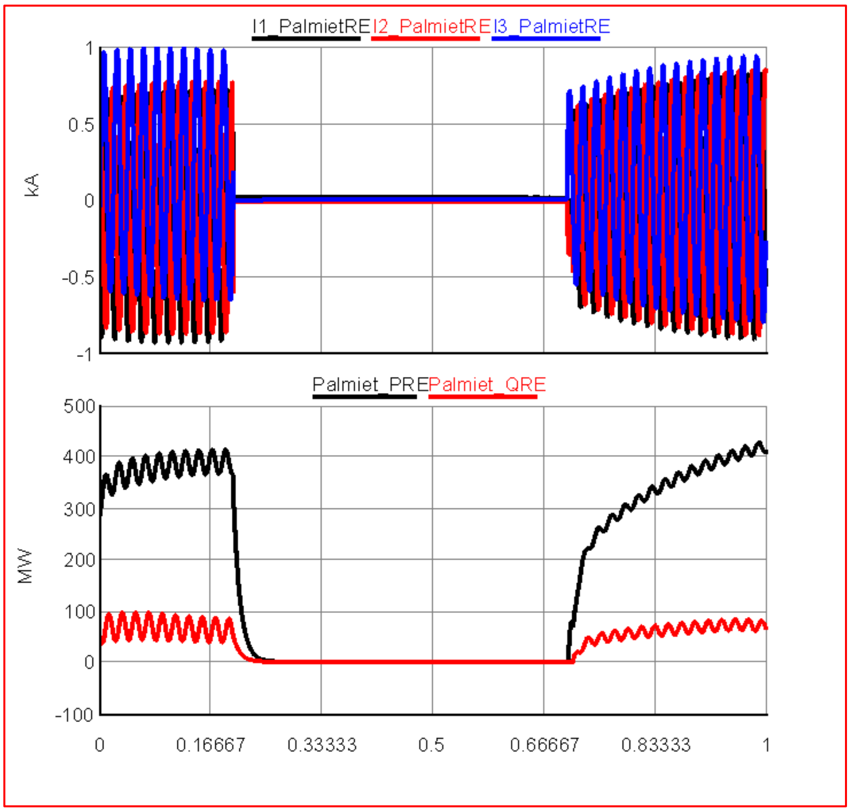

Figure 8.31: Load between Palmiet 400kV bus s/s and Pinotage 400kV bus end.

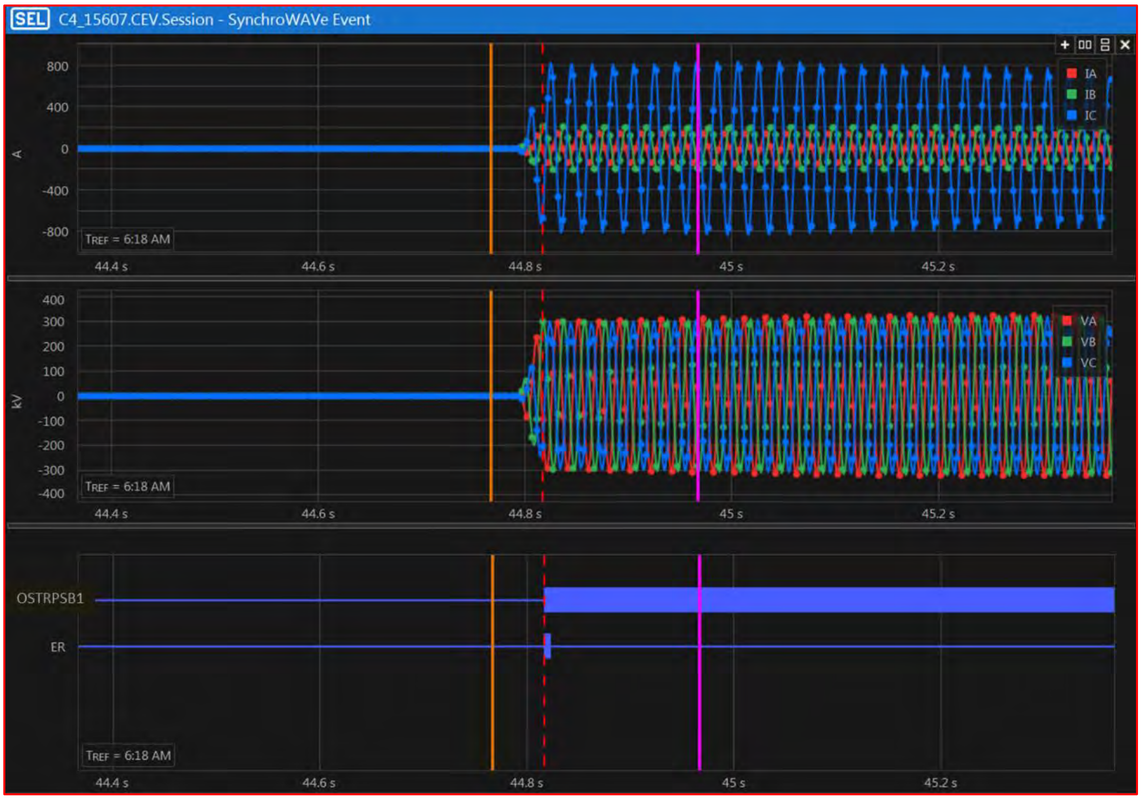

Figure 8.32: Out-of-step trip event with logical node OSTRPSB1 asserted.

8.4 Conclusion

This chapter presented Hardware-in-the-loop implementation and testing to validate the developed IEC 61850-90-5 standard. The adaptive scheme worked for both power swing bocking and pole slip tripping (OOS) conditions, the implementation of the communication standard is necessary to replace the hard-wired analogues and binary inputs for better protection situational awareness of the predictive dynamic system. The scheme is tested with the faults similar to the ones tested in the previous chapter 7.

The adaptive technique takes advantage of direct transient stability analysis methods by computing the angular difference between the system's voltages and transmitting them to protection device through PMU. As a result, out-of-step events are more predictable than traditional techniques, contributing to the growing need for smart grid as it relates to the IEC61850 standard and substation automation. This type of scheme will benefit power utility companies when it comes to rotor angle stability as it may also be applied over a wide-range of area with dispatching of Routable-GOOSE message at various stations for live situational awareness.

The thesis' deliverables are discussed in the next chapter, along with potential applications for the created methodology. Suggestions for future research work and limitations related to the thesis are also given therein.

9 CHAPTER NINE

CONCLUSION AND RECOMMENDATIONS

9.1 INTRODUCTION

Predictive dynamic maintaining stability system is becoming the most effective way of managing power system stability namely, voltage stability, frequency stability and rotor angle stability. With Load demand increasing every day, power utilities are forced to explore new ways of producing power by adapting interconnection of energy renewables to its existing grid. However, in as much as expanding their Grid they still have an obligation to maintain a secured and stable to customer service points, with this said even if an Independent Power Producer (which are the large scale and leading renewable energy utilities) is to be connected to Eskom grid for instance, the integrity of Eskom's energy production shouldn't be compromised.

This dissertation focuses on developing an IEC 61850-90-5 communication-based protection scheme. An adaptive phasor measurement unit (PMU) algorithm determines the angular difference between voltage phasors at a specific bus and the whole system then transmits these phasor quantities to the physical protection device to make an appropriate decision in light of rotor angle stability.

The portion of Eskom transmission network in the Western Cape geographic area was modified and considered as a test system study reference. A steady-state load flow analysis was carried out. Load contingencies and severe busbar faults were used in the dynamic state. The goal was to demonstrate that the rotor of the synchronous machine cannot recover withstand sudden inadvertent occurrences to equipment closer to the operating capacity. As a result a decline in electrical torque produced by synchronous generators declined as they were losing synchronism with the rest of the system and produced mechanical torque thereof, with which the impact resulted in an accelerated output speed from the control governing system which would wear out the equipment in a long run if the problem persist.

The creation of the innovative protection scheme development began with DIgSILENT PowerFactory® simulation software for non-real time simulation analysis and was further validated on RSCAD-FX to be practically implemented on the hardware-in-the loop using SEL-421 relay and virtual PMU and evaluated on RSCAD-FX RunTime platform in real-time simulation.

This Chapter summarizes the findings, major discoveries, and thesis deliverables. Section 9.2 contains the thesis' deliverables. Section 9.3 discusses the thesis deliverables' potential academic/research, and industrial applications. In section 9.4 limitations experienced in the project study is drawn. Section 9.5 proposes future work recommendations related to the rotor angle stability study for further research effort in the field of predictive dynamic maintaining system.

9.2 Thesis deliverables

This part provides a summary of the work done to achieve the thesis's goals and objectives.

9.2.1 Literature review

This study conducted a literature review to assess the advancements made in rotor angle stability and control pertaining out-of-step protection and out-of-step blocking techniques. Both the phenomenon of power system instability and the mitigating component were studied. It was investigated how wind power plants may be integrated into the distribution grid and what problems they would cause. The innovative methods for detecting loss of synchronism in large, interconnected power system were explored, the benefits introduced by incorporating an IEC-61850-90-5 standard to the OOS phenomena has also been investigated each owing to the need for interoperability of IEDs and PMUs therein.

The literature was compiled using e-books, power system textbooks, journals, previous academic theses available online, and digital library platforms, and it will serve as the direction for the study's goals.

9.2.2 Theoretical framework

The theory for power system rotor angle stability on embedded synchronous generators were developed along with multi-machine stability studies, and analysis. Also the concepts in designing protection schemes for the embedded machines were developed using digital libraries, periodicals, textbooks, and e-books.

9.2.3 Modified Eskom West Grid transmission system modelling and simulation in DigSilent PowerFactory®

Through simulations of stable power swings and unstable power swings, the effectiveness of the generator out-of-step protection strategy was examined both for main generator protection located at the synchronous machine (SEL700G) and back-up generator protection optimally placed on the outgoing transmission line (SEL-421). As a case study, the modified Eskom West Grid transmission system was taken into consideration. The DIgSILENT environment was used to develop and simulate the protection scheme on both aforementioned IEDs, and the load flow results were examined. Dynamic simulation studies were also performed in order to execute RMS/EMT fault simulation at various points on the test system for examining the reliability of the protection schemes. Quasi-dynamic simulation were also rolled out for awareness of the system contingencies and changes throughout the seasons.

From the simulation results it is quite evident that if a fault arises on the busbar closer to the running synchronous machine, that particular synchronous machine is prone to lose synchronism with the rest of the system rapidly leaving extensive vigorous damage to the machine and other equipment on the system, therefore for protection aspect it was necessary to also perform simulation scan to acquire critical clearing time of the IEDs before a substantial damage can occur on the power system equipment.

9.2.4 Power system network modelling and simulation on RSCAD-FX

On the RSCAD-FX simulation platform, the network modelling that was done in the chapter using DIgSILENT was performed again, with the aim to conduct steady state simulation analysis in an offline mode (non-real time) of RTDS. The objective of creating this network model was to successfully test if the load flow converges before embarking on creating a hardware-in-the-loop test bench for live simulation results of RTDS as this is the initial requirement in any protection technique design (Awareness of stable power flow is principal).

9.2.5 Hardware-in-the-loop testing of out-of-step protection with RTDS

Using the model developed in chapter 6 (RSCAD draft), a protection scheme was implemented and developed for generator OOS scheme incorporating only SEL-421 physical protection device. The objective of creating this test bench is to again examine stable power swing blocking and unstable power swing tripping functionality of the protection scheme using hard wire for power system control and protection in a real-time simulation platform.

Three case were conducted in order to analyse the protection scheme response with two of them being impedance faults injected on the outgoing transmission line in zone 1 and zone 2 of the line to validate power swing blocking (OSB) of the developed scheme. The last was injected on the station busbar closer to the operating synchronous machine to assess pole slipping protection of the scheme (OST). In light of these case studies, the reliability of the developed protection scheme has been validated.

9.2.6 IEC-61850-90-5 standard implementation for a predictive dynamic maintaining stability system in HIL

Utilizing the test bench developed in chapter 7, the performance of the TR IEC-61850-90-5 standard was implemented and analysed using virtual phasor measurement unit to validate angular difference between system voltages and thereby transports them to the physical devices for appropriate protection tripping decision .

IEC-61850 GOOSE messaging was also mapped between the physical SEL-421 IED and RTDS. Instead of making use of hardwired binary inputs and outputs for transporting signal to RTDS, logical nodes Pro data sets are sent via the Ethernet to the circuit breaker of the virtual test system on RSCAD-FX draft for live RunTime protection investigation in real-time simulation environment.

9.3 ACADEMIC AND INDUSTRIAL APPLICATION

This study created a test bench that academics can use to increase their knowledge of power system rotor angle stability techniques in real-time. The broader knowledge looks into advantages of using communication assisted schemes rather than the conventional techniques. This will also assist students comprehend the behaviour of the out-of-step protection and its application in the power system environment.

Enhancement of the grid stability through IEC 61850 communication standard-based protection would be of great benefit to power utilities with less wiring which often lead to much more congested protection system. Synchronising Generators of the two parties i.e. Eskom and IPPS can be quite complex and needs not to be taken lightly as this would result in major power outages so implementation of such IEC 61850-90-5 standard based predictive dynamic stability system would maintain a smart constant generating grid owing to its wide situational awareness and fast fault isolation when an out-of-step condition is detected thereby improving key performance system indexes are that put in place to govern most utility energy supply and failure for utilities to meet the targets comes with a fine so in essence utility's revenue will also be increased.

We are approaching an era where all protection devices will be time-synchronized and capable of providing accurate, high precision time tags as part of any measurement. In order to realize the possible benefits of this new age, progress in time synchronization must balance progress in other fields. For example, communication channels in streaming PMU data from remote sites to a central facility will become faster and more secure there by enhancing grid management and system stability. The value of synchronized measurement technology is presently being realized to its full extent through the deployment of large-scale projects such as the one developed in this dissertation.

9.4 PROJECT LIMITATIONS

The most unfortunate encountered limitation is the unavailability of the OOS tripping output card in the SEL700GT protection relay that is available for research use at the CSAEMS lab such that only the SEL-421 relay was utilized for practical implementation of the adaptive scheme though settings configurations and non-real time simulations were prepared for both relays.

Another limitation of this research work relates to the HIL test-bench capabilities, a wide area of the dynamic network couldn't be realised to its full extent as examining angular differences between different locations would require more than 3 physical relays optimally placed in the virtual system stations to receive data transmitted by virtual PMU's to PDC for appropriate protection tripping decision.

Despite these limitation, the findings of this study are important as they contribute both to academic and industrial applications in an exclusive way as the adaptive scheme was validated to pose better benefits than that of conventional OOS applications previously applied in previous research studies.

9.5 FUTURE WORK

The developed out-step-scheme was implemented such that it focuses only on one area of the dynamic predictive maintaining stability system. Therefore the system situational awareness perceived by the virtual PMU is only local signals with no access to remote stations awareness. Even the transportation of protection tripping logical nodes encompasses a standard GOOSE mapping not necessarily a Routable-GOOSE which is often desired by IEC-61850-90-5 standard application for a wide range of region.

The future work will focus on creating a centralised system situational awareness through phasor data concentrator (PDC) for system data quantities that can be controlled remotely in a central control station centre. Where if a pole slipping is detected at one station another generating reserve such as peaking power stations would be automatically connected to the grid while the problem of pole slipping is being cleared by out-of-step protection in that disturbed station. Further research into this area may therefore be useful since this phenomena in-turn will reduce unnecessary unplanned power outages, even in light of loadshedding there wouldn’t be a time delay in switching back customers as this would be done rapidly by the phasor data concentrator outputs.

9.6 PUBLICATION

N. Fose, S. Krishnamurthy, 2023. Experimental results and Sample Value technique evaluation based on IEC 61850-90-5 for generator out-of-step protection scheme, submitted for review on International Journal of Electrical Power and Energy Systems.

10 BIBLIOGRAPHY

D Hou and D A Tziouvaras, Schweitzer. (2004). OUT-OF-STEP PROTECTION ENHANCEMENTS D Hou and D A Tziouvaras Schweitzer Engineering Laboratories, Inc., USA. Developments in Power System Protection, 2004. Eighth IEE International Conference

Ates, Y., Boynuegri, A. R., Uzunoglu, M., Nadar, A., Yumurtacı, R., Erdinc, O., Paterakis, N. G., & Catalão, J. P. S. (2016). Adaptive protection scheme for a distribution system considering grid-connected and islanded modes of operation. Energies. https://doi.org/10.3390/en9050378

Rebizant, W., & Feser, K. (2001). Fuzzy logic application to out-of-step protection of generators. Proceedings of the IEEE Power Engineering Society Transmission and Distribution Conference. https://doi.org/10.1109/pess.2001.970179

Vieira, J. C. M., Freitas, W., Huang, Z., Xu, W., & Morelato, A. (2006). Formulas for predicting the dynamic performance of ROCOF relays for embedded generation applications. IEE Proceedings: Generation, Transmission and Distribution. https://doi.org/10.1049/ip-gtd:20045205

Alinezhad, B., & Karegar, H. K. (2017). Predictive out-of-step relay based on equal area criterion and PMU data. International Transactions on Electrical Energy Systems. https://doi.org/10.1002/etep.2327

Lamont, L., & De Kock, J. A. (2015). Developments of a predictive pole-slip protection function for synchronous generators. 2015 IEEE Energy Conversion Congress and Exposition, ECCE 2015. https://doi.org/10.1109/ECCE.2015.7309822

Adibi, M. M., Kafka, R. J., Maram, S., & Mili, L. M. (2006). On power system-controlled separation. IEEE Transactions on Power Systems. https://doi.org/10.1109/TPWRS.2006.881139

Ahmad, F., Rasool, A., Ozsoy, E., Sekar, R., Sabanovic, A., & Elitaş, M. (2018). Distribution system state estimation-A step towards smart grid. In Renewable and Sustainable Energy Reviews. https://doi.org/10.1016/j.rser.2017.06.071

Haddadi, A., Kocar, I., Karaagac, U., Gras, H., & Farantatos, E. (2019). Impact of Wind Generation on Power Swing Protection. IEEE Transactions on Power Delivery. https://doi.org/10.1109/TPWRD.2019.2896135.

Manunza, A. (2009). Out of step condition and torsional stress of synchronous generators. EEUG Meeting Technical Papers.

Centeno, V., Phadke, A. G., Edris, A., Benton, J., Gaudi, M., & Michel, G. (1997). An adaptive out-of-step relay. IEEE Power Engineering Review. https://doi.org/10.1109/MPER.1997.560665

Sauhats, A., Utans, A., Antonovs, D., & Svalovs, A. (2017). Angle control-based multi-terminal out-of-step protection system. Energies. https://doi.org/10.3390/en10030308

Yamashita, K., & Kameda, H. (2004). Out-of-step prediction logic for wide-area protection based on an autoregressive model. 2004 IEEE PES Power Systems Conference and Exposition. https://doi.org/10.1109/psce.2004.1397469

Thorp, J. S., Phadke, A. G., Horowitz, S. H., & Begovic, M. M. (1988). Some applications of phasor measurements to adaptive protection. IEEE Transactions on Power Systems. https://doi.org/10.1109/59.192936

Singh, B., Sharma, N., Tiwari, A., Verma, K., & Singh, S. (2011). Applications of phasor measurement units (PMUs) in electric power system networks incorporated with FACTS controllers. International Journal of Engineering, Science and Technology. https://doi.org/10.4314/ijest.v3i3.68423

Rockefeller, G. D., Wagner, C. L., Linders, J. R., Hicks, K. L., & Rizy, D. T. (1988). Adaptive transmission relaying concepts for improved performance. IEEE Transactions on Power Delivery. https://doi.org/10.1109/61.193943

Horowitz, S. H. (2017). Transmission line protection. In Power System Stability and Control, Third Edition. https://doi.org/10.4324/b12113

Shrestha, B., Sharma, P., & Gokaraju, R. (2013). Out-of-step protection using the analysis of electrical power Vs speed deviation in state plane. 2013 4th IEEE/PES Innovative Smart Grid Technologies Europe, ISGT Europe 2013. https://doi.org/10.1109/ISGTEurope.2013.6695490

Paudyal, S., Ramakrishna, G., & Sachdev, M. S. (2010). Application of equal area criterion conditions in the time domain for out-of-step protection. IEEE Transactions on Power Delivery. https://doi.org/10.1109/TPWRD.2009.2032326

Parmar, K. P. S., Majhi, S., & Kothari, D. P. (2012). Load frequency control of a realistic power system with multi-source power generation. International Journal of Electrical Power and Energy Systems. https://doi.org/10.1016/j.ijepes.2012.04.040

Guo, T., & Milanovic, J. V. (2016). Online Identification of Power System Dynamic Signature Using PMU Measurements and Data Mining. IEEE Transactions on Power Systems. https://doi.org/10.1109/TPWRS.2015.2453424

Ariff, M. A. M., & Pal, B. C. (2016). Adaptive Protection and Control in the Power System for Wide-Area Blackout Prevention. IEEE Transactions on Power Delivery. https://doi.org/10.1109/TPWRD.2016.2518080

Yan, J., Liu, C. C., & Vaidya, U. (2011). PMU-based monitoring of rotor angle dynamics. IEEE Transactions on Power Systems. https://doi.org/10.1109/TPWRS.2011.2111465

Messina, A. R. (2015). Wide-area monitoring of interconnected power systems. In Wide Area Monitoring of Interconnected Power Systems. https://doi.org/10.1049/PBPO077E

Eltamaly, A. M., & Abd Elghaffar, A. N. (2018). Modelling of distance protection logic for out-of-step condition in power system. Electrical Engineering. https://doi.org/10.1007/s00202-017-0667-3

So, K. H., Heo, J. Y., Kim, C. H., Aggarwal, R. K., & Song, K. B. (2007). Out-of-step detection algorithm using frequency deviation of voltage. IET Generation, Transmission and Distribution. https://doi.org/10.1049/iet-gtd:20050140

Bertsch, J., Carnal, C., Karlsson, D., McDaniel, J., & Vu, K. (2005). Wide-area protection and power system utilization. Proceedings of the IEEE. https://doi.org/10.1109/JPROC.2005.847266

Makarov, Y. V., Du, P., Lu, S., Nguyen, T. B., Guo, X., Burns, J. W., Gronquist, J. F., & Pai, M. A. (2012). PMU-based wide-area security assessment: Concept, method, and implementation. IEEE Transactions on Smart Grid. https://doi.org/10.1109/TSG.2012.2193145

Wen, M. H. F., Xu, J., & Li, V. O. K. (2013). Optimal multistage PMU placement for wide-area monitoring. IEEE Transactions on Power Systems. https://doi.org/10.1109/TPWRS.2013.2277741

Yaghobi, H. (2016). Out-of-step protection of generator using analysis of angular velocity and acceleration data measured from magnetic flux. Electric Power Systems Research. https://doi.org/10.1016/j.epsr.2015.11.003

Hashemi, S. M., & Sanaye-Pasand, M. (2019). Current-Based Out-of-Step Detection Method to Enhance Line Differential Protection. IEEE Transactions on Power Delivery. https://doi.org/10.1109/TPWRD.2018.2873698

Salomonsson, D. (2008). Modeling , Control and Protection of Low-Voltage DC Microgrids. In Power.

Phadke, A. G., & Bi, T. (2018). Phasor measurement units, WAMS, and their applications in protection and control of power systems. In Journal of Modern Power Systems and Clean Energy. https://doi.org/10.1007/s40565-018-0423-3

Laverty, D. M., Best, R. J., & Morrow, D. J. (2015). Loss-of-mains protection system by application of phasor measurement unit technology with experimentally assessed threshold settings. IET Generation, Transmission and Distribution. https://doi.org/10.1049/iet-gtd.2014.0106

Ivankovic, I., Kuzle, I., & Holjevac, N. (2017). Multifunctional WAMPAC system concept for out-of-step protection based on synchrophasor measurements. International Journal of Electrical Power and Energy Systems. https://doi.org/10.1016/j.ijepes.2016.11.005

Norgaard, P., & Holttinen, H. (2004). A Multi-Turbine Power Curve Approach. Nordic Wind Power Conference.

Che, L., Khodayar, M. E., & Shahidehpour, M. (2014). Adaptive protection system for microgrids: Protection practices of a functional microgrid system. IEEE Electrification Magazine. https://doi.org/10.1109/MELE.2013.2297031

Ohura, Y., Suzuki, M., Yanagihashi, K., Yamaura, M., Omata, K., Nakamura, T., Mitamura, S., & Watanabe, H. (1990). A predictive out-of-step protection system based on observation of the phase difference between substations. IEEE Transactions on Power Delivery. https://doi.org/10.1109/61.103664

Committee, P. S. R. (2004). IEEE Guide for Abnormal Frequency Protection for Power Generating Plants. IEEE Std C37.106-2003 (Revision of ANSI/IEEE C37.106-1987). https://doi.org/10.1109/IEEESTD.2004.94434

Aminifar, F., Fotuhi-Firuzabad, M., Shahidehpour, M., & Khodaei, A. (2011). Probabilistic multistage PMU placement in electric power systems. IEEE Transactions on Power Delivery. https://doi.org/10.1109/TPWRD.2010.2090907

Monti, A., Muscas, C., & Ponci, F. (2016). Phasor Measurement Units and Wide Area Monitoring Systems: From the Sensors to the System. In Phasor Measurement Units and Wide Area Monitoring Systems: From the Sensors to the System. https://doi.org/10.1016/C2014-0-03907-X

Ghahremani, E., & Kamwa, I. (2016). Local and wide-area PMU-based decentralized dynamic state estimation in multi-machine power systems. IEEE Transactions on Power Systems. https://doi.org/10.1109/TPWRS.2015.2400633

Apostolov, A. (2017). R-GOOSE: What it is and its application in distribution automation. CIRED - Open Access Proceedings Journal. https://doi.org/10.1049/oap-cired.2017.0494

Firouzi, S. R., Vanfretti, L., Ruiz-Alvarez, A., Hooshyar, H., & Mahmood, F. (2017). Interpreting and implementing IEC 61850-90-5 Routed-Sampled Value and Routed-GOOSE protocols for IEEE C37.118.2 compliant wide-area synchrophasor data transfer. Electric Power Systems Research. https://doi.org/10.1016/j.epsr.2016.12.006

Benmouyal, G. (2012). The Impact of Synchronous Generators Excitation Supply on Protection and Relays. Journal of Reliable Power.

Hashiesh, F., Mostafa, H. E., Khatib, A. R., Helal, I., & Mansour, M. M. (2012). An intelligent wide area synchrophasor based system for predicting and mitigating transient instabilities. IEEE Transactions on Smart Grid. https://doi.org/10.1109/TSG.2012.2187220

Phadke, A. G. (2008). The wide world of wide-area measurement. IEEE Power and Energy Magazine. https://doi.org/10.1109/MPE.2008.927476

Kezunovic, M. (2005). Fundamentals of Power System Protection. In The Electrical Engineering Handbook. https://doi.org/10.1016/B978-012170960-0/50058-X

Fang, X., Misra, S., Xue, G., & Yang, D. (2012). Smart grid - The new and improved power grid: A survey. In IEEE Communications Surveys and Tutorials. https://doi.org/10.1109/SURV.2011.101911.00087

Shrestha, B., Gokaraju, R., & Sachdev, M. (2013). Out-of-Step protection using state-plane trajectories analysis. IEEE Transactions on Power Delivery. https://doi.org/10.1109/TPWRD.2013.2245684

Sodhi, R., Srivastava, S. C., & Singh, S. N. (2011). Multi-criteria decision-making approach for multi-stage optimal placement of phasor measurement units. IET Generation, Transmission and Distribution. https://doi.org/10.1049/iet-gtd.2009.0709

Grigsby, L. L. (2017). Power system stability and control. In Power System Stability and Control, Third Edition. https://doi.org/10.4324/b12113

De La Ree, J., Centeno, V., Thorp, J. S., & Phadke, A. G. (2010). Synchronized phasor measurement applications in power systems. IEEE Transactions on Smart Grid. https://doi.org/10.1109/TSG.2010.2044815

Ali, I., Aftab, M. A., & Hussain, S. M. S. (2016). Performance comparison of IEC 61850-90-5 and IEEE C37.118.2 based wide area PMU communication networks. Journal of Modern Power Systems and Clean Energy. https://doi.org/10.1007/s40565-016-0210-y

ANIL KUMAR NM, & PARTHASARATHY K. (1969). POWER SYSTEM PROTECTION. Journal of the Institution of Engineers (India): Electrical Engineering Division.

Li, Q., Cui, T., Weng, Y., Negi, R., Franchetti, F., & Ilic, M. D. (2013). An information-theoretic approach to PMU placement in electric power systems. IEEE Transactions on Smart Grid. https://doi.org/10.1109/TSG.2012.2228242

Aminifar, F., Fotuhi-Firuzabad, M., Safdarian, A., Davoudi, A., & Shahidehpour, M. (2014). Synchrophasor Measurement Technology in Power Systems: Panorama and State-of-the-Art. IEEE Access. https://doi.org/10.1109/ACCESS.2015.2389659 System, P., & Committee, R. (1995). IEEE Guide for AC Generator Protection. Electronics.

IEEE Power System Relaying Committee. (2005). Power Swing and Out-Of-Step Considerations on Transmission Lines. Working Group D-6 Report.

Phadke, A. G. (2002). Synchronized phasor measurements ~ a historical overview. Proceedings of the IEEE Power Engineering Society Transmission and Distribution Conference. https://doi.org/10.1109/tdc.2002.1178427

Tziouvaras, D. A., & Hou, D. (2004). Out-of-step protection fundamentals and advancements. Annual Conference for Protective Relay Engineers. https://doi.org/10.1109/cpre.2004.238495 “Impact of inverter-based generation on bulk power system dynamics and short-circuit performance,” IEEE/NERC Task Force on Short-Circuit and System Performance Impact of Inverter Based Generation, PES-TR68, Jul. 2018.

J. Krata, P. Balcerek and Z. Gajic, "The new frequency difference based Out of Step protection for multiterminal transmission system," 12th IET International Conference on Developments in Power System Protection (DPSP 2014), Copenhagen, 2014, pp. 1-6, doi: 10.1049/cp.2014.0055.

J. Berdy, “Out-of-Step Protection for Generators”, GE Publication No. GER-3179. S. M. Brahma, "Distance Relay with Out-of-Step Blocking Function Using Wavelet Transform," in IEEE Transactions on Power Delivery, vol. 22, no. 3, pp. 1360-1366, July 2007, doi: 10.1109/TPWRD.2006.886773.

Y. Abdelaziz, “Adaptive protection strategies for detecting power system out-of-step conditions using neural networks,” in IEE Proceedings of Generation, Transmission and Distribution, vol. 145, pp. 387-394, 1998.

K. F. Hayes, S. M. Rovnyak, Lingyan Sun, A. Khaliq and S. Thyagarajan, "Neural networks using apparent resistance for out-of-step relaying," 2002 IEEE Power Engineering Society Winter Meeting. Conference Proceedings (Cat. No.02CH37309), New York, NY, USA, 2002, pp. 459-463 vol.1, doi: 10.1109/PESW.2002.985042.

M. -R. Jacobsen, D. Laverty, R. J. Best and J. C. Hastings, "Multi-Machine Synchronous Islanding Achieved in a Laboratory Test Bed Utilizing PMUs," 2020 31st Irish Signals and Systems Conference (ISSC), Letterkenny, Ireland, 2020, pp. 1-5, doi: 10.1109/ISSC49989.2020.9180183.

D. M. Laverty, R. J. Best, P. Brogan, I. Al Khatib, L. Vanfretti and D. J. Morrow, "The OpenPMU Platform for Open-Source Phasor Measurements," in IEEE Transactions on Instrumentation and Measurement, vol. 62, no. 4, pp. 701-709, April 2013, doi: 10.1109/TIM.2013.2240920.

A. E. Gurrola, J. Segundo-Ramírez and C. N. Gutiérrez, "Wide area control in electric power systems incorporating FACTS controllers: Review," 2014 IEEE International Autumn Meeting on Power, Electronics and Computing (ROPEC), Ixtapa, 2014, pp. 1-6, doi: 10.1109/ROPEC.2014.7036325.

Kundur, P.; Balu, N.J.; Lauby, M.G. Power System Stability and Control; McGraw-Hill: New York, NY, USA; London, UK, 1994; ISBN 007035958X.

Acosta, M.N.;Gonzalez-Longatt, F.; Topi´c, D.; Andrade, M.A. Optimal Microgrid–InteractiveReactive Power Management for Day–Ahead Operation. Energies 2021, 14, 1275.

F. Gonzalez-Longatt and J. L. Rueda Torres (eds.), Advanced Smart Grid Functionalities Based on PowerFactory, Green Energy and Technology, Springer International Publishing AG 2018 https://doi.org/10.1007/978-3-319-50532-9_1

Zhao, D., Zhu, L., Jiang, D., Qian, M., Zhao, L. & Zhang, L. 2013. Modeling Comparison on Control System of Synchronous Generator between DIgSILENT Power Factory and PSASP. International Journal of Computer and Electrical Engineering, 5(2): 229–232.

T. Van Cutsem, “Long-term Voltage Instability: Dynamic Aspects”, December 2017. www.montefiore.ulg.ac.be/~vct (current as of 2018/08/11).DIgSILENT, Technical Reference Documentation General Load, Gomaringen: DIgSILENT, 2013.

IEEE Task Force on Load Representation for Dynamic Performance, “Load Representation for Dynamic Performance Analysis”, IEEE Trans. on Power Systems, Vol. 8, No. 2, May 1993.

6J. H. Rust, Nuclear Power Plant Engineering, Haralson Publishing Company, 1979.

Tomsovic, K., Bakken, D.E., Venkatasubramanian, V. & Bose, A. 2005. Designing the next generation of real-time control, communication, and 243 computations for large power systems. Proceedings of the IEEE, 93(5): 965–979.

T. S. Ustun, S. M. Farooq and S. M. S. Hussain, "Implementing Secure Routable GOOSE and SV Messages Based on IEC 61850-90-5," in IEEE Access, vol. 8, pp. 26162-26171, 2020, doi: 10.1109/ACCESS.2020.2971011.

Acosta, M.N.; Gonzalez-Longatt, F.; Topi´c, D.; Andrade, M.A. Optimal Microgrid–Interactive Reactive Power Management for Day–Ahead Operation. Energies 2021, 14, 1275.

Kundur, P.; Balu, N.J.; Lauby, M.G. Power System Stability and Control; McGraw-Hill: New York, NY, USA; London, UK, 1994; ISBN 007035958X.

Chamorro, H.R.; Orjuela-Cañón, A.D.; Ganger, D.; Persson, M.; Gonzalez-Longatt, F.; Alvarado-Barrios, L.; Sood, V.K.; Martinez, W. Data-Driven Trajectory Prediction of Grid Power Frequency Based on Neural Models. Electronics 2021, 10, 151.

Kundur, P.; Paserba, J.; Ajjarapu, V.; Andersson, G.; Bose, A.; Canizares, C.; Hatziargyriou, N.; Hill, D.; Stankovic, A.; Taylor, C.; et al. Definition and Classification of Power System Stability IEEE/CIGRE Joint Task Force on Stability Terms and Definitions. IEEE Trans. Power Syst. 2004, 19, 1387–1401

Chamorro, H.R.; Sevilla, F.R.S.; Gonzalez-Longatt, F.; Rouzbehi, K.; Chavez, H.; Sood, V.K. Innovative primary frequency control in low-inertia power systems based on wide-area RoCoF sharing. IET Energy Syst. Integr. 2020, 2, 151–160

Sanchez, F.; Gonzalez-Longatt, F.; Bogdanov, D. Probabilistic assessment of enhanced frequency response services using real frequency time series. In Proceedings of the 2018 20th International Symposium on Electrical Apparatus and Technologies (SIELA), Bourgas, Bulgaria, 3–6 June 2018; pp. 1–4.

IEEE. IEEE Tutorial on Protection of Synchronous Generators. 2011. Available online: https://www.pes-psrc.org/kb/published/ reports/IEEEGenProtTutorial_20110506_1file.pdf (accessed on 9 October 2020).

Gonzalez-Longatt, F.; Adiyabazar, C.; Martinez, E.V. Setting and Testing of the Out-of-Step Protection at Mongolian Transmission System. Energies 2021, 14, 8170. https://doi.org/10.3390/en14238170

Gorostiza, F.S.; Gonzalez-Longatt, F. Optimised TSO-DSO interaction in unbalanced networks through frequency responsive EV clusters in virtual power plants. IET Gener. Transm. Distrib. 2020, 14, 4908–4917.

14. Rakhshani, E.; Perilla, A.; Torres, J.R.; Longatt, F.G.; Soeiro, T.B.; Van Der Meijden, M. FAPI Controller for Frequency Support innLow-Inertia Power Systems. IEEE Open Access J. Power Energy 2020, 7, 276–286

Zhang, S.; Zhang, Y. Characteristic Analysis and Calculation of Frequencies of Voltages in Out-of-Step Oscillation Power System and a Frequency-Based Out-of-Step Protection. IEEE Trans. Power Syst. 2019, 34, 205–214.

M. Basler and R. Schaefer, Understanding power-system stability, IEEE Transaction on industry applications, Vol 44, No 2, March/April 2008.

Alhejaj, S.M.; Gonzalez-Longatt, F.M. Investigation on grid-scale BESS providing inertial response support. In Proceedings of the 2016 IEEE International Conference on Power System Technology, Powercon 2016,Wollongong, NSW, Australia, 28 September– 1 October 2016.

A. B. Dehkordi, P. Neti, A.M Gole, and T.L. Maguire, Development and Validation of a Comprehensive Synchronous Machine Model for a Real−Time Environment,” IEEE Trans. Energy Conversion, Vol. 25, No. 1, March 2010.

A.B. Dehkordi, A.M Gole, and T.L. Maguire,” Permanent magnet synchronous machine model for real− time simulation”, International Conference on Power System Transients (IPST 2005), Montreal, June, 2005.

Papaspiliotopoulos, V., Kleftakis, V., Kotsampopoulos, P., Korres, G. and Hatziargyriou, N. (2014). Hardware-in-the-loop simulation for protection blinding and sympathetic tripping in distribution grids with high penetration of distributed generation. MedPower 2014, pp.1-6.

Johnson, B., Denholm, P., Kroposki, B. & Hodge, B. 2017. Achieving a 100% Renewable Grid. IEEE Power and Energy Magazine, (april): 61–73.

Kuffel, R., Ouellette, D. & Forsyth, P. 2010. Real Time Simulation and Testing Using IEC 61850. Proc. Modern Electric Power Systems conf.: 1–8.

Sallam, A.A. & Malik, O.P. 2015. Power system stability overview. Power System Stability: Modelling, Analysis and Control: 1–10

Gu, J.C., Liu, C.H., Yang, M.T. & Tsai, D.L. 2019. Research on Integrating Wind Turbine into Intelligent IEC 61850 Substation Automation. 2019 2nd Asia Conference on Energy and Environment Engineering, ACEEE 2019: 54–58.

Saadat H. Power System Analysis. International Student Edition. New York, United States of America: McGraw-Hill; 2005

Electrical Machine Dynamics. GUPTA S & LYNN, Macmillon Press Ltd, 1980.

ElectroMagnetic Transients Program (EMTP) Volume 3, Workboook 3. ALVARADO F L, DOMMEL H and BRANDWAJN V, Ref EL-4651, EPRI Research Project 2149-6, June 1989

Power System Control and Stability. ANDERSON P M and FOUAD A A, Iowa State University Press. Vol 1, 1977.

NILSSON N E & MERCURIO J, 'Synchronous Generator Capability Curve Testing and Evaluation', IEEE Trans, on Power Delivery, Vol. 9, No. 1, January 1994, pp 414 - 421.

EBERLY T W and SCHAEFER R C, 'Minimum/Maximum Excitation Limiter Performance Goals for Small Generation', IEEE Trans. Energy Conversion, Vol 10,No 4, December 1995, pp 714-721.

R. G. Farmer, "Power System Dynamics and Stability," The Electric Power Engineering Handbook, Boca Raton: CRC Press LLC, 2001, pp. 600-607.

T. Van Cutsem, "Long-term Voltage Instability: Dynamic Aspects", December 2017. www.montefiore.ulg.ac.be/~vct (current as of 2018/08/11).

J. H. Bickel, "Brief History of North American Grid – Nuclear Power Plant Disturbances", http://www.esrtllc.com/Document%20Library/1.%20Brief%20History%20of%20North%20American%20Grid%20Disturbances.pdf (current as of 2018/08/11).

Power System Stability Volume 1: Elements of Stability Calculations. KIMBARK E W, John Wiley & Sons, New York, 1984.

CLARK H K & FELTES J W, 'Industrial and Cogeneration Protection Problems Requiring Simulation', IEEE Transactions on Industry Applications, Vol 25, No.4, July/August 1989, pp 766-775

Protective Relays Application Guide. GEC Measurements, Third Edition - 1987, pp 316-319.

DINELEY J L, 'Power System Stability Part 2 - Hardware, Generators and Their Controls', IEE Power Engineering Journal, July 1991, pp 191-196.

Electric Power Systems. WEEDY B M, Third Edition, J Wiley & Sons, Chichester 1987.

SESHANNA P, 'Characteristics of an Asynchronized Synchronous Generator', Electric Machines and Electromagnetics 1982 Vol.7 No.I PP.9-25

Lewis Blackburn and Thomas J Domin, Protection Relaying Principles and Applications, third Edition, CRC press Taylor and Francis group, 2006.

Gwala A, Saha A.K.: “Simulation of 100 % stator winding internal ground fault protection in RTDS”, Southern African Universities Power Engineering Conference (SAUPEC), 2015

Gonzalez-Longatt, F.; Adiyabazar, C.; Martinez, E.V. Setting and Testing of the Out-of-Step Protection at Mongolian Transmission System. Energies 2021, 14, 8170. https://doi.org/10.3390/en14238170

Ouellette, D. (2004). Modelling an impedance relay using a real time digital simulator. Eighth IEE International Conference on Developments in Power System Protection, pp.665-668 vol.2.

McLaren, P., Kuffel, R., Wierckx, R., Giesbrecht, J. and Arendt, L. (1992). A real time digital simulator for testing relays. IEEE Transactions on Power Delivery, 7(1), pp.207-213.

APPENDIX A

SEL-421 RELAY SETTING PARAMETERS

A.1.1 setting parameters as viewed from relay terminal command.

```
=>>

=>>SHO
Group 1

Line Configuration

CTRW     := 600        CTRX     := 100        PTRY     := 3636.4    VNOMY    := 110
PTRZ     := 300.0      VNOMZ    := 110        Z1MAG    := 8.03      Z1ANG    := 83.54
Z0MAG    := 25.61      Z0ANG    := 74.66      EFLOC    := Y         LL       := 29.60


Relay Configuration

E21MP    := 2          E21XP    := N          E21MG    := 2         E21XG    := N
ECVT     := N          ESERCMP  := Y          ECDTD    := Y         ESOTF    := Y
EOOS     := Y          ELOAD    := N          E50P     := 2         E50G     := N
E50Q     := N          E51S     := 2          E81      := N         E27      := N
E59      := N          E32      := AUTO       ECOMM    := N         EBFL1    := N
E25BK1   := N          E79      := N          EMANCL   := N         ELOP     := Y1
EDEM     := N          EADVS    := N

Mho Phase Distance Element Reach

Z1MP     := 6.43       Z2MP     := 9.64

Phase Distance Element Time Delay

Z1PD     := 0.000      Z2PD     := 20.000

Mho Ground Distance Element Reach

Z1MG     := 20.49      Z2MG     := 30.73

Zero-Sequence Compensation Factor

k0M1     := 0.735      k0A1     := -12.88

Ground Distance Element Time Delay

Z1GD     := 0.000      Z2GD     := 20.000

Series Compensation

XC       := OFF

Distance Element Common Time Delay

Z1D      := 0.000      Z2D      := 20.000

Switch-Onto-Fault Scheme

ESPSTF   := N          EVRST    := N          52AEND   := OFF       CLOEND   := 10.000
SOTFD    := 10.000
CLSMON   := IN102
```

A1.2 Settings parameters continued with OOS settings

```
SOTFD    := 10.000
CLSMON   := IN102


Out-of-Step Tripping/Blocking

OOSB1    := Y         OOSB2    := Y         OSBD     := 1.875    OSBLTCH := Y
EOOST    := O         OSTD     := 1.250     X1T7     := 21.29    X1T6     := 11.56
R1R7     := 15.53     R1R6     := 5.82

Phase Instantaneous Overcurrent Pickup

50P1P    := OFF       50P2P    := OFF

Selectable Operating Qty Inv.-Time O/C Element 1
(where n = L for line, 1 for BK1, 2 for BK2)

51S1O    := 3I0L      51S1P    := 0.17      51S1C    := U3       51S1TD   := 1.96
51S1RS   := Y
51S1TC   := 32GF


Selectable Operating Qty Inv.-Time O/C Element 2
(where n = L for line, 1 for BK1, 2 for BK2)

51S2O    := 3I2L      51S2P    := 0.15      51S2C    := U3       51S2TD   := 1.00
51S2RS   := N
51S2TC   := 32QF


Directional Control Element

ORDER    := "VI"
50FP     := 0.12      50RP     := 0.08      Z2F      := 4.01     Z2R      := 4.51
a2       := 0.10      k2       := 0.20      Z0F      := 12.81    Z0R      := 13.31
a0       := 0.10
E32IV    := 1


Pole Open Detection

EPO      := 52        SPOD     := 0.500     3POD     := 0.500

Trip Logic

TR       := M1PT OR Z1GT OR M2PT OR Z2GT OR OSB OR OST
TRSOTF   := Z2P OR Z2G OR 50P1
DTA      := NA
DTB      := NA
DTC      := NA
BK1MTR   := OC1 OR PB8_PUL
ULTR     := TRGTR
ULMTR1   := NOT (52AA1 AND 52AB1 AND 52AC1)
TOPD     := 2.000     TULO     := 3         Z2GTSP   := N        67QGSP   := N
TDUR1D   := 6.000     TDUR3D   := 9.000
E3PT     := 1
E3PT1    := 1
ER       := R_TRIG Z2P OR R_TRIG Z2G OR R_TRIG 51S1 OR R_TRIG Z3P OR \
            R_TRIG Z3G OR R_TRIG OST
```

A1.3 Settings parameters continued with Metering measurements.

```
Out-o-step scheme                          Date: 12/12/2000  Time: 15:17:47.644
N_Fose                                     Serial Number: 2010316511

Event: CG                Location:   41.91                  Time Source: HIRIG
Event Number: 15657      Shot 1P: 0   Shot 3P: 0       Freq: 50.00      Group: 1
Targets:
Breaker 1: CLOSED
Breaker 2: NA
PreFault:      IA      IB      IC      IG     3I2        VA        VB        VC     V1mem
MAG(A/kV)       0       0       0       0       0     0.013     0.003     0.003     0.000
ANG(DEG)    138.7   -40.3   147.7   143.2  -171.0      12.4     136.9    -168.1      68.3

Fault:
MAG(A/kV)     104     167     600     468     465   219.698   220.145   220.435   219.603
ANG(DEG)    -12.7  -132.1   109.1   116.2  -137.2       0.0    -119.9     120.0       0.1



=>>MET

Out-o-step scheme                          Date: 12/12/2000  Time: 13:18:22.004
N_Fose                                     Serial Number: 2010316511

                      Phase Currents
                 IA        IB        IC
I MAG (A)        94.575    151.001   540.559
I ANG (DEG)      -9.63     -129.42   111.33

                      Phase Voltages               Phase-Phase Voltages
                 VA        VB        VC           VAB       VBC       VCA
V MAG (kV)       228.717   228.807   228.717      396.355   396.110   396.140
V ANG (DEG)      0.02      -120.04   120.02       30.00     -90.02    150.02

                    Sequence Currents (A)          Sequence Voltages (kV)
                  I1        3I2       3I0          V1        3V2       3V0
MAG              262.039   420.091   421.180      228.747   0.256     0.248
ANG (DEG)        -8.92     -135.10   118.24       0.00      53.26     168.64

                   A           B           C              3P
P (MW)           21.32       34.09      122.22          177.63
Q (MVAR)          3.63        5.63       18.67           27.93
S (MVA)          21.63       34.55      123.63          179.81
POWER FACTOR      0.99        0.99        0.99            0.99
                   LAG         LAG         LAG             LAG

FREQ (Hz)        50.00

=>>
```

A2.1 Relay HMI parameters with synchronous phasors inclusive

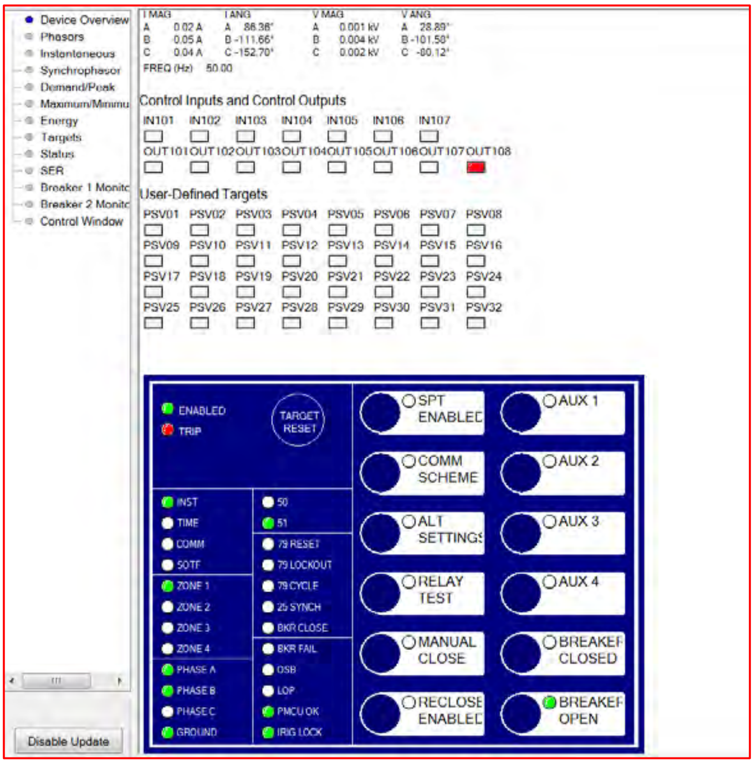

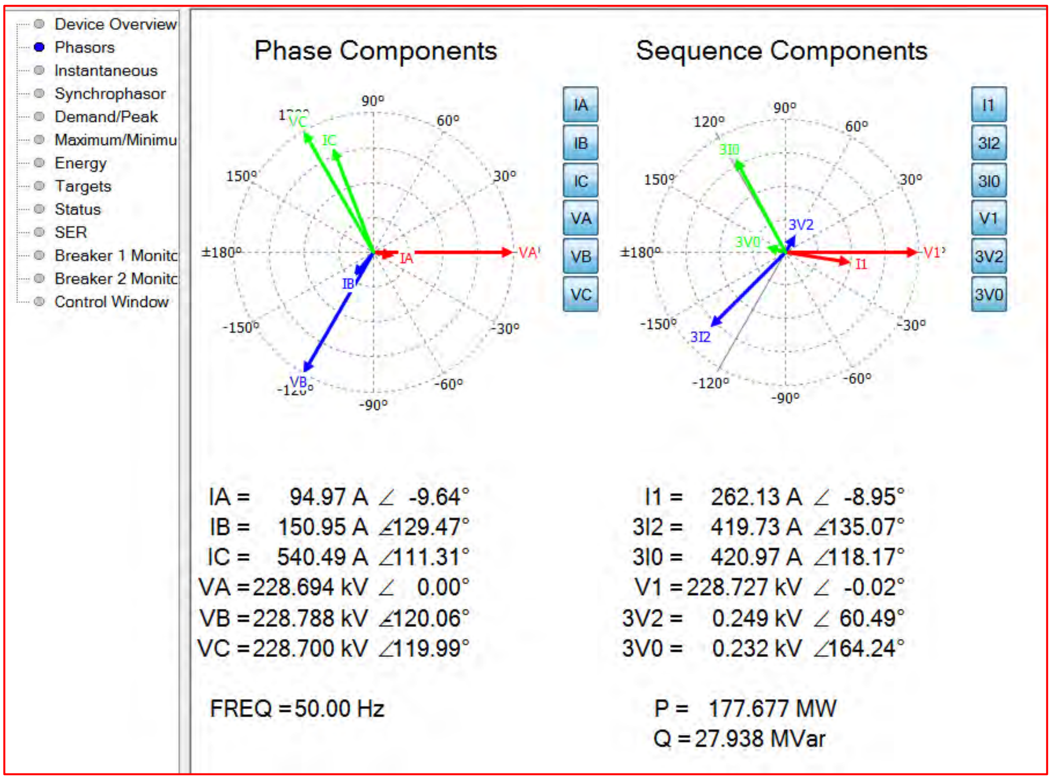

A2.2 Relay HMI instantaneous metering values

Instantaneous Metering Values

Out-o-step scheme — Date: 12/12/2000 Time: 13:23:55.918
N_Fose — Serial Number: 2010316511

	Phase Currents		
	IA	IB	IC
I MAG (A)	95.064	148.946	540.543
I ANG (DEG)	-9.59	-129.32	111.23

	Phase Voltages			Phase-Phase Voltages		
	VA	VB	VC	VAB	VBC	VCA
V MAG (kV)	228.706	228.804	228.717	396.345	396.103	396.132
V ANG (DEG)	0.02	-120.04	120.02	30.00	-90.02	150.02

	Sequence Currents (A)			Sequence Voltages (kV)		
	I1	3I2	3I0	V1	3V2	3V0
MAG	261.514	420.945	421.340	228.742	0.252	0.259
ANG (DEG)	-8.97	-134.96	117.77	0.00	54.60	167.99

	A	B	C	3P
P (MW)	21.44	33.63	122.18	177.25
Q (MVAR)	3.63	5.49	18.89	28.01
S (MVA)	21.74	34.08	123.63	179.45
POWER FACTOR	0.99 LAG	0.99 LAG	0.99 LAG	0.99 LAG

FREQ (Hz) 50.00

A2.3 Relay HMI synchrophasor metering values.

- Device Overview
- Phasors
- Instantaneous
- Synchrophasor
- Demand/Peak
- Maximum/Minimu
- Energy
- Targets
- Status
- SER
- Breaker 1 Monitc
- Breaker 2 Monitc
- Control Window

Synchrophasor Metering Values

Out-o-step scheme — Date: 12/12/2000 Time: 13:24:59.000
N_Fose — Serial Number: 2010316511

Time Quality Maximum time synchronization error: 0.000 (ms) TSOK = 1

Serial Port Configuration Error: N PMU in TEST MODE = N

Synchrophasors

	VY Phase Voltages			VY Pos. Sequence Voltage
	VA	VB	VC	V1
MAG (kV)	228.735	228.825	228.746	228.769
ANG (DEG)	172.097	52.035	-67.903	172.076

	VZ Phase Voltages			VZ Pos. Sequence Voltage
	VA	VB	VC	V1
MAG (kV)	0.006	0.004	0.001	0.003
ANG (DEG)	103.016	-44.910	139.537	84.208

	IW Phase Currents			IW Pos. Sequence Current
	IA	IB	IC	I1W
MAG (A)	95.005	146.104	540.473	260.525
ANG (DEG)	162.489	42.894	-76.712	163.114

	IX Phase Currents			IX Pos. Sequence Current
	IA	IB	IC	I1X
MAG (A)	0.027	0.052	0.094	0.039
ANG (DEG)	65.189	126.863	-5.086	-122.203

	IS Phase Currents			IS Pos. Sequence Current
	IA	IB	IC	I1S
MAG (A)	95.002	146.110	540.503	260.535
ANG (DEG)	162.473	42.914	-76.703	163.123

FREQ (Hz) 50.001 Frequency Tracking = Y
Rate-of-change of FREQ (Hz/s) 0.00

APPENDIX B

PARAMETERS IN DIGSILENT MODEL

B1.1 TGOV1 steam turbine configuration for governing control of Ankerling synchronous generators.

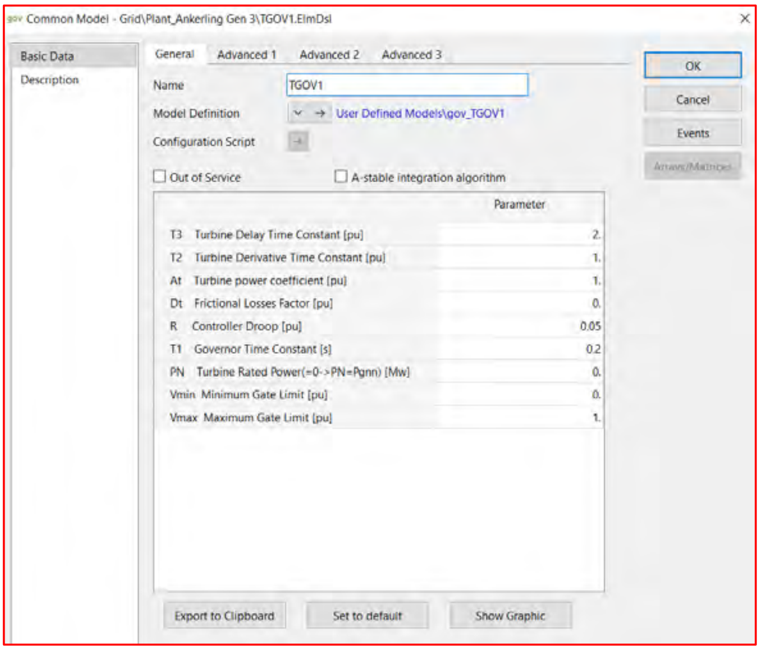

B1.2 TGOV2 steam turbine configuration for governing control of Palmiet synchronous generators.

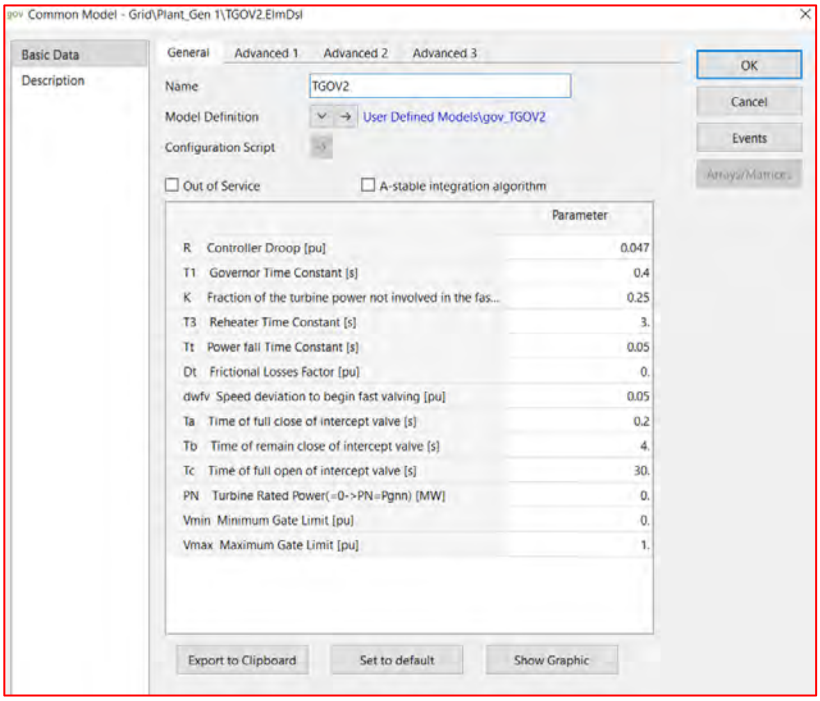

B1.3 GAST gas turbine configuration for governing control of Palmiet synchronous generators.

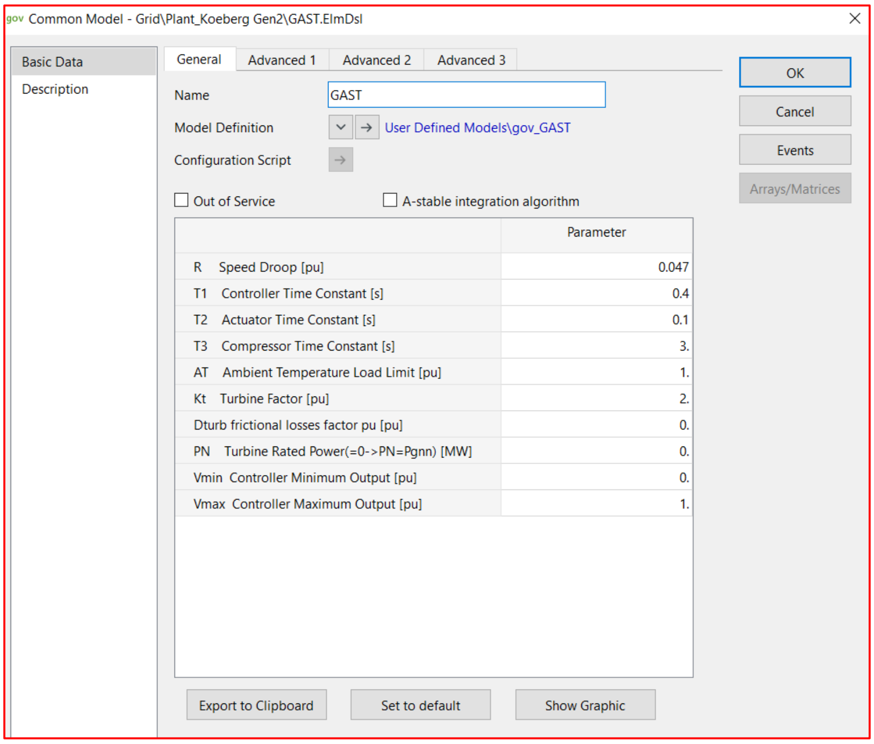

B1.4 TGOV 1 schematic of speed governor implemented in Ankerling generating units.

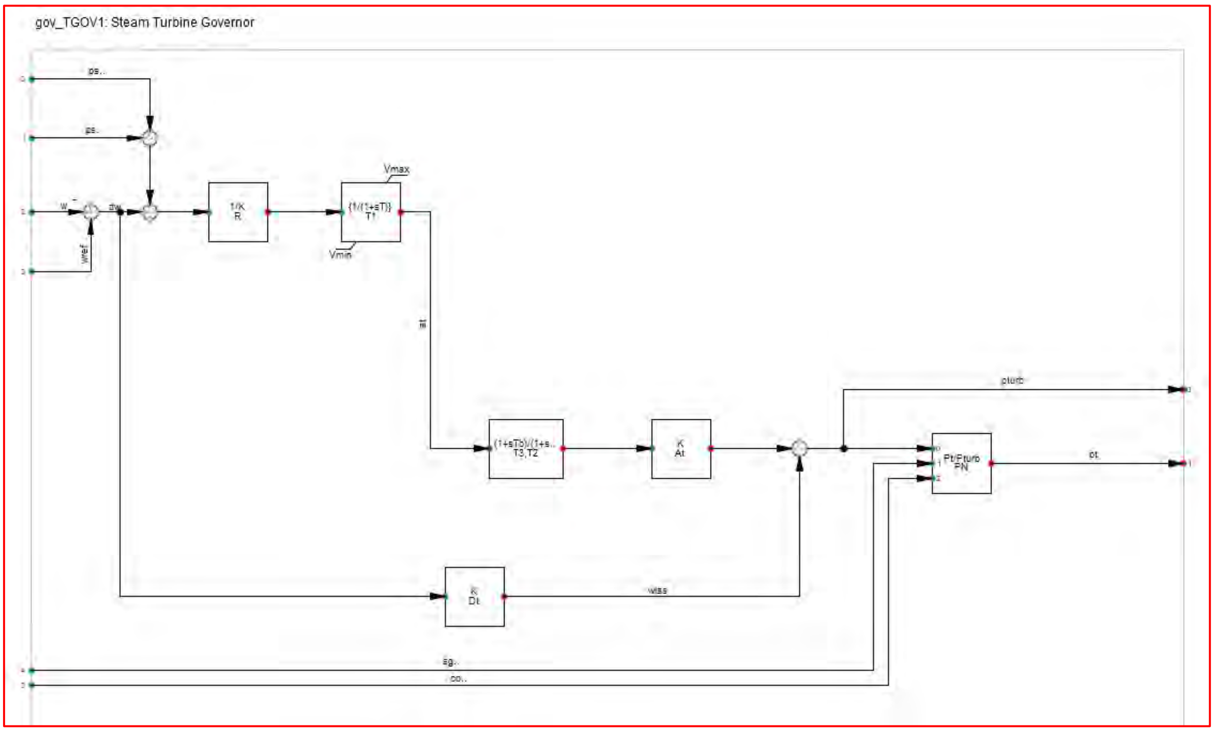

B1.5 GAST schematic of speed governor implemented in Koeberg generating units.

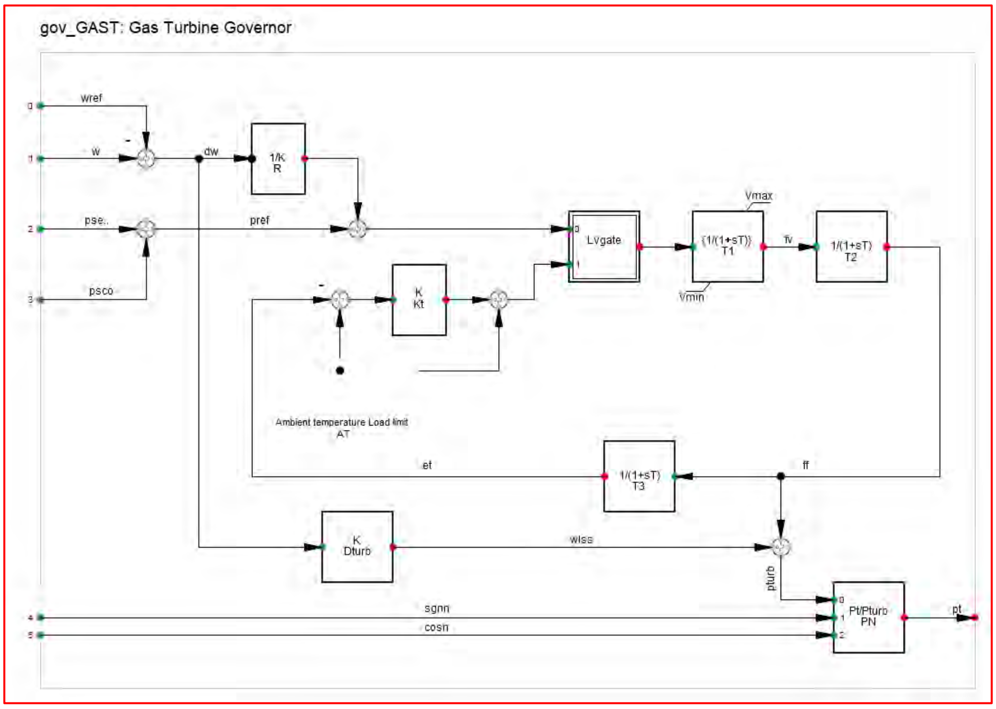

B1.6 IEET1 voltage regulator control configuration for governing control of Palmiet and Ankerling synchronous generators.

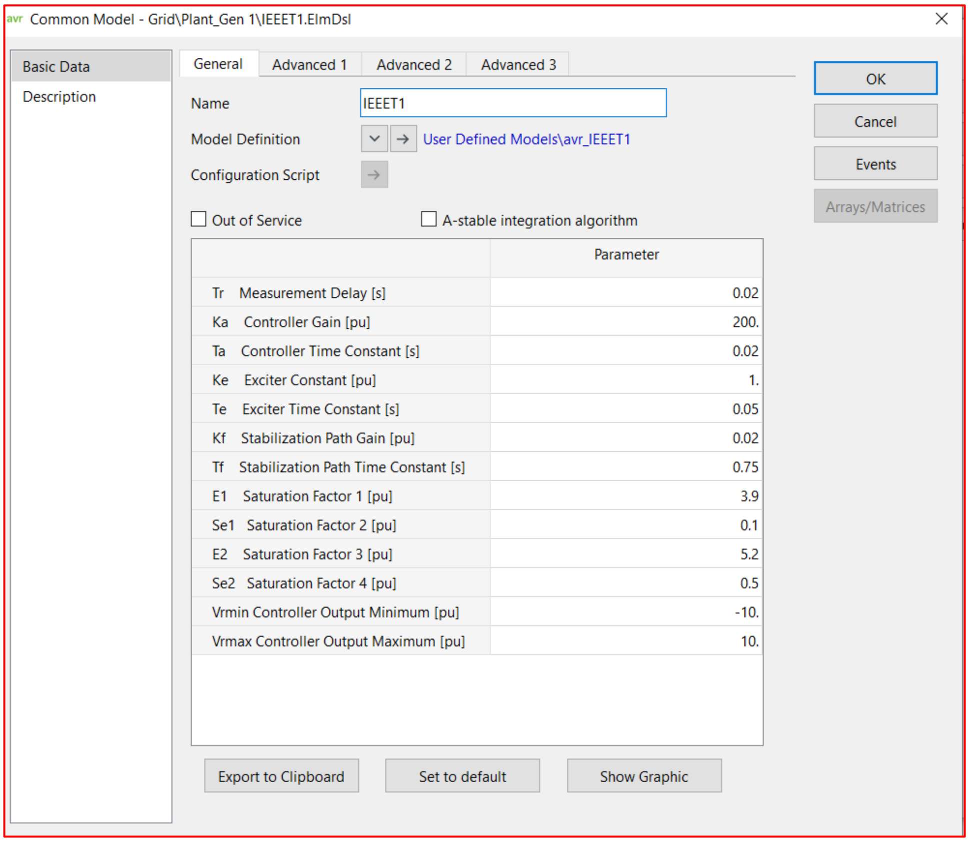

B1.7 EXSTA2 voltage regulator control configuration for dynamic control of Koeberg synchronous generators.

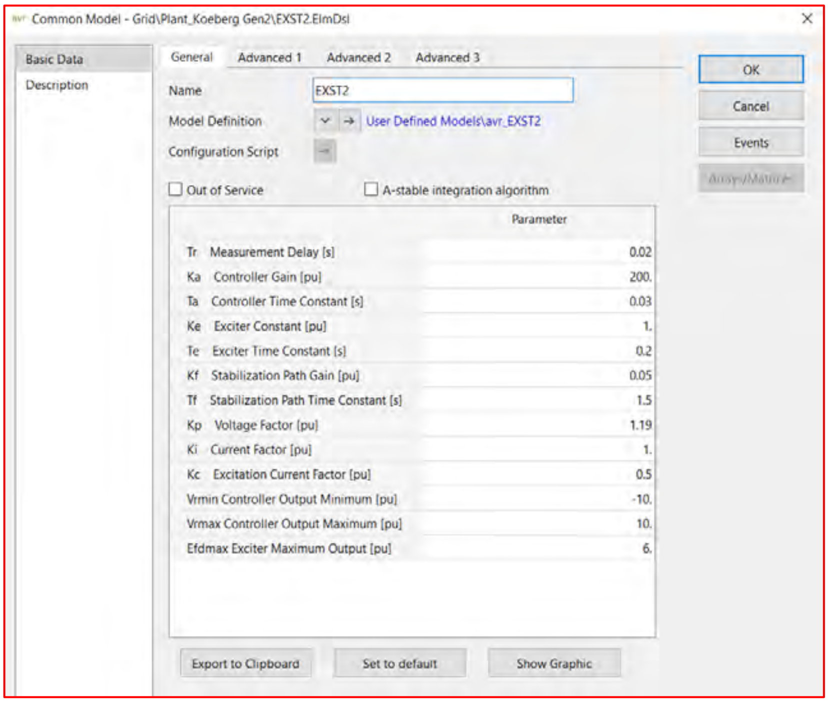

B1.6 EXSTA2 voltage regulator control schematic for dynamic control of Koeberg synchronous generators.

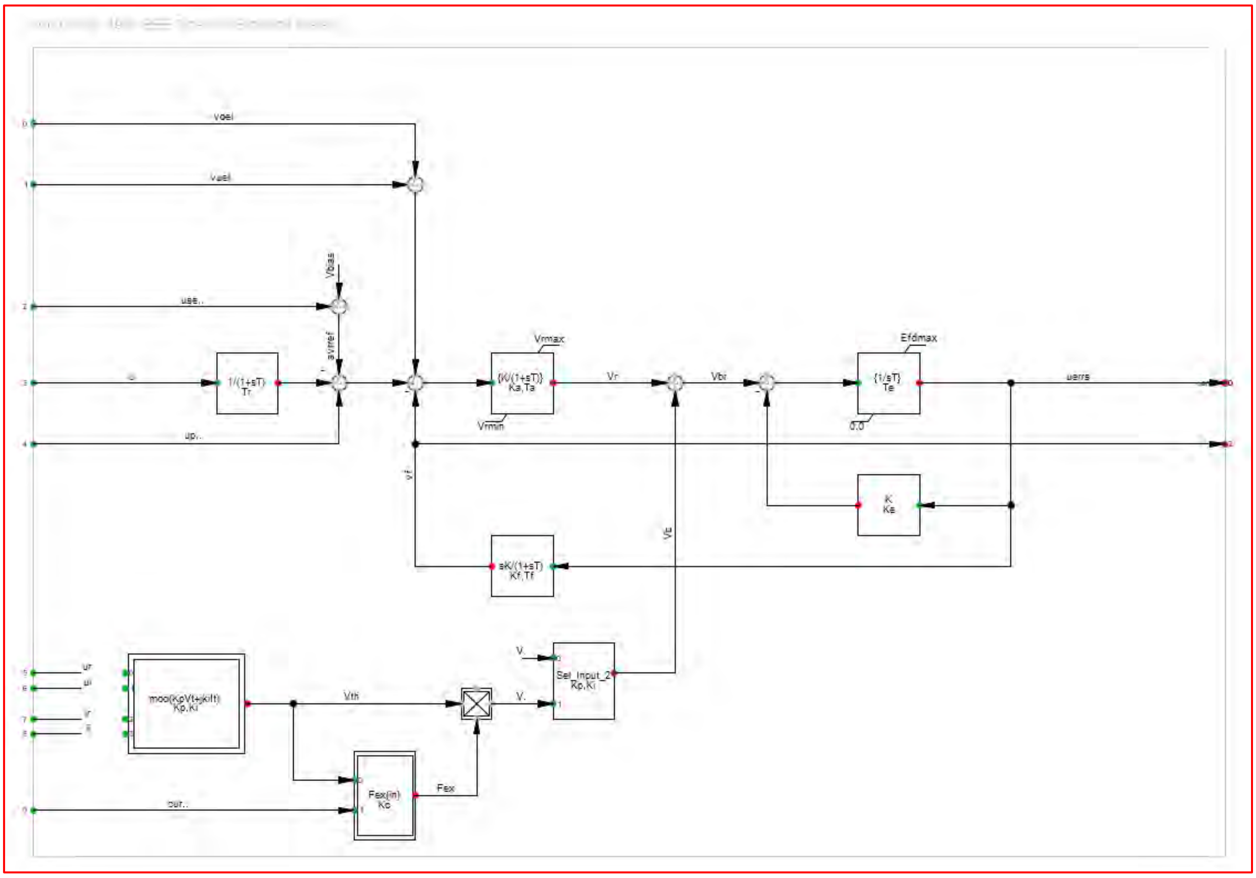

B1.7 STAB1 power system stabilizer schematic for generator control of Koeberg and Ankerling synchronous generators.

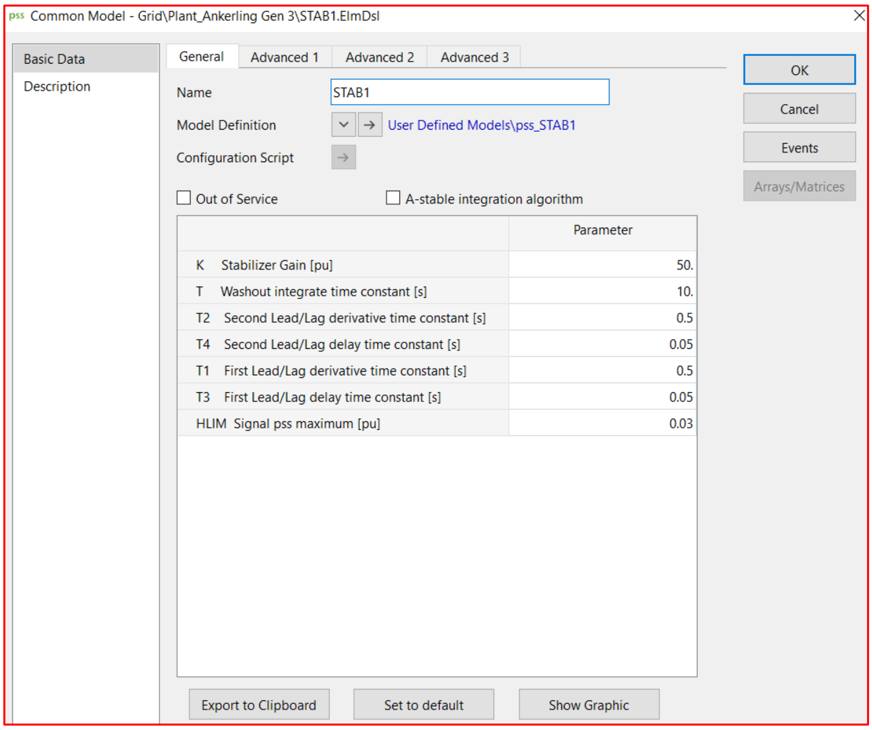

B1.8 STAB3 power system stabilizer schematic for generator control of Palmiet synchronous generators.

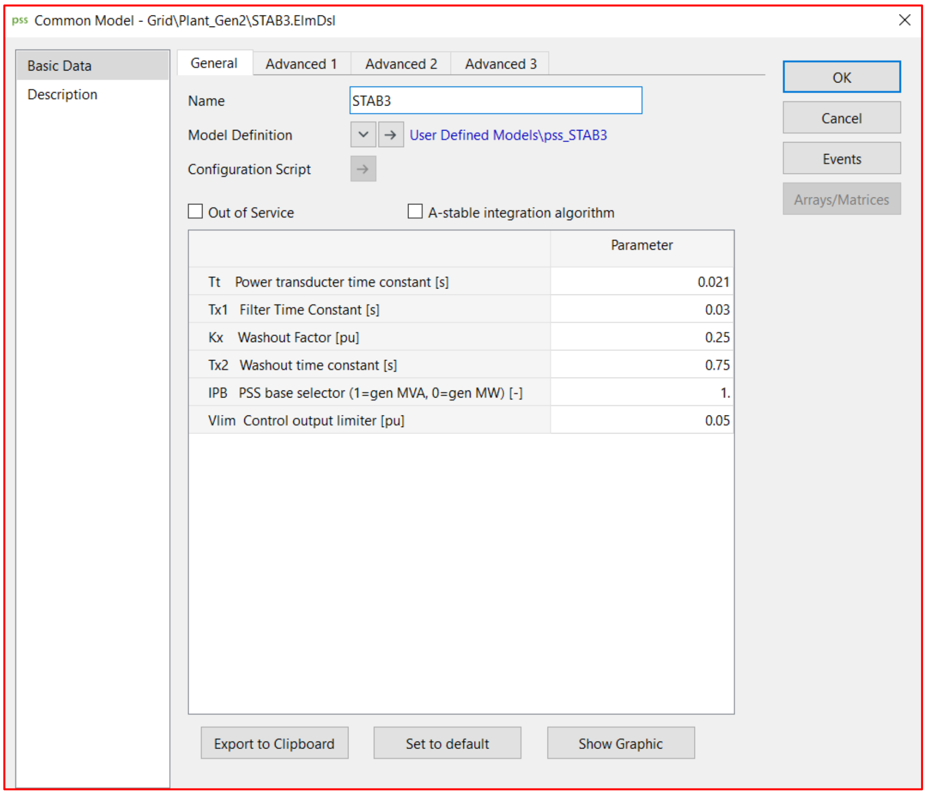

B2.1. Load flow data configuration for Palmiet_load.

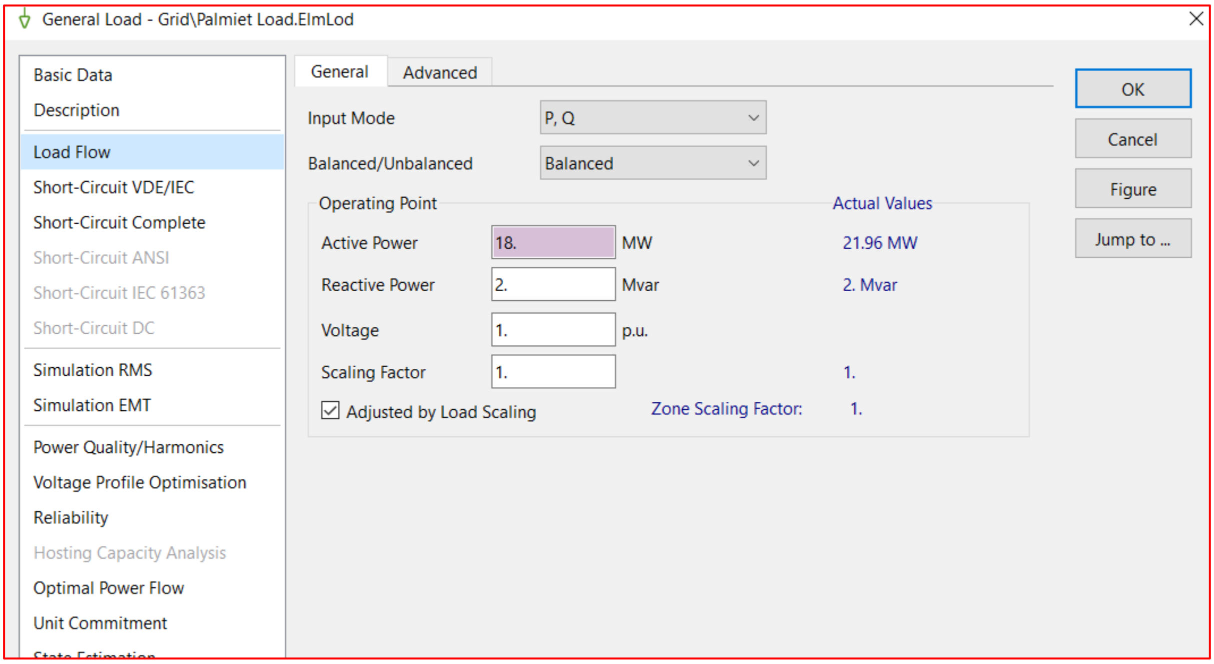

B2.2. RMS simulation data configuration for Palmiet_load P and Q co-efficient.

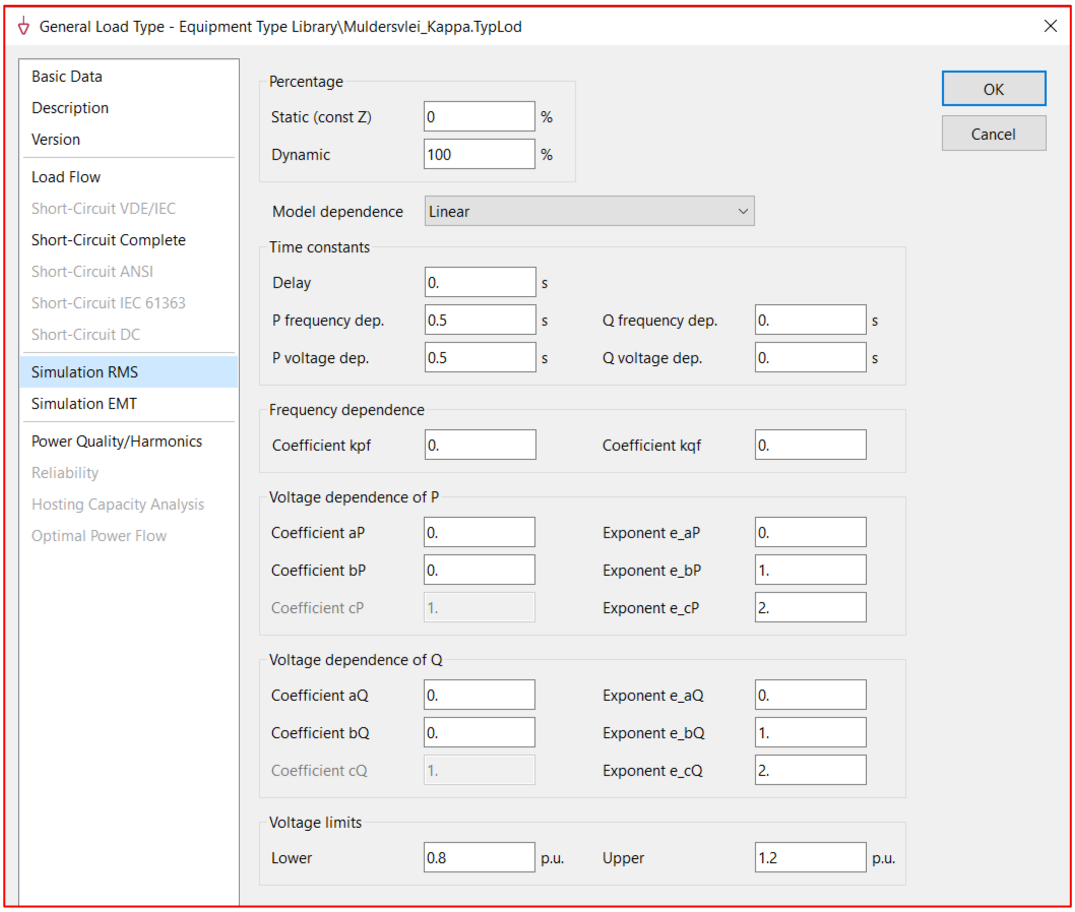

B2.3. load flow simulation data configuration for Palmiet_load P and Q co-efficient.

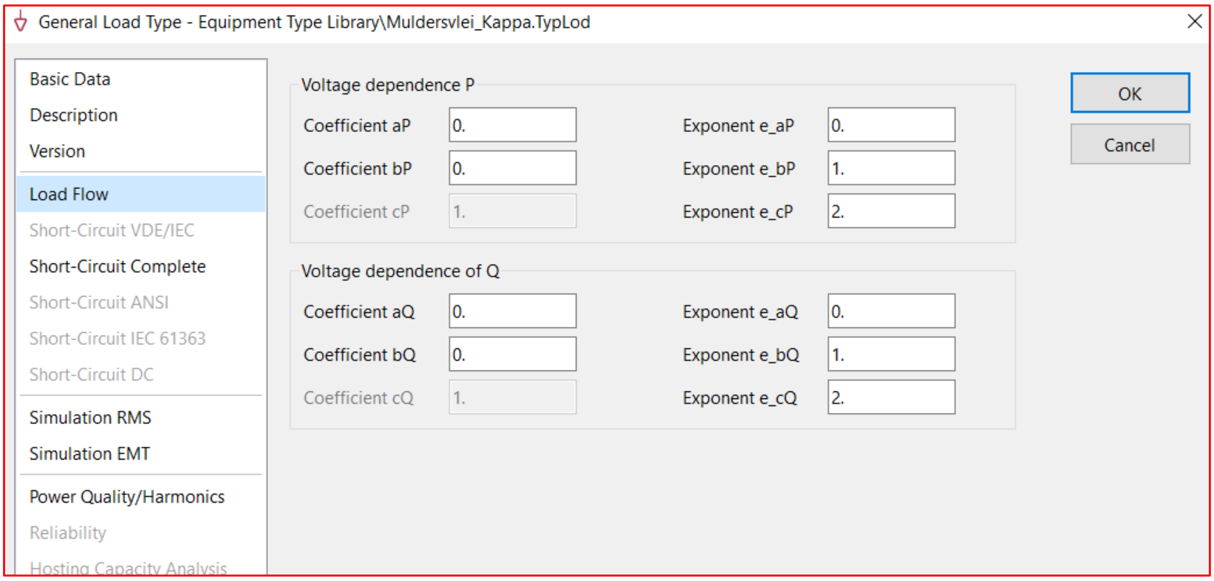

B2.4 RMS/EMT simulation events configured for Dynamic stability analysis.

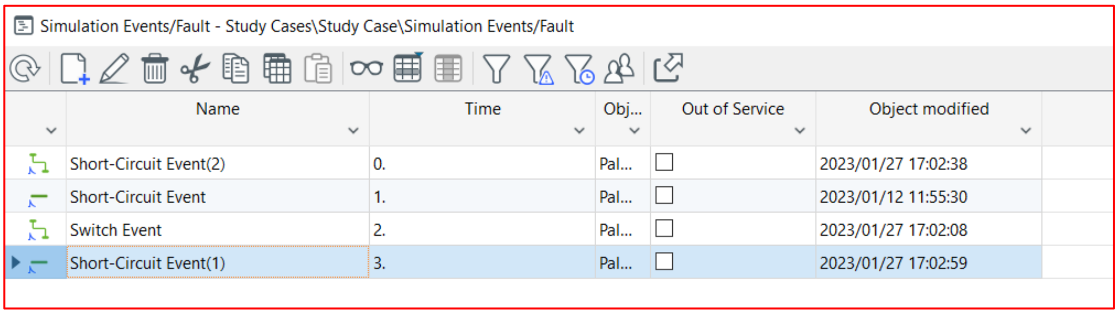

B2.5 Exemplary short-circuit event simulated on Palmiet-busbar.

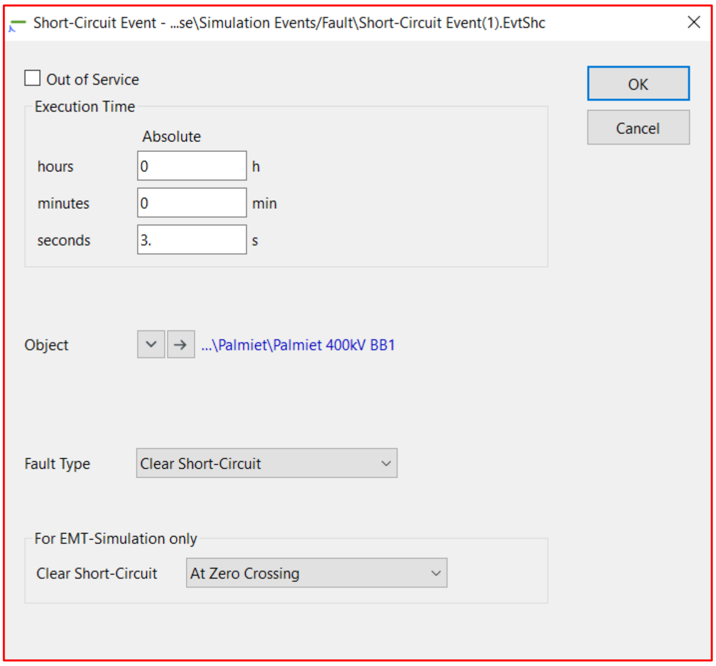

APPENDIX C

TEST SYSTEM ON RSCAD SIMULATION SOFTWARE FOR HIL TEST BENCH

C1.1 Modified Eskom West Grid transmission system on RSCAD.

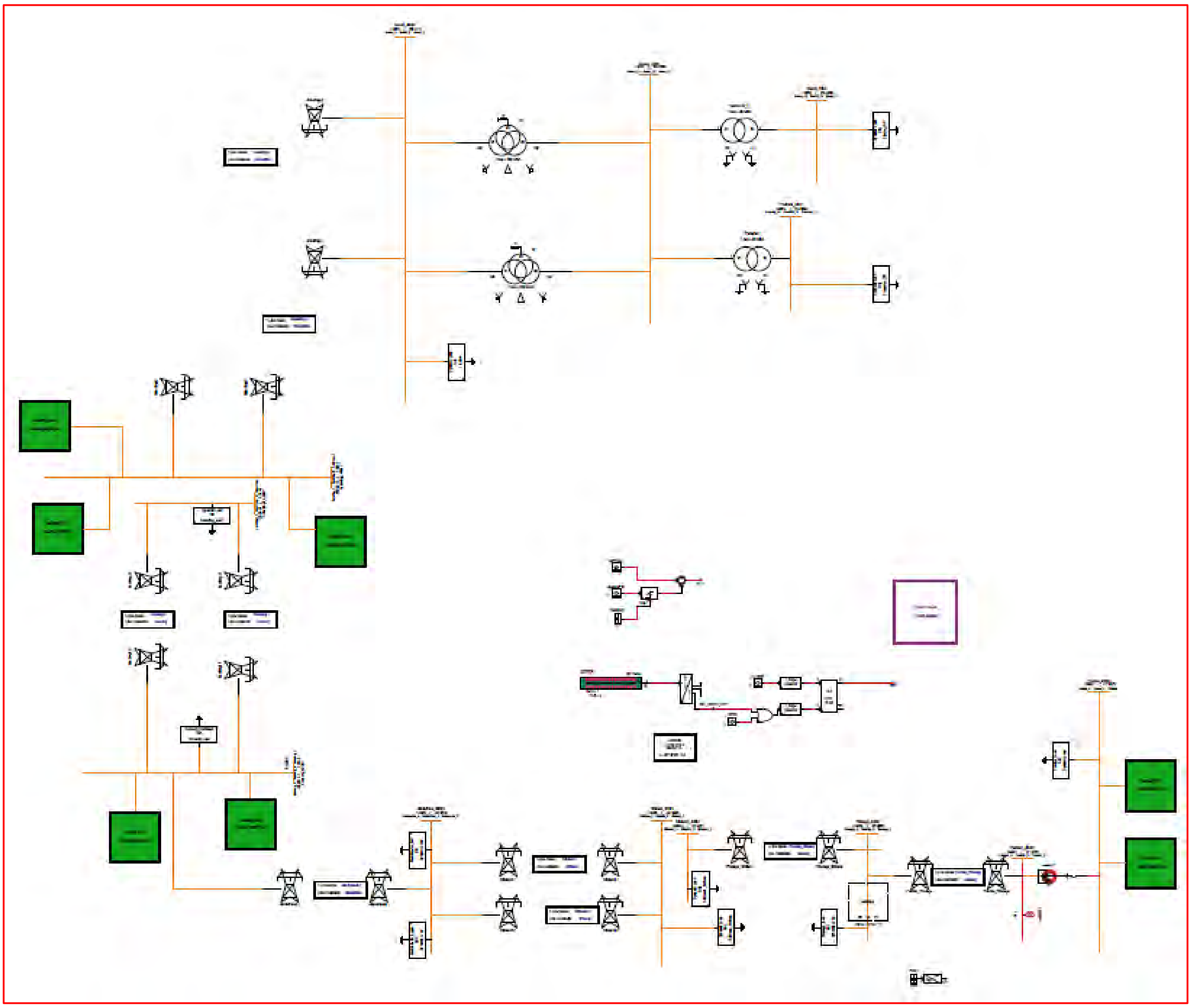

C1.2 Hardware-in-the-loop test bench to monitor rotor angle stability based on IEC 61850-90-5 and hard wire simulations.